frontiers | Research Topics

The development of biomarkers in psychiatry

Edited by
Takashi Nakano, Takahiro A. Kato, Masahiro Takamura and Shin-ichi Kano

Published in
Frontiers in Psychiatry

ISSN 1664-8714
ISBN 978-2-83251-057-5
DOI 10.3389/978-2-83251-057-5

About Frontiers

Frontiers is more than just an open access publisher of scholarly articles: it is a pioneering approach to the world of academia, radically improving the way scholarly research is managed. The grand vision of Frontiers is a world where all people have an equal opportunity to seek, share and generate knowledge. Frontiers provides immediate and permanent online open access to all its publications, but this alone is not enough to realize our grand goals.

Frontiers journal series

The Frontiers journal series is a multi-tier and interdisciplinary set of open-access, online journals, promising a paradigm shift from the current review, selection and dissemination processes in academic publishing. All Frontiers journals are driven by researchers for researchers; therefore, they constitute a service to the scholarly community. At the same time, the *Frontiers journal series* operates on a revolutionary invention, the tiered publishing system, initially addressing specific communities of scholars, and gradually climbing up to broader public understanding, thus serving the interests of the lay society, too.

Dedication to quality

Each Frontiers article is a landmark of the highest quality, thanks to genuinely collaborative interactions between authors and review editors, who include some of the world's best academicians. Research must be certified by peers before entering a stream of knowledge that may eventually reach the public - and shape society; therefore, Frontiers only applies the most rigorous and unbiased reviews. Frontiers revolutionizes research publishing by freely delivering the most outstanding research, evaluated with no bias from both the academic and social point of view. By applying the most advanced information technologies, Frontiers is catapulting scholarly publishing into a new generation.

What are Frontiers Research Topics?

Frontiers Research Topics are very popular trademarks of the *Frontiers journals series*: they are collections of at least ten articles, all centered on a particular subject. With their unique mix of varied contributions from Original Research to Review Articles, Frontiers Research Topics unify the most influential researchers, the latest key findings and historical advances in a hot research area.

Find out more on how to host your own Frontiers Research Topic or contribute to one as an author by contacting the Frontiers editorial office: frontiersin.org/about/contact

The development of biomarkers in psychiatry

Topic editors

Takashi Nakano — Fujita Health University, Japan
Takahiro A. Kato — Kyushu University, Japan
Masahiro Takamura — Shimane University, Japan
Shin-ichi Kano — University of Alabama at Birmingham, United States

Citation

Nakano, T., Kato, T. A., Takamura, M., Kano, S.-i., eds. (2022). *The development of biomarkers in psychiatry*. Lausanne: Frontiers Media SA.
doi: 10.3389/978-2-83251-057-5

Table of contents

frontiers | Frontiers in Psychiatry

TYPE Editorial
PUBLISHED 01 December 2022
DOI 10.3389/fpsyt.2022.1075993

OPEN ACCESS

EDITED AND REVIEWED BY
Michael Maes,
Chulalongkorn University, Thailand

*CORRESPONDENCE
Takashi Nakano
takashi.nakano@fujita-hu.ac.jp

SPECIALTY SECTION
This article was submitted to Computational Psychiatry, a section of the journal Frontiers in Psychiatry

RECEIVED 21 October 2022
ACCEPTED 08 November 2022
PUBLISHED 01 December 2022

CITATION
Nakano T, Takamura M, Kato TA and Kano S-i (2022) Editorial: The development of biomarkers in psychiatry.
Front. Psychiatry 13:1075993.
doi: 10.3389/fpsyt.2022.1075993

Editorial: The development of biomarkers in psychiatry

Takashi Nakano[1,2]*, Masahiro Takamura[3], Takahiro A. Kato[4] and Shin-ichi Kano[5]

[1]Department of Computational Biology, School of Medicine, Fujita Health University, Toyoake, Japan, [2]Division of Computational Science, International Center for Brain Science, Fujita Health University, Toyoake, Japan, [3]Department of Neurology, Faculty of Medicine, Shimane University, Izumo, Japan, [4]Department of Neuropsychiatry, Graduate School of Medical Sciences, Kyushu University, Fukuoka, Japan, [5]Department of Psychiatry and Behavioral Neurobiology, Heersink School of Medicine, University of Alabama at Birmingham, Birmingham, AL, United States

KEYWORDS

psychiatry, major depressive disorder, attention-deficit hyperactivity disorder (ADHD), post-traumatic stress disorder (PTSD), biomarkers

Editorial on the Research Topic
The development of biomarkers in psychiatry

Psychiatric disorders are diagnosed primarily through interviews and observations. This makes it difficult to correctly diagnose patients and select an appropriate treatment at the first visit. Thus, there is an urgent need for more objective indicators based on biological evidence. Biomarkers are objective indicators of disease presence, disease status changes, and treatment effectiveness. To date, a wide range of biomarkers, such as molecules, proteins, and physiological activities, including brain activity, have been developed. This Research Topic includes nine recent studies on the development of biomarkers for psychiatric disorders and one opinion. The proposed potential biomarkers include metabolomic profiles of blood or urine, electroencephalography (EEG) and functional magnetic resonance imaging (fMRI) measurements, volatile organic compound (VOC) profiles in exhaled breath, vocal acoustic features, and visual evoked potentials. This Research Topic multiple disorders, including major depressive disorder (MDD), post-traumatic stress disorder (PTSD), and attention-deficit hyperactivity disorder (ADHD).

Among the studies targeting MDD, Xie et al. measured resting-state brain activity using fMRI. Their results suggested disrupted causal connectivity among brain networks, including the default mode network, in drug-naive first-episode MDD patients. Sun et al. also used resting-state fMRI for patients with MDD, focusing on treatment-resistant and non-treatment-resistant depression. They found differences in some indicators of brain activity, low-frequency fluctuations, and regional homogeneity between the groups. Du et al. used visual evoked potentials, electrical signals generated at the visual cortex by a visual stimulus. Their findings suggest changes in the excitation-inhibition balance of the visual cortex in patients with MDD.

Indicators other than brain activity have also been suggested as potential biomarkers. Lueno et al. measured VOC concentrations in the exhaled breath of patients with MDD and demonstrated the possibility of using VOCs as promising biomarkers. Zhao et al. reported that vocal acoustic features could be potential biomarkers of MDD. They found altered acoustic expressions of emotion in MDD patients compared to healthy controls, suggesting a relationship between acoustic characteristics and the severity of depressive symptoms. Höller et al. investigated seasonal affective disorders using non-clinical samples. They used questionnaires and brain activity measured using EEG to predict mood decline. Höller et al. also showed that seasonality interacts with age and EEG power within the alpha frequency range.

Regarding psychiatric disorders besides mood disorders, Zhu et al. investigated the relationship between ferroptosis, iron-dependent regulated cell death, and PTSD. They applied machine-learning algorithms to blood transcriptome data and successfully predicted PTSD with ferroptosis-related genes. Tian et al. performed urinary metabolomic profiling to diagnose ADHD in children and adolescents. Levels of urine metabolites differed between patients with ADHD and healthy controls. They applied machine learning to predict ADHD using urinary metabolites and succeeded in constructing a model with good predictive ability. Myint and Halaris discussed the kynurenine pathway as a potential biomarker of psychiatric disorders. They also introduced esketamine and its possible therapeutic roles since esketamine is the only currently available medication that is directly linked to the role of the kynurenine pathway in psychiatric disorders.

Many of these studies investigated differences in biological characteristics between patients and healthy subjects or treatment-resistant and non-resistant groups; furthermore, some studies used machine learning to predict the prognosis or diagnosis. Combining biological evidence and machine learning makes it possible to predict the disorder or treatment response of a person (1). The development of machine learning and artificial intelligence has enabled us to increase the predictive value of biomarkers (2). Moreover, biomarkers can be used to predict treatment effects, which leads to tailor-made medicine according to individual characteristics (3), such as neurofeedback (4). New molecular biomarkers, such as cell-free nucleic acids and extracellular vesicles, are actively investigated (5, 6). Expanding research on the development of biomarkers will contribute to a better diagnosis and a deeper understanding of psychiatric disorders.

Author contributions

TN wrote the manuscript. All authors contributed to the article and approved the submitted version.

Conflict of interest

The authors declare that the research was conducted in the absence of any commercial or financial relationships that could be construed as a potential conflict of interest.

Publisher's note

References

1. Drysdale AT, Grosenick L, Downar J, Dunlop K, Mansouri F, Meng Y, et al. Resting-state connectivity biomarkers define neurophysiological subtypes of depression. *Nat Med.* (2017) 23:28–38. doi: 10.1038/nm.4246

2. Nakano T, Takamura M, Ichikawa N, Okada G, Okamoto Y, Yamada M, et al. Enhancing multi-center generalization of machine learning-based depression diagnosis from resting-state fMRI. *Front Psychiatry.* (2020) 11:400. doi: 10.3389/fpsyt.2020.00400

3. Nakano T, Takamura M, Nishimura H, Machizawa MG, Ichikawa N, Yoshino A, et al. Resting-state brain activity can predict target-independent aptitude in fMRI-neurofeedback training. *Neuroimage.* (2021) 245:118733. doi: 10.1016/j.neuroimage.2021.118733

4. Takamura M, Okamoto Y, Shibasaki C, Yoshino A, Okada G, Ichikawa N, et al. Antidepressive effect of left dorsolateral prefrontal cortex neurofeedback in patients with major depressive disorder: a preliminary report. *J Affect Disord.* (2020) 271:224–7. doi: 10.1016/j.jad.2020.03.080

5. Kano S, Dohi E, Rose IVL. Extracellular vesicles for research on psychiatric disorders. *Schizophr Bull.* (2019) 45:7–16. doi: 10.1093/schbul/sby127

6. Kuwano N, Kato TA, Mitsuhashi M, Sato-Kasai M, Shimokawa N, Hayakawa K, et al. Neuron-related blood inflammatory markers as an objective evaluation tool for major depressive disorder: an exploratory pilot case-control study. *J Affect Disord.* (2018) 240:88–98. doi: 10.1016/j.jad.2018.07.040

frontiers in Psychiatry

ORIGINAL RESEARCH
published: 07 March 2022
doi: 10.3389/fpsyt.2022.844434

Altered Visual Cortical Excitability Is Associated With Psychopathological Symptoms in Major Depressive Disorder

Hongheng Du[1,2], *Xue Shen*[1,2], *Xiaoyan Du*[1,2], *Libo Zhao*[1,2]* *and Wenjun Zhou*[3]*

[1] Department of Neurology, Yongchuan Hospital of Chongqing Medical University, Chongqing, China, [2] Division of Clinical Electrophysiology Center, Chongqing Key Laboratory of Cerebrovascular Disease Research, Chongqing, China, [3] Department of Ophthalmology, Yongchuan Hospital of Chongqing Medical University, Chongqing, China

Previous studies suggest that in people with major depressive disorder (MDD), there exists a perturbation of the normal balance between the excitatory and inhibitory neurotransmitter systems in the visual cortex, indicating the possibility of altered visual cortical excitability. However, investigations into the neural activities of the visual cortex in MDD patients yielded inconsistent findings. The present study aimed to evaluate the visual cortical excitability utilizing a paired-pulse stimulation paradigm in patients with MDD and to access the paired-pulse behavior of recording visual evoked potentials (VEPs) as a marker of MDD. We analyzed the amplitudes of VEPs and paired-pulse suppression (PPS) at four different stimulus onset asynchronies (SOAs) spanning 93 ms to 133 ms. Further, the relationship between PPS and the symptom severity of depression was investigated using Spearman's correlation. We found that, whereas the first VEP amplitude remained unchanged, the second VEP amplitude was significantly higher in the MDD group compared to the healthy controls. As a result, the amplitude ratio (second VEP amplitude/first VEP amplitude) increased, indicating reduced PPS and thus increased excitability in the visual cortex. Moreover, we found the amplitude ratios had a significantly positive correlation with the symptom severity of depression in MDD, indicating a clinically useful biomarker for MDD. Our findings provide new insights into the changes in the excitation-inhibition balance of visual cortex in MDD, which could pave the way for specific clinical interventions.

Keywords: major depressive disorder, cortical excitability, visual evoked potentials, paired-pulse suppression, occipital cortex

OPEN ACCESS

Edited by:
Takashi Nakano,
Fujita Health University, Japan

Reviewed by:
Tommaso Bocci,
University of Milan, Italy
Tzu-Yu Hsu,
Taipei Medical University, Taiwan

***Correspondence:**
Libo Zhao
2267254102@qq.com
Wenjun Zhou
wenjun_cqmu@163.com

Specialty section:
This article was submitted to Neuroimaging and Stimulation, a section of the journal Frontiers in Psychiatry

Received: *28 December 2021*
Accepted: *14 February 2022*
Published: *07 March 2022*

Citation:
Du H, Shen X, Du X, Zhao L and Zhou W (2022) Altered Visual Cortical Excitability Is Associated With Psychopathological Symptoms in Major Depressive Disorder. Front. Psychiatry 13:844434. doi: 10.3389/fpsyt.2022.844434

INTRODUCTION

Major depressive disorder (MDD) is a common mental disease that is characterized by affective disturbances and neurocognitive impairment, for which the development of clinically useful biomarkers remains a challenge (1).

Though the underlying mechanism of MDD has not been fully understood, wide-spread connectivity alterations in the structure and function of cortical regions, including occipital cortical abnormalities linked with impaired visual perception, have been reported in MDD patients (2). Several studies have investigated the cortical processing of different types of visual perceptions in

MDD patients, such as visual motion, visual contrast and visual integration, using psychophysical measures. The results revealed higher motion suppression (3), decreased contrast suppression (4) and deficits in integration of visual inputs in MDD (5). The psychophysical deficits in visual perception in MDD are closely related to the abnormality of biochemical changes in the occipital cortex. Using proton magnetic resonance spectroscopy, previous studies have consistently shown a decreased concentration of gamma-aminobutyric acid (GABA) in the visual cortex of MDD subjects (6–8), which can be normalized following effective therapeutic interventions (9–11). As an important inhibitory neurotransmitter, GABA was considered to mediate the center-surround suppression effect in visual perception (12). In addition to GABA, glutamate alterations have been identified in multiple cortical regions, suggesting glutamate has a function in the pathophysiology of MDD as well (13, 14). In healthy individuals, excitatory glutamate levels were found to have a positive association with GABA levels, indicating an excitation-inhibition balance in the occipital cortex. However, in MDD, there was a reduction in glutamate levels in the occipital cortex, and, more importantly, the balance between GABA and glutamate levels was disrupted (8).

Together, these findings suggest that there exists a perturbation of the normal balance between the main excitatory and inhibitory neurotransmitter systems in the occipital cortex of MDD. This begs the issue of whether the excitability of the visual cortex, determined to a great extent by GABA and glutamate, is altered in MDD. In previous studies, transcranial magnetic stimulation (TMS) of the motor cortex revealed that there was an alteration of motor cortical excitability in MDD, which could be modulated by transcranial direct current stimulation (tDCS) (15, 16). The promising intervention of tDCS for treating MDD revealed that aberrant cortical excitability played a significant part in the pathogenesis of MDD. As a result, a greater understanding of the aberrant excitability of the visual cortex may pave the way for new therapy techniques to improve visual perception in MDD patients. So far in the current literature, there are inconsistent findings about alterations involving visual cortical excitability in MDD patients. In an early investigation utilizing electrophysiological measurements, Fotiou et al. revealed that recordings of pattern-reversed visual evoked potentials (VEPs) were within the normal range in MDD patients and were not different from those in healthy controls (17). However, in the two subsequent studies, amplitudes of pattern-reversed VEPs were shown to be considerably lower in MDD patients (18, 19). More recently, Qi et al. explored the relationship between pattern glare and MDD. They discovered a high level of pattern glare in MDD patients, indicating hyper-excitability existed in the visual cortex of MDD patients (20).

Paired-pulse stimulation paradigm, which involves delivering two stimuli at different inter-stimulus intervals, are widely employed to assess cortical excitability. When paired stimuli are applied in close succession, the amplitude of the evoked potential by the second stimulus is suppressed. By comparing the suppressive influence of the second stimulus with the first stimulus, researchers can investigate the cortical excitability in the motor, visual and somatosensory cortex (21–23). High paired-pulse suppression (PPS) indicates low cortical excitability, while low PPS indicates high cortical excitability. To clarify the foregoing seemingly contradictory results, this study employed a paired-pulse stimulation method to produce VEPs. PPS was next examined in MDD patients and a group of healthy controls who were matched by gender, age, and educational level to determine visual cortical excitability. Further, the relationship between visual cortical excitability and psychopathological symptoms in MDD was investigated.

METHODS

Participants

Twenty-three individuals with MDD and 27 normal controls were enrolled in the study. All subjects were recruited from the neurology outpatient clinics of Yongchuan Hospital and provided written informed consent. This research was carried out in line with the Helsinki Declaration and approved by the Ethics Committee of Yongchuan Hospital of Chongqing Medical University (approval No. 2019114).

The diagnosis of MDD was established by two experienced psychiatrists and confirmed with the Mini International Neuropsychiatric Interview (M.I.N.I.). The population was also assessed psychometrically using the Hamilton Depression Rating Scale (HAMD).

Inclusion criteria of the MDD subjects were: (1) currently in a first or recurrent episode of MDD diagnosed according to the Diagnostic and Statistical Manual of Mental Disorders, Fifth Edition (DSM-V); (2) a total score of HAMD $\geq$17; (3) age between 18 and 60 years; (4) free from ocular diseases and with normal or corrected-to-normal visual acuity in both eyes; (5) dextromanual and able to finish the study.

Inclusion criteria of the healthy subjects were: (1) no history of psychiatric disorder; (2) a total score of HAMD $\leq$7; (3) age between 18 and 60 years; (4) free from ocular diseases and with normal or corrected-to-normal visual acuity in both eyes; (5) dextromanual and able to finish the study.

Exclusion criteria for both groups were: (1) history of neurological or other physical illness such as cardiac, respiratory, hepatic, renal, and endocrinal diseases; (2) history or family history of other psychiatric disorders; (3) presence of alcohol or substance abuse; (4) presence of psychotropic drug use; (5) subjects who are pregnant, breastfeeding or in menstrual period.

Stimulation

The paradigm of paired-pulse stimulation was the same as that used in earlier investigations (24, 25). The participants were situated in a shaded room, 50 cm away from a cathode ray tube (CRT) with a viewing angle of 23° × 17°. The CRT was set to a pixel resolution of 800 × 600 and a frame rate of 75 Hz (13.33 ms per frame). Subjects were instructed to relax with their eyes open and binocularly gaze at a small fixed cross in the center of the monitor. For paired-pulse stimulus, a black and white checkerboard pattern (check size 0.5°, contrast 36 %, mean luminance 16 cd/m^2) as the initial stimulus was displayed for one frame (13.33 ms), which corresponded to

the tube's frame rate. The first stimulus was then followed by presentations of multiple frames with a uniform gray backdrop and no variation in the mean brightness. After various stimulus onset asynchronies (SOAs), the second stimulus, presented as a checkerboard pattern with the same parameters, occurred. We used four different SOAs of 93 ms (six frames), 107 ms (seven frames), 120 ms (eight frames) and 133 ms (nine frames), which had shown paired-pulse inhibition in previous studies. The trials with these paired-pulse stimuli were spaced by 1,000 ms intertrial intervals, resulting in a frequency of around 1 Hz. For single-pulse stimulus, checkerboard patterns with identical contrast and luminance as before were displayed for one frame (13.33 ms), followed by presentations of multiple frames with a uniform gray backdrop (intertrial interval 1,000 ms, resulting in a stimulation frequency of about 1 Hz). Ten trials with paired-pulse stimuli, accompanied by 10 trials with single-pulse stimuli, constituted one cycle. Both the paired- and single-stimulus conditions were given in four successive cycles of ten stimuli, totaling 40 sweeps per condition. The VEPs were performed using a GT-2008V-III VEP system (Guo Te Medical Equipment, Chongqing, China).

Recording and Analysis

For VEP recordings, the anodal electrode was inserted on the scalp at Oz (mid-occipital location) above the visual cortex, with the reference electrode at Fz (mid-frontal position) and the ground electrode at Cz (center of the scalp). VEPs of each condition (single stimulation, and paired-pulse stimulation at SOAs of 93, 107, 120 and 133 ms) were documented in epochs from 200 ms before and 300 ms after the stimulation. After being band-pass filtered (1–100 Hz) and baseline adjusted to the Pre-stimulus, signals were averaged and those >140 μV were considered artifacts and were removed. In the single-pulse VEP recordings, C1 denoted a positive peak that occurred <100 ms after stimulus onset, while C2 denoted a negative peak that occurred more than 100 ms after the start of simulus. Considering paired-pulse VEPs, the amplitudes of the first response between C1 and C2 were termed A1 (first amplitude) and the amplitudes of the second response between C1 and C2 were termed A2 (second amplitude). To factored out the linear superposition effects in paired-pulse VEPs, the response to the single-pulse stimulation was subtracted from the paired-pulse stimulation trace, resulting in a "true" second amplitude (A2s). PPS was defined as a ratio (A2s/A1) of the amplitudes of the second (A2s) and the first (A1) peaks (**Figure 1**). The value of ratio ≥1 means that there is no suppression.

Statistics

All statistical analysis in this study was done with SPSS (version 19.0). For demographic and clinical data, χ^2 test and Student's *t* test (unpaired, two-tailed) were conducted to determine the difference between the two groups. For the amplitudes of single VEPs, Student's *t* test was performed. The paired-pulse VEP data were analyzed using a Two-way repeated measures ANOVA (Between-subject factor = group, level = 2; Within-subject factor = SOAs; level = 4) with *post-hoc t*-tests (Bonferroni corrected). To see if there was a link between PPS and HAMD-17 scores, Spearman's correlation coefficient was examined. The general linear regression analysis method is used to analyze the relationships. Differences were considered statistically significant if $p < 0.05$.

RESULTS

Demographic and Clinical Characteristics

Table 1 summarizes the demographic variables and clinical characteristics of study participants, including gender, age, education level and the scores of HAMD. No significant differences were observed between the MDD group and the healthy controls with respect to gender ($\chi^2 = 0.0480, p = 0.8267$), age ($T = 0.5020$, $p = 0.6180$) and education level ($T = 0.1181$, $p = 0.9065$). MDD patients had a significantly higher HAMD score than the control group ($T = 29.7523$, $p < 0.001$), showing that the patients were in the midst of a depressive episode when they entered the study.

Recording VEPs

Mean values and standard deviations of the response amplitudes to the single- and paired-pulse stimulus in the MDD group and the healthy controls are shown in **Table 2**. The unpaired Student's *t*-test revealed no significant changes in VEP amplitude between the two groups in the single stimulus condition ($T = 1.7707$, $p > 0.05$).

In the paired-pulse stimulus condition, the amplitude ratios (A2s/A1) in the MDD group and the control group at different SOAs (93 ms, 107 ms, 120 ms and 133 ms) were all <1.0, indicating varying degrees of PPS. The amplitude ratios increased in both groups as the value of SOAs increased, with the largest values (0.96) in the control group at a SOA of 133 ms (**Figure 2A**). The repeated measures ANOVA for the analysis of amplitude ratio (A2s/A1) indicated there were significant effects of group (MDD vs. control; $F = 100.467$, $p < 0.001$), SOA ($F = 31.237$, $p < 0.001$), and interaction between SOA and group ($F = 7.451$, $p < 0.001$) (**Table 3**). *Post-hoc t*-tests with Bonferroni correction showed the amplitude ratios (A2s/A1) were significantly higher at SOAs of 93 ms ($F = 66.481$, $p < 0.001$), 107 ms ($F = 84.846$, $p < 0.001$), 120 ms ($F = 30.536$, $p < 0.001$) and 133 ms ($F = 9.469$, $p = 0.003$) in the MDD group compared to the healthy controls (**Table 4**). A higher amplitude ratio indicated a lower PPS. Because the amplitude ratio was calculated by dividing A2s by A1, the two components were then analyzed separately to identify which component was responsible for the increased amplitude ratio in the MDD group (**Figure 2B**). For the first VEP amplitude (A1), ANOVA did not indicate any effects of group (MDD vs. control; $F = 2.592$, $p = 0.114$), SOA ($F = 2.912$, $p = 0.074$) or interaction between SOA and group ($F = 1.824$, $p = 0.156$). Regarding the second VEP amplitude after subtraction of the single VEP amplitude (A2s), there were significant effects of group (MDD vs. control; $F = 256.398$, $p < 0.001$), SOA ($F = 50.096$, $p < 0.001$), and interaction between SOA and group ($F = 17.044$, $p < 0.001$). The significant effect of group for A2s indicated that the MDD group had a substantial increase in the second VEP amplitude compared to the control group. *Post-hoc t*-tests with Bonferroni correction showed significantly higher amplitude of A2s at SOAs of 93 ms

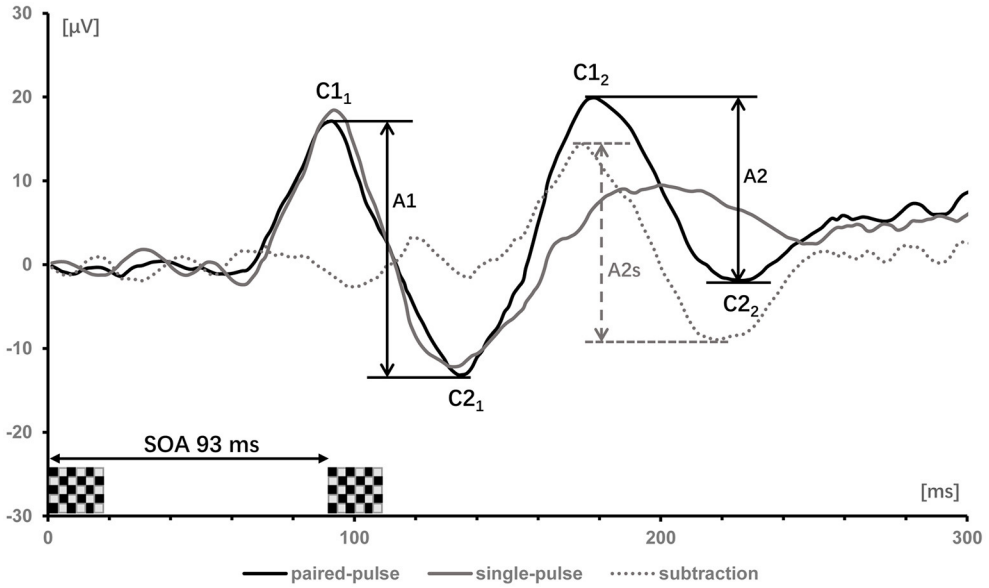

FIGURE 1 | Visually evoked potentials of one subject after single- (gray trace) and paired-pulse with SOA of 93 ms (black trace). The label C denoted the positive and negative components of the first and second response. Subtracting the single-pulse trace from the paired-pulse trace yields the dotted gray trace. The first amplitudes (A1 = $C2_1$-$C1_1$) and second amplitudes (A2 = $C2_2$-$C1_2$) in the paired-pulse trace are indicated by vertical bars; the second amplitudes (A2) after subtracting the response of a single-pulse are denoted as A2s.

TABLE 1 | Demographic and clinical data of MDDs and healthy controls.

Variables	MDD patients (*N* = 23)	Healthy controls (*N* = 27)	Test statistic	*p* value
Gender (M/F)	7/16	9/18	$\chi^2 = 0.0480$	0.8267
Education, years (SD)	13.7 (1.75)	13.6 (1.80)	$T = 0.1181$	0.9065
Age, years (SD)	30.7 (8.04)	29.7 (5.71)	$T = 0.5020$	0.6180
Age of onset, years (SD)	28.9 (7.30)	–	–	–
Duration of illness, years (SD)	1.7 (1.07)	–	–	–
Number of episodes (SD)	1.2 (0.41)	–	–	–
First/recurrent episode	18/5	–	–	–
HAMD-17 scores (SD)	23.8 (3.4)	3.4 (1.1)	$T = 29.7523$	<0.001

HAMD, Hamilton Depression Rating Scale. Each value is expressed as mean (standard deviation).

($F = 141.885, p < 0.001$), 107 ms ($F = 167.285, p < 0.001$), 120 ms ($F = 94.005$, $p < 0.001$) and 133 ms ($F = 13.171$, $p = 0.01$) in the MDD group compared to the healthy controls. So, the VEP amplitude to the second stimulus, according to our analyses, is critical in modulating paired-pulse behavior in MDD.

Relation of Paired-Pulse Suppression With Symptom Severity of Depression

PPS is regarded as a cortical excitability indicator. The above finding that the MDD group showed a reduced PPS and hence an elevated visual cortical excitability begs the question of whether PPS is related to symptom severity in MDD patients. To address this question, a linear association analysis between the degree of PPS and the symptom severity of depression was performed. The amplitude ratios (A2s/A1) used to quantify PPS were shown to have a significantly positive correlation with symptom severity as measured by HAMD scores: the greater the amplitude ratios (A2s/A1), the higher the HAMD scores suggesting higher degrees of symptom severity. **Figure 3** showed the Spearman's correlation coefficient and *p*-values for each SOA in the lower right corner of the plots (SOA 93 ms: $r = 0.4280$, $p = 0.0416$, SOA 107 ms: $r = 0.4979$, $p = 0.0156$, SOA 120 ms: $r = 0.4387$, $p = 0.0390$, SOA 133 ms: $r = 0.3476$, $p = 0.1041$). Only at a SOA of 133 ms was the correlation not significant, possibly due to the decayed PPS at long SOAs.

DISCUSSION

Previous electrophysiologic investigations on neural activities of visual cortex in MDD patients yielded inconsistent results.

TABLE 2 | Response amplitudes and their ratios for the MDD group and healthy controls.

Parameter	SOAs (ms)			
	93	107	120	133
MDD group				
A1 (μV)	34.05 ± 2.04	32.03 ± 2.26	34.24 ± 3.18	32.28 ± 2.14
A2 (μV)	22.64 ± 3.48	26.06 ± 1.83	27.54 ± 3.26	29.10 ± 2.49
A2s (μV)	29.14 ± 2.65	29.28 ± 1.96	30.66 ± 2.25	30.88 ± 2.30
Amplitude ratio (A2s/A1)	0.86 ± 0.08	0.92 ± 0.09	0.90 ± 0.10	0.96 ± 0.10
Single (μV)	32.22 ± 2.68			
Control group				
A1 (μV)	32.07 ± 3.10	32.38 ± 2.70	33.24 ± 2.29	32.76 ± 2.43
A2 (μV)	18.77 ± 2.61	20.25 ± 2.60	24.83 ± 3.15	28.08 ± 3.32
A2s (μV)	21.46 ± 1.78	21.86 ± 2.00	25.09 ± 1.71	28.41 ± 2.39
Amplitude ratio (A2s/A1)	0.67 ± 0.07	0.68 ± 0.09	0.76 ± 0.08	0.87 ± 0.10
Single (μV)	33.54 ± 2.59			

SOAs, Stimulus Onset Asynchronies. Each value is expressed as mean (standard deviation).

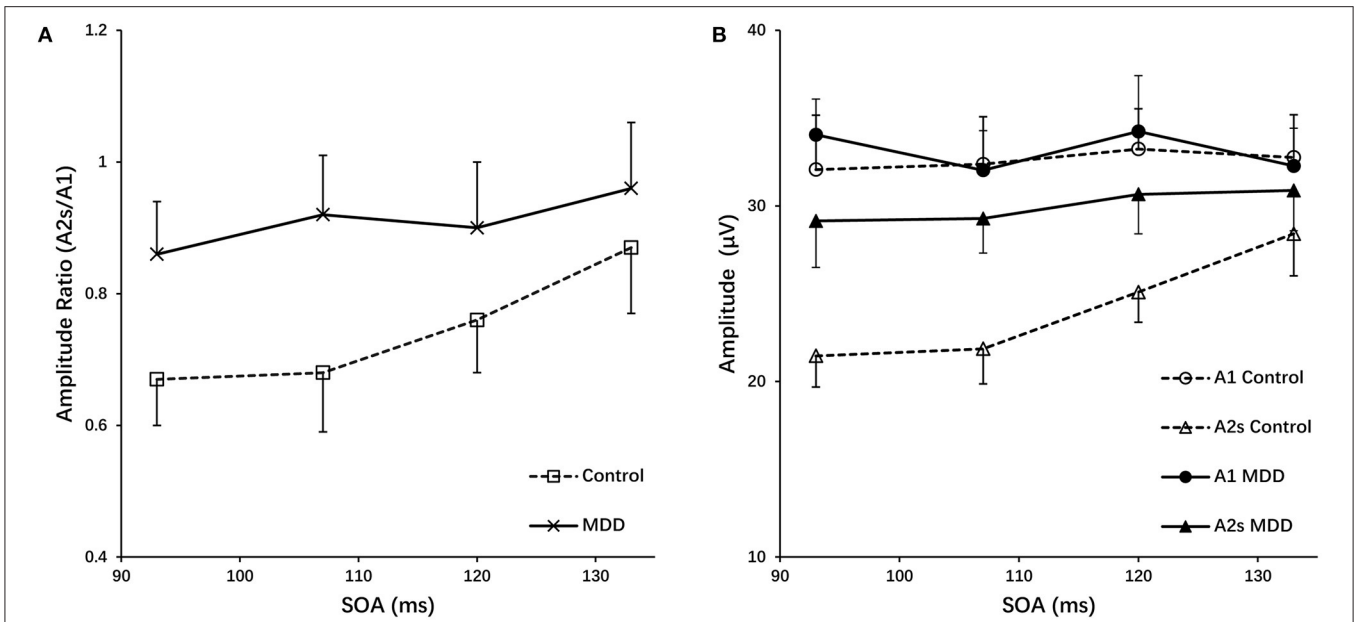

FIGURE 2 | (A) Amplitude ratios (A2s/A1) of the MDD and control group as a function of SOAs. **(B)** The first amplitudes (A1) and the second amplitudes after subtracting the response of a single-pulse (A2s) for the MDD and control group vs. SOA, grand mean ± SD.

In our results, we observed no difference in the amplitude of single-pulse VEPs between the MDD group and the healthy controls. This finding is in line with the results reported by Fotiou et al. who found no difference in the amplitude of single VEPs between MDD group and control group, but a significant alteration of VEP latency in different subtypes of MDD (17). However, our finding on single VEP is not in accordance with the two later studies (18, 19), in which amplitudes of pattern-reversed VEPs were shown to decrease significantly in MDD patients. VEPs reflect population synaptic currents and are usually termed for the type of stimulation, such as flash VEPs, pattern-reversal VEPs, or pattern-onset-offset VEPs. The inconsistency of the results might be attributed to the different types of stimulation used in the single VEP recording. Unlike the above mentioned studies, we employed the approach of pattern onset/offset VEPs, which was thought to be less vulnerable to confounding variables including inadequate fixation, eye movements, or willful defocus than pattern reversal VEPs (22). Furthermore, pattern onset/offset VEPs differs markedly from VEPs generated by other forms of stimulation, leading to a new nomenclature known as C1, C2, and C3 (26). The primary source of the C1 component of the pattern onset/offset VEPs is thought to be parvocellular areas of primary visual cortex (V1). The C2 and C3 components appear to be extrastriate in origin (27–29).

TABLE 3 | Effect of SOA, group and their interaction on amplitude ratio (A2s/A1).

Souce	df	Observed power	*p* value	*F* value
SOA	3	1.000	<0.001	31.237
Group	1	1.000	<0.001	100.467
SOA*Group	3	0.984	<0.001	7.451

SOAs, Stimulus Onset Asynchronies; df, degree of freedom.

TABLE 4 | Pairwise comparisons of amplitude ratio (A2s/A1) between MDD and control groups with *post-hoc t*-tests (Bonferroni correction).

SOAs	df	Observed power	*p* value	*F* value	SEM
93 ms	1	1.000	<0.001	66.481	0.023
107 ms	1	1.000	<0.001	84.846	0.026
120 ms	1	1.000	<0.001	30.536	0.026
133 ms	1	0.854	0.003	9.469	0.029

SOAs, Stimulus Onset Asynchronies; df, degree of freedom; SEM, Standard Error of Mean.

As a result, comparing multiple research employing different types of stimulation is challenging.

To overcome the challenges of evaluating excitability from single-pulse stimulation, paired-pulse stimulation has become a common method for investigating cortical excitability in various disorders like migraine (30), generalized anxiety (23) or dystonia (31), allowing researchers to better understand about the contributions of inhibition and facilitation in cortex, as well as changes in their balance. We aimed to investigate the visual cortical excitability using a paired-pulse stimulation method in MDD patients, and to access paired-pulse behavior of recording VEPs as a marker of MDD. According to our findings, the amplitude ratios (A2s/A1) were significantly higher in the MDD group compared to the healthy controls, indicating reduced PPS and thus increased excitability in the visual cortex. Further analysis found that, whereas the first VEP amplitude (A1) remained unchanged, the second VEP amplitude (A2s) was significantly higher in MDD patients. Moreover, we found the amplitude ratios (A2s/A1) had a significantly positive correlation with symptom severity of depression, indicating a useful clinical biomarker for MDD.

The result of increased excitability in the visual cortex of MDD patients is consistent with the findings of recent psychophysical research, in which heightened levels of pattern glare were observed in MDD, reflecting an increase in cortical excitability (20). The neurological mechanism driving pattern glare is usually assumed to be of cortical origin, i.e., cortical hyper-excitability or inadequate cortical inhibition caused by a lack of inhibitory systems unable to restrain overexcited situations (32–34). Previous research on cortical excitability in MDD has relied mostly on TMS, which is commonly utilized to evaluate motor cortical excitability, and found an interhemispheric imbalance between the prefrontal and motor cortex, which manifested as decreased excitability in the left hemisphere and increased excitability in the right (35–38). TMS was also utilized in the visual system to test cortical excitability in migraine patients (39), but not in MDD patients. However, TMS can cause phosphene perception in the visual field and incompliance in the subjects when used to measure the excitability of occipital cortex. Hoffken et al. showed that paired-pulse VEPs could indicate equivalent visual cortical excitability features while overcoming the TMS limit, since the PPS of VEPs was inversely linked with TMS-induced phosphene thresholds (40).

PPS, also denoted as forward suppression, refers to the decrease of the neural responding to the second stimuli when two stimuli are presented in short succession. The mechanisms that mediate PPS, on the other hand, are not completely understood. Short-term plasticity, a term used to describe changes in neural behavior resulting from prior activity, is often assumed to represent one possible mechanism, which involves presynaptic depletion of releasable vesicles, postsynaptic receptor desensitization or other presynaptic mechanisms depressing vesicle release (41). In addition, there is evidence for a GABAergic contribution to PPS. GABA is the primary inhibitory neurotransmitter, acting at inhibitory synapses by binding to specific $GABA_A$ and $GABA_B$ receptors. In rat auditory cortex, research has revealed that forward suppression is primarily regulated by $GABA_A$ receptor-mediated inhibition at short ISIs (42). In human motor and somatosensory cortex, drug applications of the $GABA_A$ agonist lorazepam could modulate cortical excitability by interfering with GABAergic neurotransmission (43, 44). Moreover, $GABA_B$ receptors are also implicated in the regulation of PPS, since presynaptic blockage of $GABA_B$ receptors induces a reduction in synaptic release probability, which is compatible with presynaptic inhibition of glutamate release (45). The terms "short-latency intracortical inhibition (SICI)" and "long-interval intracortical inhibition (LICI)" are used in paire-pulse TMS research to describe a phenomenon in which the conditioning stimulus reduces the response of the test stimulus at a short or long ISI, respectively. SICI is supposed to indicate $GABA_A$ receptor activity, whereas LICI is thought to reflect $GABA_B$ receptor activity. This phenomenon is thought to be related to, and maybe equivalent to, forward suppression (46). In addition to GABAergic systems, glutamate and its receptors were also considered to play an important role in modulating the PPS (47).

PPS can be altered either by changing the response to the first stimulus, or by changing the response magnitude of the second stimulus, which is considered to be controlled by different mechanisms. Modulation in PPS caused by changes in second amplitudes might indicate changes in intracortical processing, whereas the presence of altered first amplitudes reflects an involvement of thalamocortical transmission (30, 48). We observed an elevated change in the second amplitude but no changes in the first amplitude in MDD patients compared to healthy controls, thus reflecting abnormal cortical visual processing in MDD. Indeed, many lines of studies have reported that MDD is often associated with the subjective experience of altered visual perception, such as photophobia, perceived dimness and reduced visual contrast discrimination (49–51).

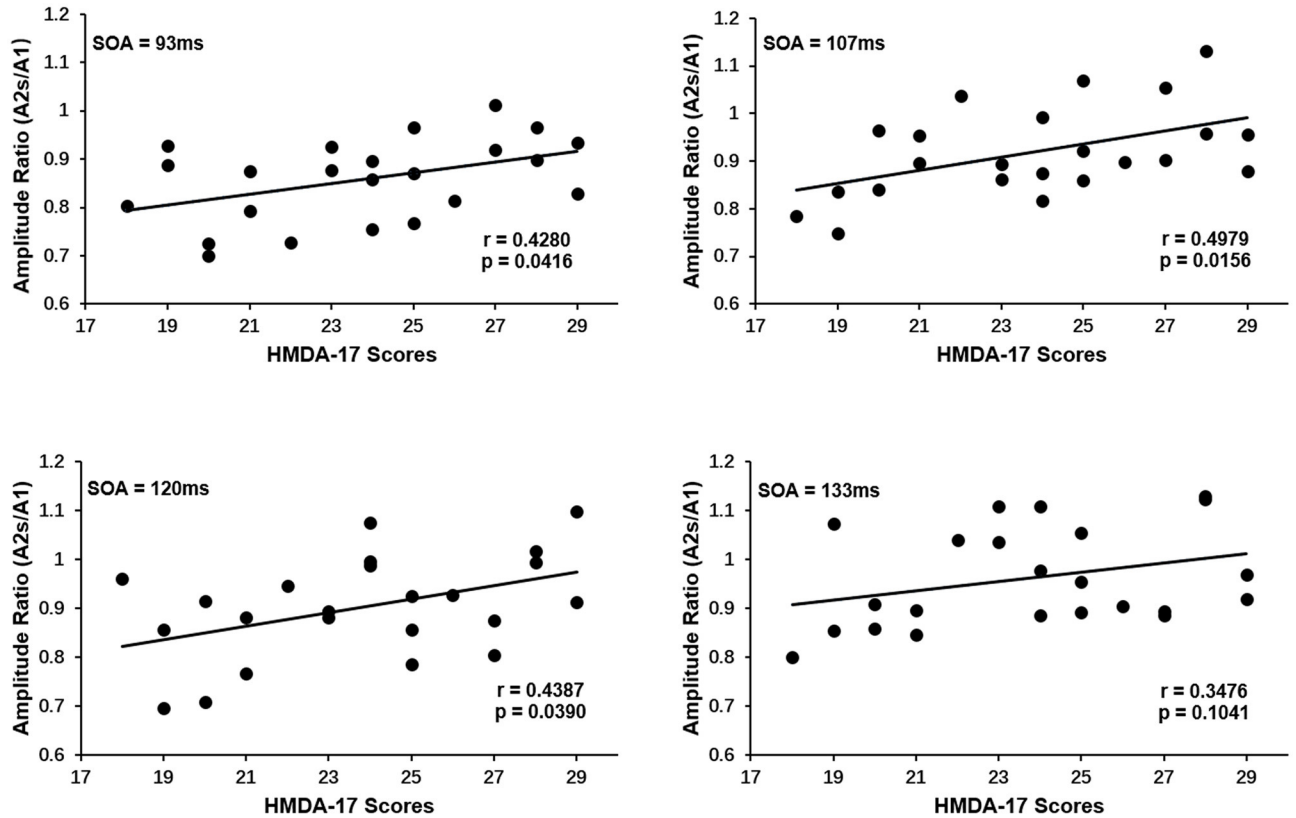

FIGURE 3 | Correlation of paired-pulse suppression with symptom severity of depression for each SOA in MDD group. An increase in the amplitude ratios (A2s/A1) is associated with an increase in HAMD-17 scores. The Spearman's correlation coefficient and p-values for each SOA were present in the lower right corner. Only at SOA of 133 ms was the correlation not significant.

Moreover, the impairment in visual perception was found to be directly related to the psychopathological symptoms of MDD (4, 8). In our study, we found PPS, as indicated by amplitude ratios (A2s/A1), was significantly related to the symptom severity of depression. It is reasonable to presume that aberrant visual cortical excitability has a significant pathophysiological role in MDD, and PPS could serve as a reliable biomarker linking the deficit of visual perception and psychopathological symptoms in MDD.

Limitations and Alternative Explanations

The paired-pulse stimulation paradigm does not allow for the assessment of separate visual substreams that are differently engaged in visual perception since both the use of a black and white checkboard and a contrast of 36% result in unspecific visual stimulation. The magnocellular pathway is more sensitive to low spatial frequency, low contrast, flicker stimuli and motion detection, whereas the parvocellular pathway is more sensitive to chromatic, high luminance contrast, high spatial frequency and stationary stimuli (52, 53). Given that MDD patients have visual motion perception, visual contrast perception, and visual integration deficits, more research should be done at various luminance contrasts, chromatic colors, and temporal frequencies to separate the possible contributions of parvo-, konio-, and magnocellular streams.

Although our results appear to point to a dysfunctional circuits occurring at the level of visual cortex in MDD, i.e., increased cortical excitability probably due to the imbalance between the excitatory and inhibitory systems, additional possibilities need to be considered. Some neurological disorders are characterized by a defective regulation of contrast gain control, including amblyopia and epilepsy (54, 55). More interestingly, the contrast gain control is likely a property of the transcallosal pathway (56), and also major depressive disorder is characterized by either atrophy or microstructural changes of the corpus callosum (57, 58). In this context, the increased cortical excitability might be attributable to a subcortical impairment in contrast gain control regulation at the corpus callosum.

Another possible explanation for the increased cortical excitability in MDD is the visual cortex's metaplasticity. The presence of mechanisms of metaplasticity could keep synaptic plasticity within a functional dynamic range in the visual cortex, i.e., homeostatic plasticity (59). Many mental diseases are often accompanied by a defective homeostatic plasticity. The elevated change in the second amplitude in MDD patients may be attributed to a deficit of homeostatic plasticity in the visual cortex, which should be explored in future studies.

CONCLUSIONS

In summary, we investigated the paired-pulse behavior of VEPs and found a reduced PPS and thus an increased excitability of the visual cortex in MDD, which may reflect abnormal cortical visual processing. Moreover, PPS had a significant correlation with the symptom severity of depression, indicating a clinically useful biomarker in MDD. Our findings provide new insights into the changes in the excitation-inhibition balance of occipital cortex in MDD.

DATA AVAILABILITY STATEMENT

The raw data supporting the conclusions of this article will be made available by the authors, without undue reservation.

ETHICS STATEMENT

The studies involving human participants were reviewed and approved by Ethics Committee of Yongchuan Hospital of Chongqing Medical University. The patients/participants provided their written informed consent to participate in this study.

AUTHOR CONTRIBUTIONS

HD performed the study, collected data, analyzed data, and drafted the article. XS and XD collected data and analyzed data. LZ designed the research and supervised the project. WZ initiated the study concept, interpreted the data, and revised the article. All authors have read the manuscript and agreed to submit it.

REFERENCES

1. Kessler RC, Sampson NA, Berglund P, Gruber MJ, Al-Hamzawi A, Andrade L, et al. Anxious and non-anxious major depressive disorder in the World Health Organization World Mental Health Surveys. *Epidemiol Psychiatr Sci*. (2015) 24:210–26. doi: 10.1017/S2045796015000189
2. Duman RS, Sanacora G, Krystal JH. Altered connectivity in depression: GABA and glutamate neurotransmitter deficits and reversal by novel treatments. *Neuron*. (2019) 102:75–90. doi: 10.1016/j.neuron.2019.03.013
3. Norton DJ, McBain RK, Pizzagalli DA, Cronin-Golomb A, Chen Y. Dysregulation of visual motion inhibition in major depression. *Psychiatry Res*. (2016) 240:214–21. doi: 10.1016/j.psychres.2016.04.028
4. Salmela V, Socada L, Soderholm J, Heikkila R, Lahti J, Ekelund J, et al. Reduced visual contrast suppression during major depressive episodes. *J Psychiatry Neurosci*. (2021) 46:E222–31. doi: 10.1503/jpn.200091
5. Zomet A, Amiaz R, Grunhaus L, Polat U. Major depression affects perceptual filling-in. *Biol Psychiatry*. (2008) 64:667–71. doi: 10.1016/j.biopsych.2008.05.030
6. Sanacora G, Gueorguieva R, Epperson CN, Wu YT, Appel M, Rothman DL, et al. Subtype-specific alterations of gamma-aminobutyric acid and glutamate in patients with major depression. *Arch Gen Psychiatry*. (2004) 61:705–13. doi: 10.1001/archpsyc.61.7.705
7. Bhagwagar Z, Wylezinska M, Jezzard P, Evans J, Ashworth F, Sule A, et al. Reduction in occipital cortex gamma-aminobutyric acid concentrations in medication-free recovered unipolar depressed and bipolar subjects. *Biol Psychiatry*. (2007) 61:806–12. doi: 10.1016/j.biopsych.2006.08.048
8. Song XM, Hu XW, Li Z, Gao Y, Ju X, Liu DY, et al. Reduction of higher-order occipital GABA and impaired visual perception in acute major depressive disorder. *Mol Psychiatry*. (2021) 102:75−90. doi: 10.1152/advan.00125.2019
9. Sanacora G, Mason GF, Rothman DL, Hyder F, Ciarcia JJ, Ostroff RB, et al. Increased cortical GABA concentrations in depressed patients receiving ECT. *Am J Psychiatry*. (2003) 160:577–9. doi: 10.1176/appi.ajp.160.3.577
10. Sanacora G, Fenton LR, Fasula MK, Rothman DL, Levin Y, Krystal JH, et al. Cortical gamma-aminobutyric acid concentrations in depressed patients receiving cognitive behavioral therapy. *Biol Psychiatry*. (2006) 59:284–6. doi: 10.1016/j.biopsych.2005.07.015
11. Sanacora G, Mason GF, Rothman DL, Krystal JH. Increased occipital cortex GABA concentrations in depressed patients after therapy with selective serotonin reuptake inhibitors. *Am J Psychiatry*. (2002) 159:663–5. doi: 10.1176/appi.ajp.159.4.663
12. Yoon JH, Maddock RJ, Rokem A, Silver MA, Minzenberg MJ, Ragland JD, et al. GABA concentration is reduced in visual cortex in schizophrenia and correlates with orientation-specific surround suppression. *J Neurosci*. (2010) 30:3777–81. doi: 10.1523/JNEUROSCI.6158-09.2010
13. Hashimoto K. Emerging role of glutamate in the pathophysiology of major depressive disorder. *Brain Res Rev*. (2009) 61:105–23. doi: 10.1016/j.brainresrev.2009.05.005
14. Humer E, Probst T, Pieh C. Metabolomics in psychiatric disorders: what we learn from animal models. *Metabolites*. (2020) 10:72. doi: 10.3390/metabo10020072
15. Veronezi BP, Moffa AH, Carvalho AF, Galhardoni R, Simis M, Bensenor IM, et al. Evidence for increased motor cortical facilitation and decreased inhibition in atypical depression. *Acta Psychiatr Scand*. (2016) 134:172–82. doi: 10.1111/acps.12565
16. Moffa AH, Martin D, Alonzo A, Bennabi D, Blumberger DM, Bensenor IM, et al. Efficacy and acceptability of transcranial direct current stimulation (tDCS) for major depressive disorder: An individual patient data meta-analysis. *Prog Neuropsychopharmacol Biol Psychiatry*. (2020) 99:109836. doi: 10.1016/j.pnpbp.2019.109836
17. Fotiou F, Fountoulakis KN, Iacovides A, Kaprinis G. Pattern-reversed visual evoked potentials in subtypes of major depression. *Psychiatry Res*. (2003) 118:259–71. doi: 10.1016/S0165-1781(03)00097-0
18. Normann C, Schmitz D, Furmaier A, Doing C, Bach M. Long-term plasticity of visually evoked potentials in humans is altered in major depression. *Biol Psychiatry*. (2007) 62:373–80. doi: 10.1016/j.biopsych.2006.10.006
19. Bubl E, Kern E, Ebert D, Riedel A, Tebartz van Elst L, Bach M. Retinal dysfunction of contrast processing in major depression also apparent in cortical activity. *Eur Arch Psychiatry Clin Neurosci*. (2015) 265:343–50. doi: 10.1007/s00406-014-0573-x
20. Qi X, Fan H, Yang X, Chen Y, Deng W, Guo W, et al. High level of pattern glare in major depressive disorder. *BMC Psychiatry*. (2019) 19:415. doi: 10.1186/s12888-019-2399-6
21. Boulogne S, Andre-Obadia N, Kimiskidis VK, Ryvlin P, Rheims S. Cortico-cortical and motor evoked potentials to single and paired-pulse stimuli: an exploratory transcranial magnetic and intracranial electric brain stimulation study. *Hum Brain Mapp*. (2016) 37:3767–78. doi: 10.1002/hbm.23274
22. Schloemer N, Lenz M, Tegenthoff M, Dinse HR, Hoffken O. Parallel modulation of intracortical excitability of somatosensory and visual cortex by the gonadal hormones estradiol and progesterone. *Sci Rep*. (2020) 10:22237. doi: 10.1038/s41598-020-79389-6
23. Huang Z, Zhan S, Chen C, Li N, Ding Y, Hou Y, et al. The effect of insomnia on cortical excitability in patients with generalized anxiety disorder. *Front Psychiatry*. (2018) 9:755. doi: 10.3389/fpsyt.2018.00755
24. Hoffken O, Grehl T, Dinse HR, Tegenthoff M, Bach M. Paired-pulse behavior of visually evoked potentials recorded in human visual cortex using patterned paired-pulse stimulation. *Exp Brain Res*. (2008) 188:427–35. doi: 10.1007/s00221-008-1374-0
25. Hoffken O, Lenz M, Hockelmann N, Dinse HR, Tegenthoff M. Noradrenergic modulation of human visual cortex excitability assessed by paired-pulse visual-evoked potentials. *Neuroreport*. (2012) 23:707–11. doi: 10.1097/WNR.0b013e3283565fb4
26. Odom JV, Bach M, Brigell M, Holder GE, McCulloch DL, Mizota A, et al. ISCEV standard for clinical visual evoked potentials: (2016 update). *Doc Ophthalmol*. (2016) 133:1–9. doi: 10.1007/s10633-016-9553-y

27. di Russo F, Pitzalis S, Spitoni G, Aprile T, Patria F, Spinelli D, et al. Identification of the neural sources of the pattern-reversal VEP. *Neuroimage*. (2005) 24:874–86. doi: 10.1016/j.neuroimage.2004.09.029
28. di Russo F, Martinez A, Sereno MI, Pitzalis S, Hillyard SA. Cortical sources of the early components of the visual evoked potential. *Hum Brain Mapp*. (2002) 15:95–111. doi: 10.1002/hbm.10010
29. Foxe JJ, Strugstad EC, Sehatpour P, Molholm S, Pasieka W, Schroeder CE, et al. Parvocellular and magnocellular contributions to the initial generators of the visual evoked potential: high-density electrical mapping of the "C1" component. *Brain Topogr*. (2008) 21:11–21. doi: 10.1007/s10548-008-0063-4
30. Hoffken O, Stude P, Lenz M, Bach M, Dinse HR, Tegenthoff M. Visual paired-pulse stimulation reveals enhanced visual cortex excitability in migraineurs. *Eur J Neurosci*. (2009) 30:714–20. doi: 10.1111/j.1460-9568.2009.06859.x
31. Prescott IA, Dostrovsky JO, Moro E, Hodaie M, Lozano AM, Hutchison WD. Reduced paired pulse depression in the basal ganglia of dystonia patients. *Neurobiol Dis*. (2013) 51:214–21. doi: 10.1016/j.nbd.2012.11.012
32. Evans BJ, Stevenson SJ. The pattern glare test: a review and determination of normative values. *Ophthalmic Physiol Opt*. (2008) 28:295–309. doi: 10.1111/j.1475-1313.2008.00578.x
33. Han D, Wegrzyn J, Bi H, Wei R, Zhang B, Li X. Practice makes the deficiency of global motion detection in people with pattern-related visual stress more apparent. *PLoS One*. (2018) 13:e0193215. doi: 10.1371/journal.pone.0193215
34. Braithwaite JJ, Broglia E, Brincat O, Stapley L, Wilkins AJ, Takahashi C. Signs of increased cortical hyperexcitability selectively associated with spontaneous anomalous bodily experiences in a nonclinical population. *Cogn Neuropsychiatry*. (2013) 18:549–73. doi: 10.1080/13546805.2013.768176
35. Concerto C, Lanza G, Cantone M, Pennisi M, Giordano D, Spampinato C, et al. Different patterns of cortical excitability in major depression and vascular depression: a transcranial magnetic stimulation study. *BMC Psychiatry*. (2013) 13:300. doi: 10.1186/1471-244X-13-300
36. Maeda F, Keenan JP, Pascual-Leone A. Interhemispheric asymmetry of motor cortical excitability in major depression as measured by transcranial magnetic stimulation. *Br J Psychiatry*. (2000) 177:169–73. doi: 10.1192/bjp.177.2.169
37. Khedr EM, Elserogy Y, Fawzy M, Elnoaman M, Galal AM. Global cortical hypoexcitability of the dominant hemisphere in major depressive disorder: a transcranial magnetic stimulation study. *Neurophysiol Clin*. (2020) 50:175–83. doi: 10.1016/j.neucli.2020.02.005
38. Levinson AJ, Fitzgerald PB, Favalli G, Blumberger DM, Daigle M, Daskalakis ZJ. Evidence of cortical inhibitory deficits in major depressive disorder. *Biol Psychiatry*. (2010) 67:458–64. doi: 10.1016/j.biopsych.2009.09.025
39. Aurora SK, Welch KM, Al-Sayed F. The threshold for phosphenes is lower in migraine. *Cephalalgia*. (2003) 23:258–63. doi: 10.1046/j.1468-2982.2003.00471.x
40. Hoffken O, Lenz M, Sczesny-Kaiser M, Dinse HR, Tegenthoff M. Phosphene thresholds correlate with paired-pulse suppression of visually evoked potentials. *Brain Stimul*. (2013) 6:118–21. doi: 10.1016/j.brs.2012.02.004
41. Bellingham MC, Walmsley B. A novel presynaptic inhibitory mechanism underlies paired pulse depression at a fast central synapse. *Neuron*. (1999) 23:159–70. doi: 10.1016/S0896-6273(00)80762-X
42. Wehr M, Zador AM. Synaptic mechanisms of forward suppression in rat auditory cortex. *Neuron*. (2005) 47:437–45. doi: 10.1016/j.neuron.2005.06.009
43. Stude P, Lenz M, Hoffken O, Tegenthoff M, Dinse H. A single dose of lorazepam reduces paired-pulse suppression of median nerve evoked somatosensory evoked potentials. *Eur J Neurosci*. (2016) 43:1156–60. doi: 10.1111/ejn.13224
44. Werhahn KJ, Kunesch E, Noachtar S, Benecke R, Classen J. Differential effects on motorcortical inhibition induced by blockade of GABA uptake in humans. *J Physiol*. (1999) 517(Pt 2):591–7. doi: 10.1111/j.1469-7793.1999.0591t.x
45. Porter JT, Nieves D. Presynaptic GABAB receptors modulate thalamic excitation of inhibitory and excitatory neurons in the mouse barrel cortex. *J Neurophysiol*. (2004) 92:2762–70. doi: 10.1152/jn.00196.2004
46. Cantone M, Bramanti A, Lanza G, Pennisi M, Bramanti P, Pennisi G, et al. Cortical plasticity in depression. *ASN Neuro*. (2017) 9:1759091417711512. doi: 10.1177/1759091417711512
47. von Gersdorff H, Schneggenburger R, Weis S, Neher E. Presynaptic depression at a calyx synapse: the small contribution of metabotropic glutamate receptors. *J Neurosci*. (1997) 17:8137–46. doi: 10.1523/JNEUROSCI.17-21-08137.1997
48. David-Jurgens M, Dinse HR. Effects of aging on paired-pulse behavior of rat somatosensory cortical neurons. *Cereb Cortex*. (2010) 20:1208–16. doi: 10.1093/cercor/bhp185
49. Anagnostou E, Vikelis M, Tzavellas E, Ghika A, Kouzi I, Evdokimidis I, et al. Photophobia in primary headaches, in essential blepharospasm and in major depression. *Int J Neurosci*. (2017) 127:673–9. doi: 10.1080/00207454.2016.1231185
50. Friberg TR, Bremer RW, Dickinsen M. Diminished perception of light as a symptom of depression: further studies. *J Affect Disord*. (2008) 108:235–40. doi: 10.1016/j.jad.2007.10.021
51. Fam J, Rush AJ, Haaland B, Barbier S, Luu C. Visual contrast sensitivity in major depressive disorder. *J Psychosom Res*. (2013) 75:83–6. doi: 10.1016/j.jpsychores.2013.03.008
52. Sartucci F, Borghetti D, Bocci T, Murri L, Orsini P, Porciatti V, et al. Dysfunction of the magnocellular stream in Alzheimer's disease evaluated by pattern electroretinograms and visual evoked potentials. *Brain Res Bull*. (2010) 82:169–76. doi: 10.1016/j.brainresbull.2010.04.001
53. Sartucci F, Orlandi G, Bonuccelli U, Borghetti D, Murri L, Orsini C, et al. Chromatic pattern-reversal electroretinograms (ChPERGs) are spared in multiple system atrophy compared with Parkinson's disease. *Neurol Sci*. (2006) 26:395–401. doi: 10.1007/s10072-006-0522-1
54. Bocci T, Nasini F, Caleo M, Restani L, Barloscio D, Ardolino G, et al. Unilateral application of cathodal tDCS reduces transcallosal inhibition and improves visual acuity in amblyopic patients. *Front Behav Neurosci*. (2018) 12:109. doi: 10.3389/fnbeh.2018.00109
55. Bocci T, Caleo M, Restani L, Barloscio D, Rossi S, Sartucci F. Altered recovery from inhibitory repetitive transcranial magnetic stimulation (rTMS) in subjects with photosensitive epilepsy. *Clin Neurophysiol*. (2016) 127:3353–61. doi: 10.1016/j.clinph.2016.06.013
56. Bocci T, Caleo M, Giorli E, Barloscio D, Maffei L, Rossi S, et al. Transcallosal inhibition dampens neural responses to high contrast stimuli in human visual cortex. *Neuroscience*. (2011) 187:43–51. doi: 10.1016/j.neuroscience.2011.04.050
57. Matsuoka K, Yasuno F, Kishimoto T, Yamamoto A, Kiuchi K, Kosaka J, et al. Microstructural Differences in the Corpus Callosum in Patients With Bipolar Disorder and Major Depressive Disorder. *J Clin Psychiatry*. (2017) 78:99–104. doi: 10.4088/JCP.15m09851
58. Ran S, Zuo Z, Li C, Yin X, Qu W, Tang Q, et al. Atrophic Corpus Callosum Associated with Altered Functional Asymmetry in Major Depressive Disorder. *Neuropsychiatr Dis Treat*. (2020) 16:1473–82. doi: 10.2147/NDT.S245078
59. Bocci T, Caleo M, Tognazzi S, Francini N, Briscese L, Maffei L, et al. Evidence for metaplasticity in the human visual cortex. *J Neural Transm (Vienna)*. (2014) 121:221–31. doi: 10.1007/s00702-013-1104-z

Conflict of Interest: The authors declare that the research was conducted in the absence of any commercial or financial relationships that could be construed as a potential conflict of interest.

Publisher's Note: All claims expressed in this article are solely those of the authors and do not necessarily represent those of their affiliated organizations, or those of the publisher, the editors and the reviewers. Any product that may be evaluated in this article, or claim that may be made by its manufacturer, is not guaranteed or endorsed by the publisher.

frontiers | Frontiers in Psychiatry

ORIGINAL RESEARCH
published: 08 April 2022
doi: 10.3389/fpsyt.2022.870079

Predictability of Seasonal Mood Fluctuations Based on Self-Report Questionnaires and EEG Biomarkers in a Non-clinical Sample

Yvonne Höller[1], Maeva Marlene Urbschat[2], Gísli Kort Kristófersson[2] and Ragnar Pétur Ólafsson[3]*

[1] Faculty of Psychology, University of Akureyri, Akureyri, Iceland, [2] School of Health Sciences, University of Akureyri, Akureyri, Iceland, [3] Faculty of Psychology, University of Iceland, Reykjavík, Iceland

Induced by decreasing light, people affected by seasonal mood fluctuations may suffer from low energy, have low interest in activities, experience changes in weight, insomnia, difficulties in concentration, depression, and suicidal thoughts. Few studies have been conducted in search for biological predictors of seasonal mood fluctuations in the brain, such as EEG oscillations. A sample of 64 participants was examined with questionnaires and electroencephalography in summer. In winter, a follow-up survey was recorded and participants were grouped into those with at least mild (N = 18) and at least moderate (N = 11) mood decline and those without self-reported depressive symptoms both in summer and in winter (N = 46). A support vector machine was trained to predict mood decline by either EEG biomarkers alone, questionnaire data from baseline alone, or a combination of the two. Leave-one-out-cross validation with lasso regularization was used with logistic regression to fit a model. The accuracy for classification for at least mild/moderate mood decline was 77/82% for questionnaire data, 72/82% for EEG alone, and 81/86% for EEG combined with questionnaire data. Self-report data was more conclusive than EEG biomarkers recorded in summer for prediction of worsening of depressive symptoms in winter but it is advantageous to combine EEG with psychological assessment to boost predictive performance.

Keywords: seasonal mood fluctuations, EEG biomarkers, cognitive vulnerabilities, prediction, machine learning, seasonal affective disorder winter depression

OPEN ACCESS

Edited by:
Masahiro Takamura, Shimane University, Japan

Reviewed by:
Peter Watson, University of Cambridge, United Kingdom
Axel Steiger, Ludwig Maximilian University of Munich, Germany

****Correspondence:***
Yvonne Höller
yvonne@unak.is

Specialty section:
This article was submitted to Computational Psychiatry, a section of the journal Frontiers in Psychiatry

Received: *05 February 2022*
Accepted: *14 March 2022*
Published: *08 April 2022*

Citation:
Höller Y, Urbschat MM, Kristófersson GK and Ólafsson RP (2022) Predictability of Seasonal Mood Fluctuations Based on Self-Report Questionnaires and EEG Biomarkers in a Non-clinical Sample. Front. Psychiatry 13:870079. doi: 10.3389/fpsyt.2022.870079

1. INTRODUCTION

Winter depression is the most common form of seasonal affective disorder (SAD), characterized by depressive symptoms in winter and remission in spring (1, 2). As compared to major depressive disorder, patients with SAD exhibit atypical depression symptoms, especially hyperphagia and hypersomnia, but scoring lower in interpersonal sensitivity and rejection avoidance (3). The condition has been reported in many regions of the world, with 1–3% of adults being affected in temperate climates (4), and being highly relevant in nordic countries with prevalence rates over 12%, e.g., in Alaska, Denmark, Norway, and Siberia (5–8). The disorder was reported to be occurring over many years for most patients, with full remission within about 9 years being found in 14% of cases, only (9), although a later study suggests higher remission rates (10). Several reports criticize the defined borders between SAD, major depression, and the DSM criteria

(11, 12). However, SAD is usually not as severe as major depression but still has socioeconomic implications as it negatively impacts quality of life and was suggested to increase the probability of unemployment (13). Because of the relatively short period of SAD compared to the typical duration of psychotherapy and the long time it takes for serotonine-selective reuptake inhibitors to show an effect it might be wise to start prevention at least two months before onset of symptoms. In turn, this requires early identification of people at-risk to develop SAD. Therefore, the search for characteristics and biomarkers with a high predictive value as well as a better understanding of vulnerabilities for SAD is highly warranted. If we could identify cognitive vulnerabilities for SAD, specific designs for psychotherapy could be developed. Both, the early estimation of the risk for SAD, and suggestions toward an effective psychotherapeutic intervention would be a tremendous improvement of mental health care.

Several attempts have been undertaken to predict sad mood in winter based on psychological examinations or biomarkers measured in summer. The best indicator for a likely occurrence of depression in winter is the individual's report on prior experience of seasonal symptoms, e.g., according to the seasonal pattern assessment questionnaire (SPAQ, 14). The SPAQ is still the most used instrument for estimating subjective experience of seasonal occurrence of depression symptoms. Furthermore, psychological research has considered cognitive vulnerabilities. In patients with SAD, there is a bias toward remembering words of negative valence more likely in the winter than in the summer (15). In addition to remembering negative words more likely, patients with depression also create more false memories than healthy controls and perceive even positive items with a less positive, i.e., more negative valence (16). Individuals with SAD estimate future negative events as more likely to happen (17), and demonstrate a high level of automatic thoughts and dysfunctional assumptions (18) as well as negative attributions (19). Such psychological features, i.e., cognitive-behavioral factors such as increased rumination, automatic thoughts and dysfunctional attitudes were shown to be not only indicative (20) but even predictive for SAD (21, 22). A ruminative response style as measured in fall predicts symptom severity in winter (21, 22) which indicates a predisposition for ruminative processes being mediators for SAD symptomatology. When examining rumination, it is crucial to distinguish between trait and state rumination (23), as induced state rumination predicts negative affect, independent of the extent of trait rumination (24). Recent theoretical accounts (25) and empirical evidence also suggest that increases in state negative affect may subsequently set of increases in state ruminative thinking in an automatic and habit-like way, and are associated with symptoms of depression and depression status (26, 27). Emotional responses were also combined with attention demands in an emotional Stroop task to predict subsequent levels of symptomatology with tests in winter and follow-up in summer (28). Performance in the Stroop task relies on cognitive flexibility, and cognitive flexibility is impaired in depression (29, 30).

Biomarkers have mainly been derived from major biological hypotheses regarding circadian rhythms, neurotransmitters, and molecular genetics (31). Circadian rhythms were suggested to play a role in SAD, where according to the phase-delay hypothesis the patient's circadian rhythm is delayed relative to the daily routine of sleeping/resting and waking/activity (4). Well in line with this hypothesis, SAD is especially common in younger subsamples who are often evening chronotypes, and in general in people with evening chronotype (32). Moreover, in patients with SAD, depressive symptoms are typically worse in the morning (33).

Another approach to identify vulnerability to SAD and, thus, find predictive biomarkers is based on neuroimaging. Since the brainstem is affected by photoperiodic changes, a large study used magnetic resonance imaging to determine a relation between brainstem volume and low mood (34). In this study, a relationship between photoperiod, volume of whole brainstem, pons and medulla, and low mood and anhedonia was found only in women, but not in men. Women with the short 5-HTTLPR genotype who suffered from SAD showed higher 5-HTT levels compared to those who did not suffer from SAD in the ventral striatum, right orbitofrontal cortex, middle frontal gyrus, left supramarginal gyrus, left precentral gyrus, and left postcentral gyrus and this difference was most pronounced during winter (35).

However, as neuroimaging and genetic testing is not widely available, the most convenient approach to predict SAD is a psychological examination. In order to boost accuracy of prediction a physiological marker could be added that is easily obtained at low cost. The electroencephalogram (EEG) is a method that is traditionally used in clinical and research settings, but commercial products for brain computer interfacing, e.g., in the gaming industry raise the hope that soon there will be easy-to-use systems available that can combine the lightweight design of devices used in non-professional settings with the accuracy needed for clinical and research questions. Indeed, it was demonstrated by a limited number of EEG studies in northern countries that EEG-biomarkers correlate with the absence of daylight and with midnight sun, and factors such as responsiveness of the brain to lighting conditions but also sleep were discussed to be the source of this variance (36, 37). The EEG is also indicative for depression and variants of it (38, 39). The earlier mentioned valence effects of memorized visual stimuli are detectable in the EEG (40), further suggesting top-down attentional modulation of emotional memory bias. Broadband lower absolute EEG-power was found in patients with major depression disorder (41), but especially in the theta (42, 43) and alpha frequency band and especially in the frontal cortex (41, 44–47). The prefrontal cortex is also involved in rumination (48–50). Interestingly, beta and alpha power varies with seasons (51, 52), and so does frontal alpha asymmetry (53). Abnormalities in beta and alpha power as well as frontal alpha asymmetry are also specific for SAD (54–58).

In this study, we aim to identify biomarkers in the EEG which, when measured in summer, allow prediction of increased depressive symptoms in winter. We aim to combine these biomarkers with personal characteristics, depressive symptoms, emotional reactivity (mood induction in an experimental task), and cognitive vulnerabilities such as rumination tendencies,

thoughts and beliefs, and habitual characteristics of negative thinking to answer the question whether it is beneficial to add EEG biomarkers to prediction models for depressive mood in winter.

2. METHODS

2.1. Ethics

We obtained prior approval from the Icelandic National Bioethics Committee on May 28th 2019 (study number 19-090-V1). All investigators signed a non-disclosure contract and written informed consent was obtained prior to inclusion from all participants.

2.2. Research Setting

The study was carried out as a collaboration between the University of Akureyri and the University of Iceland. The baseline assessment was performed between July and September 2019 in the EEG laboratory of the Faculty of Psychology at the University of Akureyri. Follow-up assessments were conducted in October, January, and April 2020 *via* online questionnaires and telephonic reminders conducted by the team at the Faculty of Psychology, University of Iceland. For the purpose of the present manuscript, only data from the follow-up in January was analyzed.

2.3. Recruitment

Participants were recruited *via* email to students at the University of Akureyri, as well as *via* advertisement in social media, directing interested individuals to a webform. Inclusion criteria were the minimum age of 18 years, proficiency in Icelandic, and the ability to give informed consent for participation. For completion of all follow-ups participants were remunerated with a voucher of 4,000 ISK for a local shop.

2.4. Procedure

Baseline assessment took about 120 min. After participants completed informed consent, a digital questionnaire, consisting of 72 custom made questions and the questionnaires as listed in Section 2.5 were answered by the participants. While participants answered the questions, the EEG was mounted with electrolyte containing a mild abrasive in order to achieve impedances below 10 kΩ. Before recordings began participants were shown the effect of muscle movement on the EEG and consequently instructed to keep movements to a minimum and asked to refrain from talking during the recordings.

The first two conditions were resting state measurements which lasted for 3 min, with eyes open and eyes closed respectively, and with the computer screen turned off. The other tasks were presented on a screen based on the Psychtoolbox in Matlab. First, in the emotional picture learning task participants were shown 60 pictures from the OASIS database (59), balanced for negative, neutral, and positive valence and low, medium, and high arousal. Participants were informed that in the subsequent task they would be asked to recall the pictures shown. The task required to indicate whether each picture represented spring, summer, fall, or winter by pressing a corresponding key on the keyboard with the right hand to ensure attention and to prime seasonal concepts. Pictures were shown with an inter-trial interval of 1 s and a variance of 0–10 screen flip intervals during which a fixation cross was presented. All pictures were shown for at least 2 s and otherwise until participants responded *via* key press. In the following the picture recall task participants were asked to freely recall and name pictures seen in the previous task. Their answers were noted by the experimenter. Subsequently, a recognition condition involved presentation of the pictures from the picture learning task but randomly intermixed with 60 new images, again balanced for valence and arousal. Participants were asked to indicate *via* keys on the keyboard whether each picture was new or previously seen. Timing of the presentation was the same as in the learning condition. The next condition was a Stroop task where participants were asked to indicate the font color of words displayed on the stimulus computer by pressing a correspondingly colored key on a keyboard. There were 105 congruent trials and 210 incongruent trials, presented in a randomized order, with an inter-trial interval of 1 s and a variance of 0–10 screen flip intervals during which a central fixation cross was presented.

In the final condition, the rumination task, participants received a printed three part form containing questions about their current emotional state and the brief state of rumination inventory (BSRI, 23). All instructions were given verbally through headphones and partly additionally on a screen. Firstly, participants completed part A on the form containing one question on their current emotional state and the 8-item BSRI. Next, an 8 min musical piece was played in order to evoke temporary sadness or dysphoria, and participants asked to freely experience any emotions they might feel. We used a musical excerpt from Prokofiev's "Russia Under the Mongolian Yoke," remastered at half speed. Prior research has shown that this approach can effectively cause a transient dysphoric mood (60–62).

Immediately after the song had finished, participants answered the forms' part B containing one question on their current emotional state. They were then instructed to wait in silence for 5 min for a challenging cognitive task. However, no cognitive task followed but the waiting period served as a free contemplation time in anticipation of a task. In the third and final part of the rumination task participants answered an 8-item BRSI and one question on their current emotional state.

On the day following the EEG recording, participants began the baseline measurement of the studies follow-up phase which consisted of a 4 day long measurement period using the mobile application ExperienceSampler (63) with which mood fluctuations over the course of a day along with activity level, fatigue, and rumination was assessed in questionnaire form. Five measurements were taken at random times each day between 9:00 a.m. and 21:00 p.m.

The three subsequent follow-up intervals, conducted in October, January, and April, had the same form as the baseline measurement with the addition of a 48 question internet survey. The internet survey consisted of the following questionnaires: Patients Health Questionnaire, Rumination Responses Scale-short form, Perceived Stress Scale, and Depression Anxiety

Stress Scales (see Section 2.5 for more details). In addition, the survey included questions on recent traveling and use of any depression treatments.

2.5. Questionnaires

We assessed subjective perception of mood and behavioral change with seasons with the seasonal pattern assessment questionnaire (SPAQ, 1). It includes 8-items regarding seasonal change in mood and behavior, pattern of seasonal change, reactivity to different climatic and atmospheric conditions and whether and to what extent those changes affect the individual (64). We used the Icelandic version, which performed compared to a diagnostic clinical interview with a sensitivity of 94%, a specificity of 73%, and a combined positive predictive value of 45% for SAD and subsyndromal SAD (65). The questionnaire is acknowledged as an effective screening tool for SAD, with an internal consistency of α=0.74–0.81 and a test-retest reliability of 0.76 at an interval of 2 months.

As mentioned in Section 2.4, we examined state rumination before and after mood induction with the 8-item BSRI (23). The Ruminative Responses Scale-short form (RRS, 66) was used to measure the degree of trait rumination.

The habit index of negative thinking (HINT, 67) measures in 12 items habitual characteristics of negative thoughts (i.e., automaticity, lack of intent and awareness, difficult to control). In addition, we measured mood with the Patient Health Questionnaire (PHQ, 68), sleep problems with the Bergen Insomnia Scale (BIS, 69), depression, anxiety, and stress with the Depression Anxiety Stress Scale (DASS, 70), positive attitudes toward ruminative thinking with the Positive Beliefs in Rumination Scale (PBRS, 71), chronotype by using the Morningness Eveningness Questionnaire—Revised (MEQ-R, 72), and to what extent people were following habits with the Creature of Habit Scale (COHS, 73). Participants were also asked about their age, gender, handedness, first language, body weight, and height from which we calculated the body mass index (BMI).

Furthermore, we asked about optimism, nutrition, mental or neurological diseases, regularly taken medication, current tiredness, bed- and waketime the night before the experiment, exercise, phase of menstrual cycle in women, and weather, but we did not include the respective data into the present manuscript.

All questionnaires and written materials used in this study were in Icelandic, therefore, only participants who were fluent in Icelandic were recruited for the study. This was ensured by having all recruitment material in Icelandic. In Iceland, 96% of the population speaks Icelandic, with 12.4% of the population being foreign citizens in 2019 according to Statistics Iceland (www.statice.is).

2.6. EEG Recording and Preprocessing

EEG data was recorded with software and hardware from Brain Products GmbH (Gilching, Germany) at a sampling rate of 1,000 Hz with an EasyCap in an extended 10-20 system, including 32 electrodes (Fp1, Fp2, F3, F4, C3, C4, P3, P4, O1, O2, F7, F8, T7, T8, P7, P8, Fz, Cz, Pz, FC1, FC2, CP1, CP2, FC5, FC6, CP5, CP6, FT9, FT10, TP9, TP10) referenced to FCz and grounded at AFz. In addition, lower vertical electrooculogram was recorded.

EEG-data was pre-processed with BrainVision Analyzer (Brain Products GmbH, Gilching, Germany). First, band-pass filters from 0.5 to 48 Hz with zero-phase shift Butterworth filters were applied. Then, data was re-referenced to common average. Next, an independent component analysis (ICA) was used such that in the backtransform the signals that include eye-blink artifacts would be removed (infomax restricted algorithm). Finally, remaining artifacts were identified and excluded automatically by the following standard thresholds: check gradient (maximal allowed voltage step: 50 microvolt/ms), check difference (maximal allowed difference of values in intervals of 200 ms: 200 microvolt), lowest activity allowed in 100 ms intervals: 0.5 microvolts. The artifacts that were identified in this way were excluded with a time-range of $\pm$200 ms.

The EEG recorded during 3 min of rest with eyes open, 3 min rest with eyes closed, the whole recall session, and the last 3 min out of 5 min of sad mood induction was segmented into equal-sized epochs of 2 s. From the learning and recall conditions 1 s starting at stimulus presentation were extracted, and they were processed separately for negative, neutral, and positive pictures for learning, and in addition for old and new pictures for recognition. From the Stroop task 500 ms from stimulus onset, and congruent and incongruent conditions were processed separately. Thus, in total, there were 15 conditions extracted from the EEG experiment that were submitted to feature extraction.

2.7. Feature Extraction

For all of these conditions and each segment we extracted features based on the multivariate autoregressive model with the functions mvfreqz.m and mvar.m from the BioSig toolbox (74) with model order 10, and partial correlation estimation with unbiased covariance estimates (75), which is an accurate estimation method (76). The multivariate parameters in the frequency domain that can be derived from these transfer functions were computed for 1 Hz frequency steps between 1 and 48 Hz. Only data from electrodes F3, F4, C3, C4, P3, P4, O1, O2, F7, F8, T7, T8, P7, P8, Fz, Cz, Pz was used. The measures that were extracted were the following:

- **Spectrum:** The auto- and the cross-spectrum, which is the Fourier transform of the cross-covariance function (77).
- **Direct causality:** Direct causality as developed by (78); this measure is not computed for each frequency.
- **Transfer function:** Related to the non-normalized directed transfer function (79).
- **Transfer function polynomial:** Frequency transform of a polynomial describing the transfer function. It is related to coherence as the absolute of the squared transfer function polynomial represents the non-normalized partial directed coherence (79).
- **Real valued coherence:** The real part of the complex-valued coherence (80) is an ordinary coherence (74).
- **Complex coherence:** The imaginary part of the complex-valued coherence (80).

- **Partial coherence:** Designed by (81) it's concept is that one channel drives the other channels if the first channel explains or accounts for the linear relation between the other two.
- **Partial directed coherence:** An extended concept of partialized coherence, measuring the relative strength of the direct interaction between pairs of signals (82).
- **Partial directed coherence factor:** An intermediate step between partial coherence and partial directed coherence by adding directionality to partial coherence and including instantaneous causality (82).
- **Generalized partial directed coherence:** In contrast to partial directed coherence, generalized partial directed coherence is invariant against scaling differences between signals (83, 84).
- **Directed transfer function:** Represents information that flows from one region to another over many possible alternative pathways (85).
- **Direct directed transfer function:** Extends directed transfer function by separating direct from indirect causal relations of signals (86).
- **Full frequency directed transfer function:** In contrast to directed transfer function, the full frequency directed transfer function is normalized with respect to all the frequencies in the predefined frequency interval (86).
- **Geweke's Granger Causality:** A bivariate version (87) of Geweke's Granger Causality (88).

Finally, we also included the power-spectral density as a feature, representing band-pass power in 1 Hz frequency steps from 1 to 48 Hz.

2.8. Features and Feature Combinations for Machine Learning

For classification, we considered three situations:

- EEG features only; each EEG feature was used individually, i.e., we conducted for each of the 15 conditions classification with each of the 16 feature vectors as described in Section 2.7.
- Questionnaire data only; We classified participants by a feature vector including their total scores in PBRS, the three mood measurements in the mood induction task individually and also the difference between the first two and the latter two, and the two rumination measurements with the BSRS in the mood induction task, SPAQ global seasonality score, HINT, DASS stress and anxiety, RSS brooding and reflection, sex, age, education, body mass index (BMI) calculated by the participants indication of height and weight, MEQ, BIS, and COHS.
- A combination of each of the EEG features and conditions with the questionnaire feature vector.

2.9. Grouping for Prediction Modeling

For machine learning we divided the sample into the group experiencing depressive symptoms in winter and a control group. For defining the borders between these groups we used the diagnostic criteria according to the DASS-21 subscale for no depression, mild depression, and moderate depression (70). The control group included participants which were not depressed at baseline in summer as well as at winter follow up in January, i.e., showing <10 points on the DASS-21 depression scale at both timepoints. For prediction we did two analyses, for mild and moderate decline of mood, i.e., increase of depressive symptoms. Both groups showed no depression at baseline (DASS-21 depression scale <10). The group with at least mild increase of depressive symptoms comprised those participants who would show a depression score on the DASS-21 of at least 10 points at follow up in January. The group with moderate increase of depressive symptoms comprised those participants who would show a depression score on the DASS-21 of at least 14 points at follow up. Thus, the group with at least mild increase of depressive symptoms overlapped with the group of at least moderate increase of depressive symptoms.

2.10. Machine Learning and Statistical Analysis

We used leave-one-out cross-validation, thus, a model was fitted for each participant to all participants but the left-out participant using the Matlab function *fitclinear* using a logistic regression as learner. The fitting procedure was performed with a regularization term strength λ of 10^{-11}.We used lasso (L1) penalty for the composition of the objective function for minimization from the sum of the average loss function, with sparse reconstruction by Separable Approximation (SpaRSA) as objective function minimization technique and 10^{-8} as gradient tolerance. The initial linear coefficient estimates were set to zeros as initial values and the learning rate was constant.

Lasso regularization reduces the number of predictors, identifies important predictors and selects among redundant predictors, which is important in the high-dimensional feature space of EEG biomarkers extracted with the multivariate autoregressive model. As λ increases, the number of nonzero components of β increases. Intuitively, the predictor coefficients β are therefore indicative for each feature's importance to the model and were therefore reported graphically with the results to demonstrate which brain regions/frequency range contributed most to the prediction of worsening of depressive symptoms in winter.

Machine learning results were gathered overall as accuracy (% of correctly classified individuals overall), specificity (% of correctly classified individuals who did not show depressive symptoms in winter, i.e., correctly classified controls), sensitivity (% of correctly classified individuals with depressive symptoms in winter), positive predictive value (PPV; % of predicted cases actually developing depressive symptoms in winter), and negative predictive value (NPV, % of not predicted actually not developing depressive symptoms in winter).

For psychological self-report questionnaires we calculated means and standard deviations separately for controls and the overall group of people experiencing mild or moderate decline of mood in winter, as well as Mann–Whitney *U*-tests comparing these two groups at baseline. A non-parametric test was chosen because the questionnaire data is ordinal, so parametric tests should not be used.

TABLE 1 | Self-reported characteristics of the control group and group with worsening of depressive symptoms in winter at baseline.

	Controls		Depressive symptoms		*U*-test	
Scale	**Mean**	**SD**	**Mean**	**SD**	**z**	***p***
Age	33.61	18.21	31.61	16.92	0.11	0.91
BIS	−20.13	25.52	−10.03	34.37	−1.43	0.15
BMI	26.06	6.79	24.82	11.37	−0.01	0.99
BSRI t1	219.52	154.05	287.25	182.97	−1.32	0.19
BSRI t3	228.56	191.93	285.8	221.62	−0.72	0.47
COHS	78.46	21.26	75.06	42.92	−1.33	0.18
DASS anxiety	2.87	4.23	8.56	6.78	−3.59	<0.001
DASS depression	2.87	2.72	3.67	3.01	−0.93	0.35
DASS stress	8.3	6.42	15	8.35	−2.88	<0.001
Education	2.8	1.36	2.78	1.31	−0.14	0.89
GSS	5.57	4.75	9.94	4.45	−3.26	<0.001
HINT	29.67	17.22	54.5	17.02	−4.22	<0.001
MEQ	35.24	36.08	21.04	41.98	1.16	0.25
Mood t1	109.95	34.35	103.98	23.21	1.46	0.14
Mood t2	77.24	38.6	82.94	41.38	−0.49	0.63
Mood t3	95.08	35.22	92.97	27.78	0.43	0.67
PBRS	23.11	6.27	24.33	3.94	−0.84	0.4
PHQ	4.11	3.09	7.83	3.55	-3.63	<0.001
RRS brooding	8.04	2.62	9.78	3.84	−2.08	0.04
RRS reflection	8.2	3.11	9.89	2.93	−2.01	0.04

BIS, Bergen insomnia scale; BMI, body mass index; BSRI, brief state rumination inventory; t1, before mood induction; t3, after mood induction; COHS, creature of habit scale; DASS, depression, anxiety, stress scales; GSS, global seasonality score; HINT, habit index for negative thinking; MEQ, morningness-eveningness questionnaire; mood, emotional state; t2, after sad music; PBRS, positive believes in rumination scale; PHQ, patient health questionnaire; RRS, ruminative response scale; SYM, group with at least mild depressive symptoms in winter.

3. RESULTS

3.1. Sample

A total of 119 participants were recruited for this study and participated in the baseline assessment in summer 2019. Among them, 89 participated in the second follow-up in winter (January 2020). After exclusion of missing data in four participants, 18 participants showed no depression at baseline and mild worsening from baseline to follow up, and 11 among those showed moderate worsening of depression from baseline to follow-up. The control group of 46 participants was free of depression at baseline as well as at follow up.

The control group sample consisted of 40 women and 6 men, while the group of participants with at least mild increase of depressive symptoms consisted of 16 women and 2 men. The odds ratio for gender to suffer from SAD is 1.8 according to (89) justifying an overall overrepresentation of female participants in our sample.

In the sample of controls/participants with at least mild worsening of depressive symptoms in winter, 8.70/0% had completed primary education, only 47.83/50% had higher education entrance qualification, 2.17/11.11% had learned a trade, 28.26/22.22% had completed undergraduate education at a university, and 10.87/11.11% had completed master or doctoral level education at a university. The native language was Icelandic in 95% of the sample, however, all participants were fluent in Icelandic.

Descriptive statistics for the self-report questionnaires, separately for the two groups as well as results from Mann-Whitney U-tests comparing the two samples are shown in **Table 1**. For some measures there is evidence that the groups are very inhomogenous. For chronotype, as measured by the MEQ, in the group experiencing at least mild depressive symptoms, the standard deviation is twice the mean, whereas for symptoms of insomnia, as measured by the BIS, the standard deviation is even three times as large as the mean.

3.2. Classification Results

For questionnaire data, only, accuracy was 76.56 for prediction of mild and 82.46 for moderate depressive symptoms in winter, with a specificity (accuracy to classify control group participants correctly) of 78.26 and 84.78 and sensitivity (accuracy to identify participants who experience depressive symptoms in winter) of 72.22 and 72.73. Positive predictive value (PPV) for at least mild depressive symptoms in winter was 56.52 and for moderate depressive symptoms it was 53.33. Negative predictive value (NPV) for at least mild depressive symptoms in winter was 87.80 and 92.86 for moderate depressive symptoms in winter. **Figure 1** shows the predictor coefficients β for each feature's importance to the model for the prediction of worsening of depressive symptoms in winter for the two classifications. Relative importance of features were highly consistent for the two prediction models. Predictive for worsening of depressive

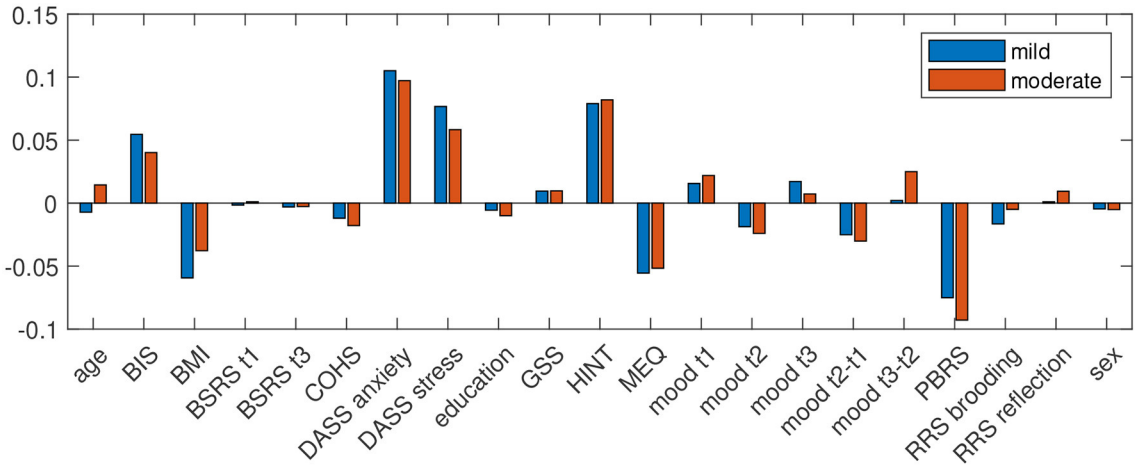

FIGURE 1 | Predictor coefficients β for each questionnaires' importance to the model for the prediction of worsening of depressive symptoms in winter to at least mild (DASS depression score $\geq$10; blue) and moderate (DASS depression score $\geq$14; red) extent.

symptoms in winter were low quality of sleep, low BMI, anxiety, stress, habits of negative thinking, eveningness, and a low degree of positive believes in rumination, measured in summer.

When using EEG data, this resulted in 15 times 16 classifications for each condition and each feature used. EEG alone for prediction of mild depressive symptoms in winter yielded best classification accuracy for partial directed coherence factor extracted during the Stroop task's matching condition (accuracy: 71.88, specificity: 80.43, sensitivity: 50). Because sensitivity was at guessing level it is safe to not interpret these results any further. PPV for at least mild depressive symptoms in winter was 50, NPV was 80.43.

EEG alone for prediction of moderate depressive symptoms in winter yielded best classification accuracy for directed transfer function during recognition of previously seen positive pictures (accuracy: 82.46, specificity: 97.83, sensitivity: 73.33%), PPV for at least moderate depressive symptoms in winter was 88.99, NPV was 93.88. Predictor coefficients β shown in **Figure 2**, showing which frequencies and brain connections were most predictive. The directed transfer function showed a broader network with interhemispheric frontal connections in the delta to theta range, frontocentral connections in the alpha-gamma range, and temporo- and fronto-occipital connections in the alpha-gamma range. Autocorrelations were also identified to be predictive right frontal, central, bilateral temporal, and right occipital in the alpha-gamma range.

EEG combined with questionnaire data yielded best classification accuracy for prediction of at least mild depressive symptoms in winter with an accuracy of 81.25 (specificity: 82.61; sensitivity: 77.78; PPV: 63.64; NPV: 90.48). This result was obtained by most biomarkers (i.e., partial directed coherence, coherence, directed transfer function, direct directed transfer function, full frequency directed transfer function, partial coherence, partial directed coherence factor, generalized partial directed coherence, and power spectral density) and most conditions (i.e., EEG data recorded during eyes closed or open, learning of neutral or positive images, recognition of recognition of new positive pictures, recognition of previously seen neutral or positive pictures, rumination, Stroop match and non-match condition). Predictor coefficients β for directed transfer function are given in **Figure 3** extracted during rest with eyes open. Again, frontal and central regions were strongly involved, across all frequency ranges. Most of the frontal involvement was autocorrelative, except for a frontocentral correlation in the higher beta and gamma range. Central correlation was highly pronounced for central-left area to all other areas in all frequency bands.

EEG combined with questionnaire data yielded best classification accuracy for prediction of at least moderate depressive symptoms in winter with an accuracy of 85.96 (specificity: 86.96; sensitivity: 81.82; PPV: 60.01; NPV: 95.24). This result was obtained by several biomarkers (i.e., spectrum, partial directed coherence, directed transfer function, partial coherence, generalized partial directed coherence) and most conditions (i.e., EEG data recorded during eyes open, learning of negative, neutral or positive images, recognition of new positive pictures, rumination, Stroop match, and non-match condition). Predictor coefficients β for directed transfer function are given in **Figure 4**, showing where in the brain oscillatory activity in a certain frequency band was most predictive for directed transfer function during rumination. Most areas were highly involved in this prediction, but fronto-occipital and temporo occipital connections on the left hemisphere dominated the higher beta-gamma range.

4. DISCUSSION

In this study we aimed to identify biomarkers in the EEG and self-reported characteristics which, when measured in

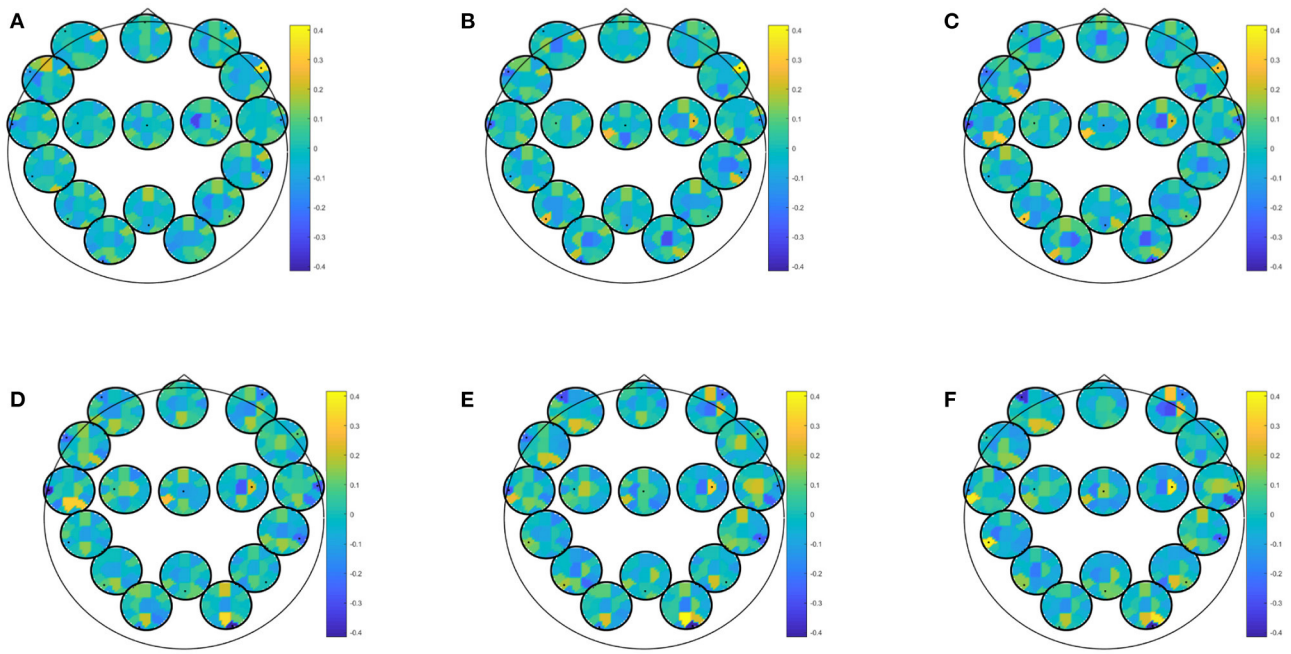

FIGURE 2 | Predictor coefficients β for directed transfer function (DTF) extracted during recognition of positive pictures. Coefficients indicate importance of the feature to the model for prediction of at least moderate depressive symptoms in winter. **(A)** Delta 1–4 Hz, **(B)** Theta 5–7 Hz, **(C)** Alpha 8–12 Hz, **(D)** Beta 13–20 Hz, **(E)** Beta 2 21–30 Hz, **(F)** Gamma 31–48 Hz.

summer, can be used for accurate prediction of whether an individual will suffer from worsening of depressive symptoms in winter. We found that indeed, a combination of cognitive aspects and EEG biomarkers allows for a better prediction than the cognitive aspects or EEG biomarkers alone. Prediction accuracy was better for prediction of at least moderate depressive symptoms as compared to mild depressive symptoms, which could be due to the clearer distinction of the group with at least moderate depressive symptoms from the control group. However, since these two groups overlap, and since the statistical power is limited for the group with at least moderate depressive symptoms we limit the discussion to the sample of at least mild depressive symptoms in winter.

4.1. Self-Reported Characteristics and Cognitive Vulnerabilities

We found that low quality of sleep, low BMI, anxiety, stress, habits of negative thinking, eveningness, and a low degree of positive believes in rumination, measured in summer predicted worsening of depressive symptoms in winter.

Insomnia or, more generally, sleep problems were related to SAD in earlier studies (5, 32, 90–96). In our sample, the variance of symptoms of insomnia was very high in the group who would develop at least mild depressive symptoms in winter, suggesting that there might be different subgroups, reflecting different paths of vulnerability that is based on the different factors causing insomnia, being either physiological or cognitive-behavioral in nature. On the one hand, increased rumination is linked to insomnia (97), but on the other hand, insomnia might be the symptom of a physiological vulnerability. It has been suggested that in some cases, insomnia could be treated by administration of melatonin (98), and there have also been attempts to treat SAD by melatonin (99, 100). Further evidence links melatonin to the serotonergic system, which in turn, is linked to depression, anxiety, and stress (101). Melatonin treatment alters the expression of genes of serotonergic neurotransmission in a mouse model of SAD (102). More evidence points to involvement of major monoamine neurotransmitters serotonin, norepinephrine, and dopamine in SAD (103). Therefore, biochemical markers such as cortisol awakening response as a marker for hypothalamic-pituitary-adrenal axis function (104) and serotonin-transporter binding (105) have been suggested. In line with the daily rhythm of cortisol, eveningness was found previously to be strongly related to seasonality and SAD (32, 95, 96). Being a serotonin-transporter-linked polymorphic region (5-HTTLPR) short allele carrier was found to be a risk factor for developing SAD (1). A genotype-dependent increase in winter of serotonin transporter binding was found to be specific for patients with winter depression (105). However, although the level of serotonin transporter binding is comparable between healthy controls and patients with winter depression during summer, the patient group shows a lower increase from summer to winter as compared to controls (105). The link to the serotonergic system is supported by predictability of relapse during winter based on depressive symptoms during tryptophan depletion in summer

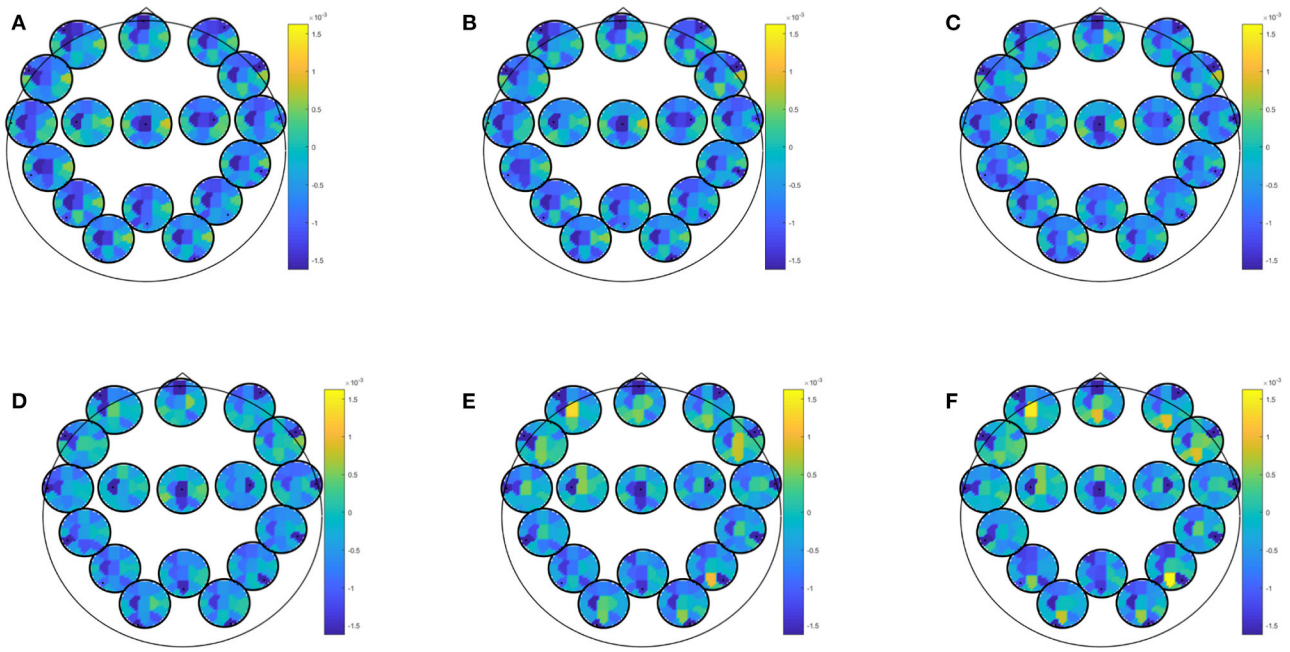

FIGURE 3 | Predictor coefficients β for questionnaire data combined with directed transfer function (DTF) extracted during rest with eyes open. Coefficients indicate importance of the feature to the model for prediction of at least mild depressive symptoms in winter. **(A)** Delta 1–4 Hz, **(B)** Theta 5–7 Hz, **(C)** Alpha 8–12 Hz, **(D)** Beta 13–20 Hz, **(E)** Beta 2 21–30 Hz, **(F)** Gamma 31–48 Hz.

(106). Possibly related to neurotransmitter systems, low vitamin D3 levels where also suggested to predict depressive symptoms increase from fall to winter (107).

The fact that melatonin was suggested as a treatment for SAD (99, 100) is closely linked to the finding that melatonin levels underly a strict circadian rhythm. Administrating melatonin at a specific time of the day triggers a change in sleeping time, which can help to ameliorate the so-called social jetlag of the evening chronotype (108). As chronotype changes with age toward more morningness, the vulnerability for anxiety and depression also decreases (109). Also in our sample, the late chronotype was predictive for depressive symptoms in winter, although the group showed a large variance in the respective score. This detail could point toward considerable inhomogeneity of the group in terms of their chronotype. Although being an evening chronotype is a risk factor for developing depressive symptoms in winter, also individuals reporting to be morning or neutral chronotypes in summer might suffer from mood decline during the dark season. Conclusions to be drawn on this end are limited, but it was also reported that chronotype self-reports do vary with the season especially in individuals with winter depression more morningness was measured in the summer than in the winter (110).

Although controls and individuals who would develop at least mild depressive symptoms in winter did not differ significantly by BMI in summer, the highly negative beta values as indicated in **Figure 1** suggest that a low BMI in summer can serve as a predictor for worsening of depressive symptoms in winter. The similarity in BMI between the two groups in summer indicates that the relationship between BMI and vulnerability to seasonal mood fluctuations is not too large. The relation between body weight and SAD has been investigated previously. A higher BMI at baseline was found to predict treatment outcome of 6 weeks light treatment (111). As emotional eating and weight gain are associated with SAD (112), our finding seems to be unexpected. However, it was shown recently that the self reported seasonal changes in weight is related to lower plasma adiponectin levels, an indicator for metabolic dysregulation (113). Therefore, it might be that the difference in weight between summer and winter is more relevant, and a lower BMI in summer might be indicative for a larger weight gain. However, this is pure speculation and needs to be addressed in future studies.

Habits of negative thinking were assessed with the HINT, where negative thoughts are characterized by automaticity, lack of intent and awareness, and difficulty to control them (67). HINT scores predicted mood worsening in winter, whereas trait ruminative brooding and reflective pondering did not. This may suggest that people experiencing their self-focused negative thoughts as being triggered more automatically and without intent, awareness, or control, are specifically vulnerable to experience upward shifts in symptoms of depression during winter.

Individuals with SAD also seem to estimate future negative events as more likely to happen (17), which is a concept

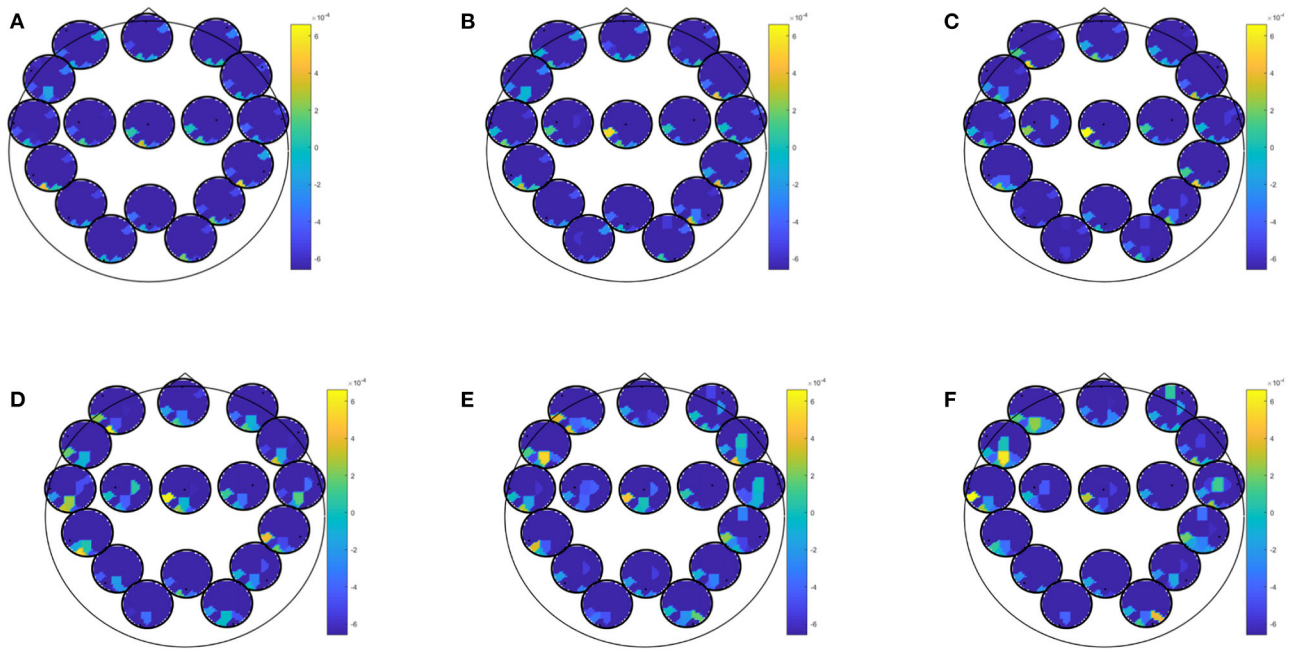

FIGURE 4 | Predictor coefficients β for questionnaire data combined with directed transfer function (DTF) extracted during rumination. Coefficients indicate importance of the feature to the model for the prediction of at least moderate worsening of depressive symptoms in winter. **(A)** Delta 1–4 Hz, **(B)** Theta 5–7 Hz, **(C)** Alpha 8–12 Hz, **(D)** Beta 13–20 Hz, **(E)** Beta 2 21–30 Hz, **(F)** Gamma 31–48 Hz.

closely related to the habit of negative thinking as well as the optimism-pessimism as assessed in our study. Endorsement of emotional adjectives and a negative attributional style are elevated in patients with SAD (114). However, in contrast to our data it was previously reported that these cognitive aspects could not be used to predict later symptom levels (114). Also, countering our expectations, a lower score in summer on the PBRS indicated a higher risk for worsening of depressive symptoms in winter. Prior research showed that rumination is linked to depression (115) and that positive beliefs about rumination are associated with ruminative thinking, mediating further a negative association with positive affect (116). While prior research suggests that increased rumination are predictive for SAD (21), we could not confirm this relationship. In our data, a negative predictor coefficient for the PBRS suggested that positive beliefs in rumination would rather protect from worsening of depressive symptoms in winter. This finding is difficult to explain but warrants further investigation. The first four items of the Icelandic translation (e.g., "I need to consider things to realize how I feel.") of the scale could have been rather interpreted as being indicative for a positive attitude toward being considerate, which might indeed be a protective factor instead of a risk factor.

Furthermore, patients with prior experience of SAD show depressive affect in response to low light intensity stimuli (21), another indicator for emotional responses to darkness. However, as this result is based on prior experience of SAD, it might rather be due to reactivated memories of sad mood during the dark period rather than an indicator for emotional response style. In line with the potential role of memory mechanisms, autobiographical memory style was examined in winter in individuals with SAD (117). It was found that the number of overly general memories that were generated in response to positive cues was related to symptom levels measured during remission in summer (117).

4.2. EEG Biomarkers

Best results for EEG alone were of guessing level for sensitivity for the prediction of mild depressive symptoms in winter, which might indicate that a mild increase of depressive symptoms can not be predicted by EEG features.

EEG alone yielded sensitivity at guessing level for prediction of mild depressive symptoms in winter, which should, therefore, not be interpreted any further.

The frontal involvement and EEG-results in general were more reliable when EEG was combined with self-report questionnaires, emphasizing further the superiority of self-report data over EEG biomarkers. Specifically, the high stability across biomarkers and conditions indicates that EEG combined with self-report data can contribute reliable additional information, but the consideration of the self-report data is crucial.

EEG studies have identified some likely structural and activational irregularities being candidates for the neurological mechanisms involved in depressive tendencies and depressive mechanisms such as rumination. For example, lowered alpha

activity in the prefrontal cortex is thought to predict higher tendency to ruminate (50). Inefficient information transfer from the left dorsolateral prefrontal cortex to the temporal lobe structures might be critical for trait rumination (48). The involvement of the frontal cortex as well as the alpha frequency range points to the role of cognitive control over negative thoughts. High alpha power is acknowledged to reflect active inhibition (118). Therefore, the involvement of alpha activity in the left hemisphere can be interpreted as reduced cortical activity. It was theorized that hypoactivation of the left frontal area leads to ruminative tendencies and consequently to negative emotional interpretation (119). The frontal cortex is also involved in cognitive flexibility (120), which has been reported to be impaired in individuals with depression (29). Specifically, in negative emotional contexts individuals with major depressive disorders were suggested to exhibit ruminative and negative automatic thoughts because they lack cognitive flexibility (30).

An abnormal activation in the lower left frontal cortex has been found to be critical regarding depressed individuals' tendency to pay greater attention to adverse stimuli (41, 47). Abnormalities in the activation or structure of the circuitry of emotion, which includes the prefrontal cortex, anterior cingulate cortex, hippocampus and amygdala have been suggested to underlie depressive disorders (121). In addition to the alpha abnormalities, abnormal synchronization of theta and beta oscillations was suggested to reflect unstable states of cognitive processing, specifically of working memory in individuals with depression (122). Analysing EEG band power beyond the alpha frequency range provided evidence which suggests that decreased theta power might be important during rumination (42), and lower power in the theta range, as well as alpha frequency band has been noted during mind wandering (43). Moreover, increases in the delta band are generally related to pathology such as mental slowing in dementia (123), as well as psychopathology (124).

4.3. Limitations

It was recently shown that machine learning performance in neuroimaging studies of depression overestimate the classification accuracy in small sample sizes (125). This is a well-known phenomenon when the number of features describing the samples exceeds the size of the sample and is not limited to neuroimaging but any modality where the feature vector is long. Certainly, our sample size is very small, as well, especially for the prediction or moderate depressive symptoms in winter. Therefore, we have chosen lasso regularization as an approach to address those problems of high-dimensional feature spaces. The prediction of moderate depressive symptoms might lead to better results because the distinction of the sample is clearer, but it might also be related to the small sample size. Therefore, we chose to not interpret those results any further. However, we also have to question whether the sample composition is representative as women outnumbered men. Although SAD is also more common among women, we had an even higher proportion of women participating in the study, which limits generalizability of the results to men. Future studies need to recruit a significant proportion of men in order to allow for interpretation of gender-specific results.

Another restriction of the study is that it was performed in Iceland, where lighting conditions might not be representative for regions with a lower latitude.

We also need to re-emphasize that this study included the GSS score as a measure for seasonality and other self-assessment questionnaires to measure depressive symptoms, while a clinical interview was not part of the study to ascertain diagnosis of SAD. Therefore, we limit our conclusions to results from a non-clinical sample with mild or moderate depressive symptoms in winter.

4.4. Future Directions

The use of psychological characteristics to predict seasonal affective occurrence can be extended to prediction of treatment response. Negative attributional style predicted poor response to pharmacotherapy in nonseasonal depression but not in seasonal affective disorder (19). It was also reported that psychic anxiety was related to response to light therapy while somatic anxiety was rather related to a negative outcome (126), and that atypical symptoms of depression predict responsiveness to light therapy (127). There have also been attempts to predict treatment outcome in order to determine which patients might respond to light therapy (128), or which patients respond better to light therapy, cognitive-behavioral therapy (129), or a combination of the two (130). When patients exhibit cognitive vulnerabilities, the use of cognitive behavior therapy might be crucial (130). In a later study cognitive vulnerability could not be replicated as prognostic or prescriptive predictor of outcome of light- vs. cognitive behavior therapy, but greater morningness was associated with less severe post-treatment depression in both treatment approaches (129). It is possible that EEG-biomarkers could add to the planning of personalized treatment of patients with SAD, both by helping to select the most appropriate therapy alongside with the consideration of cognitive vulnerabilities, as well as by identifying individuals at risk in order to initiate preventative treatment in a timely manner.

5. CONCLUSIONS

Depressive symptoms in winter may be predicted by self-report questionnaire data better than by EEG measures collected in summer, but the combination of features from both domains is advantageous and leads to higher prediction accuracy.

Our findings on relevant EEG biomarkers emphasize the importance of frontal brain regions in the vulnerability for depressive symptoms in winter as well as a broad frequency range.

DATA AVAILABILITY STATEMENT

The raw data supporting the conclusions of this article will be made available by the authors, without undue reservation.

ETHICS STATEMENT

We obtained prior approval from the Icelandic National Bioethics Committee on May 28th 2019 (study number

19-090-V1). All investigators signed a non-disclosure contract and written informed consent was obtained prior to inclusion from all participants. The patients/participants provided their written informed consent to participate in this study.

AUTHOR CONTRIBUTIONS

YH and RÓ: conceptualization. YH (for EEG): methodology. RÓ (for psychological tests): methodology. YH: software, validation, formal analysis, investigation, data curation, visualization, project administration, and funding acquisition. YH, GK, RÓ, and MU: writing—original draft preparation and writing—review and editing. YH and GK: supervision. All authors have read and agreed to the published version of the manuscript.

FUNDING

The study was supported by the Research Fund of the University of Akureyri (RHA, R1916).

ACKNOWLEDGMENTS

We thank the BS-students Anna Hjálmeig Hannesdóttir, Elísa Huld Jensdóttir, Máni Snær Hafdísarson, Sara Teresa Jónsdóttir, Sigrún María Óskarsdóttir, and Silja Hlín Magnúsdóttir at the Faculty of Psychology of the University of Akureyri for recruitment and data collection. Also many thanks to the BS-students of the Faculties of Psychology at the University of Iceland, Anton Nikolaisson Haydarly, Elena Arngrímsdóttir, Erla Ástrós Jónsdóttir, Inga Valdís Tómasdóttir, María Lovísa Breiðdal, and Ólöf Traustadóttir to sample the data in the online part of the study.

REFERENCES

1. Rosenthal NE, Sack DA, Gillin JC, Lewy AJ, Goodwin FK, Davenport Y, et al. Seasonal affective disorder. A description of the syndrome and preliminary findings with light therapy. *Arch Gen Psychiatry*. (1984) 41:72–80. doi: 10.1001/archpsyc.1984.01790120076010
2. Magnússon A, Partonen T. The diagnosis, symptomatology, and epidemiology of seasonal affective disorder. *CNS Spectr*. (2005) 10:625–34. doi: 10.1017/S1092852900019593
3. Tam EM, Lam RW, Robertson HA, Stewart JN, Yatham LN, Zis AP. Atypical depressive symptoms in seasonal and non-seasonal mood disorders. *J Affect Disord*. (1997) 44:39–44. doi: 10.1016/S0165-0327(97)01447-X
4. Magnússon A, Boivin D. Seasonal affective disorder: an overview. *Chronobiol Int*. (2003) 20:189–207. doi: 10.1081/CBI-120019310
5. Booker JM, Hellekson CJ, Putilov AA, Danilenko KV. Seasonal depression and sleep disturbances in Alaska and Siberia: a pilot study. *Arctic Med Res*. (1991) (Suppl.):281–4.
6. Levine ME. Seasonal symptoms in the sub-Arctic. *Mil Med*. (1995) 160:110–4. doi: 10.1093/milmed/160.3.110
7. Dam H, Jakobsen K, Mellerup E. Prevalence of winter depression in Denmark. *Acta Psychiatr Scand*. (1998) 97:1–4. doi: 10.1111/j.1600-0447.1998.tb09954.x
8. Magnússon A. An overview of epidemiological studies on seasonal affective disorder. *Acta Psychiat Scand*. (2000) 101:176–84. doi: 10.1046/j.0902-4441.2000.x
9. Schwartz PJ, Brown C, Wehr TA, Rosenthal NE. Winter seasonal affective disorder: a follow-up study of the first 59 patients of the National Institute of Mental Health Seasonal Studies Program. *Am J Psychiatry*. (1996) 153:1028–36. doi: 10.1176/ajp.153.8.1028
10. Cléry-Melin ML, Gorwood P, Friedman S, Even C. Stability of the diagnosis of seasonal affective disorder in a long-term prospective study. *J Affect Disord*. (2018) 227:353–7. doi: 10.1016/j.jad.2017.11.014
11. Dittmann V, Elster K, Graw P, Wirz-Justice A. Seasonal affective disorder: are the DSM-III-R criteria valid? *Psychopathology*. (1994) 27:291–7. doi: 10.1159/000284886
12. Thompson C, Raheja SK, King EA. A follow-up study of seasonal affective disorder. *Br J Psychiatry*. (1995) 167:380–4. doi: 10.1192/bjp.167.3.380
13. Tefft N. Mental health and employment: the SAD story. *Econ Hum Biol*. (2012) 10:242–55. doi: 10.1016/j.ehb.2011.08.006
14. Murray G, Allen NB, Trinder J. A longitudinal investigation of seasonal variation in mood. *Chronobiol Int*. (2001) 18:875–91. doi: 10.1081/CBI-100107522
15. Jensen CG, Hjordt LV, Stenbæk DS, Andersen E, Back SK, Lansner J, et al. Development and psychometric validation of the verbal affective memory test. *Memory*. (2016) 24:1208–23. doi: 10.1080/09658211.2015.1087573
16. Yeh ZT, Hua MS. Effects of depressive disorder on false memory for emotional information. *Depress Anxiety*. (2009) 26:456–63. doi: 10.1002/da.20453
17. Dalgleish T, Golden AMJ, Yiend J, Dunn BD. Differential predictions about future negative events in seasonal and non-seasonal depression. *Psychol Med*. (2010) 40:459–65. doi: 10.1017/S0033291709990638
18. Hodges S, Marks M. Cognitive characteristics of seasonal affective disorder: a preliminary investigation. *J Affect Disord*. (1998) 50:59–64. doi: 10.1016/S0165-0327(98)00034-2
19. Levitan RD, Rector NA, Bagby RM. Negative attributional style in seasonal and nonseasonal depression. *Am J Psychiatry*. (1998) 155:428–30. doi: 10.1176/ajp.155.3.428
20. Rohan KJ, Nillni YI, Mahon JN, Roecklein KA, Sitnikov L, Haaga DAF. Cognitive vulnerability in moderate, mild, and low seasonality. *J Nerv Ment Dis*. (2011) 199:961–70. doi: 10.1097/NMD.0b013e3182392948
21. Rohan K, Sigmon S, Dorhofer D. Cognitive-behavioral factors in seasonal affective disorder. *J Consult Clin Psychol*. (2003) 71:22–30. doi: 10.1037/0022-006X.71.1.22
22. Enggasser JL, Young MA. Cognitive vulnerability to depression in seasonal affective disorder: predicting mood and cognitive symptoms in individuals with seasonal vegetative changes. *Cogn Ther Res*. (2007) 31:3–21. doi: 10.1007/s10608-006-9076-z
23. Marchetti I, Mor N, Chiorri C, Koster EHW. The Brief State Rumination Inventory (BSRI): validation and psychometric evaluation. *Cogn Ther Res*. (2018) 42:447–60. doi: 10.1007/s10608-018-9901-1
24. Moberly N, Watkins E. Ruminative self-focus and negative affect: an experience sampling study. *J Abnorm Psychol*. (2008) 117:314–23. doi: 10.1037/0021-843X.117.2.314
25. Watkins ER, Nolen-Hoeksema S. A habit-goal framework of depressive rumination. *J Abnorm Psychol*. (2014) 123:24–34. doi: 10.1037/a0035540
26. Hjartarson KH, Snorrason I, Bringmann LF, Ögmundsson BE, Ólafsson RP. Do daily mood fluctuations activate ruminative thoughts as a mental habit? Results from an ecological momentary assessment study. *Behav Res Ther*. (2021) 140:103832. doi: 10.1016/j.brat.2021.103832
27. Hjartarson KH, Snorrason I, Bringmann LF, Ólafsson RP. *Automaticity as a Vulnerability to Depression: Daily Mood-Reactive Rumination and Early-Life Stress in People With- and Without Depression History*. (2021). Available online at: doi: 10.31234/osf.io/n3dah
28. Spinks H, Dalgleish T. Attentional processing and levels of symptomatology in Seasonal Affective Disorder (SAD): a preliminary longitudinal study. *J Affect Disord*. (2001) 62:229–32. doi: 10.1016/S0165-0327(00)00155-5
29. Murphy FC, Michael A, Sahakian BJ. Emotion modulates cognitive flexibility in patients with major depression. *Psychol Med*. (2012) 42:1373–82. doi: 10.1017/S0033291711002418

30. Deveney CM, Deldin PJ. A preliminary investigation of cognitive flexibility for emotional information in major depressive disorder and non-psychiatric controls. *Emotion*. (2006) 6:429–37. doi: 10.1037/1528-3542.6.3.429
31. Sohn CH, Lam RW. Update on the biology of seasonal affective disorder. *CNS Spectr*. (2005) 10:635–46. doi: 10.1017/S109285290001960X
32. Höller Y, Gudjónsdottir BE, Valgeirsdóttir SK, Heimisson GT. The effect of age and chronotype on seasonality, sleep problems, and mood. *Psychiatry Res*. (2021) 297:113722. doi: 10.1016/j.psychres.2021.113722
33. Graw P, Kräuchi K, Wirz-Justice A, Pöldinger W. Diurnal variation of symptoms in seasonal affective disorder. *Psychiatry Res*. (1991) 37:105–11. doi: 10.1016/0165-1781(91)90110-B
34. Majrashi NA, Ahearn TS, Waiter GD. Brainstem volume mediates seasonal variation in depressive symptoms: a cross sectional study in the UK Biobank cohort. *Sci Rep*. (2020) 10:3592. doi: 10.1038/s41598-020-60620-3
35. Nørgaard M, Ganz M, Svarer C, Fisher PM, Churchill NW, Beliveau V, et al. Brain networks implicated in seasonal affective disorder: a neuroimaging pet study of the serotonin transporter. *Front Neurosci*. (2017) 11:614. doi: 10.3389/fnins.2017.00614
36. Soroko SI, Rozhkov VP, Bekshaev SS. Features of seasonal reorganizations of the central mechanisms of regulation in children northerners with different levels of social risk. *Ross Fiziol Zh Im I M Sechenova*. (2013) 99:1435–49.
37. Demin DB, Poskotinova LV, Krivonogova EV. Comparison of electroencephalogram changes at cardiovascular training in adolescents of subpolar and polar northern territories. *Ross Fiziol Zh Im I M Sechenova*. (2014) 100:128–38.
38. de Freitas SB, Marques AA, Bevilaqua MC, de Carvalho MR, Ribeiro P, Palmer S, et al. Electroencephalographic findings in patients with major depressive disorder during cognitive or emotional tasks: a systematic review. *Braz J Psychiatry*. (2016) 38:338–46. doi: 10.1590/1516-4446-2015-1834
39. Höller Y, Uhl A, Bathke A, Thomschewski A, Butz K, Nardone R, et al. Reliability of EEG measures of interaction: a paradigm shift is needed to fight the reproducibility crisis. *Front Hum Neurosci*. (2017) 11:441. doi: 10.3389/fnhum.2017.00441
40. Kuchinke L, Fritsch N, Müller CJ. Evaluative conditioning of positive and negative valence affects P1 and N1 in verbal processing. *Brain Res*. (2015) 1624:405–13. doi: 10.1016/j.brainres.2015.07.059
41. Ding X, Yue X, Zheng R, Bi C, Li D, Yao G. Classifying major depression patients and healthy controls using EEG, eye tracking and galvanic skin response data. *J Affect Disord*. (2019) 251:156–61. doi: 10.1016/j.jad.2019.03.058
42. Shim M, Im CH, Lee SH. Disrupted cortical brain network in post-traumatic stress disorder patients: a resting-state electroencephalographic study. *Transl Psychiatry*. (2017) 7:e1231. doi: 10.1038/tp.2017.200
43. Atchley R, Klee D, Oken B. EEG frequency changes prior to making errors in an easy stroop task. *Front Hum Neurosci*. (2017) 11:521. doi: 10.3389/fnhum.2017.00521
44. Gollan JK, Hoxha D, Chihade D, Pflieger ME, Rosebrock L, Cacioppo J. Frontal alpha EEG asymmetry before and after behavioral activation treatment for depression. *Biol Psychol*. (2014) 99:198–208. doi: 10.1016/j.biopsycho.2014.03.003
45. Kaiser AK, Gnjezda MT, Knasmüller S, Aichhorn W. Electroencephalogram alpha asymmetry in patients with depressive disorders: current perspectives. *Neuropsychiatr Dis Treat*. (2018) 14:1493–504. doi: 10.2147/NDT.S137776
46. Park Y, Jung W, Kim S, Jeon H, Lee SH. Frontal alpha asymmetry correlates with suicidal behavior in major depressive disorder. *Clin Psychopharm Neurosci*. (2019) 17:377–87. doi: 10.9758/cpn.2019.17.3.377
47. Cisler JM, Koster EHW. Mechanisms of attentional biases towards threat in anxiety disorders: an integrative review. *Clin Psychol Rev*. (2010) 30:203–16. doi: 10.1016/j.cpr.2009.11.003
48. Ferdek MA, van Rijn CM, Wyczesany M. Depressive rumination and the emotional control circuit: an EEG localization and effective connectivity study. *Cogn Affect Behav Neurosci*. (2016) 16:1099–113. doi: 10.3758/s13415-016-0456-x
49. Rosenbaum D, Thomas M, Hilsendegen P, Metzger F, Häußinger F, Nuerk HC, et al. Stress-related dysfunction of the right inferior frontal cortex in high ruminators: an fNIRS study. *Neuroimage Clin*. (2018) 18:510–7. doi: 10.1016/j.nicl.2018.02.022
50. Putnam K, McSweeney L. Depressive symptoms and baseline prefrontal EEG alpha activity: a study utilizing ecological momentary assessment. *Biol Psychol*. (2008) 77:237–40. doi: 10.1016/j.biopsycho.2007.10.010
51. Machleidt W, Gutjahr L. Ultradian periodicity, diurnal and circannual rhythms in the electroencephalogram. *Fortschr Neurol Psychiatr*. (1984) 52:135–45. doi: 10.1055/s-2007-1002011
52. Barbato G, Cirace F, Monteforte E, Costanzo A. Seasonal variation of spontaneous blink rate and beta EEG activity. *Psychiatry Res*. (2018) 270:126–33. doi: 10.1016/j.psychres.2018.08.051
53. Velo JR, Stewart JL, Hasler BP, Towers DN, Allen JJB. Should it matter when we record? Time of year and time of day as factors influencing frontal EEG asymmetry. *Biol Psychol*. (2012) 91:283–91. doi: 10.1016/j.biopsycho.2012.06.010
54. Allen JJ, Iacono WG, Depue RA, Arbisi P. Regional electroencephalographic asymmetries in bipolar seasonal affective disorder before and after exposure to bright light. *Biol Psychiatry*. (1993) 33:642–6. doi: 10.1016/0006-3223(93)90104-L
55. Volf NV, Senkova NI, Danilenko KV, Putilov AA. Hemispheric language lateralization in seasonal affective disorder and light treatment. *Psychiatr Res*. (1993) 47:99–108. doi: 10.1016/0165-1781(93)90059-P
56. Teicher MH, Glod K, Ito Y. Hemispheric asymmetry of EEG and T2 relaxation time in seasonal affective disorder (SAD) pre- and post-light therapy. In: *SLTBR: Abstracts of the Annual Meeting of the Society for Light Treatment and Biological Rhythms*. Wheat Tidge, CO (1996). p. 9.
57. Passynkova N, Volf N. Seasonal affective disorder: Spatial organization of EEG power and coherence in the depressive state and in light-induced and summer remission. *Psychiatry Res*. (2001) 108:169–85. doi: 10.1016/S0925-4927(01)00122-6
58. Volf NV, Passynkova NR. EEG mapping in seasonal affective disorder. *J Affect Disord*. (2002) 72:61–9. doi: 10.1016/S0165-0327(01)00425-6
59. Kurdi B, Lozano S, Banaji MR. Introducing the open affective standardized image set (OASIS). *Behav Res Methods*. (2017) 49:457–70. doi: 10.3758/s13428-016-0715-3
60. Jarrett RB, Minhajuddin A, Borman PD, Dunlap L, Segal ZV, Kidner CL, et al. Cognitive reactivity, dysfunctional attitudes, and depressive relapse and recurrence in cognitive therapy responders. *Behav Res Ther*. (2012) 50:280–6. doi: 10.1016/j.brat.2012.01.008
61. Lau MA, Segal ZV, Williams JMG. Teasdale's differential activation hypothesis: implications for mechanisms of depressive relapse and suicidal behaviour. *Behav Res Ther*. (2004) 42:1001–17. doi: 10.1016/j.brat.2004.03.003
62. Ólafsson RP, Gudmundsdóttir SJ, Björnsdóttir TD, Snorrason I. A Test of the habit-goal framework of depressive rumination and its relevance to cognitive reactivity. *Behav Ther*. (2020) 51:474–87. doi: 10.1016/j.beth.2019.08.005
63. Thai S, Page-Gould E. ExperienceSampler: an open-source scaffold for building smartphone apps for experience sampling. *Psychol Methods*. (2017) 23:729–39. doi: 10.31234/osf.io/gxv5b
64. Murray G. The Seasonal Pattern Assessment Questionnaire as a measure of mood seasonality: a prospective validation study. *Psychiatr Res*. (2003) 120:53–9. doi: 10.1016/S0165-1781(03)00147-1
65. Magnússon A. Validation of the Seasonal Pattern Assessment Questionnaire (SPAQ). *J Affect Disord*. (1996) 40:121–9. doi: 10.1016/0165-0327(96)00036-5
66. Treynor W, Gonzalez R, Nolen-Hoeksema S. Rumination reconsidered: a psychometric analysis. *Cogn Ther Res*. (2003) 27:247–59. doi: 10.1023/A:1023910315561
67. Verplanken B, Friborg O, Wang CE, Trafimow D, Woolf K. Mental habits: metacognitive reflection on negative self-thinking. *J Pers Soc Psychol*. (2007) 92:526–41. doi: 10.1037/0022-3514.92.3.526
68. Kroenke K, Spitzer RL, Williams JB. The PHQ-9: validity of a brief depression severity measure. *J Gen Intern Med*. (2001) 16:606–13. doi: 10.1046/j.1525-1497.2001.016009606.x
69. Pallesen S, Bjorvatn B, Sivertsen NBIH, Hjornevik M, Morin CM. A new scale for measuring insomnia: the Bergen Insomnia Scale. *Percept Motor Skills*. (2008) 107:691–706. doi: 10.2466/pms.107.3.691-706
70. Lovibond PF, Lovibond SH. The structure of negative emotional states: comparison of the Depression Anxiety Stress Scales (DASS) with the beck

depression and anxiety inventories. *Behav Res Ther*. (1995) 33:335–43. doi: 10.1016/0005-7967(94)00075-U
71. Watkins E, Moulds M. Positive beliefs about rumination in depression—A replication and extension. *Pers Indiv Differ*. (2005) 39:73–82. doi: 10.1016/j.paid.2004.12.006
72. Horne JA, Ostberg O. A self-assessment questionnaire to determine morningness-eveningness in human circadian rhythms. *Int J Chronobiol*. (1976) 4:97–110. doi: 10.1037/t02254-000
73. Ersche KD, Lim TV, E WLH, Robins TW, Stochl J. Creature of habit: a self-report measure of habitual routines and automatic tendencies in everyday life. *Pers Indiv Differ*. (2017) 116:73–85. doi: 10.1016/j.paid.2017.04.024
74. Schlögl A, Brunner C. BioSig: a free and open source software library for BCI research. *Computer*. (2008) 41:44–50. doi: 10.1109/MC.2008.407
75. Marple S. *Digital Spectral Analysis With Applications*. Upper Saddle River: Prentice Hall (1987).
76. Schlögl A. A comparison of multivariate autoregressive estimators. *Signal Process*. (2006) 86:2426–9. doi: 10.1016/j.sigpro.2005.11.007
77. Murthy V. Estimation of the cross-spectrum. *Ann Math Stat*. (1963) 34:1012–21. doi: 10.1214/aoms/1177704024
78. Kaminski M, Ding M, Truccolo W, Bressler S. Evaluating causal relations in neural systems: granger causality, directed transfer function and statistical assessment of significance. *Biol Cybern*. (2001) 85:145–57. doi: 10.1007/s004220000235
79. Eichler M. On the evaluation of information flow in multivariate systems by the directed transfer function. *Biol Cybern*. (2006) 94:469–82. doi: 10.1007/s00422-006-0062-z
80. Nolte G, Bai O, Wheaton L, Mari Z, Vorbach S, Hallett M. Identifying true brain interaction from EEG data using the imaginary part of coherency. *Clin Neurophysiol*. (2004) 115:2292–307. doi: 10.1016/j.clinph.2004.04.029
81. Gersch W, Goddard G. Epileptic focus location: spectral analysis method. *Science*. (1970) 169:701–2. doi: 10.1126/science.169.3946.701
82. Baccalá L, Sameshima K. Partial directed coherence: a new concept in neural structure determination. *Biol Cybern*. (2001) 84:463–74. doi: 10.1007/PL00007990
83. Baccalá L, Takahashi D, Sameshima K. Generalized partial directed coherence. In: Sanei S, Chambers J, McWhirter J, Hicks Y, Constantinides A, editors. *Proceedings of the 15th International Conference on Digital Signal Processing (DSP)*. Wales; New York, NY: IEEE (2007). p. 162–6. doi: 10.1109/ICDSP.2007.4288544
84. Taxidis J, Coomber B, Mason R, Owen M. Assessing cortico-hippocampal functional connectivity under anesthesia and kainic acid using generalized partial directed coherence. *Biol Cybern*. (2010) 102:327–40. doi: 10.1007/s00422-010-0370-1
85. Kaminski M, Blinowska K. A new method of the description of the information flow in the brain structures. *Biol Cybern*. (1991) 65:203–10. doi: 10.1007/BF00198091
86. Korzeniewska A, Maczak M, Kaminskí M, Blinowska K, Kasicki S. Determination of information flow direction among brain structures by a modified directed transfer function (dDTF) method. *J Neurosci Methods*. (2003) 125:195–207. doi: 10.1016/S0165-0270(03)00052-9
87. Bressler S, Richter C, Chen Y, Ding M. Cortical functional network organization from autoregressive modeling of local field potential oscillations. *Stat Med*. (2007) 26:3875–85. doi: 10.1002/sim.2935
88. Geweke J. Measures of conditional linear dependence and feedback between time series. *J Am Stat Assoc*. (1982) 77:304–13. doi: 10.1080/01621459.1982.10477803
89. Magnússon A, Stefánsson JG. Prevalence of seasonal affective disorder in Iceland. *Arch Gen Psychiatry*. (1993) 50:941–6. doi: 10.1001/archpsyc.1993.01820240025002
90. Albert PS, Rosen LN, Alexander JRJ, Rosenthal NE. Effect of daily variation in weather and sleep on seasonal affective disorder. *Psychiatry Res*. (1991) 36:51–63. doi: 10.1016/0165-1781(91)90117-8
91. Anderson JL, Rosen LN, Mendelson WB, Jacobsen FM, Skwerer RG, Joseph-Vanderpool JR, et al. Sleep in fall/winter seasonal affective disorder: effects of light and changing seasons. *J Psychosom Res*. (1994) 38:323–37. doi: 10.1016/0022-3999(94)90037-X
92. Koorengevel KM, Beersma DGM, Den Boer JA, Van Den Hoofdakker RH. Sleep in seasonal affective disorder patients in forced desynchrony: an explorative study. *J Sleep Res*. (2002) 11:347–56. doi: 10.1046/j.1365-2869.2002.00319.x
93. Johnsen MT, Wynn R, Bratlid T. Is there a negative impact of winter on mental distress and sleeping problems in the subarctic: the Tromso study. *BMC Psychiatry*. (2012) 12:225. doi: 10.1186/1471-244X-12-225
94. Tonetti L, Fabbri M, Erbacci A, Martoni M, Natale V. Association between seasonal affective disorder and subjective quality of the sleep/wake cycle in adolescents. *Psychiatry Res*. (2014) 215:624–7. doi: 10.1016/j.psychres.2013.12.023
95. Borisenkov MF, Petrova NB, Timonin VD, Fradkova LI, Kolomeichuk SN, Kosova AL, et al. Sleep characteristics, chronotype and winter depression in 10-20-year-olds in northern European Russia. *J Sleep Res*. (2015) 24:288–95. doi: 10.1111/jsr.12266
96. Sandman N, Merikanto I, Määttänen H, Valli K, Kronholm E, Laatikainen T, et al. Winter is coming: nightmares and sleep problems during seasonal affective disorder. *J Sleep Res*. (2016) 25:612–9. doi: 10.1111/jsr.12416
97. Ballesio A, Ottaviani C, Lombardo C. Poor cognitive inhibition predicts rumination about insomnia in a clinical sample. *Behav Sleep Med*. (2019) 17:672–81. doi: 10.1080/15402002.2018.1461103
98. Low TL, Choo FN, Tan SM. The efficacy of melatonin and melatonin agonists in insomnia - an umbrella review. *J Psychiatr Res*. (2020) 121:10–23. doi: 10.1016/j.jpsychires.2019.10.022
99. Danilenko KV, Putilov AA. Melatonin treatment of winter depression following total sleep deprivation: waking EEG and mood correlates. *Neuropsychopharmacology*. (2005) 30:1345–52. doi: 10.1038/sj.npp.1300698
100. Nussbaumer-Streit B, Greenblatt A, Kaminski-Hartenthaler A, Van Noord MG, Forneris CA, Morgan LC, et al. Melatonin and agomelatine for preventing seasonal affective disorder. *Cochrane Database Syst Rev*. (2019) 6:CD011271. doi: 10.1002/14651858.CD011271.pub3
101. Graeff FG, Guimar aes FS, De Andrade TG, Deakin JF. Role of 5-HT in stress, anxiety, and depression. *Pharmacol Biochem Behav*. (1996) 54:129–41. doi: 10.1016/0091-3057(95)02135-3
102. Nagy AD, Iwamoto A, Kawai M, Goda R, Matsuo H, Otsuka T, et al. Melatonin adjusts the expression pattern of clock genes in the suprachiasmatic nucleus and induces antidepressant-like effect in a mouse model of seasonal affective disorder. *Chronobiol Int*. (2015) 32:447–57. doi: 10.3109/07420528.2014.992525
103. Levitan RD. The chronobiology and neurobiology of winter seasonal affective disorder. *Dialog Clin Neurosci*. (2007) 9:315–24. doi: 10.31887/DCNS.2007.9.3/rlevitan
104. Agustini B, Bocharova M, Walker AJ, Berk M, Young AH, Juruena MF. Has the sun set for seasonal affective disorder and HPA axis studies? A systematic review and future prospects. *J Affect Disord*. (2019) 256:584–93. doi: 10.1016/j.jad.2019.06.060
105. Mc Mahon B, Andersen SB, Madsen MK, Hjordt LV, Hageman I, Dam H, et al. Seasonal difference in brain serotonin transporter binding predicts symptom severity in patients with seasonal affective disorder. *Brain*. (2016) 139(Pt 5):1605–14. doi: 10.1093/brain/aww043
106. Neumeister A, Habeler A, Praschak-Rieder N, Willeit M, Kasper S. Tryptophan depletion: a predictor of future depressive episodes in seasonal affective disorder? *Int Clin Psychopharmacol*. (1999) 14:313–5. doi: 10.1097/00004850-199909000-00006
107. Kerr DCR, Zava DT, Piper WT, Saturn SR, Frei B, Gombart AF. Associations between vitamin D levels and depressive symptoms in healthy young adult women. *Psychiatry Res*. (2015) 227:46–51. doi: 10.1016/j.psychres.2015.02.016
108. Roenneberg T, Wirz-Justice A, Merrow M. Life between clocks: daily temporal patterns of human chronotypes. *J Biol Rhythms*. (2003) 18:80–90. doi: 10.1177/0748730402239679
109. Druiven SJM, Hovenkamp-Hermelink JHM, Knapen SE, Kamphuis J, Haarman BCM, Penninx BWJH, et al. Stability of chronotype over a 7-year follow-up period and its association with severity of depressive and anxiety symptoms. *Depress Anxiety*. (2020) 37:466–74. doi: 10.1002/da.22995
110. Putilov AA. State- and trait-like variation in morning and evening components of morningness-eveningness in winter depression. *Nord J Psychiatry*. (2017) 71:561–9. doi: 10.1080/08039488.2017.1353642
111. Dimitrova TD, Reeves GM, Snitker S, Lapidus M, Sleemi AR, Balis TG, et al. Prediction of outcome of bright light treatment in patients with

seasonal affective disorder: discarding the early response, confirming a higher atypical balance, and uncovering a higher body mass index at baseline as predictors of endpoint outcome. *J Affect Disord*. (2017) 222:126–32. doi: 10.1016/j.jad.2017.06.038
112. Kräuchi K, Reich S, Wirz-Justice A. Eating style in seasonal affective disorder: who will gain weight in winter? *Compr Psychiatry*. (1997) 38:80–7. doi: 10.1016/S0010-440X(97)90085-7
113. Akram F, Gragnoli C, Raheja UK, Snitker S, Lowry CA, Stearns-Yoder KA, et al. Seasonal affective disorder and seasonal changes in weight and sleep duration are inversely associated with plasma adiponectin levels. *J Psychiatr Res*. (2020) 122:97–104. doi: 10.1016/j.jpsychires.2019.12.016
114. Dalgleish T, Spinks H, Golden AM, du Toit P. Processing of emotional information in seasonal depression across different cognitive measures. *J Abnorm Psychol*. (2004) 113:116–26. doi: 10.1037/0021-843X.113.1.116
115. Takano K, Van Grieken J, Raes F. Difficulty in updating positive beliefs about negative cognition is associated with increased depressed mood. *J Behav Ther Exp Psychiatry*. (2019) 64:22–30. doi: 10.1016/j.jbtep.2019.02.001
116. Kubiak T, Zahn D, Siewert K, Jonas C, Weber H. Positive beliefs about rumination are associated with ruminative thinking and affect in daily life: evidence for a metacognitive view on depression. *Behav Cogn Psychother*. (2014) 42:568–76. doi: 10.1017/S1352465813000325
117. Dalgeish T, Spinks H, Yiend J, Kuyken W. Autobiographical memory style in seasonal affective disorder and its relationship to future symptom remission. *J Abnorm Psychol*. (2001) 110:335–40. doi: 10.1037/0021-843X.110.2.335
118. Klimesch W. EEG alpha and theta oscillations reflect cognitive and memory performance: a review and analysis. *Brain Res Rev*. (1999) 29:169–95. doi: 10.1016/S0165-0173(98)00056-3
119. Disner SG, Beevers CG, Haigh EA, Beck AT. Neural mechanisms of the cognitive model of depression. *Nat Rev Neurosci*. (2011) 12:467–77. doi: 10.1038/nrn3027
120. Kim C, Johnson NF, Cilles SE, Gold BT. Common and distinct mechanisms of cognitive flexibility in prefrontal cortex. *J Neurosci*. (2011) 31:4771–9. doi: 10.1523/JNEUROSCI.5923-10.2011
121. Davidson RJ, Pizzagalli D, Nitschke JB, Putnam K. Depression: perspectives from affective neuroscience. *Annu Rev Psychol*. (2002) 53:545–74. doi: 10.1146/annurev.psych.53.100901.135148
122. Li Y, Kang C, Wei Z, Qu X, Liu T, Zhou Y, et al. Beta oscillations in major depression -signalling a new cortical circuit for central executive function. *Sci Rep*. (2017) 7:18021. doi: 10.1038/s41598-017-18306-w
123. Cassani R, Estarellas M, San-Martin R, Fraga FJ, Falk TH. Systematic review on resting-state EEG for Alzheimer's disease diagnosis and progression assessment. *Dis Mark*. (2018) 2018:5174815. doi: 10.1155/2018/5174815
124. Newson JJ, Thiagarajan TC. EEG frequency bands in psychiatric disorders: a review of resting state studies. *Front Hum Neurosci*. (2019) 12:521. doi: 10.3389/fnhum.2018.00521
125. Flint C, Cearns M, Opel N, Redlich R, Mehler DMA, Emden D, et al. Systematic misestimation of machine learning performance in neuroimaging studies of depression. *Neuropsychopharmacology*. (2021) 46:1510–7. doi: 10.1038/s41386-021-01020-7
126. MacKenzie B, Levitan RD. Psychic and somatic anxiety differentially predict response to light therapy in women with seasonal affective disorder. *J Affect Disord*. (2005) 88:163–6. doi: 10.1016/j.jad.2005.07.003
127. Nagayama H, Sasaki M, Ichii S, Hanada K, Okawa M, Ohta T, et al. Atypical depressive symptoms possibly predict responsiveness to phototherapy in seasonal affective disorder. *J Affect Disord*. (1991) 23:185–9. doi: 10.1016/0165-0327(91)90099-E
128. Terman M, Amira L, Terman JS, Ross DC. Predictors of response and nonresponse to light treatment for winter depression. *Am J Psychiatry*. (1996) 153:1423–9. doi: 10.1176/ajp.153.11.1423
129. Camuso JA, Rohan KJ. Cognitive vulnerabilities as prognostic predictors of acute and follow-up outcomes in seasonal affective disorder treatment with light therapy or cognitive-behavioral therapy. *Cogn Ther Res*. (2020) 44:468–82. doi: 10.1007/s10608-020-10086-4
130. Sitnikov L, Rohan KJ, Evans M, Mahon JN, Nillni YI. Cognitive predictors and moderators of winter depression treatment outcomes in cognitive-behavioral therapy vs. light therapy. *Behav Res Ther*. (2013) 51:872–81. doi: 10.1016/j.brat.2013.09.010

Conflict of Interest: The authors declare that the research was conducted in the absence of any commercial or financial relationships that could be construed as a potential conflict of interest.

Publisher's Note: All claims expressed in this article are solely those of the authors and do not necessarily represent those of their affiliated organizations, or those of the publisher, the editors and the reviewers. Any product that may be evaluated in this article, or claim that may be made by its manufacturer, is not guaranteed or endorsed by the publisher.

frontiers | Frontiers in Psychiatry

ORIGINAL RESEARCH
published: 28 April 2022
doi: 10.3389/fpsyt.2022.815678

Vocal Acoustic Features as Potential Biomarkers for Identifying/Diagnosing Depression: A Cross-Sectional Study

*Qing Zhao, Hong-Zhen Fan, Yan-Li Li, Lei Liu, Ya-Xue Wu, Yan-Li Zhao, Zhan-Xiao Tian, Zhi-Ren Wang, Yun-Long Tan and Shu-Ping Tan**

Peking University HuiLongGuan Clinical Medical School, Beijing Huilongguan Hospital, Beijing, China

Background: At present, there is no established biomarker for the diagnosis of depression. Meanwhile, studies show that acoustic features convey emotional information. Therefore, this study explored differences in acoustic characteristics between depressed patients and healthy individuals to investigate whether these characteristics can identify depression.

Methods: Participants included 71 patients diagnosed with depression from a regional hospital in Beijing, China, and 62 normal controls from within the greater community. We assessed the clinical symptoms of depression of all participants using the Hamilton Depression Scale (HAMD), Hamilton Anxiety Scale (HAMA), and Patient Health Questionnaire (PHQ-9), and recorded the voice of each participant as they read positive, neutral, and negative texts. OpenSMILE was used to analyze their voice acoustics and extract acoustic characteristics from the recordings.

Results: There were significant differences between the depression and control groups in all acoustic characteristics ($p < 0.05$). Several mel-frequency cepstral coefficients (MFCCs), including MFCC2, MFCC3, MFCC8, and MFCC9, differed significantly between different emotion tasks; MFCC4 and MFCC7 correlated positively with PHQ-9 scores, and correlations were stable in all emotion tasks. The zero-crossing rate in positive emotion correlated positively with HAMA total score and HAMA somatic anxiety score ($r = 0.31$, $r = 0.34$, respectively), and MFCC9 of neutral emotion correlated negatively with HAMD anxiety/somatization scores ($r = -0.34$). Linear regression showed that the MFCC7-negative was predictive on the PHQ-9 score ($\beta = 0.90$, $p = 0.01$) and MFCC9-neutral was predictive on HAMD anxiety/somatization score ($\beta = -0.45$, $p = 0.049$). Logistic regression showed a superior discriminant effect, with a discrimination accuracy of 89.66%.

Conclusion: The acoustic expression of emotion among patients with depression differs from that of normal controls. Some acoustic characteristics are related to the severity of depressive symptoms and may be objective biomarkers of depression. A systematic method of assessing vocal acoustic characteristics could provide an

OPEN ACCESS

Edited by:
Takahiro A. Kato,
Kyushu University, Japan

Reviewed by:
Bingxin Zhao,
Purdue University, United States
Tingshao Zhu,
Institute of Psychology (CAS), China

****Correspondence:***
Shu-Ping Tan
shupingtan@126.com

Specialty section:
This article was submitted to Mood Disorders, a section of the journal Frontiers in Psychiatry

Received: *15 November 2021*
Accepted: *30 March 2022*
Published: *28 April 2022*

Citation:
Zhao Q, Fan H-Z, Li Y-L, Liu L, Wu Y-X, Zhao Y-L, Tian Z-X, Wang Z-R, Tan Y-L and Tan S-P (2022) Vocal Acoustic Features as Potential Biomarkers for Identifying/Diagnosing Depression: A Cross-Sectional Study. Front. Psychiatry 13:815678. doi: 10.3389/fpsyt.2022.815678

accurate and discreet means of screening for depression; this method may be used instead of—or in conjunction with—traditional screening methods, as it is not subject to the limitations associated with self-reported assessments wherein subjects may be inclined to provide socially acceptable responses rather than being truthful.

Keywords: depression, acoustic characteristics, MFCC, biomarker, zero-crossing rate

INTRODUCTION

Depression is a serious mental illness that can result in a significant decline in a patient's social functioning and quality of life. According to a 2019 epidemiological survey in China, the lifetime prevalence of depression was 3.4%, and the 12-month prevalence was 2.1%—both of which are higher than the prevalence rates for most other psychiatric disorders (1). Currently, the diagnosis of depression is primarily dependent upon the subjective judgment of experienced psychiatrists. However, accurately distinguishing negative emotions from depression is challenging, and objective and effective auxiliary diagnostic methods for depression are lacking. These are among the possible reasons that depression is easily missed. For example, in primary care settings, only one-third of people with mild depression are correctly diagnosed (2). After experiencing a first depressive episode, the recurrence rate within 3 years is more than 30%, and some patients have recurrent episodes; thus, the course of the disease can be chronic, placing a heavy burden on both patients and society (3, 4). Consequently, the use of any potential objective biomarker for accurately diagnosing depression warrants in-depth investigation.

The speech of depressed patients is different from that of normal people. The patients usually show lower intonation and less speech. Many studies have suggested that there are abnormal acoustic features in depressed patients (5, 6). This suggests that acoustic features may be an objective biomarker of depression. Therefore, to determine an appropriate biomarker to investigate, we considered the question, "What is the physical process of speech?" The brain organizes prosodic information and produces neuromuscular instructions that control the activities of muscles and tissues related to phonation movement. Next, the airflow stream out of the lungs either causes the vocal cords to vibrate (when the glottis is closed) or passes through the vocal cord smoothly (when the glottis is open). The oropharyngeal muscle forms the main channel of phonation, which is equivalent to a filter that can amplify or attenuate the sound of a specific frequency (7).

Regarding the content of speech, it mainly consists of two different types of information: "what" is being said, including the literal meaning of the information expressed, and "how" it is said, which connotes the emotion and rhythm information in the expression. The speech of a depressed patient can convey not only verbal information, such as negative, pessimistic, and suicidal ideas, but also considerable non-verbal information, including slow reaction and speech, lack of attention, and low volume of voice. "Voice," in this context, is a non-verbal form of emotional expression (8). Emotion affects speech by changing the physiological characteristics of the vocal system (9), breathing, and muscle tone while listeners perceive the emotion of the speaker through specific neural pathways (10).

Depressed patients tend to show less speech production, have a low intonation, and pause often, all of which are characteristics of this mental disorder. Acoustic characteristics of speech that people can hear directly, such as the length of a pause, pause variability, and the speech/pause ratio, differ between people with and without depression, and studies have verified that some of these characteristics indicate depression severity (11–14). These reported findings suggest that voice analysis may be used to gauge the severity of depression objectively. However, the aforementioned characteristics are easily affected by unstable environmental factors. Therefore, the mel-frequency cepstral coefficient (MFCC) is often considered a superior method for distinguishing differences in voice emotion characteristics and analyzing the subtle differences in voice emotions perceived by human ears (15).

MFCCs can be used to identify changes in the vocal tract (16) and can be calculated in the following steps: (1) calculating the fast Fourier transform spectrum from the frequency, (2) extracting filter bank output of mel scale allocation according to human auditory features, and (3) obtaining the cepstrum coefficient from the discrete cosine transformation. Ozdas et al. (17) found that MFCC has an accuracy of 75% in distinguishing between depressed patients and normal controls. Akkaralaertsest and Yingthawornsuk (18) also believed that there were characteristic differences in MFCC of depressed patients' speech that could help identify depressed patients with or without high suicide risk, to some extent.

In addition to the MFCC, other characteristics can indicate the voice mood. The fundamental frequency (F0) is the basic frequency generated by the vibration of the vocal cords. Results from a 4-week sertraline/placebo double-blind controlled trial showed that the mean fundamental frequency of the depression group that responded to the treatment increased from baseline; meanwhile, the frequency remained consistent or decreased from baseline for the depression group that did not respond to the treatment (19). Additionally, the zero-crossing rate (ZCR), which refers to the number of times a signal passes through the zero axis in a certain time, can be used to identify voiceless and voiced sounds that are characteristic expressions of phonetic emotions. A Chinese study found the ZCR has an accuracy of 67–70% to distinguish depressed individuals from those without depression (20). However, a Japanese study found no significant difference in ZCR between the depression and normal groups (5). Furthermore, although the harmonic-to-noise ratio (HNR) reflects the ratio of the sound signal strength to noise signal strength, few studies have investigated the relationship between

depressive symptoms and acoustic characteristics, such as ZCR, MFCC, HNR, and F0.

Additionally, although previous studies that used small sample sizes and included limited acoustic characteristics have shown that depressed patients present abnormal acoustic characteristics, no studies to date have verified the correlation between acoustic characteristics and clinical symptoms. Hence, there is a lack of explanation for the psychopathology of abnormal acoustic characteristics. It is unclear whether acoustic features can partly reflect the severity of emotional symptoms and whether the severity of depression can be evaluated by certain acoustic features.

To address this limitation, the present study surveyed a relatively large sample of depressed patients and healthy controls. Using MFCC, ZCR, HNR, and F0, which are known to reflect the emotional changes of the voice, we aimed to verify the relationship between acoustic characteristics and severity of depression and the significance of acoustic characteristics in disease discrimination. We also conducted a preliminary exploration of the psychopathological mechanism of abnormal acoustic characteristics.

We hypothesized that the acoustic characteristics of depressed patients and normal people differ and are related to depressive symptoms and that acoustic characteristics can help distinguish depressed patients from normal individuals to some extent. If acoustic characteristics can be used as objective biomarkers of depression to provide a diagnostic reference, it may help decrease the rate of misdiagnosis and missed diagnosis, promote early identification and treatment of depression, and ultimately improve the patient's prognosis. Since acoustic characteristics can be obtained automatically, exploring the acoustic characteristics that can predict the severity of anxiety and depression was conducive to promoting the intelligent evaluation of depressive disorder severity. Moreover, it can also promote the development of artificial intelligence ability to identify depression and provide Internet-based medical treatment to patients, which can have far-reaching implications.

MATERIALS AND METHODS

Participants

We recruited 71 patients from Beijing Huilongguan Hospital from 2018 to 2020. An experienced psychiatrist conducted detailed mental and physical examinations of the participants. The inclusion criteria were as follows: (1) diagnosed with depression according to the Diagnostic and Statistical Manual of Mental Disorders (DSM–IV), (2) aged 18–60 years, (3) attained junior high school education or above, and (4) able to read Chinese fluently. The exclusion criteria were as follows: (1) diagnosed with severe cerebrovascular disease, brain injury, and other nervous system diseases; (2) having a serious physical disease; (3) having accompanying substance abuse (except tobacco) problems; and (4) diagnosed with acute nasolaryngology and respiratory system diseases affecting the vocal cords. Sixty-two healthy controls with no current or previous mental illness were recruited from the surrounding community and screened by the Mini-International Neuropsychiatric Interview. The remaining inclusion and exclusion criteria were the same as those used in the patient group.

This study was approved by the Ethics Committee of Beijing Huilongguan Hospital. A specific psychiatrist explained the details of the study to all the participants; meanwhile, their information was strictly confidential. Audio data would be stored on a specific hard disk. Participants took part in voluntarily and there would be no penalty for withdrawal at any time. Written informed consent was obtained from all participants.

Measures

All participants provided their general information, and the depression group completed clinical symptom evaluation questionnaires, including the 17-item Hamilton Depression Scale (HAMD-17), Hamilton Anxiety Scale (HAMA), and Patient Health Questionnaire (PHQ-9). The HAMD-17 is a commonly used depression rating scale comprising 17 symptom items across five domains including anxiety/somatization, weight, cognitive impairment, retardation, sleep disturbance (21, 22). The HAMA is a commonly used 14-item anxiety rating scale for measuring "physical anxiety" and "mental anxiety;" each item is scored from 0 (not present) to 4 (very severe) (23). We also used the PHQ-9, a simple and effective 9-item self-assessment tool for depression wherein each item is rated on a scale from 0 to 3 (24). Higher scores on these scales indicate greater severity of symptoms.

All participants were seated in a noise-controlled room (background sound less than 30 dB). After a 3-min rest period, voices were recorded using a fixed ISK BM-5000 microphone (sampling frequency: 44 kHz, bit rate: 1,058 kbps). The participants were asked to read three paragraphs in their natural tone. Each paragraph contained about 200 Chinese characters, which described one of the three different emotions: positive, negative, and neutral. The positive emotion text depicted scenes from the Chinese New Year and included words such as "happy," "smile," "play games," "delicious," "singing and dancing," and so on. The negative emotion text included "punishment," "trouble," "worry," "anxious," "worry," "slander," "pain," "dark clouds," and so on. The neutral emotion text described a bridge using location, shape, and other descriptors that did not contain any emotion-related words. Word stimulations can induce different emotional and physiological responses (25, 26) and might influence acoustic differences between the depression group and control group (6). However, it is not clear whether the different emotional stimuli could play a role in the discriminant analysis, so we explored this further. After reading a paragraph, the participants were asked to rest for 1 min before moving on to the next paragraph. Voices were analyzed with OpenSMILE v2.1.0 (27) using the feature set of INTERSPEECH 2009 Emotion Challenge pre-set configuration (IS09_emotion.conf). The mean values of the following acoustic features within the utterance segments were calculated for the 12 dimensions of MFCC, ZCR, HNR, and F0.

Statistical Analyses

All statistical analyses were performed using the SPSS 21.0. For normally distributed continuous variables, the independent sample *t*-test was used for comparison between groups.

TABLE 1 | Demographic and clinical characteristics of all participants $N = 133$.

Characteristics	Depression group ($n = 71$)	Control group ($n = 62$)	Group comparison	
	Mean ± SD	Mean ± SD	t/χ^2	p
Age (years)	34.90 ± 9.32	36.67 ± 8.56	1.15	0.25
Gender (Male,%)	33.80%	31.30%	0.1	0.85
Education (years)	16.25 ± 2.05	15.86 ± 1.83	−1.17	0.24
Age of onset (years)	27.59 ± 6.25	NA	NA	NA
Disease duration (years)	7.31 ± 6.02	NA	NA	NA
HAMA score	21.3 ± 9.93	NA	NA	NA
HAMD score	16.09 ± 6.24	NA	NA	NA
PHQ-9 score	13.13 ± 6.61	NA	NA	NA

HAMA, Hamilton Anxiety Scale; HAMD, Hamilton Depression Scale; PHQ-9, Patient Health Questionnaire.

Categorical data were analyzed using the chi-square test. Multivariate analysis of variance was used to compare the differences in acoustic characteristics between groups, with gender, age, and education level as covariates. To address the problem of multiple comparisons (15 acoustic features), a false discovery rate (FDR) procedure was further performed at a q-value of 0.05 over all acoustic features together. Spearman correlation analysis was performed to explore the relationship between depression symptom scores and acoustic characteristics. Further, multiple linear regression was conducted to explore the relation between clinical symptom and acoustic characteristics.

To choose the more suitable discriminant model, the discriminant effect on the depression group and normal control group was tested *via* logistic regression (LR) and support vector machine (SVM) models, respectively, both of which were used frequently in previous studies. Due to its superior discriminant effect, the LR model was selected for further analysis. All machine learning processes were completed with scikit-learn in Python 3.8. All parameters were performed by default to avoid the influence of manual intervention on discrimination results. The f_classif method in the feature_selection module of scikit-learn was used to screen all of acoustic features. The LR analysis was performed again based on the 20 selected variables, while analyzing the contribution of each variable to the classification. We performed a 10-fold cross validation of the classification and divided the dataset into the training set and the test set at a 7:3 ratio. The test data was only used for the validation of the discriminant model and were not used in any training process. Figures were generated from Matplotlib, a popular data visualization package for Python (38).

RESULTS

General Demographic Data of the Two Groups

We enrolled 71 patients with depression and 62 healthy controls in Beijing, China. There were no significant differences in age, gender, or education between the two groups (**Table 1**). The depression group was accompanied by obvious symptoms of anxiety. The group's psychic anxiety score of HAMA was 12.30 ± 5.12, while the somatic anxiety score of HAMA was 9.16 ± 6.00. The subscale scores of HAMD were 6.35 ± 3.13 (anxiety/somatization score), 0.57 ± 0.69 (weight score), 1.97 ± 1.44 (cognition score), 4.49 ± 2.02 (retardation score), and 2.86 ± 1.86 (insomnia score).

Multivariate Analysis of Variance of Acoustic Characteristics Between Depression and Normal Control Groups

A multivariate analysis of variance (ANOVA)—with gender, age, and education level as covariates—showed significant inter-group main effects of all of the acoustic characteristics ($p < 0.0001$), which survived FDR-correction. For η^2 0.01, 0.06, and 0.14 were considered small, moderate, and large effect sizes, respectively. ZCR, F0, MFCC1-5, MFCC7-10 showed a large effect size, and the remaining features showed a moderate effect size. Only MFCC2, MFCC3, MFCC8, and MFCC9 had statistically significant conditional main effects in the positive, neutral, and negative emotion tasks (η^2 = 0.06, 0.09, 0.05, and 0.02, respectively), but none of the acoustic characteristics had a group × condition interaction effect (**Table 2**).

Correlation Between Depressive Symptom Scores and Acoustic Characteristics of the Depression Group

Since there were significant differences between the groups for each acoustic characteristic indicator, we performed a Spearman correlation analysis for all acoustic features and the PHQ-9, HAMA, and HAMD scores. The results showed that MFCC4 and MFCC7 had significant positive correlations with the PHQ-9 score, regardless of the positive, neutral, or negative emotion tasks. ZCR in the positive condition task showed a significant correlation with the HAMA total score ($r = 0.31$) and with the HAMA somatic anxiety subscale score ($r = 0.34$). MFCC9 in the neutral task showed a negative correlation with the anxiety/somatization subscale score of the HAMD ($r = -0.34$). The remaining acoustic characteristics did not show a significant correlation with depressive symptoms (**Table 3**).

Linear Regression Analysis Between Clinical Symptom Scores and Acoustic Features

In linear regression, the PHQ-9 score was a dependent variable, while age, gender, education, MFCC4, and MFCC7 were independent variables. To avoid high collinearity of the same features under different emotion tasks, we selected MFCC4-neutral and MFCC7-negative, which had the highest correlation coefficient with the PHQ-9 score. Stepwise method was used. The result showed statistically significant effects, $F = 7.25$, $R^2 = 0.20$, $p = 0.01$ (**Table 4**).

Then, the HAMD anxiety/somatization score was used as a dependent variable, while MFCC9-neutral, age, gender, and education were independent variables. Similarly, stepwise method was used. Here too, linear regression showed statistically significant effects, $F = 4.15$, $R^2 = 0.11$, $p = 0.049$ (**Table 4**).

TABLE 2 | Differences in acoustic characteristics between the depression and control groups under different emotional tasks *N* = 133.

	Depression group(*n* = 71)Mean (*SD*)			Control group(*n* = 62)Mean (*SD*)			Group effect		
	Positive	Neutral	Negative	Positive	Neutral	Negative	*F*	*p*	η^2
ZCR (10^{-2})	4.91 (1.78)	5.08 (1.76)	5.01 (1.82)	6.34 (0.82)	6.67 (0.80)	6.63 (0.82)	128.07	<0.0001*	0.25
HNR (10^{-2})	34.59 (8.97)	35.78 (9.03)	35.14 (9.10)	31.30 (3.46)	31.78 (3.36)	31.52 (3.88)	34.09	<0.0001*	0.08
F0	38.68 (38.55)	44.23 (41.60)	41.26 (39.33)	13.61 (11.84)	17.60 (12.77)	15.67 (14.99)	85.13	<0.0001*	0.18
MFCC1	−6.01 (5.25)	−6.54 (5.07)	−6.64 (5.13)	−10.88 (1.49)	−11.73 (1.45)	−11.68 (1.46)	181.35	<0.0001*	0.32
MFCC2	−0.84 (4.20)	0.81 (3.99)	0.70 (3.94)	−6.23 (1.84)	−4.23 (1.61)	−4.46 (1.63)	265.72	<0.0001*	0.41
MFCC3	−2.69 (2.72)	−1.24 (3.01)	−1.27 (2.76)	−5.99 (2.26)	−4.16 (2.30)	−4.28 (2.34)	158.39	<0.0001*	0.29
MFCC4	−3.56 (4.07)	−4.47 (4.30)	−3.77 (4.06)	−7.33 (2.24)	−8.06 (2.23)	−7.49 (2.24)	119.36	<0.0001*	0.23
MFCC5	−5.92 (4.79)	−6.50 (4.55)	−6.04 (4.65)	−9.26 (2.37)	−9.55 (2.32)	−9.32 (2.31)	68.58	<0.0001*	0.15
MFCC6	−7.13 (5.64)	−6.74 (5.46)	−6.78 (5.37)	−9.55 (2.31)	−9.00 (2.01)	−9.19 (2.14)	28.66	<0.0001*	0.07
MFCC7	−4.49 (3.08)	−5.14 (2.95)	−4.80 (2.98)	−8.19 (2.68)	−8.84 (2.27)	−8.51 (2.32)	171.70	<0.0001*	0.31
MFCC8	−3.36 (3.60)	−4.93 (3.73)	−4.47 (3.64)	−6.36 (2.16)	−8.08 (2.09)	−7.55 (2.01)	99.82	<0.0001*	0.20
MFCC9	−3.14 (3.24)	−3.95 (2.63)	−3.78 (3.05)	−5.11 (2.07)	−5.97 (1.59)	−5.83 (1.67)	67.17	<0.0001*	0.15
MFCC10	−4.62 (4.14)	−3.90 (3.78)	−4.50 (4.15)	−8.14 (2.93)	−7.42 (2.26)	−8.08 (2.68)	130.32	<0.0001*	0.25
MFCC11	−3.98 (2.57)	−3.68 (2.95)	−4.02 (2.94)	−5.55 (2.30)	−5.00 (2.42)	−5.40 (2.42)	32.37	<0.0001*	0.08
MFCC12	−2.07 (1.86)	−2.18 (1.78)	−2.40 (1.94)	−3.41 (2.01)	−3.39 (1.89)	−3.75 (2.02)	48.35	<0.0001*	0.11

**Indicates survived FDR-correction.*
ZCR, zero-crossing rate; HNR, harmonic-to-noise ratio; F0, fundamental frequency; MFCC, mel-frequency cepstral coefficient.

TABLE 3 | The correlation between depressive symptom severity and acoustic characteristics.

	PHQ-9 score	HAMA total score	HAMA somatic anxiety score	HAMD anxiety/ somatization score
ZCR-positive	−0.13	0.31*	0.34*	0.18
MFCC4-positive	0.39*	−0.06	0.02	−0.05
MFCC4-neutral	0.42*	−0.02	0.01	0.02
MFCC4-negative	0.36*	−0.10	−0.09	−0.09
MFCC7-positive	0.43*	0.10	0.11	−0.11
MFCC7-neutral	0.41*	0.14	0.17	−0.14
MFCC7-negative	0.46*	0.09	0.12	−0.05
MFCC9-neutral	−0.02	−0.09	−0.07	−0.34*

**p < 0.05.*
PHQ-9, Patient Health Questionnaire; HAMA, Hamilton Anxiety Scale; HAMD, Hamilton Depression Scale; ZCR, zero-crossing rate; MFCC, mel-frequency cepstral coefficient.

TABLE 4 | Linear regression analysis between PHQ-9 score and MFCC7-negative.

	β	SE	*t*	*p*	95% confidence interval of β	
					Lower bound	Upper bound
PHQ-9 score						
(constant)	17.00	1.79	9.49	<0.001	13.34	20.65
MFCC7-negative	0.90	0.33	2.69	0.01	0.22	1.58
HAMD anxiety/somatization score						
(Constant)	4.33	1.11	3.92	<0.001	2.09	6.58
MFCC9-neutral	−0.45	0.22	−2.04	0.049	−0.91	−0.001

Discriminant Analysis of Acoustic Characteristics of the Depression Group

The LR model showed better discriminant results than SVM between the depression and control groups, with a discrimination accuracy of 89.66% and AUC of 0.98. A recall of 0.94 signified that 94% of depression patients were predicted as the depressed group, and precision of 0.89 signified that 89% of participants in the predicted depressed group were actually depression patients. Further, 83% of the healthy controls were predicted to be in the control group, and 91% of the participants in the predicted control group were actually healthy controls. The discrimination accuracy of the SVM model and the AUC were 86.21% and 0.95, respectively (see **Table 5** and **Figure 1**).

TABLE 5 | The discriminant result of grouping by different classifiers.

Indicator	LR		SVM	
	Depression group	Control group	Depression group	Control group
Precision	0.89	0.91	0.93	0.79
Recall	0.94	0.83	0.82	0.92
F1 score	0.91	0.87	0.87	0.85

LR, Logistic Regression; SVM, support vector machine.

Figure 2 shows the 20 acoustic features with the largest contribution to discrimination in the LR model. Concerning acoustic features—particularly MFCC1-negative, MFCC6-neutral—with contributions greater than 0, the larger the value, the more likely the participant is to be identified as depressed. In contrast, when these acoustic features have contributions less than 0, the smaller the value, the more likely the participant is to be identified as depressed.

DISCUSSION

There were significant differences in acoustic characteristics between the depression and normal control groups, after controlling for gender, age, and education. Only MFCC2,

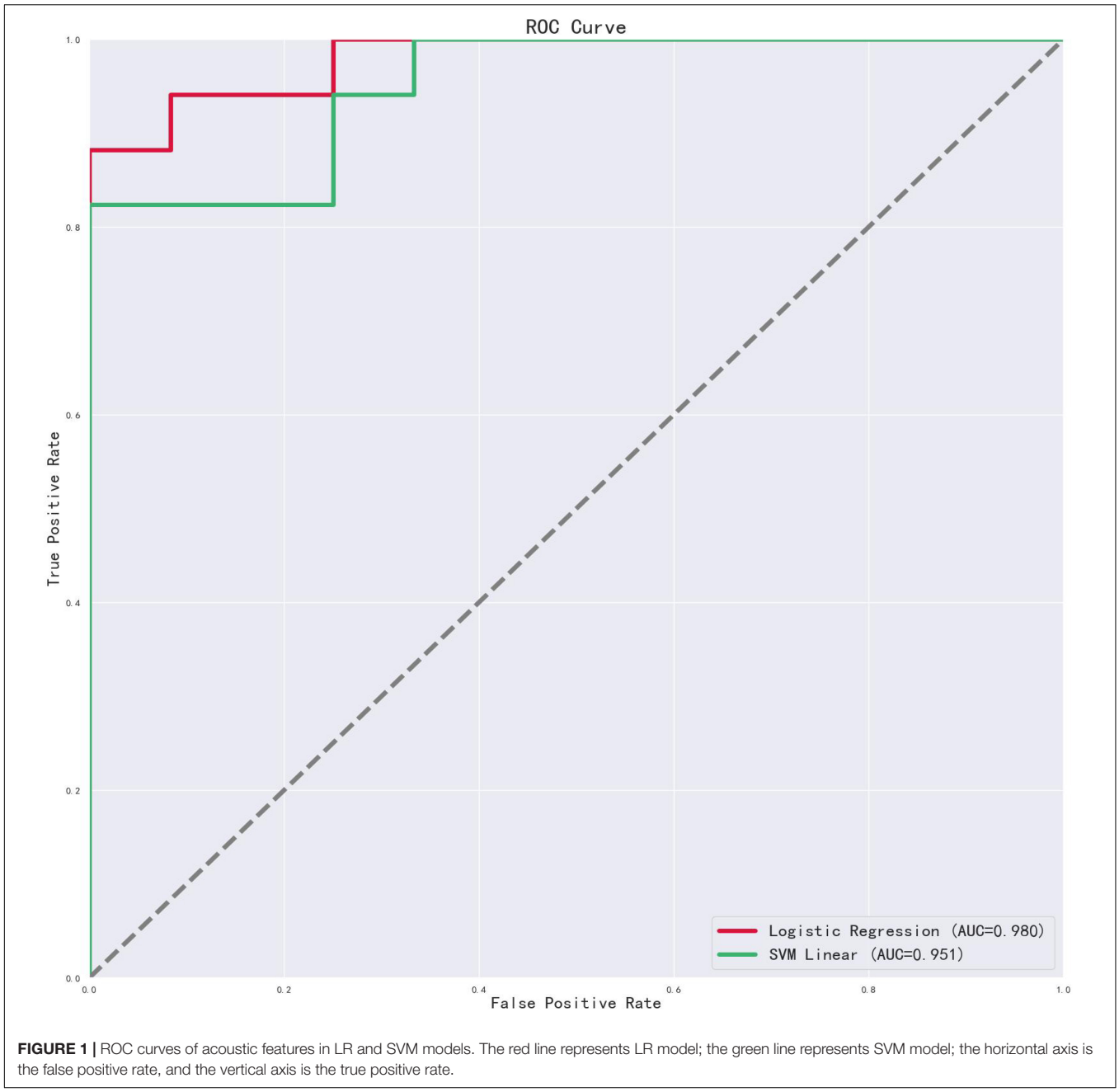

FIGURE 1 | ROC curves of acoustic features in LR and SVM models. The red line represents LR model; the green line represents SVM model; the horizontal axis is the false positive rate, and the vertical axis is the true positive rate.

MFCC3, MFCC8, and MFCC9 showed differences during the positive, neutral, and negative emotion tasks. This suggests that there are differences in some acoustic features under different implicit emotional task patterns. Taguchi et al. also found that MFCC2 was higher in depressed patients than in normal controls, which is consistent with our results, but they did not report an association between MFCC and depressive symptom severity (5). These inconsistent results may be due to differences in language, disease stages, and speech recording methods. Another study from China found that MFCC5 and MFCC7 of the depression group were consistently lower than those of the control group across different emotional and situational tasks, and F0 was lower while ZCR was higher for the depression group in the reading text task, which was contrary to the findings of the present study (6). This inconsistency may be attributed to the different clinical characteristics of depression, such as anxiety and psychomotor retardation. The accuracy of identifying depression using acoustic characteristics was close to 90%. These results suggest that acoustic features may comprise a useful biomarker for diagnosing depression. Moreover, ZCR, MFCC4, MFCC7, and MFCC9 were associated with depressive and anxiety symptoms severity. MFCC7-negative can predict a PHQ-9 score; meanwhile, MFCC9-neutral can predict an anxiety/somatization score. Therefore, we believed that MFCC7

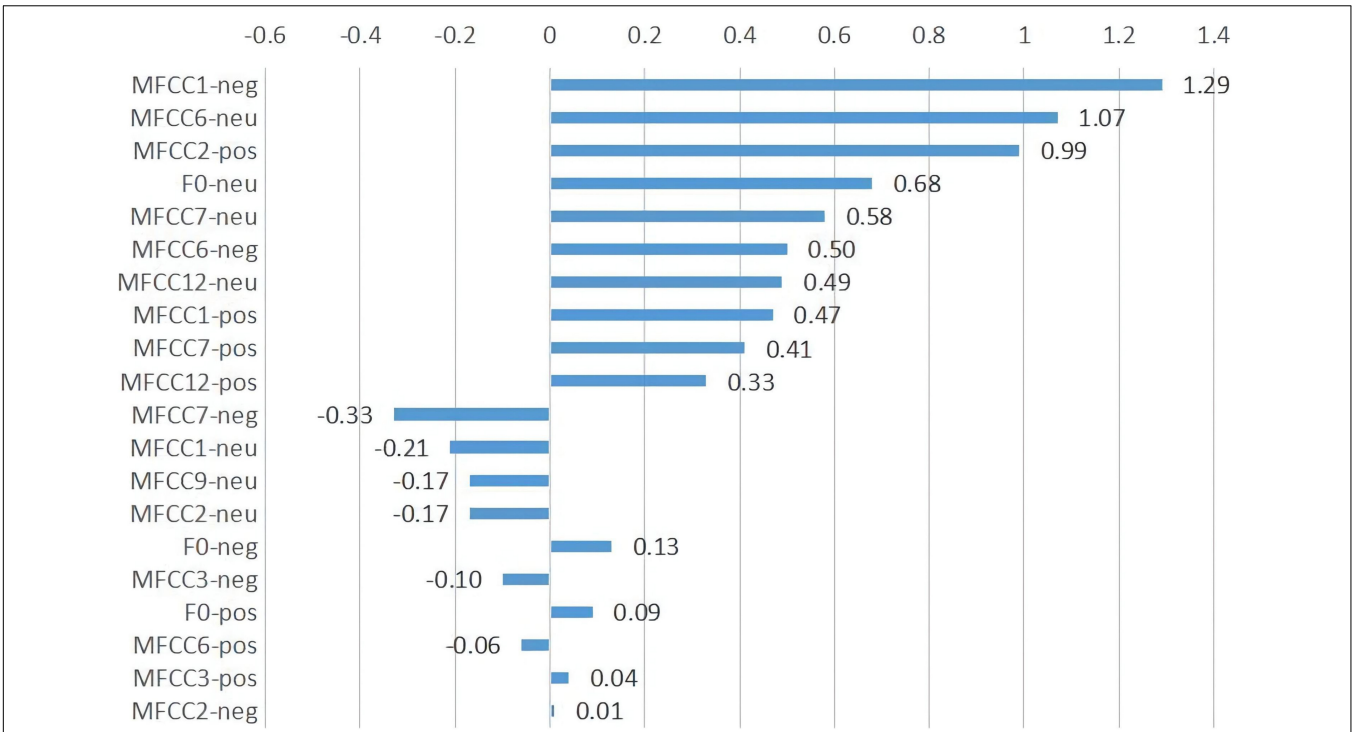

FIGURE 2 | The 20 acoustic features with the largest contribution in LR model. pos, positive emotion task; neg, negative emotion task; neu, neutral emotion task.

and MFCC9 can partly reflect the severity of depressive and anxiety symptoms and have the potential to be quantitative, objective indicators in evaluating disease severity.

Patients with depression often have autonomic nervous function disorders, and the muscle tone of their vocal tract can be affected by the disease, which may be one of the factors that distinguish depressed patients' acoustic characteristics from those of healthy individuals. Patients with depression often feel tired, and a study suggests that sympathetic nervous system activity is enhanced, and parasympathetic nervous system activity is weakened during fatigue (28). Changes in the autonomic nervous system cause disturbances in the respiratory rate (29), and this may affect the airflow from the lungs to the vocal tract. Muscle tension is also a common symptom of depression (30). Changes in muscle tone can alter the dynamics of the vocal tract, limiting joint movement (31), which in turn slows speech and affects sound frequency. Air passes through the vocal cords and glottis, and the vocal tract acts as a filter that amplifies and attenuates different sound frequencies through movement, adjusting the spectrum of the glottis waveform (32). In a previous study, MFCC was associated with muscle movement of the vocal tract on MRI scans (16); MFCC can also reflect voice mood and is minimally affected by age and sex (5). We found that ZCR, MFCC4, MFCC7, and MFCC9 were associated with depression symptom severity. However, how depression affects muscle movement of the vocal tract that causes such changes in the specific frequencies of the patient's voice remains unknown.

Speakers can constantly monitor and adjust their voice by using their speech as feedback in the auditory circuit (32). In the central auditory pathway, 5-hydroxytryptamine (5-HT) exists in many structures from the cochlear nucleus to the auditory cortex. It is one of the most important neurotransmitters in auditory processing; 5-HT neurons in the inferior colliculus can adjust the frequency of perceived tones by changing the response latency of neurons (33). Female patients with depression show reduced tolerance to sound, also known as auditory hypersensitivity (34). People with low expression of 5-HT transporter perceived sounds as clearer than those with high expression, showing a higher signal-to-noise ratio and volume (35). Therefore, patients with depression may also be more sensitive than healthy individuals when hearing the sounds of their own voices. Due to the low 5-HT function, the perceived frequency of their own sounds may change. Through auditory feedback, patients may tend to have lower intonation and acoustic features, which are different from those of normal controls when speaking.

Rats express their emotions through ultrasonic vocalizations, and different emotions correspond to different frequencies of ultrasound; ultrasonic vocalizations in anxious conditions due to isolation are associated with 5-HT. Drugs that act on the 5-HT receptor, such as some serotonin reuptake inhibitors and serotonin 5-HT_{1A} receptor agonists, dose-dependently reduce isolation-induced ultrasound vocalizations in rats (36). Serotonin reuptake transporter gene-deficient rats exhibited more anxious behavior, accompanied by changes in the ultrasonic vocal structure, and they were less likely to make orectic 50 kHz vocalizations when exploring novel environments (37). The above studies on animals suggest that 5-HT may be related to the frequency and behavior of the sound emitted. However, there

are no studies on human vocalization and 5-HT. Given that 5-HT plays an important role in the pathogenesis of depression, our results lead us to suspect that 5-HT may be involved in the pathological mechanism of the abnormal acoustic characteristics of depressed patients.

Limitations

Although the findings of this study have implications for improving the diagnosis of depression, there are some inherent limitations to the study design. First, the exploratory cross-sectional design of this study precluded causal inferences. Longitudinal follow-ups of patients with depression, including observation of the entire course of disease with and without drug treatment, need to be carried out in the future. Second, the clinical symptom assessment in this study was simple; future studies should include more dimensions of depression, including the assessment of suicide risk and autonomic nervous function. Third, the experimental paradigm of this study was relatively simple and warrants further expansion to simulate different scenarios, help gain a comprehensive understanding of the changes in the acoustic characteristics of depressed patients, and fully evaluate their accuracy as objective biomarkers of depression. Furthermore, this study only included Chinese Mandarin samples, whether the specific language or other cultural factors may influence the generalizability of the results is still unclear. Finally, although we performed a 10-fold cross validation, a larger sample size and independent validation datasets may be more effective for verifying our conclusions.

CONCLUSION

The change in acoustic characteristics in patients with depression may not be caused by a single factor, and the specific underlying mechanism remains unclear. However, the acoustic characteristics of depressed patients were significantly different from those of the normal control group in this study, and the accuracy of depression classification based on acoustic features was very high. These findings suggest that acoustic characteristics may become objective biomarkers of depression; this may help clinicians make objective diagnosis of depression, reduce the rate of missed diagnosis and misdiagnosis, and promote the development of Internet medical treatment.

DATA AVAILABILITY STATEMENT

The raw data supporting the conclusions of this article will be made available by the authors, without undue reservation.

ETHICS STATEMENT

The studies involving human participants were reviewed and approved by the Ethics Committee of Beijing Huilongguan Hospital. The patients/participants provided their written informed consent to participate in this study.

AUTHOR CONTRIBUTIONS

S-PT, Z-RW, and Y-LT contributed to the conception and design of the study. QZ performed the statistical analysis and wrote the first draft of the manuscript. S-PT reviewed and revised the manuscript. H-ZF, Y-LZ, and Z-XT organized the database. Y-LL, LL, and Y-XW contributed to provision of study materials and patients. All authors contributed to the manuscript revision, as well as read and approved the submitted version.

FUNDING

This work was funded by the Funds of Beijing Science and Technology Project (code: Z191100006619104) and the Natural Science Foundation of Beijing (code: 7202072). The funding sources of this study had no role in the study design, data collection, and analysis, decision to publish, or preparation of the article.

ACKNOWLEDGMENTS

We express our gratitude to all participants of this study. We would like to thank Editage (www.editage.cn) for English language editing.

REFERENCES

1. Huang Y, Wang Y, Wang H, Liu Z, Yu X, Yan J, et al. Prevalence of mental disorders in China: a cross-sectional epidemiological study. *Lancet Psychiatry.* (2019) 6:211–24.
2. Mitchell AJ, Rao S, Vaze A. Can general practitioners identify people with distress and mild depression? A meta-analysis of clinical accuracy. *J Affect Disord.* (2011) 130:26–36. doi: 10.1016/j.jad.2010.07.028
3. Lam RW, McIntosh D, Wang J, Enns MW, Kolivakis T, Michalak EE, et al. Canadian network for mood and anxiety treatments (CANMAT) 2016 clinical guidelines for the management of adults with major depressive disorder: section 1. disease burden and principles of care. *Can J Psychiatry.* (2016) 61:510–23. doi: 10.1177/0706743716659416
4. Liu Q, He H, Yang J, Feng X, Zhao F, Lyu J. Changes in the global burden of depression from 1990 to 2017: findings from the global burden of disease study. *J Psychiatr Res.* (2020) 126:134–40. doi: 10.1016/j.jpsychires.2019.08.002
5. Taguchi T, Tachikawa H, Nemoto K, Suzuki M, Nagano T, Tachibana R, et al. Major depressive disorder discrimination using vocal acoustic features. *J Affect Disord.* (2018) 225:214–20. doi: 10.1016/j.jad.2017.08.038
6. Wang J, Zhang L, Liu T, Pan W, Hu B, Zhu T. Acoustic differences between healthy and depressed people: a cross-situation study. *BMC Psychiatry.* (2019) 19:300. doi: 10.1186/s12888-019-2300-7
7. Krajewski J, Schnieder S, Sommer D, Batliner A, Schuller B. Applying multiple classifiers and non-linear dynamics features for detecting sleepiness from speech. *Neurocomputing.* (2012) 84:65–75.5.
8. Grabowski K, Rynkiewicz A, Lassalle A, Baron-Cohen S, Schuller B, Cummins N, et al. Emotional expression in psychiatric conditions: new technology for clinicians. *Psychiatry Clin Neurosci.* (2019) 73:50–62. doi: 10.1111/pcn.12799

9. Tolkmitt FJ, Scherer KR. Effect of experimentally induced stress on vocal parameters. *J Exp Psychol Hum Percept Perform.* (1986) 12:302–13. doi: 10.1037//0096-1523.12.3.302
10. Schirmer A, Adolphs R. Emotion perception from face, voice, and touch: comparisons and convergence. *Trends Cogn Sci.* (2017) 21:216–28. doi: 10.1016/j.tics.2017.01.001
11. France DJ, Shiavi RG, Silverman S, Silverman M, Wilkes DM. Acoustical properties of speech as indicators of depression and suicidal risk. *IEEE Trans Biomed Eng.* (2000) 47:829–37. doi: 10.1109/10.846676
12. Alpert M, Pouget ER, Silva RR. Reflections of depression in acoustic measures of the patient's speech. *J Affect Disord.* (2001) 66:59–69. doi: 10.1016/s0165-0327(00)00335-9
13. Cannizzaro M, Harel B, Reilly N, Chappell P, Snyder PJ. Voice acoustical measurement of the severity of major depression. *Brain Cogn.* (2004) 56:30–5. doi: 10.1016/j.bandc.2004.05.003
14. Mundt JC, Snyder PJ, Cannizzaro MS, Chappie K, Geralts DS. Voice acoustic measures of depression severity and treatment response collected *via* interactive voice response (IVR) technology. *J Neurolinguist.* (2007) 20:50–64. doi: 10.1016/j.jneuroling.2006.04.001
15. Li H, Xu X, Wu G, et al. Research on speech emotion feature extraction based on MFCC. *J Electr Measur Instrument.* (2017) 31:448–53.
16. Zhu Y, Kim YC, Proctor MI, Narayanan SS, Nayak KS. Dynamic 3-D visualization of vocal tract shaping during speech. *IEEE Trans Med Imaging.* (2013) 32:838–48. doi: 10.1109/TMI.2012.2230017
17. Ozdas A, Shiavi RG, Wilkes DM, Silverman MK, Silverman SE. Analysis of vocal tract characteristics for near-term suicidal risk assessment. *Methods Inf Med.* (2004) 43:36–8. doi: 10.1055/s-0038-1633420
18. Akkaralaertsest T, Yingthawornsuk T. Comparative analysis of vocal characteristics in speakers with depression and high-risk suicide[J]. *Int J Comp Theory Engine.* (2015) 7:448. doi: 10.7763/ijcte.2015.v7.1001
19. Mundt JC, Vogel AP, Feltner DE, Lenderking WR. Vocal acoustic biomarkers of depression severity and treatment response. *Biol Psychiatry.* (2012) 72:580–7. doi: 10.1016/j.biopsych.2012.03.015
20. Long H, Guo Z, Wu X, Hu B, Liu Z, et al. Detecting depression in speech: comparison and combination between different speech types[C]//2017 IEEE International Conference on Bioinformatics and Biomedicine (BIBM). *IEEE.* (2017) 2017:1052–8.
21. Hamilton M. A rating scale for depression. *J Neurol Neurosurg Psychiatry.* (1960) 23:56–62.
22. Zhao B, Li Z, Wang Y, Ma X, Wang X, Wang X, et al. Can acupuncture combined with SSRIs improve clinical symptoms and quality of life in patients with depression? Secondary outcomes of a pragmatic randomized controlled trial. *Complement Ther Med.* (2019) 45:295–302. doi: 10.1016/j.ctim.2019.03.015
23. Hamilton M. The assessment of anxiety states by rating. *Br J Med Psychol.* (1959) 32:50–5. doi: 10.1111/j.2044-8341.1959.tb00467.x
24. Löwe B, Unützer J, Callahan CM, Perkins AJ, Kroenke K. Monitoring depression treatment outcomes with the patient health questionnaire-9. *Med Care.* (2004) 42:1194–201. doi: 10.1097/00005650-200412000-00006
25. Wu D, Yao S, Guo W. Difference ERPs effects of the difference introduction on the recognition of Chinese emotional content words in healthy subjects[C]//2005 International Conference on Neural Networks and Brain. *IEEE* (2005) 2:1303–6.
26. Xu S, Yin H, Wu D. Initial establishment of the Chinese Affective Words Categorize System used in research of emotional disorder[J]. *Chin. Mental Health J.* (2008) 22:770–4.
27. Eyben F, Weninger F, Gross F, Schuller B. Recent developments in openSMILE, the munich open-source multimedia feature extractor. *MM 2013 - Proceedings of the 2013 ACM Multimedia Conference*. New York, NY: ACM (2013).
28. Tanaka M, Tajima S, Mizuno K, Ishii A, Konishi Y, Miike T, et al. Frontier studies on fatigue, autonomic nerve dysfunction, and sleep-rhythm disorder. *J Physiol Sci.* (2015) 65:483–98. doi: 10.1007/s12576-015-0399-y
29. Kreibig SD. Autonomic nervous system activity in emotion: a review. *Biol Psychol.* (2010) 84:394–421. doi: 10.1016/j.biopsycho.2010.03.010
30. Maes M. "Functional" or "psychosomatic" symptoms, e.g. a flu-like malaise, aches and pain and fatigue, are major features of major and in particular of melancholic depression. *Neuro Endocrinol Lett.* (2009) 30:564–73.
31. Roy N, Nissen SL, Dromey C, Sapir S. Articulatory changes in muscle tension dysphonia: evidence of vowel space expansion following manual circumlaryngeal therapy. *J Commun Disord.* (2009) 42:124–35. doi: 10.1016/j.jcomdis.2008.10.001
32. Postma A. Detection of errors during speech production: a review of speech monitoring models. *Cognition.* (2000) 77:97–132. doi: 10.1016/s0010-0277(00)00090-1
33. Hurley LM, Thompson AM, Pollak GD. Serotonin in the inferior colliculus[J]. *Hearing Res.* (2002) 168:1–11.
34. Gopal KV, Briley KA, Goodale ES, Hendea OM. Selective serotonin reuptake inhibitors treatment effects on auditory measures in depressed female subjects. *Eur J Pharmacol.* (2005) 520:59–69. doi: 10.1016/j.ejphar.2005.07.019
35. Selinger L, Zarnowiec K, Via M, Clemente IC, Escera C. Involvement of the Serotonin Transporter Gene in Accurate Subcortical Speech Encoding. *J Neurosci.* (2016) 36:10782–90. doi: 10.1523/JNEUROSCI.1595-16.2016
36. Wöhr M, van Gaalen MM, Schwarting RK. Affective communication in rodents: serotonin and its modulating role in ultrasonic vocalizations. *Behav Pharmacol.* (2015) 26:506–21. doi: 10.1097/FBP.0000000000000172
37. Golebiowska J, Hołuj M, Potasiewicz A, Piotrowska D, Kuziak A, Popik P, et al. Serotonin transporter deficiency alters socioemotional ultrasonic communication in rats. *Sci Rep.* (2019) 9:20283. doi: 10.1038/s41598-019-56629-y
38. Hunter, J. D. Matplotlib: a 2D graphics environment. *Comput. Sci. Eng.* (2007) 9:90–5. doi: 10.1109/MCSE.2007.55

Conflict of Interest: The authors declare that the research was conducted in the absence of any commercial or financial relationships that could be construed as a potential conflict of interest.

frontiers | Frontiers in Psychiatry

ORIGINAL RESEARCH
published: 18 May 2022
doi: 10.3389/fpsyt.2022.858768

Disrupted Causal Connectivity Anchored on the Right Anterior Insula in Drug-Naive First-Episode Patients With Depressive Disorder

*Haiyan Xie[1], Qinger Guo[2], Jinfeng Duan[3], Xize Jia[4,5], Weihua Zhou[3], Haozhe Sun[6], Ping Fang[1] and Hong Yang[7]**

[1] Department of Psychiatry, The Fourth Affiliated Hospital, College of Medicine, Zhejiang University, Yiwu, China, [2] Department of Radiology, The Fourth Affiliated Hospital, College of Medicine, Zhejiang University, Yiwu, China, [3] Department of Psychiatry, The First Affiliated Hospital, College of Medicine, Zhejiang University, Hangzhou, China, [4] School of Teacher Education, Zhejiang Normal University, Jinhua, China, [5] Key Laboratory of Intelligent Education Technology and Application of Zhejiang Province, Zhejiang Normal University, Jinhua, China, [6] School of Social Sciences, Heriot-Watt University, Edinburgh, United Kingdom, [7] Department of Radiology, The First Affiliated Hospital, College of Medicine, Zhejiang University, Hangzhou, China

OPEN ACCESS

Edited by:
Takahiro A. Kato, Kyushu University, Japan

Reviewed by:
Bochao Cheng, Sichuan University, China
Xiaohua Cao, First Hospital of Shanxi Medical University, China

***Correspondence:**
Hong Yang
1307017@zju.edu.cn

Specialty section:
This article was submitted to Neuroimaging and Stimulation, a section of the journal Frontiers in Psychiatry

Received: *20 January 2022*
Accepted: *30 March 2022*
Published: *18 May 2022*

Citation:
Xie H, Guo Q, Duan J, Jia X, Zhou W, Sun H, Fang P and Yang H (2022) Disrupted Causal Connectivity Anchored on the Right Anterior Insula in Drug-Naive First-Episode Patients With Depressive Disorder. Front. Psychiatry 13:858768. doi: 10.3389/fpsyt.2022.858768

Object: Major depressive disorder (MDD) has been demonstrated to be associated with abnormalities in neural networks. However, few studies examined information flow in the salience network (SN). This study examined abnormalities in the causal connectivity between the SN and whole brain in drug-naive first-episode patients with MDD in the resting state.

Methods: Based on the Diagnostic and Statistical Manual of Mental Disorders (DSM-5) diagnostic criteria, 23 drug-naive first-episode MDD patients and 20 matched healthy individuals were recruited and underwent a resting-state magnetic resonance scan. The acquired functional image data were preprocessed using resting-state functional magnetic resonance imaging (rs-fMRI) data analysis toolkit plus (RESTplus). Then, using the data processing & analysis for brain imaging (DPABI) software and a coefficient-based general component analysis method with the right anterior insula (rAI) as the region of interest (ROI), the causal connectivity of the SN with the whole brain and its correlation with cognitive and mental performance were examined in the resting state.

Results: (1) The MDD group showed a significantly higher Hamilton Depression Rating Scale total score and significantly higher scores for anxiety, cognitive disturbance, and block factors compared with normal controls. (2) Compared with control: from whole brain to the rAI, the MDD group showed a lower causal connectivity in the left inferior frontal gyrus; from the rAI to the whole brain, the MDD group showed a lower causal connectivity in the right cingulate gyrus, the right precuneus, and extending to paracentral lobule but higher causal connectivity in the left inferior and middle frontal gyrus. (3) In the MDD group, from rAI to the whole brain, the causal connectivity values for the right cingulate gyrus/precuneus were negatively correlated with the score of Stroop Color-Word Test A, B, and C as well as interference times.

Conclusion: Our results indicated disrupted causal connectivity among the default mode network (DMN), the central executive network (CEN), and SN in drug-naive first-episode MDD patients. Especially, our results suggest a unique role for rAI in the ordered or hierarchical information processing, presumed to include bottom-up and top-down reciprocal influences among the three networks in MDD.

Keywords: major depressive disorder, right insula, causal connectivity, salience network, default mode network, central executive network, stroop test

INTRODUCTION

Characterized as persistent negative emotions, a lack of motivation and changes in cognitive functions, major depressive disorder (MDD) is one of the most common mental disorders (1). According to the "Depression and Other Common Mental Disorders: Global Health Estimates" issued by the World Health Organization (WHO) in February 2017, the total number of people living with depression worldwide is 322 million. The World Health Organization ranked depressive disorders as the single largest contributor to non-fatal health loss (7.5% of all years lived with disability). Although depression does great harm to individuals, its pathogenesis largely remains unclear.

The brain is a complex network with extensive interconnections in structure and function among different parts of the brain. Functional coordination among brain regions requires the exchange of information among different regions. This information exchange plays an important part in complex cognitive processes (2). With the technique of resting-state functional magnetic resonance imaging (rs-fMRI), it was found that depression results from the dysfunction of multiple brain regions caused by connectivity abnormalities (3, 4). Previously, related studies have mainly focused on functional networks related to movement control, cognitive processing, emotional processing, etc., such as default mode network (DMN), central executive network (CEN), and salience network (SN) (3, 5–7).

The SN is mainly composed of the insular cortex, the dorsal side of the anterior cingulate gyrus, the amygdala, and the temporal lobe. It controls the signal transmission between the CEN and DMN, acting as a regulatory "switch," such as attention to the external environment for the CEN and the monitoring of internal information for the DMN (8). According to the review by Menon, an important cause of the depressive disorder is likely to function abnormalities in salience information detection between the networks and the destruction of the internal and external information mapping functions, i.e., abnormal conversion between the DMN and CEN caused by anterior insular dysfunction in the SN, which in turn leads to abnormal behavioral responses to internal and external stimuli and events (6).

The SN may change with the emotion processing process, and the insula, as a core node of the SN, i.e., a cross-boundary region in processing cognitive functions, internal states, and emotional perceptions, plays a very important interactive role in the monitoring of endogenous stimuli and exogenous information (9). Therefore, in studies of the SN that employ the seed point-based functional connectivity method, the insular cortex is often used as the region of interest. The anterior insula (AI) is the control center that regulates the dynamic interactions involving brain networks and plays a very important role in autocorrelated mental activities involving external attention and internal orientation, having a right-side advantage (7). Several studies have linked the AI to both the processing of mutual feeling states and adaptive switching between functional networks, making this region an ideal candidate for exploring potential neural circuit dysfunction in emotional disorders (10, 11).

Causal connectivity refers to the direct or indirect causal influence of one brain area on another brain area (12, 13). Granger causality analysis (GCA) is a relatively data-driven analytical method for connectivity, analyzing the direction of information flow between brain regions based on the time series of information processing and thus enabling a description of resting-state brain networks (13, 14). A regression coefficient-based algorithm has been proposed in which signed regression coefficients are used to assess the Granger effect: a positive value indicates an excitatory effect and a negative value indicates an inhibitory effect or negative feedback (15). This method can more truly reflect brain activity, with low computational complexity, making the calculations easier. Using regression coefficient-based GCA, our previous research found that depression patients in the resting state exhibit abnormalities in the frontal lobe network, confirming that MDD patients have impaired top-down cognitive control (16).

Therefore, in this study, with coefficient-based GCA method and the right anterior insula (rAI) as the seed point, we examined the direction of information flow between the SN and the whole brain and their correlations with cognitive and mental performance in drug-naive first-episode MDD patients in the resting state. We hypothesized that there would be the abnormalities in the causal connectivity between the rAI and DMN or CEN meanwhile the abnormal GCA would be correlated with clinical psychological scale scores in MDD patients.

MATERIALS AND METHODS

Subjects

Study Group

Twenty-three depression patients (seven men and 16 women; outpatients and inpatients) of the Psychiatry Department, First Affiliated Hospital, Zhejiang University School of Medicine,

were included in the study (MDD group). According to the clinical interview and the Structured Clinical Interview for DSM, the diagnosis was unanimously ascertained by two licensed psychiatrists with intermediate professional titles. The inclusion criteria were as follows: met the diagnostic criteria for depression in "Diagnostic and Statistical Manual of Mental Disorders (DSM-5)" as well as the International Classification of Disease (ICD-10) diagnostic criteria for depression; first episode of depression and had not yet received treatment; education of junior high school or above; right-handed; and Hamilton Depression Rating Scale (HAM-D) (17-item) score $\geq$17 points.

Control Group

Twenty normal individuals (six men and 14 women), matched for age, education, and right-handedness, were recruited from hospital staff, students, and volunteers from nearby communities. The inclusion criteria were as follows: healthy adults without a history of mental illness or a family history of mental illness; education of junior high school or above; and HAM-D score $\leq$ seven points.

The general exclusion criteria were as follows: (1) treated depression; (2) a history of diseases with abnormal brain structure, epilepsy or significant medical illness; (3) any other mental disorders (except MDD in patients) after clinical interviews and Structured Clinical Interview screening; (4) any family history of mental illness; (5) a history of alcohol and drug abuse; (6) women pregnant, lactating or in a menstrual period, and (7) magnetic resonance imaging (MRI) contraindications, such as metallic implants, retractors or braces, and claustrophobia.

Moreover, patients with MDD usually have cognitive executive function impairment (17). Considering of immature or possibly declined cognitive function (18), 18–45-year-old patients were chosen as subjects. This study was approved by the local Medical Ethics Committee of First Affiliated Hospital of Zhejiang University, and each subject signed an informed consent form.

Clinical Assessments and Neuropsychological Tests

The severity of mood symptoms was assessed using the 17-item HAM-D, which is categorized into six dimensions, i.e., anxiety, weight, cognitive disturbance, diurnal variation, block and sleep disorders. In this study, we only analyzed the scores for anxiety, cognitive disturbance, and block factors, as well as the HAM-D total score.

Two well-known neuropsychological tests, Stroop Color-Word Test (SCWT) (19) and Trail-making test (TMT) (20), were performed on each subject, including attention, memory, processing speed, behavior inhibition and executive function. The two tests have been proved to reveal cognitive deficits in patients with MDD in many studies.

The SCWT A and SCWT B were conducted to measure selective attention and processing speed, SCWT C and SCWT interference were used to measure behavioral inhibition and executive function. SCWT A asked subjects to read aloud three written colors printed in black ink as quickly as possible. SCWT B required the subjects to name the color as quickly as possible. Finally, the subjects were required to name the ink color of a color word as fast as possible to finish SCWT C. The color word was not the same as the ink color. The performance for each condition was recorded as the processing time per item in seconds. The reaction time difference in SCWT C relative to SCWT B is the SCWT interference. There were two subtasks: write and read aloud color names that differ from printed ink colors.

The TMT was divided into two parts, which were used to evaluate attention and executive function. For the TMT-A, subjects were asked to draw lines quickly to connect consecutive numbers. It measured visuo-spatial attention and performance speed. For the TMT-B, subjects were asked to connect numbers and letters alternately in ascending order as quickly as possible, the part measured mental flexibility, ability to shift attention, and strategy. Task completion was measured in seconds.

Image Acquisition

The MRI data were collected on a Philips Achieva 3.0 T scanner in the First Affiliated Hospital of Medical College of Zhejiang University. The participants were asked to lie on the scanner with their eyes closed, do not think about anything in particular, and do not fall asleep. An echo-planar imaging (EPI) sequence was used for functional magnetic resonance imaging. The parameters were as follows: repetition time (TR), 2000 ms; echo time (TE), 35 ms; flip angle, 90°; slice thickness/interval, 5.0/1.0 mm; and number of volumes (or time points), 200. A total of 24 transverse slices were used to cover the whole brain, with all slices arranged in parallel with the anterior-posterior commissure. A gradient-echo sequence was also used to obtain high-resolution T1-weighted structural MRI images. The parameters were as follows: TR/TE, 8/4 ms; flip angle, 8°; matrix size, 240 × 240; slice thickness, 1 mm; and field of view, 240 mm × 240 mm.

Imaging Data Preprocessing

Preprocessing of rs-fMRI data was performed using Resting-State fMRI Data Analysis Toolkit (RESTplus) (http://restfmri.net/forum/RESTplus) (21), including (1) removal of the first 10 time points for steady magnetization and participant adaptation; (2) slice timing correction; (3) head motion correction; (4) performing spatial normalization to the Montreal Neurological Institute (MNI) space by using new segment to the structural images (resampling voxel size = 3 mm × 3 mm × 3 mm); (5) spatial smoothing using an isotropic Gaussian kernel of 6 mm full width at half maximum (FWHM); (6) removal of the linear drift within the time series; (7) regressing out the effects of head movement (Friston 24 parameter model), the cerebrospinal fluid (CSF) signal noise, and the white matter signal noise from the fMRI data (22); and (8) band-pass filtering (0.01–0.08 Hz). One participant in the healthy control group was excluded because head motion is larger than 3.0 mm or 3.0°.

As a powerful approach, GCA may be confounded by varied hemodynamic response functions (HRFs) across the brain. We then employed a blind deconvolution method to control the varied HRF which has been demonstrated in detail by Wu et al. (23). The method considers the HRF modeled from the spikes of large amplitude Blood Oxygen on Lever Depending (BOLD) signal based on the assumption that such spikes represent spontaneous neural activities. The lack of explicit inputs for

modeling signal dynamics and estimating the underlying neural signal remains a challenge for rs-fMRI data compared with task-based fMRI (22, 23). It has been argued that this makes the representation of BOLD-level causal influences to underlying neural-level causal influences more difficult (24). The approach solves these problems by performing deconvolution of the HRF with the BOLD signal, which allows the extraction of neuronal variables from the signal, thus being closer to neural-level causal models. In accordance with Wu et al. (23), a threshold of 1.2 standard deviations was used for determining spikes and 15 s for a maximum lag between a neural event and BOLD response.

Granger Causality Analysis

To study the influence of depression on the brain, we used a sphere centered at the rAI [MNI coordinate (51, 33, −3)] with a 6-mm radius as the seed region for the GCA (25). The driving effects and feedback effects were calculated between the time series of seed region and the time series of each voxel in the whole brain by using GCA in this study. The bivariate coefficient GCA was performed using REST softwarche (http://www.restfmri.net) (26). Granger causality estimates the causal effect of the seed-to-whole-brain and whole-brain-to-seed. In the current study, the times series of the seed was defined as X, and the time series of each voxel was Y. A positive coefficient from X to Y indicates that X has a Granger causal influence on Y (i.e., positive influence). Similarly, a negative coefficient from X to Y suggests that the activity in region X exerts an opposing directional influence on the activity in region Y (i.e., negative influence). The coefficient maps for all subjects were *z*-transformed to improve normality.

Statistical Analysis

Two-sample *t*-tests were performed to compare the GCA maps between patients with depression and the healthy control group. All the statistical analyses were conducted within a gray matter mask (using a gray matter probability template with a threshold of 0.2). The Gaussian random field theory correction was used for the *T*-maps with a threshold of voxel $p < 0.05$, cluster $p < 0.05$, and edge connected. The analyses were performed using data processing & analysis for brain imaging (DPABI) (27). Finally, we extracted the mean GCA value in the areas of significant difference in gray matter, Pearson correlation analysis was performed between the mean GCA value and the score of HAM-D, SCWT, and TMT in patients.

RESULTS

Demographic, Clinical, and Neuropsychological Test Results

As shown in **Table 1**, there is no significant difference between the two groups in age, sex, and education level ($p > 0.05$). In addition, there was no significant difference in the SCWT and TMT between the two groups ($p > 0.05$), but a significant difference in the total HAM-D score ($t = 18.41$, $p < 0.01$) and in the scores for anxiety ($t = 11.69$, $p < 0.01$), cognitive disturbance ($t = 7.50$, $p < 0.01$) and block factors ($t = 19.31$, $p < 0.01$) between the two groups.

TABLE 1 | Demographics and clinical characteristics of the subjects.

Variables (mean ± SD)	MDD ($n = 23$)	NC ($n = 20$)	*P*-value
Age (years)	31.526 ± .86	30.107 ± .52	0.449[b]
Gender (male/female)	7/16	6/14	0.975[a]
Education (years)	12.133 ± .86	12.403 ± .13	0.741[b]
Illness duration (months)	11.871 ± 0.92	/	/
HAM-D score	25.095 ± .57	1.251 ± .68	0.000[b]
Anxiety factors	7.392 ± .37	0.701 ± .03	0.000[b]
Cognitive disturbance factors	4.482 ± .59	0.100 ± .30	0.000[b]
Block factors	8.391 ± .75	0.350 ± .67	0.000[b]
TMT A	58.872 ± 9.05	59.204 ± 3.06	0.976[b]
TMT B	110.395 ± 6.89	106.858 ± 5.97	0.873[b]
SCWT A	49.152 ± 7.68	45.961 ± 2.87	0.733[b]
SCWT B	74.522 ± 3.47	64.052 ± 4.20	0.131[b]
SCWT C	115.03 ± 3.44	104.42 ± 5.55	0.295[b]
SCWT interference	40.391 ± 7.67	40.301 ± 7.73	0.761[b]

MDD, major depressive disorder; NC, normal control; HAM-D, Hamilton Depression Rating Scale; TMT, Trail-making test; SCWT, Stroop Color-Word Test.
[a] The P-value was obtained by chi-square test.
[b] The P-values were obtained by Mann–Whitney U test.

TABLE 2 | Significant group differences in Granger causality analysis.

Regions	MNI (x, y, z)	Cluster size (mm^3)	*t*-value	*P*-value
Causal inflow to the rAI from the whole brain				
lIFG	−51, 24, 27	114	−3.7167	<0.05
Causal outflow from the rAI to the whole brain				
rCC	3, −24, 48	56	−3.8407	<0.05
rPreC	3, −24, 48	136	−3.8407	<0.05
PCL	3, −24, 48	77	−3.8407	<0.05
lIFG	−39, 21, 24	64	3.4310	<0.05
lMFG	−39, 21, 24	104	3.4310	<0.05

rAI, right anterior insula; rCC, right cingulate cortex; rPreC, right precuneus; PCL, Paracentral lobule; lIFG, left inferior frontal gyrus; lMFG, left middle frontal gyrus.

Granger Causality Analysis

From the whole brain to the region of interest (ROI) (Y to X), in the left inferior frontal gyrus (lIFG), causal connectivity in the MDD group was lower than that in the control group. The MDD group did not show any region with causal connectivity that was higher than that in the control group.

From the ROI to the whole brain (X to Y), for the following regions, the causal connectivity in the MDD group was lower than that in the control group: right cingulate cortex (rCC), right precuneus (rPreC), and paracentral lobule (PCL); from the ROI to the whole brain (X to Y), in the left middle frontal gyrus (lMFG) and lIFG, the causal connectivity in the MDD group were higher than that in the control group. It was shown in **Table 2** and **Figure 1**.

Correlation Analysis

In the MDD group, the signals within the cluster range that were statistically significant between two groups were directly

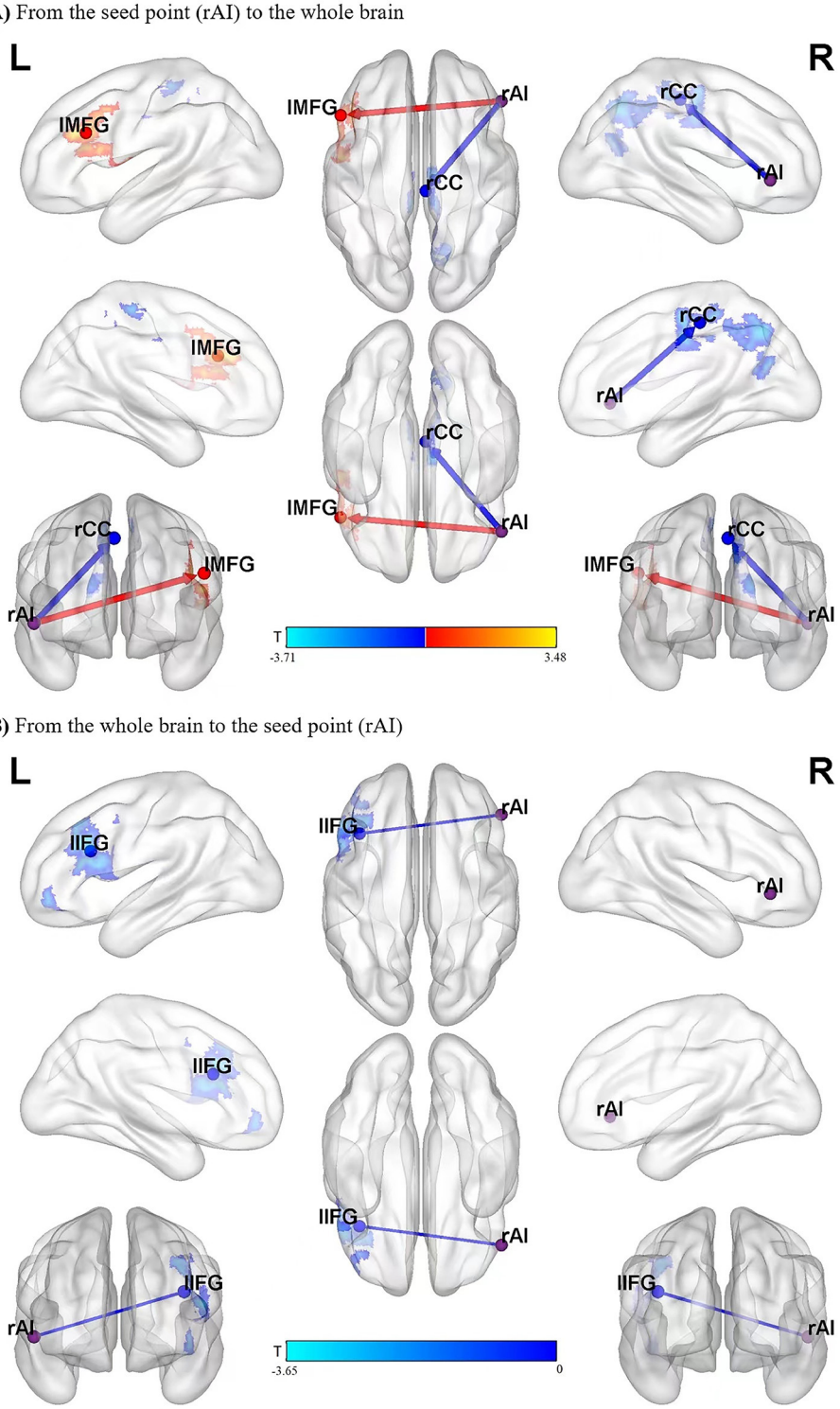

FIGURE 1 | Blue areas show brain regions where MDD patients had reduced causal effects than controls, while red-yellow colored areas show brain regions where patients had increased causal effects than controls. The color bar represents *t*-values. The significant results of GCA between the two groups **(A,B)**. rAI, right anterior insula; rCC, right cingulate cortex; lMFG, left middle frontal gyrus; lIFG, left inferior frontal gyrus.

extracted and analyzed based on the correlation with the scores from the scales, the results showed that from the seed point to the whole brain, the causal connectivity values for the right cingulate gyrus/right precuneus were negatively correlated with SCWT A, SCWT B, SCWT C, and SCWT interference time but not significantly correlated with the HAM-D total score and the score for each factor. They were shown in **Figure 2**.

DISCUSSION

In this study, with a seed point-based GCA, we found that the causal connectivity from lIFG (a key node of the CEN) to the rAI (a key node of the SN) in the MDD was lower than that in the controls. Moreover, the causal connectivity from the rAI to rCC, rPreC, and PCL (the key nodes of the DMN) in the MDD group was lower than that in the normal group, while the causal connectivity from the rAI to lMFG and lIFG in the MDD was higher than that in the normal group. The results suggest aberrant information flow between the SN and the DMN or CEN in drug-naive first-episode MDD patients. Moreover, the decrease in the causal connectivity from the rAI to the components of the DMN (rPreC/rCC) was negatively correlated with the SCWT A, B, and C and interference time.

In recent years, the DMN, CEN, and SN have been hotspot networks of depressive disorder. The ability to switch neural resources between DMN, SN, and CEN has been considered to be the key mechanism of adaptive emotion regulation (28). DMN is associated with spontaneous brain activities involving episode-related memory retrieval and the monitoring of the external environment and exogenous stimuli as well as the state of the self-reflection and the regulation of endogenous information, which in turn is related to the advanced cognitive perception and emotional processing (29). The CEN is closely related to attention and working memory, and controls the network's involvement in cognitive tasks, playing an important role in adaptive cognitive control. The SN is mainly involved in assessing external affairs and responding accordingly to connect to the CEN and DMN. The study (30) found that MDD patients show connectivity abnormalities in internal functions of the SN and that the decrease in functional connectivity within the rAI of the SN is correlated to the severity of depressive symptoms and abnormal DMN/CEN interactions. Another study (31) reported that functional connectivity increased between the SN and CEN as well as the dynamic interaction between the DMN and CEN decreased for MDD. However, these studies on functional connectivity did not take into account the direction of information flow between the triple network model, which is important to understand the causality of DMN, CEN, and SN in MDD.

In this study, we found that abnormal the causal connectivity between the rAI and the frontal lobe, including decreased from the lIFG to the rAI, but increased from the rAI to lMFG and lIFG. The frontal lobe lesions can change cognitive function and behavioral and decision-making capacity, while affecting emotion and mood. Abnormalities in the functional connectivity of the frontal cortex in patients with depression have been reported in many imaging studies (16, 32–35). Our result showed that the unidirectional causal effect of the lIFG on the rAI was reduce, it suggested the patients decreased externally oriented task information flow (top-to-down), and impaired the lIFG function that related to higher demand or a specific cognitive process (36). The unidirectional causal effect of the rAI on the lMFG and lIFG was increased in patients in our study, which may suggest, in the early stage of the MDD, as feedback or compensatory, increased self-referential cognition information flow (down-to-top) to general reorganization of brain functioning. The frontal lobe is a key part of the CEN. According to the triple model proposed by Menon (6), SN might play a central role in mediating the transformation of the functional connectivity in CEN, which is related to the externally oriented task, especially the region rAI in SN. Our results indicated the impaired triple model in MDD.

We found that the causal connectivity from rAI to DMN nodes (rCC/rPreC and PCL) is decreased. The precuneus/cingulate cortex, which belongs to the posterior sub-network, is an important part of DMN. It has been reported that a change in the resting-state functional connectivity between the rCC and rAI indirectly reflects changes in the emotional regulation function of MDD patients (37). Precuneus as a key node of DMN has been reported to be participated in the self-consciousness and self-related mental representations, the dysfunctions of precuneus were related to depressive symptoms, such as somatic complaints, negative bias in interpreting bodily feedback and negative emotional memory, some key features of MDD (38). Yuen GS et al. adopted the rAI as the seed point and found that the rAI and bilateral precuneus had abnormal functional connectivity in the depression group (39). In addition, we also found that the causal connectivity from the rAI to the PCL was lower in the MDD group than that in the controls. The PCL (an important part of the CEN)participates in a variety of complex functions and is critical for somatic motor processing, regulating subjective well-being, and emotion processing (40). The decline of information flow from the rAI to the PCL may be one of the pathological mechanisms that cause non-specific physical symptoms in patients with depression. In our study, decreased causal connectivity from rAI to rCC/rPreC and PCL suggested the decreased down-top information flow, which may be related to the breakdown of this presumed hierarchical processing system from sensory to higher cognitive regions, mediated by core limbic regions (e.g., insula) in MDD. In patients, those results also proved the impaired triple model (6) – that SN has a core role in mediating the conversion of the functional connectivity between the DMN, which is related to self-referential cognition.

We found that the two groups did not differ significantly on the SCWT and TMT, i.e., in terms of the psychometric measurements of cognitive functions using the SCWT and TMT, the scores for the two groups did not differ significantly. This was just similar to our GCA results – decreased causal connectivity from the frontal lobe to the rAI, but increased causal connectivity from the rAI to the frontal lobe which suggested, in the early stage of the MDD, like feedback or compensatory, increased self-referential cognition function to general reorganization of

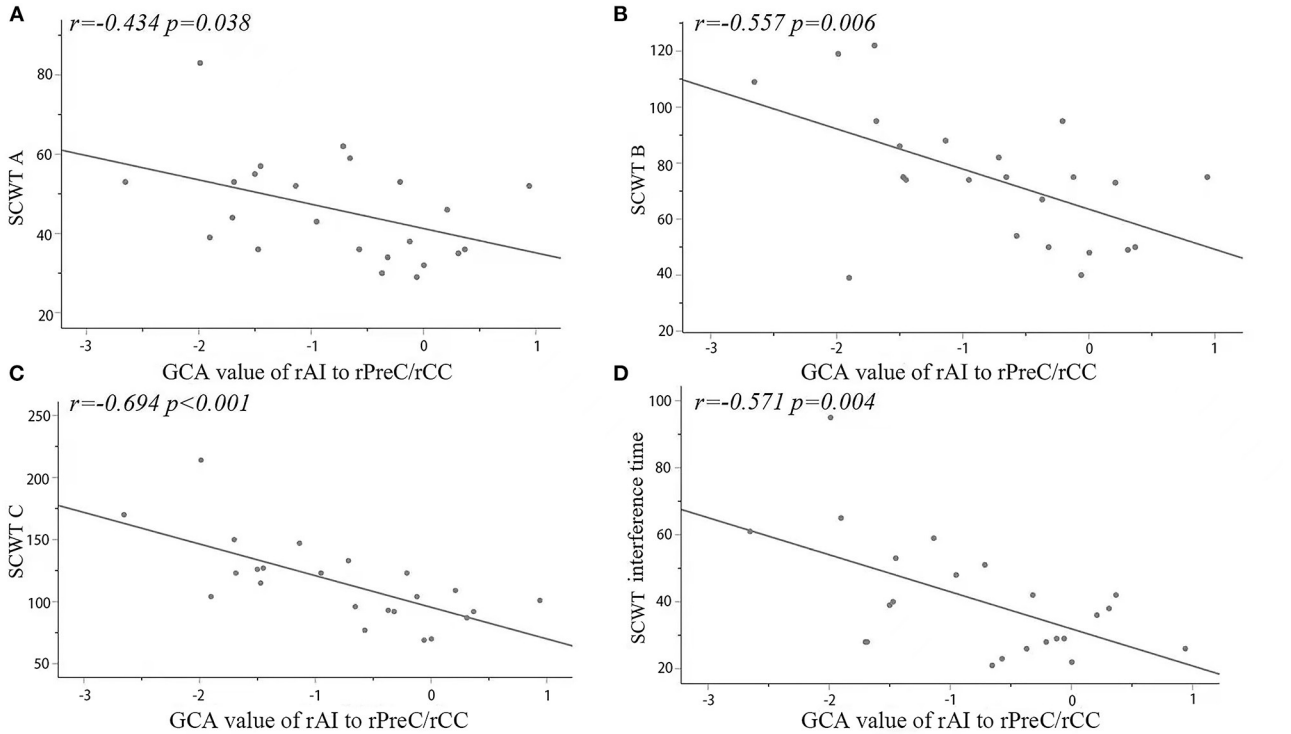

FIGURE 2 | Significantly negative correlations between the causal connectivity values and the SCWT **(A–C)** and interference times in the rPreC/rCC from the seed point to the whole brain in the MDD group. The correlations of the GCA values with the SCWT in the MDD group **(D)**. rAI, right anterior insula; rPreC, right precuneus; rCC, right cingulate cortex; SCWT, Stroop Color-Word Test.

brain functioning. In addition, the higher education level in our subjects might be another influencing factor. The study has shown that individuals with a high level of education have greater cognitive reserves than those with a low level of education, enabling those individuals to better withstand brain damage and maintain function (41).

A meta-analysis conducted by McDermott et al. (42) confirmed that depression severity is positively correlated with cognitive deficits in terms of episodic memory and processing speed. We observed that the change in the GCA from the rAI to the rPreC/rCC was negatively correlated with the Stroop test cards A, B, and C and interference times. Subtest A measures automatic processing and the flexibility of attention; subtest B measures controlled processing and the concentration of attention; and subset C measures the selective attention and response inhibition of executive functions. Our results suggested that, in the early stage of the MDD, the impairment in cognitive function might be the beginning with attention concentration, selective attention of executive function, and response inhibition function, and they were progressed with the severity of the depression.

In summary, we found the abnormal information flow among DMN, CEN, and SN in drug-naive MDD patients. It suggested that the rAI had an important role in orderly or hierarchical information processing, which was considered to include bottom-up (sensory to multimodal) and top-down (multimodal to sensory) reciprocal influences among the three networks. Our results also suggest that in the early stage of MDD, as feedback or compensatory, MDD patients can increase self-referential cognition function to reorganize brain function.

LIMITATIONS

This study used depression patients who had only one episode of depression, had not taken any medication, and did not have other mental illnesses, thus avoiding interference from factors, such as past medication use and chronic disease. However, there are still some limitations. First, the sample size was small, which may cause biases in the results. Second, the seed point-based choice has a substantial impact on the results, and the selection criteria are highly arbitrary and lack unified standards; therefore, the bias related to the brain area of interest generates incomplete results and results that are dependent on assumptions. Lastly, similar to most rs-fMRI studies, we used a TR of two s, leading to very limited time resolution. This problem can be solved by developing sub-second whole brain scan sequences.

CONCLUSION

In conclusion, our results indicated disrupted causal connectivity among DMN, CEN, and SN in the first-episode patients with

depressive disorder. Especially, our results showed that the anterior insula had a unique role in orderly or hierarchical information processing, which was considered to include bottom-up (sensory to multimodal) and top-down (multimodal to sensory) reciprocal influences among the three networks in depressive disorder. Our results also suggested that the information flow involves in the execution, memory, and attention function of the brain from SN to DMN was decreased with the severity of the depression.

DATA AVAILABILITY STATEMENT

The raw data supporting the conclusions of this article will be made available by the authors, without undue reservation.

ETHICS STATEMENT

The studies involving human participants were reviewed and approved by Ethical Committee approval was received from the Ethics Committee of First Affiliated Hospital, Zhejiang University School of Medicine (Approval No. 2016-27). The patients/participants provided their written informed consent to participate in this study.

AUTHOR CONTRIBUTIONS

HX designed the research, collected samples, and wrote the original of manuscript. QG, JD, WZ, and PF collected samples, supervised data, and conducted quality control. XJ and HS analyzed the data. HY supervised and designed the research, collected samples, and revised the manuscript. All authors contributed to the article and approved the submitted version.

FUNDING

This study was supported by the Basic Public Welfare Research Program of Zhejiang Province (Grant No. LGF20H090013), the Key Research and Development Program, Ministry of Science and Technology of People's Republic of China (Grant No. 2019YFC0121003), the Science Technology Department of Zhejiang Province (Grant No. 2017C33096), and the Health and Family Planning Commission of Zhejiang Province (Grant No. 2015107509).

ACKNOWLEDGMENTS

We sincerely appreciate all the subjects and their families for participating in our study.

REFERENCES

1. Lu S, Peng H, Wang L, Vasish S, Zhang Y, Gao W, et al. Elevated specific peripheral cytokines found in major depressive disorder patients with childhood trauma exposure: a cytokine antibody array analysis. *Compr Psychiatry.* (2013) 54:953–61. doi: 10.1016/j.comppsych.2013.03.026
2. Bullmore E, Sporns O. Complex brain networks: graph theoretical analysis of structural and functional systems. *Nat Rev Neurosci.* (2009) 10:186–98. doi: 10.1038/nrn2575
3. Hamilton JP, Chen MC, Gotlib IH. Neural systems approaches to understanding major depressive disorder: an intrinsic functional organization perspective. *Neurobiol Dis.* (2013) 52:4–11. doi: 10.1016/j.nbd.2012.01.015
4. Drevets WC, Price JL, Furey ML. Brain structural and functional abnormalities in mood disorders: implications for neurocircuitry models of depression. *Brain Struct Funct.* (2008) 213:93–118. doi: 10.1007/s00429-008-0189-x
5. Raichle ME, Macleod AM. Snyder AZ, Powers WJ, Gusnard DA, Shulman GL. A default mode of brain function. *Proc Natl Acad Sci USA.* (2001) 98:676–82. doi: 10.1073/pnas.98.2.676
6. Menon V. Large-scale brain networks and psychopathology: a unifying triple network model. *Trends Cogn Sci.* (2011) 15:483–506. doi: 10.1016/j.tics.2011.08.003
7. Seeley WW, Menon V, Schatzberg AF, Keller J, Glover GH, Kenna H, et al. Dissociable intrinsic connectivity networks for salience processing and executive control. *J Neurosci.* (2007) 27:2349–56. doi: 10.1523/JNEUROSCI.5587-06.2007
8. Whitfield-Gabrieli S, Ford JM. Default mode network activity and connectivity in psychopathology. *Annu Rev Clin Psychol.* (2012) 8:49–76. doi: 10.1146/annurev-clinpsy-032511-143049
9. Chen X, Duan MJ, He H. Yang M, Klugah-Brown B, Xu H, et al. Functional abnormalities of the right posterior insula are related to the altered self-experience in schizophrenia. *Psychiatry Res Neuroimaging.* (2016) 256:26–32. doi: 10.1016/j.pscychresns.2016.09.006
10. Terasawa Y, Fukushima H. Umeda S. How does interoceptive awareness interact with the subjective experience of emotion? An fMRI study. *Hum Brain Mapp.* (2013) 34:598–612. doi: 10.1002/hbm.21458
11. Sridharan D, Levitin DJ, Menon V. A critical role for the right fronto-insular cortex in switching between central-executive and default-mode networks. *Proc Natl Acad Sci USA.* (2008) 105:12569–74. doi: 10.1073/pnas.0800005105
12. Deshpande G, Hu XP. Investigating effective brain connectivity from fMRI data: past findings and current issues with reference to Granger causality analysis. *Brain Connect.* (2012) 2:235–45. doi: 10.1089/brain.2012.0091
13. Deshpande G, Santhanam P, Hu XP. Instantaneous and causal connectivity in resting state brain networks derived from functional MRI data. *Neuroimage.* (2011) 54:1043–52. doi: 10.1016/j.neuroimage.2010.09.024
14. Jiao Q, Lu GM, Zhang ZQ, Zhong Y, Wang ZG, Guo YX, et al. Granger causal influence predicts BOLD activity levels in the default mode network. *Hum Brain Mapp.* (2011) 32:154–61. doi: 10.1002/hbm.21065
15. Chen G, Hamilton JP, Thomason ME, Gotlib IH, Saad ZS, Cox RW. Granger causality *via* vector auto-regression tuned for fMRI data analysis. *ISMRM 17th Scientific Meetin.* (Hawaii) (2009).
16. Feng Z, Xu SL, Huang ML, Shi YS, Xiong B, Yang H. Disrupted causal connectivity anchored on the anterior cingulate cortex in first-episode medication-naive major depressive disorder. *Prog Neuropsychopharmacol Biol Psychiatry.* (2016) 64:124–30. doi: 10.1016/j.pnpbp.2015.07.008
17. Lim J, Oh IK, Han C, Huh YJ, Jung IK, Patkar AA, et al. Sensitivity of cognitive tests in four cognitive domains in discriminating MDD patients from healthy controls: a meta-analysis. *Int Psychogeriatri.* (2013) 25:1543–57. doi: 10.1017/S1041610213000689
18. Lockwood KA, Alexopoulos GS, Van Gorp WG. Executive dysfunction in geriatric depression. *Am J Psychiatry.* (2002) 159:1119–26. doi: 10.1176/appi.ajp.159.7.1119
19. Periáñez JA, Lubrini G, García-Gutiérrez A, Ríos-Lago M. Construct validity of the stroop color-word test: influence of speed of visual search, verbal fluency, working memory, cognitive flexibility, and conflict monitoring. *Arch Clin Neuropsychol.* (2021) 36:99–111. doi: 10.1093/arclin/acaa034
20. Arnett JA, Labovitz SS. Effect of physical layout in performance of the trail making test. *Psychol Assess.* (1995) 7:220–21.
21. Jia XZ, Sun JW Ji GJ, Liao W, Lv YT, Wang J, et al. Percent amplitude of fluctuation: a simple measure for resting-state fMRI signal at single voxel level. *PLoS ONE.* (2020) 15:e0227021. doi: 10.1371/journal.pone.0227021

22. Friston K. Hierarchical Models in the Brain. *PLoS Comput Biol.* (2008) 4:e1000211. doi: 10.1371/journal
23. Wu GR, Liao W, Stramaglia S, Ding JR, Chen H, Marinazzo D, et al. Blind Deconvolution Approach to Recover Effective Connectivity Brain Networks from Resting State FMRI Data. *Med Image Anal.* (2013) 17:365–74. doi: 10.1016/j.media.2013.01.003
24. Smith JC, Nielson KA, Woodard JL, Seidenberg M, Durgerian S, Antuono P, et al. Interactive effects of physical activity and APOE-ε4 on BOLD semantic memory activation in healthy elders. *Neuroimage.* (2011) 54:635–44. doi: 10.1016/j.neuroimage.2010.07.070
25. Liu CH, Guo J. Lu SL,Tang LR, Fan J, Wang CY,et al. Increased salience network activity in patients with insomnia complaints in major depressive disorder. *Front Psychiatry.* (2018) 9:1–9. doi: 10.3389/fpsyt.2018.00093
26. Song XW, Dong ZY, Long XY Li SF, Zuo XN, Zhu CZ, et al. REST: a toolkit for resting-state functional magnetic resonance imaging data processing. *PLoS ONE.* (2011) 6:e25031. doi: 10.1371/journal.pone.0025031
27. Yan CG, Wang XD, Zuo XN, Zang YF. DPABI. Data processing & analysis for (resting-state) brain imaging. *Neuroinformatics.* (2016) 14:339–51. doi: 10.1007/s12021-016-9299-4
28. Ellard KK, Zimmerman JP, Kaur N, Van Dijk KR, Roffman JL, Nierenberg AA, et al. Functional connectivity between anterior insula and key nodes of frontoparietal executive control and salience networks distinguish bipolar depression from unipolar depression and healthy controls. *Biol Psychiatry Cogn Neurosci Neuroimaging.* (2018) 3:473–84. doi: 10.1016/j.bpsc.2018.01.013
29. Grimm S, Boesiger P, Beck J, Schuepbach D, Bermpohl F, Walter M. et al. Altered negative BOLD responses in the default-mode network during emotion processing in depressed subjects. *Neuropsychopharmacol.* (2009) 34:932–43. doi: 10.1038/npp.2008.81
30. Manoliu A, Meng C, Brandl F, Doll A, Tahmasian M, Scherr M, et al. Insular dysfunction within the salience network is associated with severity of symptoms and aberrant inter-network connectivity in major depressive disorder. *Front Hum Neurosci.* (2013) 7:930. doi: 10.3389/fnhum.2013.00930
31. Zheng HN, Xu LL, Xie FF, Guo XJ, Zhang JC, Yao L, et al. The altered triple networks interaction in depression under resting state based on graph theory. *Bio Res Int.* (2015) 2015:386326. doi: 10.1155/2015/386326
32. Zhang JR, Wang JH, Wu QZ, Kuang WH, Huang XQ, He Y, et al. Disrupted brain connectivity networks in drug-naive, first-episode major depressive disorder. *Biol Psychiatry.* (2011) 70:334–42. doi: 10.1016/j.biopsych.2011.05.018
33. Cullen KR, Gee DG, Klimes-Dougan B, Gabbay V, Hulvershorn L, Mueller BA, et al. A preliminary study of functional connectivity in comorbid adolescent depression. *Neurosci Lett.* (2009) 460:227–31. doi: 10.1016/j.neulet.2009.05.022
34. Sheline YI, Price JL, Yan Z, Mintun MA. Resting-state functional MRI in depression unmasks increased connectivity between networks via the dorsal nexus. *Proc Natl Acad Sci USA.* (2010) 107:11020–5. doi: 10.1073/pnas.1000446107
35. Lai CH, Wu YT. Decreased inter-hemispheric connectivity in anterior subnetwork of default mode network and cerebellum: significant findings in major depressive disorder. *Int J Neuropsychopharmacol.* (2014) 17:1935–42. doi: 10.1017/S1461145714000947
36. Batista AX, Bazán PR, Conforto AB, Martins MGM, Hoshino M, Simon SS, et al. Resting state functional connectivity and neural correlates of face-name encoding in patients with ischemic vascular lesions with and without the involvement of the left inferior frontal gyrus. *Cortex.* (2019) 113:15–28. doi: 10.1016/j.cortex.2018.11.016
37. Rzepa E, McCabe C. Decreased anticipated pleasure correlates with increased salience network resting state functional connectivity in adolescents with depressive symptomatology. *J Psychiatr Res.* (2016) 82:40–7. doi: 10.1016/j.jpsychires.2016.07.013
38. Zhong X, Pu WD, Yao SQ. Functional alterations of fronto-limbic circuit and default mode network systems in first-episode, drug-naïve patients with major depressive disorder: a meta-analysis of resting-state fMRI data. *J Affect Disord.* (2016) 206:280–6. doi: 10.1016/j.jad.2016.09.005
39. Yuen GS, Gunning-Dixon FM, Hoptman MJ, AbdelMalak B, McGovern AR, Seirup JK, et al. The salience network in the apathy of late-life depressionInt. *J Geriatr Psychiatry.* (2014) 29:1116–24. doi: 10.1002/gps.4171
40. Zhang R, Zhang LH, Wei SN, Wang PS, Jiang XW, Tang YQ, et al. Increased amygdala-paracentral lobule/precuneus functional connectivity associated with patients with mood disorder and suicidal behavior. *Front Hum Neurosci.* (2021) 14:585664. doi: 10.3389/fnhum.2020.585664
41. Zhang SS, Ou RW, Chen XP, Yang J, Zhao B, Yuan XY, et al. Correlative factors of cognitive dysfunction in PD patients: a cross-sectional study from Southwest China. *Neurol Res.* (2016) 38:434–40. doi: 10.1080/01616412.2016.1139320
42. McDermott LM, Ebmeier KP. A meta-analysis of depression severity and cognitive function. *J Affect Disord.* (2009) 119:1–8. doi: 10.1016/j.jad.2009.04.022

Conflict of Interest: The authors declare that the research was conducted in the absence of any commercial or financial relationships that could be construed as a potential conflict of interest.

Publisher's Note: All claims expressed in this article are solely those of the authors and do not necessarily represent those of their affiliated organizations, or those of the publisher, the editors and the reviewers. Any product that may be evaluated in this article, or claim that may be made by its manufacturer, is not guaranteed or endorsed by the publisher.

frontiers | Frontiers in Psychiatry

ORIGINAL RESEARCH
published: 20 May 2022
doi: 10.3389/fpsyt.2022.819498

Urinary Metabolomic Study in a Healthy Children Population and Metabolic Biomarker Discovery of Attention-Deficit/Hyperactivity Disorder (ADHD)

Xiaoyi Tian[1,2†], Xiaoyan Liu[3†], Yan Wang[1], Ying Liu[1], Jie Ma[1], Haidan Sun[3], Jing Li[3], Xiaoyue Tang[3], Zhengguang Guo[3], Wei Sun[3], Jishui Zhang[4*] and Wenqi Song[1,2*]*

[1] Department of Clinical Laboratory, Beijing Children's Hospital, Capital Medical University, National Center for Children's Health, Beijing, China, [2] Beijing Advanced Innovation Center for Big Data-Based Precision Medicine, Beihang University & Capital Medical University, Beijing, China, [3] Proteomics Research Center, Institute of Basic Medical Sciences, School of Basic Medicine, Peking Union Medical College, Chinese Academy of Medical Sciences (CAMS), Beijing, China, [4] Department of Mental Health, Beijing Children's Hospital, Capital Medical University, National Center for Children's Health, Beijing, China

Objectives: Knowledge of the urinary metabolomic profiles of healthy children and adolescents plays a promising role in the field of pediatrics. Metabolomics has also been used to diagnose disease, discover novel biomarkers, and elucidate pathophysiological pathways. Attention-deficit/hyperactivity disorder (ADHD) is one of the most common psychiatric disorders in childhood. However, large-sample urinary metabolomic studies in children with ADHD are relatively rare. In this study, we aimed to identify specific biomarkers for ADHD diagnosis in children and adolescents by urinary metabolomic profiling.

Methods: We explored the urine metabolome in 363 healthy children aged 1–18 years and 76 patients with ADHD using high-resolution mass spectrometry.

Results: Metabolic pathways, such as arachidonic acid metabolism, steroid hormone biosynthesis, and catecholamine biosynthesis, were found to be related to sex and age in healthy children. The urinary metabolites displaying the largest differences between patients with ADHD and healthy controls belonged to the tyrosine, leucine, and fatty acid metabolic pathways. A metabolite panel consisting of FAPy-adenine, 3-methylazelaic acid, and phenylacetylglutamine was discovered to have good predictive ability for ADHD, with a receiver operating characteristic area under the curve (ROC–AUC) of 0.918. A panel of FAPy-adenine, N-acetylaspartylglutamic acid, dopamine 4-sulfate, aminocaproic acid, and asparaginyl-leucine was used to establish a robust model for ADHD comorbid tic disorders and controls with an AUC of 0.918.

Keywords: urinary metabolomics, childhood ADHD, biomarkers, healthy children, mass spectrometry

OPEN ACCESS

Edited by:
Takahiro A. Kato,
Kyushu University, Japan

Reviewed by:
Aihua Zhang,
Heilongjiang University of Chinese Medicine, China
Amelia Palermo,
University of California, Los Angeles, United States

***Correspondence:**
Wei Sun
sunwei@ibms.pumc.edu.cn
Jishui Zhang
zhangjishui@163.com
Wenqi Song
songwenqi1218@163.com

† These authors have contributed equally to this work and share first authorship

Specialty section:
This article was submitted to Child and Adolescent Psychiatry, a section of the journal Frontiers in Psychiatry

Received: *21 November 2021*
Accepted: *19 April 2022*
Published: *20 May 2022*

Citation:
Tian X, Liu X, Wang Y, Liu Y, Ma J, Sun H, Li J, Tang X, Guo Z, Sun W, Zhang J and Song W (2022) Urinary Metabolomic Study in a Healthy Children Population and Metabolic Biomarker Discovery of Attention-Deficit/Hyperactivity Disorder (ADHD). Front. Psychiatry 13:819498. doi: 10.3389/fpsyt.2022.819498

INTRODUCTION

Metabolomics, an innovative analytical profiling technique, aims to detect the whole set of metabolites of low molecular weight present in body fluid. In recent years, it has already shown great potential in exploring the physiological status of healthy populations and in discovering subtle metabolic discrepancies in some specific disorders (1–4).

Urine samples can be collected through non-invasive protocols. Metabolic phenotyping of urine in a healthy population reflects the real-time dynamics of growth and development of the body and documents the physiological status of individuals (1, 2, 5). Some previous urinary metabolomic studies have revealed dynamic metabolic changes associated with age, sex, body mass index (BMI), dietary intake, and demographics in healthy children (1, 6–8), even in healthy neonates (2). Researchers have found that sex deeply influences both quantitative and qualitative urinary organic acid levels in healthy children aged 1–36 months, and the effect of sex is age-dependent (5). Metabolites that correlated with age included creatinine, creatine, glycine, betaine/TMAO, citrate, succinate, and acetone in children aged 12 years and younger (9). The metabolite profile of human urine also allows the prediction of sex and age with high accuracy in adults (10). Sili Fan et al. found that urinary metabolic signatures were globally distinct between healthy male and female children, and the levels of α-ketoglutarate and 4-hydroxybutyric acid increased 2.3-fold and 4.41-fold in male children compared to female children, respectively (11). In the urine of adult female children, succinate, citrate, hippurate, glycine, and malic acid are higher (11, 12), whereas creatine, stearate, alpha-ketoglutarate, and 4-hydroxybutyrate are higher in healthy male children than in female children (11). Due to rapid growth and development in early life, the characteristics of the urinary metabolome are different between children and adults. However, large-scale metabolome studies in healthy children aged 1–18 years are lacking. A high-quality urinary metabolome for children of all ages is in great demand for investigating the metabolic changes in healthy children at each stage throughout early childhood, characterizing early-life physical and environmental exposures and assessing their general health status. Characterizing healthy children's urinary metabolic features and their associations with age and sex can provide a standard reference metabolome, thus helping to assess disease metabolic disturbances and seek detectable biomarkers that differentiate health from disease.

Metabolomics has also been widely employed in identifying specific metabolic fingerprints in neuropsychiatric disorders in children, such as autism spectrum disorder (ASD) (13, 14) and attention-deficit/hyperactivity disorder (ADHD) (15). ADHD is a childhood-onset neurodevelopmental disorder marked by persistent and impaired inattention, hyperactivity/impulsivity, or both (16). It is one of the most common psychiatric disorders in childhood and adolescence, affecting approximately 7% of children worldwide (17), and it is more common in male children. ADHD adversely affects children's emotional, behavioral, cognitive, academic, and social functions (18). Currently, the diagnosis of ADHD mainly depends on behavioral analysis, which is subjective and inconsistent, especially for children. It is imperative to investigate objective laboratory biomarkers for ADHD diagnosis. Recently, a few studies have proposed potential serum biomarkers, such as mono- and polyunsaturated fatty acids and the kynurenine pathway, in children and adults with ADHD, suggesting a potential linkage between metabolic characteristics and ADHD disease pathophysiology (15, 19–21). Bonvicini et al. performed a systematic review and meta-analysis of 6 biochemical studies and found lower serum docosahexaenoic acid (DHA) levels in adults with ADHD (19). Evangelisti et al. examined serum levels of tryptophan and other metabolites of the kynurenine pathway in children with ADHD. They found increased serum levels of tryptophan and kynurenine and reduced levels of kynurenic acid, anthranilic acid, and xanthurenic acid. The AUC of anthranilic acid was 0.88 (95% CI = 0.83–0.94) (22). In contrast to obtaining blood samples, urine is easy to collect in children due to its non-invasive procedures of collection. Urine can potentially provide crucial metabolic information. The applications of urine metabolomics are very promising in biomarker discovery for disease etiology, diagnosis, and prognosis (4, 23). However, there have been fewer urinary metabolomic studies on childhood ADHD.

In this study, we collected urine samples from 363 healthy children aged 1–18 years and 76 patients with ADHD (with or without comorbid tic disorders) for non-targeted metabolite profiling. We sought to (a) define metabolite associations with demographic factors, age, and sex in healthy children in a larger sample, (b) evaluate different urine metabolic profiles between patients with ADHD and healthy controls, and (c) compare different urine metabolic patterns between ADHD patients with/without tic disorders. We found that sex and age can influence interindividual variations in the urine metabolome of healthy children. Differences in urine metabolites were found in patients with ADHD. We constructed a differential metabolite pattern that could simultaneously discriminate three different types of psychiatric status (normal, ADHD, and ADHD with tic disorders). Furthermore, we discovered a biomarker panel that could distinguish ADHD from healthy controls with higher diagnostic values. Here, to the best of our knowledge, for the first time, we have identified novel urinary metabolites that could help to classify children with or without ADHD.

MATERIALS AND METHODS

Cohort

All healthy participants aged 1–18 years were recruited through school voluntarily. Informed consent forms were obtained from each participant's legally authorized representative (parent or guardian). The online health questionnaires based on the inclusion and exclusion criteria were completed by their guardians (24). Healthy volunteers were checked and examined by trained pediatricians according to standard operating procedures. All physical examination indices, including routine urine tests and biochemical tests, were in the normal range. Strict exclusion criteria, such as all types of genetic diseases and clinical

laboratory values indicating acute or chronic disease, were applied. Based on physiological developmental characteristics of children and a previous study (24), we determined five age-specific partitions of the enrolled healthy participants for boys and girls: 1–3 years, 4–6 years, 7–10 years, 11–14 years, and 15–18 years of age.

A senior child psychiatrist interviewed the participants according to the Diagnostic and Statistical Manual of Mental Disorders, Fifth Edition (DSM-5), criteria (25). Conners' parent rating scales were completed by each patient's parents. A continuous performance test (CPT) (26) was administered to all the patients by a technician to obtain behavioral measures of attention. Patients with ADHD with comorbid tic disorders were examined by the Yale Global Tic Severity Scale (YGTSS) (27). Furthermore, experienced child psychiatrists conducted a neurocognitive assessment and physical examination to exclude any neurological disorder other than ADHD. Children with brain damage, a neurological disorder, a genetic disorder, epilepsy, or any other neurological disorder reported during the collection of personal history or anamnesis were excluded. Children who exhibited an IQ of 80 or lower according to the Combined Raven's Test (CRT) or who were receiving drug treatment were also excluded. In this study, 76 outpatients with ADHD were recruited from Beijing Children's Hospital. A total of 44 pediatric patients with ADHD and 32 children with both ADHD and chronic tic disorder were enrolled and randomly selected as the training group and validation group. The clinical features of the training and validation groups were similar. Biomarkers for ADHD with or without comorbid tic disorder were identified based on profiling analysis of 31 patients with ADHD, 21 ADHD patients with a tic disorder, and 46 age- and sex-matched healthy controls. An independent batch of patients with ADHD (13 ADHD and 11 ADHD with tic) and 17 healthy controls were used for external validation of the potential biomarkers using logistic regression.

Urine Sample Collection and Preprocessing

Urine samples were collected and preprocessed according to guidelines (28, 29). Throughout the study, all urine samples were collected from the first urination in the morning under fasting conditions. In clean, dry specimen tubes from the same manufacturer, 10 ml of midstream samples were collected. Samples were centrifuged (3,000 g for 10 min) within 1 h of the collection; the supernatants were isolated, aliquoted, and stored at −80°C until analysis. Samples were shipped at cold temperatures. Freeze–thaw cycles were avoided.

Urine Sample Preparation

Urine samples were prepared using the method described in our previous study (30). Briefly, 200 μl morning midstream urine samples were mixed with 400 μl acetonitrile to precipitate proteins. The mixture was vortexed for 30 s and centrifuged at 14,000 g for 10 min. After drying under vacuum, the supernatant was reconstituted with 200 μl 2% acetonitrile/water. Additionally, 10 kDa molecular weight cut-off ultracentrifugation filters (Millipore Amicon Ultra, MA, United States) were used to remove small proteins from the urine samples before transferring the samples to an autosampler.

The QC standard was prepared by mixing aliquots from all urine samples to assess the stability and repeatability of the analytical process.

LC-HRMS Analysis

Urine sample analyses were conducted by a Waters ACQUITY H-class LC system coupled with an LTQ-Orbitrap mass spectrometer (MS) (Thermo Fisher Scientific, MA, United States). Urinary metabolites were separated with a 29-min gradient on a Waters HSS C18 column (3.0 mm × 100 mm, 1.7 μm) at a flow rate of 0.5 ml/min. Mobile phase A was 0.1% formic acid in H_2O, and mobile phase B was acetonitrile. The gradient was set as follows: 0–1 min, 2% solvent B; 1–8 min, 2%–98% solvent B; 8–8.1 min, 98%–100% solvent B; 8.1–12 min, 100% solvent B; 12–12.1 min, 100%–2% solvent B; and 12.1–17 min, 2% solvent B. The column temperature was 45°C. The full MS acquisition ranged from 100 to 1,000 m/z at a resolution of 60 K in MS1 and 15 K in MS2. The MS1 automatic gain control target was 1×10^6, and the maximum injection time (IT) was 100 ms. The MS2 automatic gain control target was set as 5×10^5, and the maximum IT was 50 ms. The higher-energy collisional dissociation (HCD) fragmentation mode was used to dissociate differential metabolites with the optimal collision energy of 20, 40, 60, or 80 eV. Every urine sample was randomly injected into 3 technical replicates to reduce the experimental bias. All samples were randomly injected into the LC–MS system within a single analysis (within 12 days).

A quality control (QC) sample consisting of representative samples from populations with different genders and ages was used to monitor analytical performance throughout the run and was analyzed at an interval of every 10 samples. Overall, 42 injections were performed during the whole analysis. The analysis showed stable conditions with only a small variation ($< \pm 2$ SD) (**Supplementary Figure 1**). These results provided some assurances that the platform had essential repeatability and stability throughout the analytical run.

Data Processing

The raw data files obtained with LC-MS systems consist of a complex three-dimensional data format comprising retention time, m/z values, and density or abundance on each axis. This comprehensive information needs to be processed before any statistical techniques are applied to analyze the data. Data processing consists of certain steps, and one of them is converting the raw data produced by the instrument into a two-dimensional data matrix. Since data collection in metabolomic studies is carried out using special commercial software that works with LC-MS systems, the raw data obtained from the instruments should be converted to an open standard format such as mzML by using suitable software. After this conversion, the data can be used in many commercial and public programs to create data matrices using a public metabolomics software tool such as XCMS, Progenesis QI, and MetaboAnalyst. All these software are useful in terms of peak picking (EIC: extracted ion

chromatography), deconvolution, and peak alignment. In this study, commercial software, Progenesis QI, was used for peak picking, alignment, and normalization. The data were normalized using "Normalize to the total compound."

Further data preprocessing, including missing value estimation (50% rule), log transformation, and Pareto scaling, was carried out online using Metabo Analyst 5.0, a web-based tool[1]. Variables whose CV% (coefficient of variation) was more than 30% and missed in 50% or more samples were removed for further statistical analysis. Pattern recognition analysis (principal component analysis, PCA; orthogonal partial least squares discriminant analysis, OPLS-DA) was performed using SIMCA 14.0 (Umetrics, Sweden) software. The *Wilcoxon* rank-sum test was used to evaluate the significance of variables between the disease and control groups. Quantification of differentially expressed biomarkers was performed using EIC peak areas extracted and integrated by progenesis QI. Differential variables were selected according to the following rules: (1) adjusted P-value < 0.05, (2) fold change > 1.5, and (3) VIP value > 1.0.

Feature Annotation and Metabolite Identification

Differential features were divided into several targeted lists. The lists were imported to the "MS2 method", such as lists for targeted data-dependent analysis. The MS/MS spectra were further imported into Progenesis QI for metabolite annotation. In this study, two databases were used for MS/MS matching: (1) Metlin MS/MS library (Waters, version 1.0.6499.51447, commercial, composed of authentic standard spectra obtained by orbitrap and TOF mass spectrometry) and (2) fragment library constructed using theoretical fragments calculated by the theoretical fragmentation algorithm, the "MetFrag" algorithm (31). The detailed compound identification information (.csv file) included compound ID, adducts, formula, score, MS/MS score, mass error (in ppm), isotope similarity, theoretical isotope distribution, web link, and m/z values. Confirmation of the differential compounds was performed by the parameter of score value, calculated from mass error, isotope similarity, and fragmentation similarity (fragmentation score). The score value ranged from 0 to 60. According to the score results of the reference standards, the threshold was set at 35.0. Isotope similarity is calculated by comparing the measured isotope distribution of a precursor ion with the theoretical. The more reliable the compound identification, the higher the values obtained. Metabolite function annotation was performed using the KEGG metabolism pathway database, combined with manual annotation by reference searching. The predictive accuracy of biomarkers was assessed using the receiver operating characteristic (ROC) curve plotted in MetaAnalyst 4.0.

[1]http://www.metaboanalyst.ca

RESULTS

Population Characteristics

We recruited a total of 350 healthy children (178 males and 172 females) aged 1–18 years, including five age stages (1–3 years, 4–6 years, 7–10 years, 11–14 years, and 15–18 years), 44 patients with ADHD, and 32 children with both ADHD and tic disorder. The workflow of our study is shown in **Figure 1**. The characteristics of the population included in this analysis

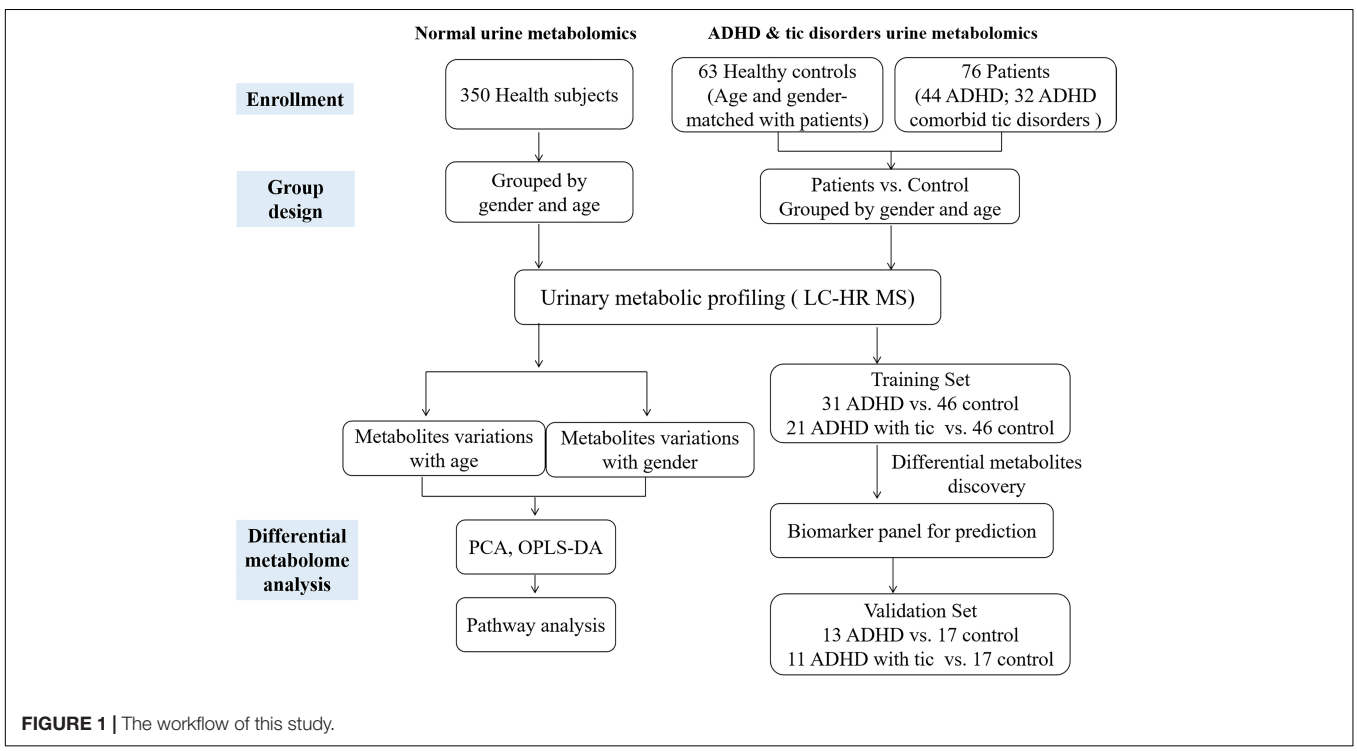

FIGURE 1 | The workflow of this study.

TABLE 1 | Basic characteristics of the subjects enrolled in this study.

(1a) Numbers of healthy controls in different age stages

Age stage	Male	Female	Total
Aged 1-3 (years)	29	25	54
Aged 4-6 (years)	30	29	59
Aged 7-10 (years)	39	40	79
Aged 11-14 (years)	39	39	78
Aged 15-18 (years)	41	39	80
Total	178	172	350

(1b) Means and standard deviations for age used in analysis of the three groups

	ADHD without tic disorders	ADHD comorbid tic disorders	Healthy control
Cases	44	32	63
Age (years)	7.9 ± 2.0	8.7 ± 1.8	7.8 ± 1.8
Gender (Male/Female)	38/6	28/4	58/5

are summarized in **Table 1** and **Supplementary Table 1**. We analyzed urinary metabolic profiling and explored the metabolite variations associated with age and sex.

Gender Variations in Children in Different Age Groups

We performed unsupervised principal component analysis (PCA) and supervised orthogonal partial least squares method-discriminant analysis (OPLS-DA) to explore the tendency of metabolic profiling variations between male and female children in five different age groups. The resulting score plot is shown in **Supplementary Figure 2**. Unsupervised PCA of different age groups showed the tendency that most male samples clustered together, although some male dots overlapped with the female samples (**Supplementary Figure 2**). Class separation could be obviously observed for all male and female children in five different age groups using an OPLS-DA model. Scatter plots showed that sex differences in urine metabolomics in each age group were apparent (**Supplementary Figure 2** and **Figure 2A**). To validate the OPLS-DA model, the use of 100 permutation tests showed no overfitting of the models (**Supplementary Figure 2**).

Metabolites identified in sets with different age groups were selected by using the cut-off of OPLS-DA variable importance in projection (VIP) score of >1.0 and a P-value <0.05. The ratio of expression levels between female and male children is shown in **Supplementary Tables 2A–F**. We identified 73, 30, 28, 33, 69, and 64 metabolites to be significantly different between female and male children in sets aged 1–3, 4–6, 7–10, 11–14, and 15–18, and in all age groups, respectively (**Supplementary Tables 2A∼F**). Approximately half of the differential metabolites showed higher levels in female children, including 5′-methylthioadenosine, indoleacrylic acid, kynuramine, and tauroursodeoxycholic acid. Higher levels of the metabolites of L-Dopa, 3,4-methyleneazelaic acid, and 3-hydroxyhexanoyl carnitine, etc., were found in boys (**Supplementary Tables 2A∼F**).

We applied pathway enrichment analysis to analyze gender-dependent metabolism status in children. **Figure 2B** shows the sex-dependent metabolism pathways in all age groups. Arachidonic acid metabolism, valine-leucine-isoleucine biosynthesis, glycerolipid metabolism, etc., were found to be gender-dependent in children in different age groups (**Figure 2B**). **Table 2** shows gender-dependent metabolism pathways of five different age groups: spermidine and spermine biosynthesis, estrone metabolism, etc., were found to be gender-dependent in healthy children aged 1–3 years; arachidonic acid and bile acid metabolism in children aged 4–6 years; glutamate, leucine, androsterone and fatty acid metabolism, etc., in children aged 7–10 years; proline and androsterone metabolism in children aged 11–14 years; and catecholamine, bile acid, estrone, and tyrosine metabolism, etc., in children aged 15–18 years.

Age Variations in Female and Male Groups

Both the OPLS-DA and PCA models showed the obvious tendency of metabolic profiling variations with age (**Figures 2C,D** and **Supplementary Figure 3**). Five age groups, including 1–3 years, 4–6 years, 7–10 years, 11–14 years, and 15–18 years, were compared. Both the female and male groups showed the same age-dependent metabolic status (**Figures 2C,D**). Notably, one hundred permutation tests showed no overfitting of the two models (**Supplementary Figure 3**).

According to the significance threshold, 250 metabolites were identified as key molecules with a significant correlation with age in the boy group (**Supplementary Table 3**) and 243 metabolites were identified in the girl group (**Supplementary Table 4**). These differential metabolites were submitted for further pathway analysis. **Figures 2E,F** show the relative intensity change trend among the five age groups of male and female children, respectively. Catecholamine biosynthesis, pantothenate and CoA biosynthesis, vitamin B6, androstenedione, and estrone metabolism were found to change with age in boys. In girls, metabolites involved in phenylacetate metabolism, pantothenate and CoA biosynthesis, and pterin biosynthesis were age-dependent (**Table 3** and **Figures 2E,F**).

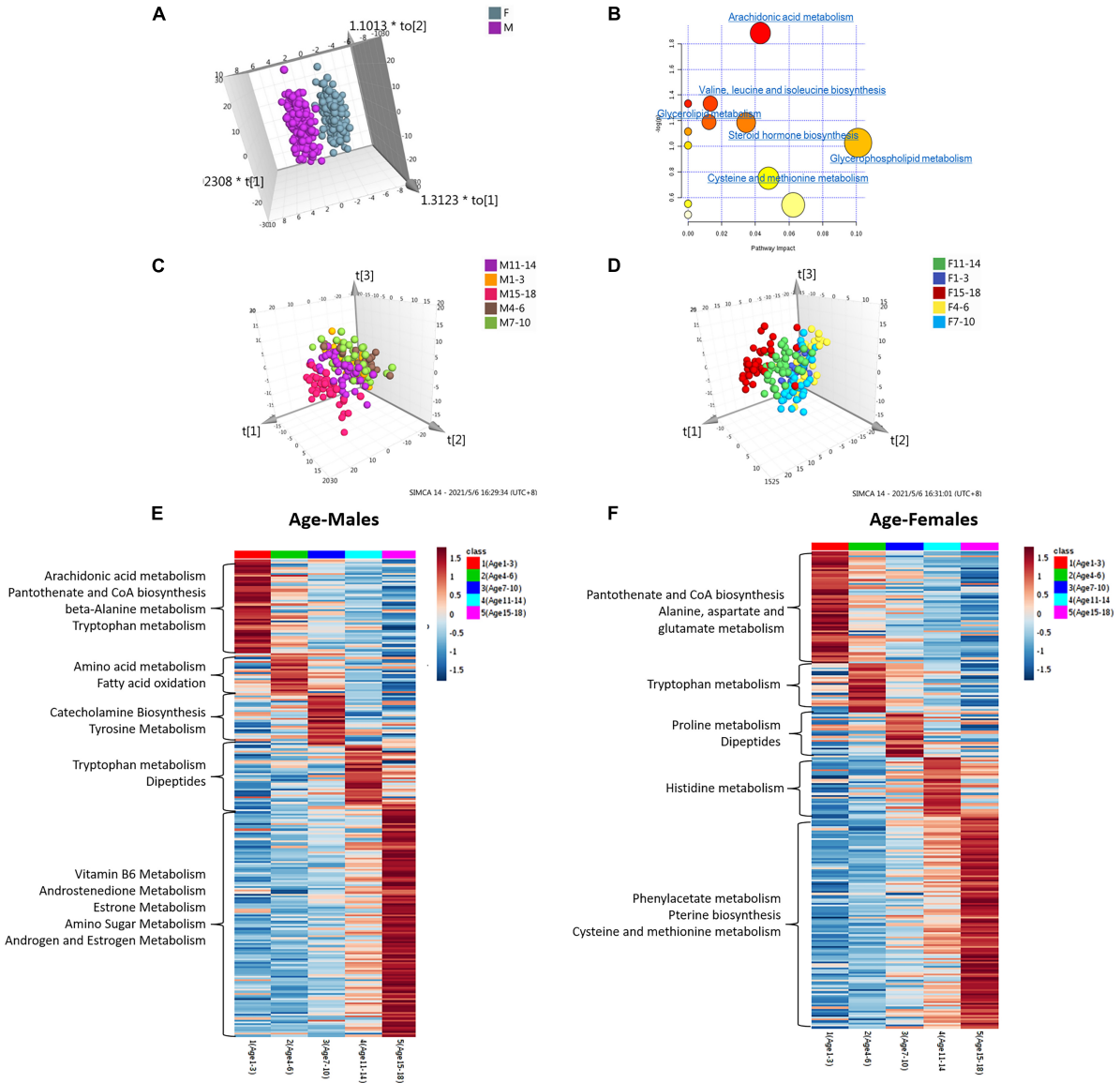

FIGURE 2 | Analysis of metabolome interindividual variations and related factors (gender and age). **(A)** The score plot of the OPLS-DA model between female and male children of all ages. **(B)** Pathway overrepresentation analysis of differential metabolites in the two sex groups. The analysis was carried out with the metabolites in changes ($P < 0.05$). Pathway impact values were plotted against the *X*-axis, and *P*-values were plotted against the *Y*-axis. The node color is determined by its *P*-values, and the node size is proportional to the pathway impact values. (c,d) The score plot of the OPLS-DA model of male children **(C)** and female children **(D)** with different age stages. **(E,F)** Age-dependent metabolic pathways were enriched based on metabolites with the highest level in each age group. The KEGG database was the background pathway database.

Attention-Deficit/Hyperactivity Disorder Biomarker Discovery

From the above results, we found that age and sex are important factors affecting metabolism, so we used age- and sex-matched healthy control subjects to analyze urine metabolomics differences between the ADHD and control groups. Both unsupervised PCA and supervised OPLS-DA suggested apparent discrimination between the two groups (**Supplementary Figures 4A∼B**). Differential metabolites were selected according to the VIP value (VIP > 1). Notably, sixty significantly differential metabolites were identified (**Supplementary Table 5**). The data indicate that metabolites involved in dihydrolipoamide, 3-methylazelaic acid, and phenylacetylglutamine were upregulated in patients with ADHD, whereas the metabolites isohomovanillic acid, indanone, and dopamine 4-sulfate were downregulated.

ROC curves were used to evaluate the diagnostic accuracy of the differential metabolites for ADHD. A metabolite panel consisting of FAPy-adenine, N-acetylaspartylglutamic acid, and dopamine 4-sulphate was found to have the best prediction accuracy for ADHD. The area under the curve (AUC) was 0.923

TABLE 2 | Gender dependent metabolism pathways of five age groups.

Age stages	Metabolism pathways
Aged 1-3 (years)	Spermidine and spermine biosynthesis; Estrone metabolism; Mitochondrial beta-oxidation of short chain saturated fatty acids; Propanoate metabolism; Methionine metabolism; Valine, leucine and isoleucine degradation
Aged 4-6 (years)	Arachidonic acid metabolism; Bile acid metabolism
Aged 7-10 (years)	Glutamate metabolism; Bile acid metabolism; Fatty acid metabolism; Leucine metabolism; Androsterone metabolism
Aged 11-14 (years)	Leukotriene E4 metabolism; Proline metabolism; Androsterone metabolism
Aged 15-18 (years)	Catecholamine biosynthesis; Estrone metabolism; Bile acid biosynthesis; Androgen and estrogen metabolism; Tyrosine metabolism

TABLE 3 | Age dependent metabolism pathways in male and female children.

Gender	Age-dependent metabolism pathways
Male	Arachidonic acid metabolism, Pantothenate and CoA biosynthesis, Beta-alanine metabolism, Tryptophan metabolism, Amino acid metabolism, Fatty acid oxidation, Catecholamine biosynthesis, Tyrosine metabolism, Tryptophan metabolism, Dipeptides, Vitamin B6 metabolism, Androstenedione metabolism, Estrone metabolism, Amino sugar metabolism, Androgen and estrogen metabolism
Female	Pantothenate and CoA biosynthesis, Alanine, aspartate and glutamate metabolism, Tryptophan metabolism, Proline metabolism, Dipeptides, Histidine metabolism, Phenylacetate metabolism, Pterin biosynthesis, Cysteine and methionine metabolism

for the training set (**Table 4**), the sensitivity was 94.2%, and the specificity was 82.6%. Furthermore, an independent batch of patients with ADHD (13 with ADHD and 11 ADHD with tic) and 17 healthy controls were used for external validation of the potential biomarkers. External validation achieved an AUC of 0.877 (**Table 4** and **Supplementary Figure 4C**).

Furthermore, we explored the urine metabolic differences between ADHD without tic disorder and healthy controls. PCA was performed, and the analysis showed apparent discrimination between the control samples and the ADHD disease groups (**Figure 3A**). Furthermore, an OPLS-DA model established for differential metabolite selection also showed apparent discrimination (**Supplementary Figure 5A**). A total of 34 significantly differential metabolites were identified in children with ADHD without tic disorders (**Supplementary Table 6**). Pathway power analysis indicated that tyrosine metabolism, biopterin metabolism, drug metabolism-cytochrome P450, caffeine metabolism, tryptophan metabolism, and N-glycan degradation were differentially regulated in ADHD (**Figure 3C**). A metabolite panel consisting of FAPy-adenine, 3-methylazelaic acid, and phenylacetylglutamine was used to construct a robust model for distinguishing between the healthy group and the ADHD without tic disorder group. The AUC of the panel was 0.918 for the training set (**Table 4**), and its sensitivity and specificity were above 0.8 (**Supplementary Figure 6A**). The AUC for the external validation set was 0.96 (**Table 4** and **Figure 3E**).

Using the same strategy as above, PCA and OPLS-DA models were performed to visualize the metabolomic differences between ADHD comorbid with tic disorder and healthy control subjects. Both PCA and OPLS-DA showed apparent discrimination between the two groups (**Figure 3B**, **Supplementary Figure 5B**). Then, 42 differential metabolites were identified in children with ADHD with comorbid tic disorders (**Supplementary Table 7**). These differential metabolites involve pathways of tyrosine metabolism, biopterin metabolism, sialic acid metabolism, tryptophan metabolism, N-glycan biosynthesis, amino sugar metabolism, glycolysis, gluconeogenesis, and pentose phosphate metabolism (**Figure 3D**). A metabolite panel consisting of FAPy-adenine, N-acetylaspartylglutamic acid, dopamine 4-sulfate, aminocaproic acid, and asparaginyl-leucine was found to have a good distinction between the healthy group and the ADHD with tic disorder group. The AUC-ROC of the panel was 0.918 for the training set (**Table 4**), and it achieved sufficient sensitivity (0.83) and higher specificity (0.91) (**Supplementary Figure 6B**). The AUC-ROC was 0.918 for the external validation set (**Table 4** and **Figure 3F**).

In addition, we examined the main metabolic characteristics of ADHD patients with and without comorbid tic disorder and healthy controls. Metabolites showing the highest level for each group were submitted for pathway analysis, indicating the specific metabolic characteristics for each group. Arginine biosynthesis, pentose and glucuronate interconversions, and alanine, aspartate, and glutamate metabolism were the main metabolic features in the healthy group. Compared with the control group, the two disease groups showed similar metabolic features. Leucine metabolism and fatty acid metabolism showed higher activity in ADHD patients with a tic disorder. In ADHD without tic disorder, glutamate metabolism was active (**Supplementary Figure 7**).

TABLE 4 | ROC of three groups.

	Disease vs. Normal[a]	ADHD vs. Normal[b]	ADHD comorbid tic disorders vs. Normal[c]
	AUC	AUC	AUC
Training Set	0.923	0.918	0.918
Validation Set	0.877	0.96	0.918

a The panel includes FAPy-adenine, N-Acetylaspartylglutamic acid and Dopamine 4-sulfate.
b The panel includes FAPy-adenine, 3-Methylazelaic acid and Phenylacetylglutamine.
c The panel includes FAPy-adenine, N-Acetylaspartylglutamic acid, Dopamine 4-sulfate, Aminocaproic acid and Asparaginyl-Leucine.

DISCUSSION

The analytical platforms to be used for metabolomic studies should be able to simultaneously analyze hundreds of metabolites from complex biological samples and also allow monitoring of changes in these metabolites. However, none of the

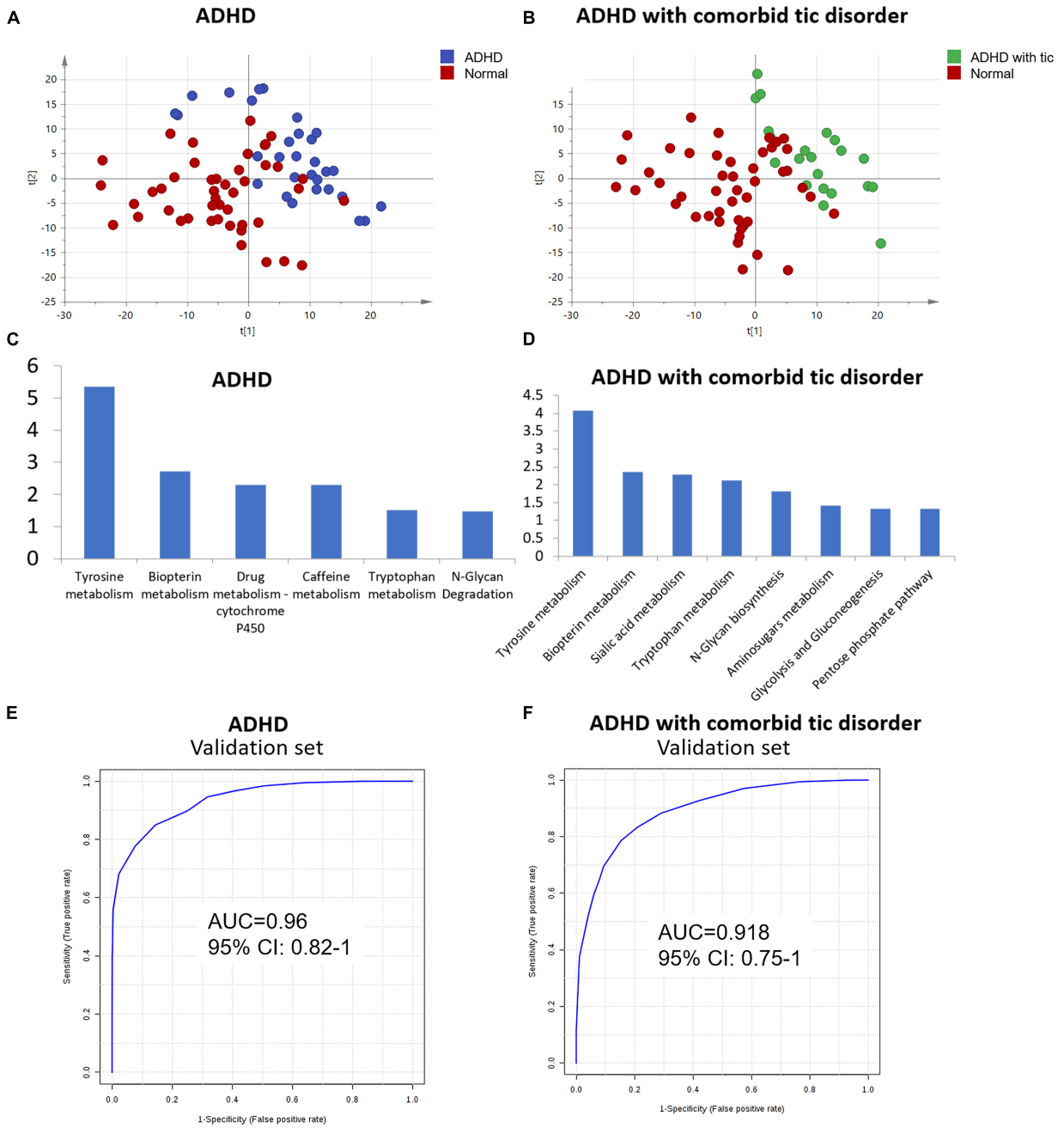

FIGURE 3 | Analysis of metabolome interindividual variations and related factors. **(A)** The score plot of the PCA model between ADHD without tic disorder and normal controls. **(B)** The score plot of PCA based on urine profiling of ADHD comorbid with tic disorder and normal controls. **(C,D)** Enriched pathway of metabolites for ADHD with/without tic disorder. **(E,F)** ROC plot of the validation set of ADHD patients with/without tic disorder.

current analytical platforms available today has the power to fully measure the whole metabolome, and this may be due to the physicochemical diversity of these metabolites, e.g., hydrophilic carbohydrates, volatile alcohols and ketones, amino and non-amino organic acids, and hydrophobic lipids. Analytical techniques, such as NMR, GC-MS, and LC-MS, are the most commonly used analytical methods for metabolomic studies. Different analytical methods showed differences in resolution and sensitivity, which would contribute to the number of identified metabolites. In this study, the LC-MS method was used for biomarker discovery. LC-MS shows higher resolution and sensitivity than NMR and GC-MS and could identify more metabolites (32, 33).

The spectra data files obtained with LC-MS systems consist of a complex three-dimensional data format, comprising retention time, m/z values, and density or abundance on each axis. Data

processing consists of certain steps, and one of them is converting the raw spectra data produced by the instrument into a two-dimensional data matrix, named peak picking and alignment procedures. Several tools, including XCMS, Progenesis QI, and MetaboAnalyst, could perform peak picking. The accuracy of peak picking is imperative in the analysis of LC-MS-based metabolomic data (34). In this study, peak alignment was carried out automatically, using a QC run as the reference. The alignment vector is used for quality control. The quality evaluation results indicated that the score values for all the samples were greater than 80% (35).

Compared to previous adult urine metabolomic studies, there are relatively few studies on healthy children. Due to rapid growth and development in early life, each age range in the childhood period has different metabolic features. In this study, we characterized the urine metabolic profiles of a large sample size of healthy children among five different age groups (from 1 to 18 years of age) using the LC–MS/MS platform. Our results showed that the urinary metabolic signature of children was associated with sex and age parameters. Urine is a sensitive matrix that can reflect physiological and pathological changes. Urine metabolomics reflects the disturbance in disease states and is commonly used for the diagnosis of neuropsychiatric diseases. Urine samples are routinely collected easily from young children. Our study identified seven urinary metabolites that could be used as effective biomarker panels for ADHD diagnosis and could help to elucidate the underlying molecular pathological mechanisms of the disease.

Gender-Dependent Metabolism Status in the Healthy Children Population

Previous studies have highlighted the impact of sex on the urinary metabolome in adults (10, 36–38). Manuela J. Rist et al. found that urine metabolite profiles could predict sex in healthy adults with an accuracy of prediction of approximately 90% (10). Several studies also underlined that sex was one of the most relevant biological variables significantly influencing metabolomic profiles in children. Scalabre and coworkers (7) investigated the influence of age on the newborns' urine metabolome during the first 4 months of life using ^{1}H-NMR spectroscopy combined with multivariate statistical analyses. They did not find any statistically significant differences between male and female children. However, Caterino et al. (5) investigated sex influences on 72 organic acids measured through GC–MS analysis in the urine of 291 children aged 1–36 months and stratified them into four age groups. They demonstrated that sex deeply influenced urinary organic acid levels, and the sex-induced variations depended on age. López-Hernández and their team (2) identified and quantified 136 metabolites in the urine of 48 healthy neonates collected in the first 24 h of life, and sex differences were found for 15 metabolites.

In this study, we included healthy children aged 1–18 years and almost equal numbers of healthy male and female subjects (50.9% boys/49.1% girls). Interestingly, our results suggest that gender differences in the urinary metabolome are already present during childhood, even from the early years of life (1–3 years of age). Our pathway analysis revealed strong differences in steroid hormone biosynthesis and valine-leucine and isoleucine biosynthesis between female and male children in all age groups. In addition, our results showed that the influence of sex was linked to age, and the single age group presented some specificity. The metabolic phenotypes of boys showed the presence of significantly higher concentrations of 3-hydroxydodecanoyl carnitine and 3-hydroxyhexanoyl carnitine and lower 11-beta-hydroxyandrosterone-3-glucuronide and valyl-proline compared to girls in all age groups. Carnitine plays important role in fatty acid oxidation and branched-chain amino acid metabolism. It can facilitate fatty acids to shuttle the mitochondrial membrane by combining with fatty acids to form acyl-carnitines. 3-Hydroxydodecanoyl carnitine and 3-hydroxyhexanoyl carnitine belong to the family of acyl-carnitines, which are beta-oxidation products of fatty acids (39). Previous studies have reported that healthy adult male subjects (19–69 years) had higher levels of urinary metabolites related to fatty acid oxidation (carnitine, acetylcarnitine) than female subjects (38), and newborns had a markedly increased acylation degree of carnitine in urine compared with healthy boys (8–15 years) (40). In this study, we confirmed gender-specific acylcarnitine metabolites in urine in younger children aged 1–3 years. Elevated carnitine and its related metabolites in male children relative to female children may suggest a greater usage of fats for energy metabolism for male children at rest vs. female children (38).

Age-Dependent Metabolism Status in the Healthy Children Population

Urine and serum metabolomics were reported to reveal dynamic metabolic changes associated with age both in children (1, 7–9) and in the adult population (10, 36, 41). However, to date, most metabolome studies in children have covered a relatively narrow age range. Here, we provided an overview of the dynamic metabolic changes in a large cohort of healthy children, comprising all age groups from 1 to 18 years of age, which potentially provided complete information on rapid physical growth during the childhood period. Since we observed that sex played an important role in urine metabolism profiling, we analyzed age variation in boys (males) and girls (females). We found that pantothenic acid urinary concentration decreases with age both in boys and girls. Pantothenic acid is an essential micronutrient and serves as a cofactor in the synthesis of coenzyme A, which is essential for the metabolism and synthesis of the TCA cycle and fatty acid oxidation (42). Aureìlien Scalabre et al. also observed that urinary pantothenate decreased with age and weight in newborns under 4 months of age (7).

In addition, we found that the pathways of catecholamine biosynthesis, vitamin B6, estrone, and androstenedione metabolism changed with age in boys; phenylacetate metabolism and pterin biosynthesis were age-dependent in girls. Age-related differences in urinary catecholamine excretion both in adults and in children have been reported by several studies (43–47). There was a sex difference, with lower values in girls and women than in their male counterparts (48, 49). The 24-h urinary excretion

of dopamine (DA) was significantly inversely related to age in adult women but not in men (47). However, Anne et al. found that there was a linear relationship between age and the excretion of the urinary catecholamine metabolites epinephrine (E), DA, vanillylmandelic acid (VMA), and homovanillic acid (HVA) in children aged 3–16 years (45). Dalmaz et al. also determined catecholamines (DA, E, and norepinephrine (NE)) in human urine from one day of age to adulthood. They observed that the maturation process of the sympathoadrenal system is not achieved at birth; both sympathetic and glandular function remain low during a prolonged period in childhood, reaching full maturation probably near the fifth year of life (44). Here, we found that urinary DA, HVA, and 6-hydroxydopamine levels changed with age in males/boys, reaching a peak at the age of 7–10 years. In addition, androstenedione, androstanol, and their glucuronide metabolites showed high levels during prepubescence (11–14 years) and puberty (15–18 years). Our results demonstrated that age-dependent metabolic profile changes revealed not only rapid growth occurring in childhood but also sex maturation.

Attention-Deficit/Hyperactivity Disorder Biomarker Discovery

Currently, metabolic strategies have been used to characterize specific metabolic phenotypes associated with ADHD disorders, and several metabolites have been identified (3, 15, 19). The urinary metabolism of ADHD has not been sufficiently investigated thus far in children. It is essential to determine an accurate and sensitive non-invasive diagnostic biomarker of ADHD for children in whom disease diagnosis is more difficult. In our study, a panel based on three urinary metabolites was found to have high accuracy for ADHD disease, and a pattern based on three urinary metabolites, namely, FAPy-adenine, 3-methylazelaic acid, and phenylacetylglutamine, was found to have high sensitivity and specificity for ADHD without tic disorders, as was a panel based on five urinary metabolites for ADHD with tic disorders.

We compared the urinary metabolic profile between the pediatric ADHD cases and the age- and gender-matched healthy controls, and we observed a total of 60 metabolites that could significantly differentiate cases with ADHD from the healthy controls. Our metabolic pathway analysis showed that amino acid metabolism (e.g., L-norleucine and citrulline) and fatty acid metabolism (e.g., aminocaproic acid and 3-methylazelaic acid) pathways were associated with ADHD. Previous ADHD studies have suggested that metabolites in blood serum involved in fatty acids contribute to the distinction between adults diagnosed with ADHD and control groups (21, 50). In our study, we found that the content of 3,4-methylenepimelic acid in urine was decreased in ADHD groups, and aminocaproic acid and 3-methylazelaic acid were increased in patients with ADHD. Although the specific pathological mechanisms of these fatty acids are not yet clear, our results indicated that fatty acid metabolism in patients with ADHD was disturbed.

Dopamine (DA) is a member of the catecholamine family of neurotransmitters. The correlation between DA and ADHD is the most widely studied. DA is synthesized by converting tyrosine into levodopa (L-DOPA), which can then be converted into DA. Extensive neurobiological, pharmacological, and neuroimaging evidence suggests that ADHD is characterized by defects in DA production or metabolic disorders (44, 45). In our study, we found that urinary metabolites belonging to the tyrosine metabolic pathways displayed the largest differences between patients with ADHD and healthy controls. The change in urinary metabolites involving tyrosine metabolic pathways may indirectly reflect dopamine metabolic profile alterations in ADHD. Moreover, we found that the urinary levels of the main degradation metabolites of DA, dopamine 4-sulfate and isohomovanillic acid, were decreased in children diagnosed with ADHD. Sulfation is one of the major degradative pathways of DA, and the main excretion products of DA found in human urine are homovanillic acid and its sulfates (46). Several studies have found changes in urinary levels of dopamine and its metabolites (homovanillic acid, dihydroxyphenylalanine, and dihydroxyphenylacetic acid) in patients with ADHD (47). Our results are consistent with previous reports and indicate that urinary DA metabolites could be potential diagnostic candidates. However, taking into consideration the complexities of dopamine production and metabolism, the relationship between urinary metabolic alternation and the molecular mechanism of ADHD remains to be fully elucidated. Urinary nucleosides and deoxynucleosides are mainly known as metabolites of RNA turnover and oxidative damage of DNA. FAPy-adenine is an oxidized DNA base. Oxidized nucleosides are biochemical markers for some neurodegenerative diseases (Alzheimer's disease) (51). Combined with the other two metabolites, dopamine 4-sulphate and N-acetylaspartylglutamic acid, FAPy-adenine obtained higher diagnostic accuracy (ROC-AUC was above 0.8). However, its pathological mechanism in ADHD needs to be explored further.

CONCLUSION

This study provided an overview of the dynamic urinary metabolic changes in children from 1 to 18 years of age. These results may be potentially useful in assessing the biological age (as opposed to chronological) of young humans as well as in providing a deeper understanding of the confounding factors in the application of metabolomics. Such a large-scale cohort may pave the way for the future building of urine metabolomic reference profiles in healthy children and may provide insight into the complex metabolic changes in children's growth and development.

ADHD is more difficult to diagnose in children, as the disease diagnosis depends on the parent's scale and physicians' diagnostic procedure, which has been criticized for strong subjectivity. Here, our pilot study encouraged the application of a panel of metabolites in ADHD diagnosis and offered the opportunity to standardize and improve disease diagnostic assessment.

Our study has several limitations that should be mentioned. First, while the ADHD-specific urinary metabolites were

validated in one independent sample cohort in our study, the sample size was still relatively small, which may have reduced the statistical power of the study. Our findings need to be further validated with a larger sample. In the future, we will collect more samples to validate the findings. Second, we found urinary metabolite markers between children with ADHD and healthy controls; however, the causal relationships between these peripheral biomarkers and central nervous system disease remain unknown. Furthermore, we will carry out the functional study of these urinary metabolites in animal models of childhood ADHD. It could increase our understanding of the pathological mechanism of ADHD.

DATA AVAILABILITY STATEMENT

The original contributions presented in the study are included in the article/**Supplementary Material**, further inquiries can be directed to the corresponding authors.

ETHICS STATEMENT

The studies involving human participants were reviewed and approved by the Ethics Committee of Beijing Children's Hospital. Written informed consent to participate in this study was provided by the participants' legal guardian/next of kin. Written informed consent was obtained from the individual(s), and minor(s)' legal guardian/next of kin, for the publication of any potentially identifiable images or data included in this article.

AUTHOR CONTRIBUTIONS

XTi, XL, JL, and XTa performed the experiments. ZG, HS, and YL verified the methodology. YW, YL, and JM collected urine samples and clinical data. XTi and XL wrote the manuscript. WSu, JZ, and WSo designed the study. All authors contributed to the article and approved the submitted version.

FUNDING

This project has received fundings from the Special Fund of the Pediatric Medical Coordinated Development Center of Beijing Hospitals Authority (Award number: XTCX201815, Recipient: WSo), the Beihang University and Capital Medical University Advanced Innovation Centre for Big Data-Based Precision Medicine Plan (Award number: BHME-201910, Recipient: WSo), Beijing Talents Fund (Award number: 2018000021469G278, Recipient: XTi), National Natural Science Foundation of China (Award number: 82170524, Recipient: WSu and Award number: 31901039, Recipient: XL), Beijing Medical Research (Award number: 2018-7, Recipient: WSu), and CAMS Innovation Fund for Medical Sciences (Award number: 2021-1-I2M-016, Recipient: WSu).

SUPPLEMENTARY MATERIAL

The Supplementary Material for this article can be found online at: https://www.frontiersin.org/articles/10.3389/fpsyt.2022.819498/full#supplementary-material

REFERENCES

1. Lau CHE, Siskos AP, Maitre L, Robinson O, Athersuch TJ, Want EJ, et al. Determinants of the urinary and serum metabolome in children from six European populations. *BMC Med.* (2018) 16:202. doi: 10.1186/s12916-018-1190-8
2. López-Hernández Y, Oropeza-Valdez JJ, Blanco-Sandate JO, Herrera-Van Oostdam AS, Zheng J, Chi Guo A, et al. The urinary metabolome of healthy newborns. *Metabolites.* (2020) 10:165. doi: 10.3390/metabo10040165
3. Yang J, Yan B, Zhao B, Fan Y, He X, Yang L, et al. Assessing the causal effects of human serum metabolites on 5 major psychiatric disorders. *Schizophr Bull.* (2020) 46:804–13. doi: 10.1093/schbul/sbz138
4. Alves S, Paris A, Rathahao-Paris E. Mass spectrometry-based metabolomics for an in-depth questioning of human health. *Adv Clin Chem.* (2020) 99:147–91. doi: 10.1016/bs.acc.2020.02.009
5. Caterino M, Ruoppolo M, Villani GRD, Marchese E, Costanzo M, Sotgiu G, et al. Influence of sex on urinary organic acids: a cross-sectional study in children. *Int J Mol Sci.* (2020) 21:582. doi: 10.3390/ijms21020582
6. Moco S, Collino S, Rezzi S, Martin FPJ. Metabolomics perspectives in pediatric research. *Pediatr Res.* (2013) 73:570–6. doi: 10.1038/pr.2013.1
7. Scalabre A, Jobard E, Demède D, Gaillard S, Pontoizeau C, Mouriquand P, et al. Evolution of newborns' urinary metabolomic profiles according to age and growth. *J Proteome Res.* (2017) 16:3732–40. doi: 10.1021/acs.jproteome.7b00421
8. Chiu CY, Yeh KW, Lin G, Chiang MH, Yang SC, Chao WJ, et al. Metabolomics reveals dynamic metabolic changes associated with age in early childhood. *PLoS One.* (2016) 11:e0149823. doi: 10.1371/journal.pone.0149823
9. Gu H, Pan Z, Xi B, Hainline BE, Shanaiah N, Asiago V, et al. 1H NMR metabolomics study of age profiling in children. *NMR Biomed.* (2009) 22:826–33. doi: 10.1002/nbm.1395
10. Rist MJ, Roth A, Frommherz L, Weinert CH, Krüger R, Merz B, et al. Metabolite patterns predicting sex and age in participants of the Karlsruhe metabolomics and nutrition (KarMeN) study. *PLoS One.* (2017) 12:e0183228. doi: 10.1371/journal.pone.0183228
11. Fan S, Yeon A, Shahid M, Anger JT, Eilber KS, Fiehn O, et al. Sex-associated differences in baseline urinary metabolites of healthy adults. *Sci Rep.* (2018) 8:11883. doi: 10.1038/s41598-018-29592-3
12. Psihogios NG, Gazi IF, Elisaf MS, Seferiadis KI, Bairaktari ET. Gender-related and age-related urinalysis of healthy subjects by NMR-based metabonomics. *NMR Biomed.* (2008) 21:195–207. doi: 10.1002/nbm.1176
13. Gevi F, Zolla L, Gabriele S, Persico AM. Urinary metabolomics of young Italian autistic children supports abnormal tryptophan and purine metabolism. *Mol Autism.* (2016) 7:47. doi: 10.1186/s13229-016-0109-5
14. Glinton KE, Elsea SH. Untargeted metabolomics for autism spectrum disorders: current status and future directions. *Front Psychiatry.* (2019) 10:647. doi: 10.3389/fpsyt.2019.00647
15. Bonvicini C, Faraone SV, Scassellati C. Common and specific genes and peripheral biomarkers in children and adults with attention-deficit/hyperactivity disorder. *World J Biol Psychiatry.* (2018) 19:80–100. doi: 10.1080/15622975.2017.1282175
16. Faraone SV, Asherson P, Banaschewski T, Biederman J, Buitelaar JK, Ramos-Quiroga JA, et al. Attention-deficit/hyperactivity disorder. *Nat Rev Dis Prim.* (2015) 1:15020.

17. Thomas R, Sanders S, Doust J, Beller E, Glasziou P. Prevalence of attention-deficit/hyperactivity disorder: a systematic review and meta-analysis. *Pediatrics.* (2015) 135:e994–1001. doi: 10.1542/peds.2014-3482
18. Posner J, Polanczyk GV, Sonuga-Barke E. Attention-deficit hyperactivity disorder. *Lancet.* (2020) 395:450–62.
19. Bonvicini C, Faraone SV, Scassellati C. Attention-deficit hyperactivity disorder in adults: a systematic review and meta-analysis of genetic, pharmacogenetic and biochemical studies. *Mol Psychiatry.* (2016) 21:872–84. doi: 10.1038/mp.2016.74
20. Aarsland TIM, Landaas ET, Hegvik TA, Ulvik A, Halmøy A, Ueland PM, et al. Serum concentrations of kynurenines in adult patients with attention-deficit hyperactivity disorder (ADHD): a case–control study. *Behav Brain Funct.* (2015) 11:36. doi: 10.1186/s12993-015-0080-x
21. Irmisch G, Richter J, Thome J, Sheldrick AJ, Wandschneider R. Altered serum mono– and polyunsaturated fatty acid levels in adults with ADHD. *Atten Defic Hyperact Disord.* (2013) 5:303–11. doi: 10.1007/s12402-013-0107-9
22. Evangelisti M, De Rossi P, Rabasco J, Donfrancesco R, Lionetto L, Capi M, et al. Changes in serum levels of kynurenine metabolites in paediatric patients affected by ADHD. *Eur Child Adolesc Psychiatry.* (2017) 26:1433–41. doi: 10.1007/s00787-017-1002-2
23. Yap IKS, Angley M, Veselkov KA, Holmes E, Lindon JC, Nicholson JK. Urinary metabolic phenotyping differentiates children with autism from their unaffected siblings and age-matched controls. *J Proteome Res.* (2010) 9:2996–3004. doi: 10.1021/pr901188e
24. Ni X, Song W, Peng X, Shen Y, Peng Y, Li Q, et al. Pediatric reference intervals in China (PRINCE): design and rationale for a large, multicenter collaborative cross-sectional study. *Sci Bull.* (2018) 63:1626–34. doi: 10.1016/j.scib.2018.11.024
25. Association AP. *Diagnostic and Statistical Manual of Mental Disorders*. 5th ed. Arlington, VA: American Psychiatric Publishing (2013).
26. Epstein JN, Erkanli A, Conners CK, Klaric J, Costello JE, Angold A. Relations Between continuous performance test performance measures and ADHD behaviors. *J Abnorm Child Psychol.* (2003) 31:543–54. doi: 10.1023/a:1025405216339
27. Leckman JF, Riddle MA, Hardin MT, Ort SI, Swartz KL, Stevenson J, et al. The yale global tic severity scale: initial testing of a clinician-rated scale of tic severity. *J Am Acad Child Adolesc Psychiatry.* (1989) 28:566–73. doi: 10.1097/00004583-198907000-00015
28. Bi H, Guo Z, Jia X, Liu H, Ma L, Xue L. The key points in the pre-analytical procedures of blood and urine samples in metabolomics studies. *Metabolomics.* (2020) 16:68. doi: 10.1007/s11306-020-01666-2
29. González-Domínguez R, González-Domínguez Á, Sayago A, Fernández-Recamales Á. Recommendations and best practices for standardizing the pre-analytical processing of blood and urine samples in metabolomics. *Metabolites.* (2020) 10:229. doi: 10.3390/metabo10060229
30. Liu X, Cheng X, Liu X, He L, Zhang W, Wang Y, et al. Investigation of the urinary metabolic variations and the application in bladder cancer biomarker discovery. *Int J Cancer.* (2018) 143:408–18. doi: 10.1002/ijc.31323
31. Allen F, Pon A, Wilson M, Greiner R, Wishart D. CFM-ID: a web server for annotation, spectrum prediction and metabolite identification from tandem mass spectra. *Nucleic Acids Res.* (2014) 42:W94–9. doi: 10.1093/nar/gku436
32. Zeki Ö C, Eylem CC, Reçber T, Kır S, Nemutlu E. Integration of GC-MS and LC-MS for untargeted metabolomics profiling. *J Pharm Biomed Anal.* (2020) 190:113509. doi: 10.1016/j.jpba.2020.113509
33. Crook AA, Powers R. Quantitative NMR-based biomedical metabolomics: current status and applications. *Molecules.* (2020) 25:5128. doi: 10.3390/molecules25215128
34. Fiehn O, Wohlgemuth G, Scholz M, Kind T, Lee DY, Lu Y, et al. Quality control for plant metabolomics: reporting MSI-compliant studies. *Plant J.* (2008) 53:691–704. doi: 10.1111/j.1365-313X.2007.03387.x
35. Zhang J, Yang W, Li S, Yao S, Qi P, Yang Z, et al. An intelligentized strategy for endogenous small molecules characterization and quality evaluation of earthworm from two geographic origins by ultra-high performance HILIC/QTOF MS(E) and progenesis QI. *Anal Bioanal Chem.* (2016) 408:3881–90. doi: 10.1007/s00216-016-9482-3
36. Thévenot EA, Roux A, Xu Y, Ezan E, Junot C. Analysis of the human adult urinary metabolome variations with age, body mass index, and gender by implementing a comprehensive workflow for univariate and OPLS statistical analyses. *J Proteome Res.* (2015) 14:3322–35.
37. Wu J, Gao Y. Physiological conditions can be reflected in human urine proteome and metabolome. *Expert Rev Proteomics.* (2015) 12:623–36. doi: 10.1586/14789450.2015.1094380
38. Slupsky CM, Rankin KN, Wagner J, Fu H, Chang D, Weljie AM, et al. Investigations of the effects of gender, diurnal variation, and age in human urinary metabolomic profiles. *Anal Chem.* (2007) 79:6995–7004. doi: 10.1021/ac0708588
39. Steiber A, Kerner J, Hoppel CL. Carnitine: a nutritional, biosynthetic, and functional perspective. *Mol Aspects Med.* (2004) 25:455–73. doi: 10.1016/j.mam.2004.06.006
40. Cederblad G, Finnström O, Mårtensson J. Urinary excretion of carnitine and its derivatives in newborns. *Biochem Med.* (1982) 27:260–5. doi: 10.1016/0006-2944(82)90029-1
41. Saito K, Maekawa K, Kinchen JM, Tanaka R, Kumagai Y, Saito Y. Gender– and age-associated differences in serum metabolite profiles among Japanese populations. *Biol Pharm Bull.* (2016) 39:1179–86. doi: 10.1248/bpb.b16-00226
42. Velazquez-Arellano A, Hernandez-Vazquez ADJ. Vitamins as cofactors for energy homeostasis and their genomic control, with special reference to biotin, thiamine, and pantothenic acid. In: Caterina RDE, Martinez JA, Kohlmeier M editors. *Principles of Nutrigenetics and Nutrigenomics*. (Cambridge, MA: Academic Press) (2020). p. 271–7. doi: 10.1016/b978-0-12-804572-5.00035-5
43. Moyer TP, Jiang NS, Tyce GM, Sheps SG. Analysis for urinary catecholamines by liquid chromatography with amperometric detection: methodology and clinical interpretation of results. *Clin Chem.* (1979) 25:256–63. doi: 10.1093/clinchem/25.2.256
44. Dalmaz Y, Peyrin L, Sann L, Dutruge J. Age-related changes in catecholamine metabolites of human urine from birth to adulthood. *J Neural Transm.* (1979) 46:153–74. doi: 10.1007/BF01250336
45. Prémel-Cabic A, Turcant A, Allain P. Normal reference intervals for free catecholamines and their acid metabolites in 24-h urines from children, as determined by liquid chromatography with amperometric detection. *Clin Chem.* (1986) 32:1585–7. doi: 10.1093/clinchem/32.8.1585
46. Haap M, Blaschka F, Lehmann R, Hoyer A, Müssig K. Association between urinary catecholamine excretion and urine volume. *Horm Metab Res.* (2019) 51:531–8. doi: 10.1055/a-0926-3532
47. Gerlo EA, Schoors DF, Dupont AG. Age– and sex-related differences for the urinary excretion of norepinephrine, epinephrine, and dopamine in adults. *Clin Chem.* (1991) 37:875–8. doi: 10.1093/clinchem/37.6.875
48. Lakatua DJ, Nicolau GY, Bogdan C, Plinga L, Jachimowicz A, Sackett-Lundeen L, et al. Chronobiology of catecholamine excretion in different age groups. *Prog Clin Biol Res.* (1987) 227B:31–50.
49. Hansen Åse M, Garde Anne H, Christensen-Jytte M, Eller-Nanna H, Netterstrøm B. Reference intervals and variation for urinary epinephrine, norepinephrine and cortisol in healthy men and women in Denmark. *Clin Chem Lab Med.* (2001) 39:842–9. doi: 10.1515/CCLM.2001.140
50. Young GS, Maharaj NJ, Conquer JA. Blood phospholipid fatty acid analysis of adults with and without attention deficit/hyperactivity disorder. *Lipids.* (2004) 39:117–23. doi: 10.1007/s11745-004-1209-3
51. Gabbita SP, Lovell MA, Markesbery WR. Increased nuclear DNA oxidation in the brain in Alzheimer's disease. *J Neurochem.* (1998) 71:2034–40. doi: 10.1046/j.1471-4159.1998.71052034.x

Conflict of Interest: The authors declare that the research was conducted in the absence of any commercial or financial relationships that could be construed as a potential conflict of interest.

frontiers | Frontiers in Psychiatry

OPINION
published: 28 June 2022
doi: 10.3389/fpsyt.2022.913303

Imbalances in Kynurenines as Potential Biomarkers in the Diagnosis and Treatment of Psychiatric Disorders

*Aye-Mu Myint and Angelos Halaris**

Department of Psychiatry, Loyola University School of Medicine and Loyola University Medical Center, Maywood, IL, United States

Keywords: kynurenine, glutamate, GABA, treatment resistant depression (TRD), esketamine

INTRODUCTION

Psychiatric disorders are heterogeneous in many aspects. Due to this heterogeneity, many hypotheses have been proposed especially in regards to understanding the etiopathology of these disorders. A variety of molecules and their associated systems have been proposed as presumptive etiological factors in different psychiatric disorders. Based on some of these hypotheses, many pharmacological agents have been developed over the course of over half a century. It is impossible to state whether a certain hypothesis is right or wrong. Each hypothesis may be applicable to certain individuals, for a certain condition and/or specific symptoms. In the majority of psychiatric syndromes, more than a single system is involved in the pathophysiology of the disorder in a given individual. As a matter of fact, in most of these patients, an array of different molecules act synergistically as a network, at times facilitatory and at times inhibitory. However, there are certain molecules or systems that play a key role in the network of several molecules. For example, chronic subclinical imbalances in the immune system is such a key etiopathogical determinant. Furthermore, imbalances in the kynurenine pathway resulting mainly through imbalances in the immune system, play a key role in dysregulations in several other systems, such as serotonergic, glutamatergic, dopaminergic, noradrenergic and Gamma amino-butyric acid (GABAergic) neurotransmissions (1).

The kynurenine pathway (**Figure 1**) has been reported to be involved in several psychiatric disorders (2–6). Medications, such as escitalopram, reportedly reduce neurotoxicity in depression (7). Recently, based on knowledge of the kynurenine pathway, and involvement of NMDA-R in chronic depression and suicide, a new medication which acts through NMDA-R antagonism, esketamine nasal spray, was developed and approved by the United States Food and Drug Administration (FDA) for treatment resistant depression (8) and in emergency situations to prevent suicide in severe depression (9). Based on the fact that the kynurenine pathway has a huge network with other neurochemical pathways, questions remain whether esketamine might also be therapeutically useful in other psychiatric conditions.

In this minireview, we analyzed the knowledge and information we have regarding the involvement of the kynurenine pathway in different psychiatric disorders, its complex interactions with other neuronal and neurochemical systems, and the introduction of innovative therapeutic agents, notably esketamine, and its possible therapeutic roles since esketamine is the only currently available medication which is directly link to the role of kynurenine pathway in psychiatric disorders. Nevertheless, the role of timely administration of anti-inflammatory agents is also discussed as a preventive measure for treatment resistant depression.

OPEN ACCESS

Edited by:
Takahiro A. Kato, Kyushu University, Japan

Reviewed by:
Magdalena Sowa-Kucma, University of Rzeszow, Poland

***Correspondence:**
Angelos Halaris
ahalaris@luc.edu

Specialty section:
This article was submitted to Molecular Psychiatry, a section of the journal Frontiers in Psychiatry

Received: *11 April 2022*
Accepted: *27 May 2022*
Published: *28 June 2022*

Citation:
Myint A-M and Halaris A (2022) Imbalances in Kynurenines as Potential Biomarkers in the Diagnosis and Treatment of Psychiatric Disorders. Front. Psychiatry 13:913303. doi: 10.3389/fpsyt.2022.913303

The blue, green and red colored text and arrows indicate the metabolic pathway itself. Blue color depicts the neutral nature in terms of neurotoxicity while the red color depicts neurotoxicity and green color depicts neuroprotection. The black color lines and texts indicate the network. The dotted arrows depict the inhibitory effect, while the complete arrows depict the excitatory or stimulatory effect. The double headed arrow indicate the antagonism in action. The thickness of the arrow indicates the strength of the effect.

KYNURENINE PATHWAY IN RELATION TO OTHER NEUROCHEMICALS

Kynurenine Pathway and Serotonergic System

The kynurenine pathway is directly related to the serotonergic system. Serotonin is synthesized from tryptophan which is an essential amino acid. This amino acid can also be degraded into kynurenine in the tryptophan metabolic pathway. This degradation can occur through one of two enzymes, tryptophan 2,3-dioxygenase (TDO) or indolamine 2,3-dioxygenase (IDO) (10–12). The enzyme TDO is activated by the stress hormone cortisol (13, 14), while the IDO enzyme is activated by the pro-inflammatory cytokines, such as interferon γ (IFN γ), interleukin 6 (IL6) and tumor necrosis factor α (TNF α) (15, 16). Therefore, chronic inflammation or the unregulated chronic imbalance in the immune system, as well as stress can activate the tryptophan degradation pathway, the kynurenine pathway. This increased degradation of tryptophan will lead to reduction in the availability of tryptophan for serotonin synthesis and ultimately reduction in the synthesis of serotonin. Serotonergic deficiency has been closely associated with depressive mood, and reversal of serotonergic deficiency by serotonin reuptake inhibitors (SSRI's) restores mood at least in a percentage of depressed patients.

Kynurenine (KYN), the degradation product of tryptophan by the enzymes, IDO or TDO, is further degraded to kynurenic acid (KYNA) via kynurenine amino transferases (KATs), or to 3-hydroxy kynurenine (3-HK) by kynurenine monooxygenase (KMO). 3-HK is further degraded to quinolinic acid (QUIN), the final product of which is nicotinamide adenine dinucleotide (NAD). QUIN is the antagonist of the NMDA type of the glutamate receptor. NMDA receptors are important in information processing in neurons, as well as in toxicity (17). On the other hand, KYNA is a NMDA-R agonist and considered to be neuroprotective against QUIN induced neurotoxicity (18). Since KMO enzymatic activity is enhanced by the pro-inflammatory cytokine, IFN γ, formation of QUIN is enhanced in cases of chronic immune activation. KMO activity is suppressed by the anti-inflammatory cytokine, IL4 (19). Enhanced QUIN can induce excitotoxicity through the NMDA-R and, in turn, neurotoxicity. These processes might, at least partially, contribute to treatment resistance or chronicity in depression and expand our understanding of the etiopathology of depression beyond serotonin depletion (20). In addition, this mechanism may not be confined only to depression since other disorders such as schizophrenia and bipolar disorders are also chronic disorders.

Kynurenine Pathway and Glutamatergic System

Since QUIN is the antagonist of the NMDA type of the glutamate receptor, when there is chronic uncorrected immune activation, the formation of QUIN is enhanced and its synergistic

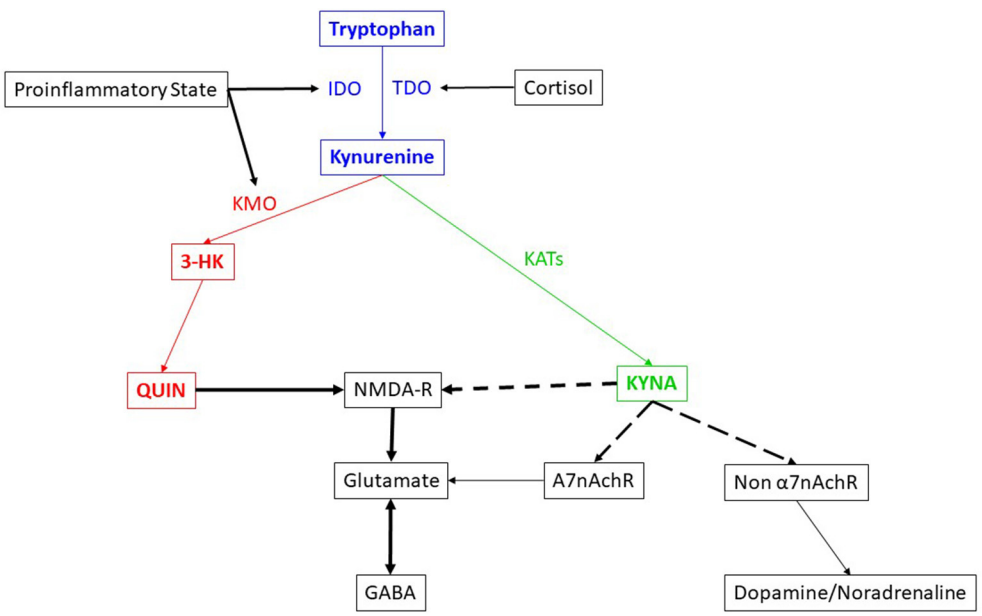

FIGURE 1 | Brief description of the kynurenine pathway and its interaction with other systems.

agonistic action to Glutamate at the NMDA-R is also enhanced. This increase of QUIN can occur with or without increase in KYNA, the metabolite from the other arm of the KYN pathway. Sometimes, KYNA becomes even decreased, since the pathway is shifted to the arm of QUIN and in this manner, QUIN can induce neurotoxicity. Although this outcome might not be directly involved in inducing the symptoms of depression or schizophrenia or bipolar disorder or any specific symptoms of a psychiatric disorder, it could definitely induce neurotoxicity and neurodegeneration which could eventually result in treatment resistance or chronicity of the psychiatric illness (20).

However, KYNA which is a NMDA-R antagonist, and is generally considered as a protective metabolite against QUIN (21), can also be toxic, since it is also an antagonist of all ionotropic excitatory amino acid receptor activities (19). Its abnormal accumulation beyond physiological levels could induce glutamatergic hypo-functioning and might diminish cognitive function (22). Moreover, while one of the tryptophan metabolites, 5-hydroxyindole (5HI), activates the α7-nicotinic acetylcholine receptor (α7nAchR) and induces glutamate release (23, 24), KYNA is an antagonist of a7nAchR (25). Since KYNA downregulates the permissive role of 5HI activation at the α 7nAchR, the accumulation of KYNA could suppress α7nAchR function and induce disruption of auditory sensory gating (26). This is considered to be a causal factor in psychotic symptoms development.

In summary, the above referenced imbalances in the metabolism of the kynurenine pathway play an important role in psychiatric disorders in regards to aspects of acute psychotic symptom development as well as chronicity or treatment resistance. In addition, the neurotoxicity and cognitive disturbances through the enhanced degradation of KYN into KYNA and QUIN might play a role in neurodegenerative disorders. This would explain the connection between depression and dementia.

Kynurenine Pathway and Dopaminergic/Noradrenergic System

In addition, 5HI inhibits the non- α7nAchR mediated release of noradrenaline, dopamine and acetylcholine (27), while KYNA regulates the activity and expression of non-a7nAchR based on dosage and length of exposure (25). Through this action, the abnormal accumulation of KYNA might disturb dopaminergic and noradrenergic neurotransmission as well. It has long been known that noradrenergic and dopaminergic neurotransmission play important roles in both mood disorders and schizophrenia.

Kynurenine Pathway and GABAergic System

Although not through the direct action of kynurenines on the GABAergic pathway, the kynurenine pathway has an association with GABAergic neurotransmission through its NMDA receptor activity. In this subsection, the interaction between GABAergic and glutamatergic transmission in general, and its associations with psychiatric and neuropsychiatric disorders will be briefly described.

To maintain optimal central nervous system (CNS) function, a balance between excitatory and inhibitory synaptic transmission is essential for long-term stability and function of neuronal networks. Traditionally, excitatory and inhibitory neurotransmission systems have been associated with the glutamatergic and GABAergic systems, respectively. Homeostatic synaptic plasticity depends on signaling cascades regulating in parallel the efficacy of glutamatergic and GABAergic transmission and homeostatic synaptic plasticity (28). In this context, glutamine (Gln) is a precursor of several neurotransmitter amino acids, notably. the excitatory amino acids, glutamate (Glu) and aspartate (Asp), and the inhibitory amino acid, γ-amino butyric acid (GABA). Gln is present in the CNS and participates in a variety of metabolic pathways. Disturbances of Gln metabolism and/or transport contribute to changes in glutamatergic or GABAergic transmission associated with brain pathology (29).

Dysfunction of the GABAergic/glutamatergic network in telencephalic brain structures may be the major pathogenetic mechanism underlying psychotic symptoms in schizophrenia and bipolar disorder. GABAergic neuropathology may underlie the disturbance of the reciprocal interaction between GABAergic interneurons and principal glutamatergic pyramidal neurons and this may induce positive and negative symptoms and cognitive dysfunction that are observed in psychotic patients (30, 31). Many studies have suggested that schizophrenia and bipolar disorder are diseases characterized by a deficit of GABAergic transmission with consequent glutamatergic and monoaminergic network dysfunction (32–34).

Stress has long been recognized as a major contributory factor to medical and psychiatric illnesses. Prolonged stress and different forms of experimental stress suppress the inhibitory action of GABA, thereby causing hyperactivation of glutamatergic stimulation of Corticotrophin releasing factor (CRF) producing cells and exhaustion of the hypothalamo-pituitary-adrenal (HPA) axis resulting in low levels of glucocorticoids. This is sometimes referred to as "the GABAergic deficit hypothesis of major depressive disorder" (35, 36). Since cortisol, a stress hormone enhances the tryptophan degradation, increased formation of kynurenine pathway metabolites plays a role in enhanced glutamatergic neurotransmission through NMDA-R activity.

An imbalance between excitatory and inhibitory neurotransmission systems may also underlie the synaptic dysfunction caused by β-amyloid (Aβ) peptides (37–40). Pharmacological treatments aimed at modulating excitatory and/or inhibitory neurotransmission may be helpful in improving symptoms of Alzheimer's Disease (AD). It has been suggested that strategies aimed at reestablishing the balance between both systems, particularly in early stages of AD, may be effective in halting, if not reversing, the functional deficits caused by Aβ (40–42). The correlation between kynurenine pathway (KP) metabolites and AD with major emphasis on its two functionally contrasting neuroactive metabolites, KYNA and QUIN the reader is referred to this review article (43).

A significant non-invasive imaging tool that is presently available to elucidate brain biochemistry, especially as it relates to the highly complex neuronal pathways, such the pathways summarily reviewed in this article, is magnetic resonance spectroscopy (MRS). Using ^{13}C label, ^{13}C MRS can visualize

the role of glutamate/GABA neurotransmission in disorders referred to above, notably AD, schizophrenia, and bipolar disorder (44).

KYNURENINE PATHWAY INVOLVEMENT IN PSYCHIATRIC DISORDERS

Mood Disorder

As stated earlier, in the case of a pro-inflammatory state and IDO activation, there will be reduced serotonin availability for serotonergic neurotransmission. The pro-inflammatory status in major depressive disorder, documented in numerous studies, would activate not only IDO but also KMO enzyme activities and this activation may in turn shift KYN metabolism to the 3-HK and QUIN arm. It has been proposed that the increase in these toxic metabolites, may make the astrocyte–microglia–neuronal network vulnerable to environmental factors, such as stress. It has also been proposed that an impaired glial-neuronal network, induced by the unbalanced KYN pathway, may contribute to the recurrence and chronicity of major depressive disorder (20). The neurotoxic metabolites may then induce astrocytic and neuronal apoptosis, which would weaken the function of the glial–neuronal network. Loss of astrocyte function could also impair glutamate–glutamine metabolism through the glutamine synthetase enzyme, which occurs mainly in astrocytes (45).

In medication-naïve or medication-free patients with major depressive disorder, an imbalance has been demonstrated between these neuroprotective and neurotoxic pathways, with reduction in the protective metabolite, KYNA (2). The ratio between KYNA and KYN, which indicates how much of the KYN would be degraded into KYNA, was significantly lower in depressed patients than healthy controls. After a 6-week medication trail with currently available antidepressants, mainly selective serotonin reuptake inhibitors (SSRI's), the metabolic imbalance in the KYN pathway could not be reversed. This imbalance might, in the long term, induce neurodegenerative changes and these, in turn, might induce chronicity and treatment resistance. In our study (5) on QUIN immunoreactivity in post-mortem brain tissues from patients with major depressive disorder or bipolar depression and normal controls, we demonstrated that QUIN immunoreactivity was increased in the prefrontal cortex area in the brains of patients with major depression and patients with bipolar depression who committed suicide. However, in our postmortem immunohistochemical investigation, we observed decreased QUIN immuno-stained microglia in the hippocampal area of the depressed patients (46). This could be due to the fact that QUIN enhanced expression in the brain is area specific, or, that there was a failure to detect QUIN expression due to cell loss in hippocampal area. Another study on KYN metabolites concentrations in the cerebrospinal fluid (CSF) of suicidal patients with different psychiatric disorders also demonstrated the increase in QUIN concentration regardless of the psychiatric disorders (47). This indicates that the KYN metabolites imbalance in the brain in suicidal patients is not limited only to major depression.

Kynurenine Pathway Involvement in Schizophrenia

Regarding the KYN pathway in schizophrenia, a study of KYNA concentrations in post-mortem brain tissue in different cortical regions revealed increased KYNA in the samples from schizophrenic patients compared with a control sample, particularly in the prefrontal cortex (48). In another investigation of the anterior cingulate cortex, a small and non-significant increase of KYNA in medicated schizophrenics was observed (49). Our postmortem histochemical study in brain tissue from chronically medicated patients showed reduced QUIN staining in the hippocampal area (50). These studies raised the question of whether the increase in KYNA might be associated with antipsychotic medication. However, increased levels of KYNA were also observed in the cerebrospinal fluid of schizophrenic patients (51). Since most of the patients in this study were drug-naïve first-episode patients, this increase could not have been caused by antipsychotic treatment. It was hypothesized that accumulation of KYNA may lead to schizophrenic symptoms (52). Our finding in medication-naïve schizophrenic patients indicated increased plasma 3-HK and decreased plasma KYNA compared to healthy controls, and this was reversed after 6 weeks of antipsychotic treatment. This finding would be an indirect indicator of the accumulation of 3-HK due to enhanced KMO activity (4) in those patients which might further lead to increased QUIN formation. In addition, a recent study on KYN metabolites in brain tissue failed to show either increased KYNA or decreased QUIN in schizophrenia (53). Thus, the findings regarding KYN metabolites in schizophrenia are inconclusive.

While increased KYNA could induce psychotic symptoms, increased QUIN could also induce neurotoxicity and probably also suicide. Therefore, it is not very conclusive in management of schizophrenia via manipulation of KYN metabolites.

Kynurenine Pathway and Drug Discoveries

Based on all findings from basic, preclinical and clinical studies, ketamine, an NMDA antagonistic medication, has received major interest over the last two decades (54, 55). A study has demonstrated that a single infusion of ketamine could induce reduction in Montgomery Asberg Depression Rating Score (MADRS) and suicidal ideation score in treatment resistant patients with major depression or bipolar depression (56). An even stronger but short-term effect was demonstrated with (S)-ketamine, an enantiomer of ketamine (9). Although (S)-ketamine is four times more potent at the NMDA receptor than another enantiomer (R)-ketamine (57), the (R)-isoform showed a longer-term effect on depressive symptom reduction (58). The improvement of suicidal ideation was also documented with intranasal ketamine (59). In 2019, esketamine as an intranasal antidepressant for treatment resistant depression, was approved by FDA (8). Esketamine is also now approved for use in major depressive disorder patients presenting with suicidal ideation or intent.

As discussed above, increased QUIN concentration in CSF of suicidal patients is not limited to major depression. A question could be raised whether indications for the use of esketamine could be expanded to other psychiatric emergency conditions beyond major depression.

FUTURE PERSPECTIVES

In previous studies, both QUIN immunohistochemical expression in the anterior cingulate cortex (5) and increased QUIN CSF concentration (47) were documented in suicidal patients with different psychiatric disorders. However, in hippocampus of both depressed and schizophrenic patients in general (both suicide victims and those who died due to other causes), we could not demonstrate increased QUIN immunohistochemical expression (46, 50), but we found decreased expression instead. This raises the question whether the imbalance in QUIN expression between different brain areas could induce compulsive and aggressive behavior, such as suicide in those patients with psychiatric disorders, notably mood and schizophrenic disorders. If this were to be the case, further opportunities could present themselves in drug development. Carefully and closely observed clinical studies should be performed to achieve the preventive treatment for suicide in both depressive disorders and psychotic disorders.

Moreover, based on the findings which indicated the role of inflammatory state in inducing increased tryptophan degradation and imbalance in KYN metabolites, to prevent the development of treatment resistance in psychiatric disorders through timely use of anti-inflammatory medication should also be considered.

Since it is not easy to analyze the KYN metabolites in the specific brain regions, new invention in imaging technology to achieve a surrogate marker for this imbalance in the KYN metabolites in the different brain region could be very useful to take preventive measures for suicide and neurotoxicity.

AUTHOR CONTRIBUTIONS

Both authors contributed to the concept, design, and writing of this mini review article. Both authors contributed to the article and approved the submitted version.

REFERENCES

1. Myint AM. Kynurenines: from the perspective of major psychiatric disorders. *FEBS J.* (2012) 279:1375–85. doi: 10.1111/j.1742-4658.2012.08551.x
2. Myint AM, Leonard BE, Steinbusch HW, Kim YK. Th1, Th2, and Th3 cytokine alterations in major depression. *J Affect Disord.* (2005) 88:167–73. doi: 10.1016/j.jad.2005.07.008
3. Kim YK, Myint AM, Lee BH, Han CS, Lee SW, Leonard BE, et al. T-helper types 1, 2, and 3 cytokine interactions in symptomatic manic patients. *Psychiatry Res.* (2004) 129:267–72. doi: 10.1016/j.psychres.2004.08.005
4. Kim YK, Myint AM, Lee BH, Han CS, Lee HJ, Kim DJ, et al. Th1, Th2 and Th3 cytokine alteration in schizophrenia. *Prog Neuropsychopharmacol Biol Psychiatry.* (2004) 28:1129–34. doi: 10.1016/j.pnpbp.2004.05.047
5. Steiner J, Walter M, Gos T, Guillemin GJ, Bernstein HG, Sarnyai Z, et al. Severe depression is associated with increased microglial quinolinic acid in subregions of the anterior cingulate gyrus: evidence for an immune-modulated glutamatergic neurotransmission? *J Neuroinflammation.* (2011) 8:94. doi: 10.1186/1742-2094-8-94
6. Veen C, Myint AM, Burgerhout KM, Schwarz MJ, Schütze G, Kushner SA, et al. Tryptophan pathway alterations in the postpartum period and in acute postpartum psychosis and depression. *J Affect Disord.* (2016) 189:298–305. doi: 10.1016/j.jad.2015.09.064
7. Halaris A, Myint AM, Savant V, Meresh E, Lim E, Guillemin G, et al. Does escitalopram reduce neurotoxicity in major depression? *J Psychiatr Res.* (2015) 66–7:118–26. doi: 10.1016/j.jpsychires.2015.04.026
8. Kim J, Farchione T, Chen Q, Temple R. Esketamine for treatment-resistant depression - first FDA approved antidepressant in a new class. *N Engl J Med.* (2019) 381:1–4. doi: 10.1056/NEJMp1903305
9. Canuso CM, Singh JB, Fedgchin M, Alphs L, Lane R, Lim P, et al. Efficacy and safety of intranasal esketamine for the rapid reduction of symptoms of depression and suicidality in patients at imminent risk for suicide: results of a double-blind, randomized, placebo-controlled study. *Am J Psychiatry.* (2018) 175:620–30. doi: 10.1176/appi.ajp.2018.17060720
10. Watanabe Y, Fujiwara M, Yoshida R, Hayaishi O. Stereospecificity of hepatic L-tryptophan 2,3-dioxygenase. *Biochem J.* (1980) 189:393–405. doi: 10.1042/bj1890393
11. Heyes MP, Saito K, Major EO, Milstien S, Markey SP, Vickers JH. A mechanism of quinolinic acid formation by brain in inflammatory neurological disease Attenuation of synthesis from L-tryptophan by 6-chlorotryptophan and 4-chloro-3-hydroxyanthranilate. *Brain.* (1993) 116:1425–50. doi: 10.1093/brain/116.6.1425
12. Mellor AL, Munn DH. Tryptophan catabolism and T-cell tolerance: immunosuppression by starvation? *Immunol Today.* (1999) 20: 469–473. doi: 10.1016/S0167-5699(99)01520-0
13. Knox WE. Two mechanisms which increase in vivo the liver tryptophan peroxidase activity: specific enzyme adaptation and stimulation of the pituitary adrenal system. *Br J Exp Pathol.* (1951) 32:462–9.
14. Salter M, Pogson CI. The role of tryptophan 2,3-dioxygenase in the hormonal control of tryptophan metabolism in isolated rat liver cells effects of glucocorticoids and experimental diabetes. *Biochem J.* (1985) 229:499–504. doi: 10.1042/bj2290499
15. Carlin JM, Borden EC, Sondel PM, Byrne GI. Biologic-response-modifier-induced indoleamine 2,3-dioxygenase activity in human peripheral blood mononuclear cell cultures. *J Immunol.* (1987) 139:2414–8.
16. Yasui H, Takai K, Yoshida R, Hayaishi O. Interferon enhances tryptophan metabolism by inducing pulmonary indoleamine 2,3-dioxygenase: its possible occurrence in cancer patients. *Proc Natl Acad Sci USA.* (1986) 83:6622–6. doi: 10.1073/pnas.83.17.6622
17. Verkersky A, Kirchhoff F. Glutamate-mediated neuronal-glial transmission. *J Anat.* (2007) 210:651–60. doi: 10.1111/j.1469-7580.2007.00734.x
18. Musso T, Gusella GL, Brooks A, Longo DL, Varesio L. Interleukin-4 inhibits indoleamine 2,3-dioxygenase expression in human monocytes. *Blood.* (1994) 83:1408–11. doi: 10.1182/blood.V83.5.1408.1408
19. Perkins MN, Stone TW. An iontophoretic investigation of the actions of convulsant kynurenines and their interaction with the endogenous excitant quinolinic acid. *Brain Res.* (1982) 247:184–7. doi: 10.1016/0006-8993(82)91048-4
20. Myint AM, Kim YK. Cytokine-serotonin interaction through IDO: a neurodegeneration hypothesis of depression. *Med Hypotheses.* (2003) 61:519–25. doi: 10.1016/S0306-9877(03)00207-X
21. Guillemin GJ, Kerr SJ, Smythe GA, Smith DG, Kapoor V, Armati PJ, et al. Kynurenine pathway metabolism in human astrocytes: a paradox for neuronal protection. *J Neurochem.* (2001) 78:842–53. doi: 10.1046/j.1471-4159.2001.00498.x
22. Olney JW, Labruyere J, Wang G, Wozniak DF, Price MT, Sesma MA. NMDA antagonist neurotoxicity: mechanism and prevention. *Science.* (1991) 254:1515–8. doi: 10.1126/science.1835799
23. Zwart R, De Filippi G, Broad LM, McPhie GI, Pearson KH, Baldwinson T, et al. 5-Hydroxyindole potentiates human alpha 7 nicotinic receptor-mediated responses and enhances acetylcholine-induced glutamate release in cerebellar slices. *Neuropharmacology.* (2002) 43:374–84. doi: 10.1016/S0028-3908(02)00094-1
24. Mannaioni G, Carpenedo R, Moroni F. 5-hydroxyindole causes convulsions and increases transmitter release in the CA1 region of the rat hippocampus. *Br J Pharmacol.* (2003) 138:245–53. doi: 10.1038/sj.bjp.0705007
25. Hilmas C, Pereira EF, Alkondon M, Rassoulpour A, Schwarcz R, Albuquerque EX. The brain metabolite kynurenic acid inhibits alpha7 nicotinic receptor activity and increases nonalpha7 nicotinic receptor

expression: physiopathological implications. *J Neurosci.* (2001) 21:7463–73. doi: 10.1523/JNEUROSCI.21-19-07463.2001
26. Shepard PD, Joy B, Clerkin L, Schwarcz R. Micromolar brain levels of kynurenic acid are associated with a disruption of auditory sensory gating in the rat. *Neuropsychopharmacology.* (2003) 28:1454–62. doi: 10.1038/sj.npp.1300188
27. Grilli M, Raiteri L, Patti L, Parodi M, Robino F, Raiteri M, et al. Modulation of the function of presynaptic alpha7 and non-alpha7 nicotinic receptors by the tryptophan metabolites, 5-hydroxyindole and kynurenate in mouse brain. *Br J Pharmacol.* (2006) 149:724–32. doi: 10.1038/sj.bjp.0706914
28. Tyagarajan SK, Fritschy JM. GABA(A) receptors, gephyrin, and homeostatic synaptic plasticity *J Physiol.* (2010) 588:101–106. doi: 10.1113/jphysiol.2009.178517
29. Albrecht J, Sidoryk-Wegrzynowicz M, Zielińska M, Aschner M. Roles of glutamine in neurotransmission. *Neuron Glia Biol.* (2010) 6:263–76. doi: 10.1017/S1740925X11000093
30. Lewis DA, González-Burgos G. Neuroplasticity of neocortical circuits in schizophrenia. *Neuropsychopharmacology.* (2008) 33:141–65. doi: 10.1038/sj.npp.1301563
31. Lisman JE, Coyle JT, Green RW, Javitt DC, Benes FM, Heckers S, et al. Circuit-based framework for understanding neurotransmitter and risk gene interactions in schizophrenia Trends. *Neurosci.* (2008) 31:234–42. doi: 10.1016/j.tins.2008.02.005
32. Benes FM, Lim B, Matzilevich D, Walsh JP, Subburaju S, Minns M. Regulation of the GABA cell phenotype in hippocampus of schizophrenics and bipolars. *Proc Natl Acad Sci USA.* (2007) 104:10164–9. doi: 10.1073/pnas.0703806104
33. Guidotti A, Auta J, Davis JM, Dong E, Grayson DR, Veldic M, et al. GABAergic dysfunction in schizophrenia: new treatment strategies on the horizon. *Psychopharmacology.* (2005) 180:191–205. doi: 10.1007/s00213-005-2212-8
34. Guidotti A, Auta J, Chen Y, Davis JM, Dong E, Gavin DP, et al. Epigenetic GABAergic targets in schizophrenia and bipolar disorder. *Neuropharmacology.* (2011) 60:1007–16. doi: 10.1016/j.neuropharm.2010.10.021
35. Luscher B, Shen Q, Sahir N. The GABAergic deficit hypothesis of major depressive disorder. *Mol Psychiatry.* (2011) 16:383–406. doi: 10.1038/mp.2010.120
36. Fogaça MV, Duman RS. Cortical GABAergic dysfunction in stress and depression: new insights for therapeutic interventions. *Front Cell Neurosci.* (2019) 13:87. doi: 10.3389/fncel.2019.00087
37. Sun B, Halabisky B, Zhou Y, Palop JJ Yu G, Mucke L, Gan L. Imbalance between GABAergic and glutamatergic transmission impairs adult neurogenesis in an animal model of Alzheimer's disease. *Cell Stem Cell.* (2009) 5:624–33. doi: 10.1016/j.stem.2009.10.003
38. Palop JJ, Mucke L. Synaptic depression and aberrant excitatory network activity in Alzheimer's disease: two faces of the same coin? *Neuromolecular Med.* (2010) 12:48–55. doi: 10.1007/s12017-009-8097-7
39. Palop JJ, Mucke L. Network abnormalities and interneuron dysfunction in Alzheimer disease. *Nat Rev Neurosci.* (2016) 17:777–92. doi: 10.1038/nrn.2016.141
40. Verret L, Mann EO, Hang GB, Barth AM, Cobos I, Ho K, et al. Inhibitory interneuron deficit links altered network activity and cognitive dysfunction in Alzheimer model. *Cell.* (2012) 149:708–21. doi: 10.1016/j.cell.2012.02.046
41. Huang Y, Mucke L. Alzheimer mechanisms and therapeutic strategies. *Cell.* (2012) 148:1204–22. doi: 10.1016/j.cell.2012.02.040
42. Mucke L, Selkoe DJ. Neurotoxicity of amyloid β-protein: synaptic and network dysfunction. *Cold Spring Harb Perspect Med.* (2012) 2:a006338. doi: 10.1101/cshperspect.a006338
43. Sharma R, Razdan K, Bansal Y, Kuhad A. Rollercoaster ride of kynurenines: steering the wheel towards neuroprotection in Alzheimer's disease. *Expert Opin Therap Targets.* (2018) 22:849–67. doi: 10.1080/14728222.2018.1524877
44. Mandal PK, Guha Roy R, Samkaria A, Maroon JC, Arora Y. *In vivo* 13 C magnetic resonance spectroscopy for assessing brain biochemistry in health and disease. *Neurochem Res.* (2022) 47:1183–201. doi: 10.1007/s11064-022-03538-8
45. Lavoie J, Giguere JF, Layrargues GP, Butterworth RF. Activities of neuronal and astrocytic marker enzymes in autopsied brain tissue from patients with hepatic encephalopathy. *Metab Brain Dis.* (1987) 2:283–90. doi: 10.1007/BF00999698
46. Busse M, Busse S, Myint AM, Gos T, Dobrowolny H, Müller UJ, et al. Decreased quinolinic acid in the hippocampus of depressive patients: evidence for local anti-inflammatory and neuroprotective responses? *Eur Arch Psychiatry Clin Neurosci.* (2015) 265:321–9. doi: 10.1007/s00406-014-0562-0
47. Erhardt S, Lim CK, Linderholm KR, Janelidze S, Lindqvist D, Samuelsson M et al. Connecting inflammation with glutamate agonism in suicidality. *Neuropsychopharmacol.* (2013) 38:743–52. doi: 10.1038/npp.2012.248
48. Schwarcz R, Rassoulpour A, Wu HQ, Medoff D, Tamminga CA, Roberts RC. Increased cortical kynurenate content in schizophrenia. *Biol Psychiatry.* (2001) 50:521–30. doi: 10.1016/S0006-3223(01)01078-2
49. Miller CL, Llenos IC, Dulay JR, Weis S. Upregulation of the initiating step of the kynurenine pathway in postmortem anterior cingulate cortex from individuals with schizophrenia and bipolar disorder. *Brain Res.* (2006) 1073–4:25–37. doi: 10.1016/j.brainres.2005.12.056
50. Gos T, Myint AM, Schiltz K, Meyer-Lotz G, Dobrowolny H, Busse S, et al. Reduced microglial immunoreactivity for endogenous NMDA receptor agonist quinolinic acid in the hippocampus of schizophrenia patients. *Brain Behav Immun.* (2014) 41:59–64. doi: 10.1016/j.bbi.2014.05.012
51. Erhardt S, Blennow K, Nordin C, Skogh E, Lindstrom LH, Engberg G. Kynurenic acid levels are elevated in the cerebrospinal fluid of patients with schizophrenia. *Neurosci Lett.* (2001) 313:96–8. doi: 10.1016/S0304-3940(01)02242-X
52. Erhardt S, Schwieler L, Engberg G. Kynurenic acid and schizophrenia. *Adv Exp Med Biol.* (2003) 527:155–65. doi: 10.1007/978-1-4615-0135-0_18
53. Afia AB, Vila È, MacDowell KS, Ormazabal A, Leza JC, Haro JM, et al. Kynurenine pathway in post-mortem prefrontal cortex and cerebellum in schizophrenia: relationship with monoamines and symptomatology. *J Neuroinflammation.* (2021) 18:198. doi: 10.1186/s12974-021-02260-6
54. Oye I, Paulsen O, Maurset A. Effects of ketamine on sensory perception: evidence for a role of N-methyl-D-aspartate receptors. *J Pharmacol Exp Ther.* (1992) 260:1209–13.
55. Miller OH, Yang L, Wang CC, Hargroder EA, Zhang Y, Delpire E, et al. GluN2B-containing NMDA receptors regulate depression-like behavior and are critical for the rapid antidepressant actions of ketamine. *Elife.* (2014) 3:e03581. doi: 10.7554/eLife.03581.009
56. Price RB, Nock MK, Charney DS, Mathew SJ. Effects of intravenous ketamine on explicit and implicit measures of suicidality in treatment-resistant depression. *Biol Psychiatry.* (2009) 66:522–6. doi: 10.1016/j.biopsych.2009.04.029
57. Sinner B, Graf BM. Ketamine. *Handb Exp Pharmacol.* (2008) 313–33. doi: 10.1007/978-3-540-74806-9_15
58. Singh JB, Fedgchin M, Daly E, Xi L, Melman C, De Bruecker G, et al. Intravenous esketamine in adult treatment-resistant depression: a double-blind, double-randomization, placebo-controlled study. *Biol Psychiatry.* (2016) 80:424– 431. doi: 10.1016/j.biopsych.2015.10.018
59. Daly EJ, Singh JB, Fedgchin M, Cooper K, Lim P, Shelton RC, et al. Efficacy and safety of intranasal esketamine adjunctive to oral antidepressant therapy in treatment resistant depression: a randomized clinical trial. *JAMA Psychiatry.* (2018) 75:139–48. doi: 10.1001/jamapsychiatry.2017.3739

Conflict of Interest: The authors declare that the research was conducted in the absence of any commercial or financial relationships that could be construed as a potential conflict of interest.

Publisher's Note: All claims expressed in this article are solely those of the authors and do not necessarily represent those of their affiliated organizations, or those of the publisher, the editors and the reviewers. Any product that may be evaluated in this article, or claim that may be made by its manufacturer, is not guaranteed or endorsed by the publisher.

frontiers | Frontiers in Psychiatry

ORIGINAL RESEARCH
published: 12 July 2022
doi: 10.3389/fpsyt.2022.819607

Volatile Organic Compounds From Breath Differ Between Patients With Major Depression and Healthy Controls

*Marian Lueno[1], Henrik Dobrowolny[1], Dorothee Gescher[1], Laila Gbaoui[2], Gabriele Meyer-Lotz[1], Christoph Hoeschen[2] and Thomas Frodl[1,3]**

[1] Department of Psychiatry and Psychotherapy, Otto von Guericke University Magdeburg, Magdeburg, Germany, [2] Institute of Medical Engineering, Otto von Guericke University Magdeburg, Magdeburg, Germany, [3] Department of Psychiatry, Psychotherapy and Psychosomatics, University Hospital, RWTH Aachen, Aachen, Germany

Major depressive disorder (MDD) is a widespread common disorder. Up to now, there are no easy and frequent to use non-invasive biomarkers that could guide the diagnosis and treatment of MDD. The aim of this study was to investigate whether there are different mass concentrations of volatile organic compounds (VOCs) in the exhaled breath between patients with MDD and healthy controls. For this purpose, patients with MDD according to DSM-V and healthy subjects were investigated. VOCs contained in the breath were collected immediately after awakening, after 30 min, and after 60 min in a respective breath sample and measured using PRT-MS (proton-transfer-reaction mass spectrometry). Concentrations of masses m/z 88, 89, and 90 were significantly decreased in patients with MDD compared with healthy controls. Moreover, changes during the time in mass concentrations of m/z 93 and 69 significantly differed between groups. Differentiation between groups was possible with an AUCs of 0.80–0.94 in ROC analyses. In this first study, VOCs differed between patients and controls, and therefore, might be a promising tool for future studies. Altered masses are conceivable with energy metabolism in a variety of biochemical processes and involvement of the brain–gut–lung–microbiome axis.

Keywords: depression, biomarker, breath gas, volatile organic compounds, classification, clinical utility

OPEN ACCESS

Edited by:
Masahiro Takamura, Shimane University, Japan

Reviewed by:
Kiran Veer Sandhu, University College Cork, Ireland
Krishna Chandra Persaud, The University of Manchester, United Kingdom

***Correspondence:**
Thomas Frodl
tfrodl@ukaachen.de

Specialty section:
This article was submitted to Molecular Psychiatry, a section of the journal Frontiers in Psychiatry

Received: *08 December 2021*
Accepted: *13 June 2022*
Published: *12 July 2022*

Citation:
Lueno M, Dobrowolny H, Gescher D, Gbaoui L, Meyer-Lotz G, Hoeschen C and Frodl T (2022) Volatile Organic Compounds From Breath Differ Between Patients With Major Depression and Healthy Controls. Front. Psychiatry 13:819607. doi: 10.3389/fpsyt.2022.819607

INTRODUCTION

Mental Health disorders are on the rise in every country in the world. Estimates in Europe are almost €800 billion (US$1 trillion) a year—more than cancer, cardiovascular disease, and diabetes do cost together (1). One of the most common psychiatric diseases is major depressive disorder (MDD) which can effectively be treated with psychotherapy and/or antidepressants. However, still one-third of the patients do not respond to at least two different antidepressant trials and might need it as early as possible with different treatment options (2).

Unfortunately, there are currently no easy and frequently applicable non-invasive biomarkers available that could help to facilitate diagnosis of a depressive episode or that could guide to the most effective therapy. Noteworthy, currently there are ongoing studies on biomarkers

in the area of MDD using, e.g., neuroimaging, inflammation markers, hormones, markers for oxidative stress, and genetics. Significant differences were described for MDD compared with healthy controls for functional and structural neuroimaging (3) and as well as analyses of the immune system and inflammation (4). Moreover, the dysregulation of the hypothalamic–pituitary–adrenal (HPA) hormone axis has been well described in MDD (5). In a recent meta-analysis on prospective studies that aimed to predict MDD onset, relapse and recurrence by imaging, genetic information, inflammation markers, and hormone markers, only cortisol was detected to be a significant predictor (6). Thus, signatures related to the cortisol/stress-system seem to be of major relevance. With respect to cortisol tests the cortisol awakening response (CAR) is one of the most straightforward measures of dynamics of the HPA axis and can be obtained reliably (7). The CAR is thought to reflect the sensitivity of the HPA axis to the natural challenge awakening. However, overall, no widely accepted clinical biomarkers for MDD have been developed (8).

The aforementioned measures currently under investigation are invasive blood tests, except the test for cortisol when measured in saliva, which, however, is unpleasant to collect for the participants. It is not convenient for patients to give numerous blood samples throughout the day or even over several days in order to follow the disease course longitudinally. Moreover, functional neuroimaging is expensive and time consuming and it is not feasible to scan patients several times as a routine procedure. A non-invasive longitudinal measurement would certainly increase the information on individual disease characteristics and the dynamics of these during the disease in patients. Thus, new non-invasive markers are highly needed.

One of these possible methods might be breath gas analysis. The exhaled breath gas includes volatile organic compounds (VOCs) that are exhaled shortly after their production, and thus, can deliver information about the acute state of the human being. Therefore, breath biomarkers could provide new insights into metabolic and pathophysiological processes. Breath gas analysis is already clinically implemented, e.g., for alcohol tests. It was found to have predictive power for hyper- or hypoglycemia in human studies (9) and in diet-based studies with mice suffering from obesity (10). Other areas of research with breath gas analysis are pulmonary diseases such as asthma (11) or liver diseases (12).

Currently to our knowledge, no study exists that investigated whether VOCs in breath differ between patients with MDD and healthy controls, although metabolic changes are well known in patients with MDD.

The aim of this study was therefore primarily to identify potential VOCs in breath that differ between patients and controls. Second, we were interested to investigate the change of breath gas markers during the awakening time, since the awakening time was previously under focus of cortisol research in depression. As a third objective, we were interested to examine whether breath gas analysis might have the potential to differentiate between patients and controls and to investigate if multiple measurements over the first hour after awakening might improve classification. Furthermore, we tested for the influence of hospital environment and medication on the detected mass concentrations.

MATERIALS AND METHODS

Participants

From our psychiatric service 26 patients with DSM-V MDD diagnosis and 25 healthy controls were recruited in a prospective design. All the patients were in therapy either as inpatients or outpatients and at time of investigation were mildly to severely depressed. Inclusion criteria for patients were MDD according to DSM-V and age between 18 and 65 years. The latter applied to healthy controls too, who were recruited from the local community matched for age and sex to the patients included into the study. Exclusion criteria for participants were a known alcohol or drug dependency. Neurological disorders and diseases affecting the brain function were further excluded (e.g., hypo- or hyperthyroidism) and also acute internal disorders. Our participants reported no acute gastrointestinal disease. Furthermore, for the patients a current psychotic disorder, depressive episodes with psychotic symptoms, comorbid personality disorder, and suicidal intent were not allowed. Moreover, other psychiatric axis 1 disorders were excluded. For healthy controls any history of a psychiatric disorder was an exclusion criterion. All the patients and controls had to give written informed consent to participate in the study.

Clinical Assessments

All the subjects were investigated clinically and diagnosis were confirmed using the SCID diagnostic interview (13) by an additional independent investigator. Moreover, they have been examined using standardized questionnaires for psychiatric symptoms: Hamilton Depression Scale (HAMD) (14), Clinical Global Impression (CGI) (15), and Beck Depression Inventory (BDI) (16). The current medication and also the medication during the last 2 weeks before study inclusion were documented for the group of patients receiving antidepressants. Furthermore, the past clinical course was assessed from interviews and case notes within the psychiatric services in particular to stage the recurrence of the disease. Moreover, previous other doctors' reports were collected. Thus, as exact as possible treatment history for medications and psychotherapy were obtained.

Breath Gas Analysis

We measured the VOC concentrations as counts per seconds in the breath gas of all the participants (patients as well as controls) with Proton-Transfer-Reaction Mass Spectrometry (PTR-MS). Breath gas probes were taken at awakening, after 30 min, and after 60 min. Awakening was defined when participants got out of the bed in the morning. All the breath gas collection was carried out after awakening in patients and controls on an empty stomach, to avoid contamination with acute food intake or smoking effects. Participants were instructed to sit calm for 2 min and to breath normally and then to start breath gas sampling. Since breath gas was collected at awakening, after 30 min, and after 60 min, tedlar bags were used, which are special tubes for collecting air and

breath. No further preparation such as freezing or making use of condensation is necessary. For better detection of the exact substances, we carried out six probes with the PTR-MS system as well as a more sophisticated system based on a time-of-flight (TOF) analyzer unit. The sensitivity and specificity of such a system is by far better than the quadrupole-based system.

Smoking influences some of the VOCs. In the smokers benzene, xylene isomers, styrene, ethylbenzene, acetonitrile, and furan derivatives and also hydrocarbons have been detected in exhaled breath (17). With regards to smoking the patients and test persons behavior was documented and moreover, it can clearly be detected with breath gas analysis and the VOCs concerned were excluded from the analysis.

Therefore, we selected those VOCs that are already known from breath research and are not related to smoking. We determined an effect-size for group differences between patients and controls as $d = 1.37$ for comparison of single values and an effect size of 15 per group. For this first proof of concept study, we intended thus to recruit 25 patients and controls to allow also for covariates to be included in the analyses.

Data Analysis

Group differences between patients and controls and interactive effects between groups and time (during awakening) were analyzed using general linear models for repeated measures. Correction for multiple comparison was applied using false discovery rate (FDR) and significance was assumed with $p = 0.05$. Cliffs Delta statistics was used to indicate effect sizes for differences between patients and controls irrespective of distribution of values. Effects of antidepressant medication and the clinical environment (inpatients and outpatients) were analyzed further.

Moreover, a random forest analysis for feature extraction was used to cope with the structure of the test set and the measured values. For cross-validation, the data set was divided into ten randomly chosen training and validation data sets in the ratio of 75 and 25%. The algorithm tries to keep the number of patients and healthy subjects in each randomly chosen data set equal. In each validation of the trained random forest model, the importance of each measured value is calculated using the permutation method. After that, calculated importance values were summed for each measured mass. Subsequently, the five masses with the highest summed importance values were then used for logistic regression. Based on the obtained formulas for combination of markers we obtained the predicted values for the model in the test sample. These models were available to our statistician, not to performers or assessors. The obtained results and reference standards were confirmed in the validation sample. A ROC analysis was then carried out to identify sensitivity, specificity, and accuracy for discrimination between patients with MDD and healthy controls.

RESULTS

There are no significant differences between patients and controls in terms of gender, age, BMI, alcohol consumption and education (**Table 1**). Per definition, patients with MDD show significant higher depression severity compared to healthy controls. When performing the study, no adverse events did occur.

Group Comparison

In the analysis of the group and time by group effects, masses were included into repeated measurement ANCOVAs. Interestingly, concentrations of m/z 88 [$F(1/50) = 11.2$, $p = 0.0016$, $p_{FDR} = 0.0373$], m/z 89 [$F(1/50) = 10.5$, $p = 0.0022$, $p_{FDR} = 0.0373$] and m/z 90 [$F(1/50) = 11.6$, $p = 0.0013$, $p_{FDR} = 0.0373$] were significantly decreased in patients with MDD compared with the healthy controls. No significant time effects or time × group interactions were found for these masses (**Figure 1**). The following masses were altered, but did not survive false discovery rate (FDR) correction: m/z 42 was increased in patients with MDD compared with healthy controls [$F(1/50) = 8.3$, $p = 0.006$, $p_{FDR} = 0.084$]. Decreased in patients with MDD compared with healthy controls were m/z 70 [$F(1/50) = 5.3$, $p = 0.025$, $p_{FDR} = 0.156$), m/z 74 ($F(1/50) = 5.6$, $p = 0.022$, $p_{FDR} = 0.154$], m/z 85 [$F(1/50) = 6.3$, $p = 0.016$, $p_{FDR} = 0.128$], m/z 91 [$F(1/50) = 7$, $p = 0.011$, $p_{FDR} = 0.121$], and m/z 93 [$F(1/50) = 6.6$, $p = 0.013$, $p_{FDR} = 0.121$].

Moreover, different time courses during the awakening for the concentrations of the m/z 93 [$F(1/50) = 5.2$, $p = 0.007$ with assumed sphericity] and 69 [$F(1/50) = 2.6$, $p = 0.091$ with Greenhouse–Geisser correction] were detected between patients with MDD and controls (**Supplementary Figure 1**). The difference between m/z 93 at 30 min minus baseline was

TABLE 1 | Description of the sample.

	Control N = 25	MDD N = 26	Sig.
Gender	$f = 13$, $m = 12$	$f = 16$, $m = 10$	Chi = 0.47, $p = 0.49$
Age (years)	34.4 ± 8.2	37.9 ± 12.6	t = 1.2, $p = 0.24$
Education (years)	12.04 ± 3.2	12.15 ± 2.6	t = 0.14, $p = 0.89$
BMI (kg/m^2)	24.7 ± 4.0	27.3 ± 7.8	t = 1.5, $p = 0.21$
CGI	0.0	3.6, ± 1.4	t = 13.2, $p < 0.001$
BDI-II	1.7, ± 3.8	32.6, ± 10.8	t = 13.5, $p < 0.001$
HDRS	0.12, ± 0.44	17.2, ± 4.9	t = 17.2, $p < 0.001$
Smoking	Yes = 8	Yes = 0	Chi = 9.1, $p = 0.003$
Alcohol	Yes = 5	Yes = 5	Chi = 0.005, $p = 0.95$
Marital status			Chi = 9.3
Single	5	9	$p = 0.09$
Relationship	14	6	
Married	6	6	
Divorced		5	
Medication class	n.a.		n.a.
None		7	
SSRI		7	
SNRI		4	
NASSA		5	
Others		3	

Depicted are mean values and SDs. SSRI, serotonin reuptake inhibitors; SNRI, serotonin and noradrenaline reuptake inhibitors; NASSA, noradrenaline and selective serotonergic antidepressants (e.g., mirtazapine), others (1 = valdoxane, 1 = nortiptiline, and 1 = bupropione).

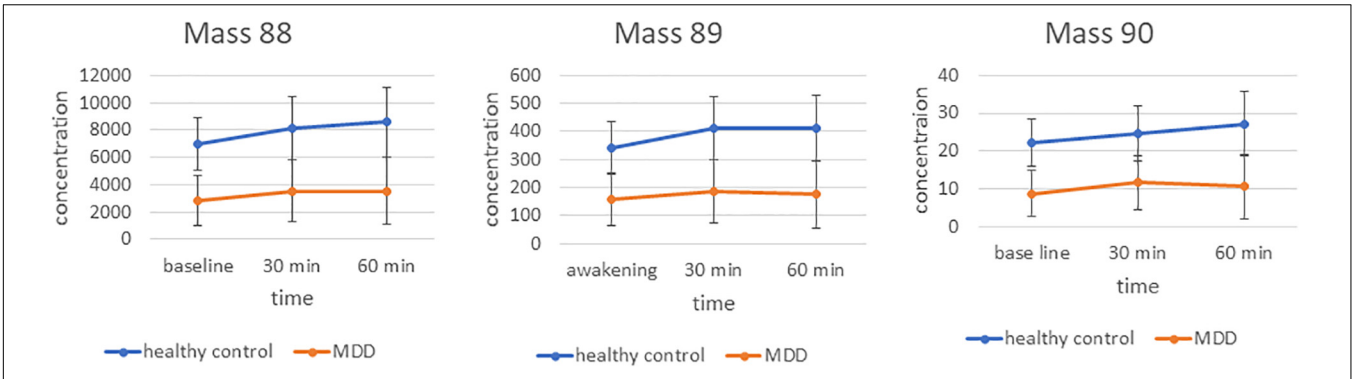

FIGURE 1 | Time course and differences between groups for markers 88, 89, and 90 m/z. Mean concentration in counts per second.

significantly higher for patients with MDD compared with the controls [$F(1/50 = 13.5$, $p = 0.00074$, $p_{FDR} = 0.011$]. The difference between m/z 69 at 60 min minus 30 min is significantly different between groups as well [$F(1/50) = 4.6$, $p = 0.037$, $p_{FDR} = 0.041$].

Candidate Selection and Evaluation Using Random Forest Analysis

In order to test whether markers not showing significant differences in the multiple testing corrected ANCOVA might contribute to differentiation between groups a random forest analysis was automatically run on those masses showing uncorrected significant differences (**Supplementary Tables 1**, **2**). The random forest analysis was run for each effect size threshold ten times with varying training and validation samples that were automatically chosen by the software. Taking breath gas markers from baseline measurements at awakening resulted in good accuracy of 80%. This was improved by adding measurements from the 30 and 60 min time points as well. Moreover, including the differences between measurement points (increase, decrease over time) further improved the accuracy. From the random forest analysis most important markers for the models are derived (**Figure 2**).

Composite Marker and Classification Analysis Based on Logistic Regression

Based on the selected markers from the random forest analysis, we further investigated the classification accuracy in our test and the validation samples. Prediction accuracy was already high for the most important VOC (m/z 74) measured 60 min after awakening even in the validation sample (AUC 0.81). Taking the three best markers from the random forest analysis (m/z 74 at 60 min, m/z 94 at 60 min, and m/z 93 at 30 min) showed a very good accuracy in the validation sample (AUC 0.93). Adding the next markers to the model does not further improve the classification (**Figure 3**).

Adding the marker m/z 69 showed very good classification. The classification was as following: AUC = 0.96 in the test sample and AUC = 0.91 in the validation sample (**Supplementary Figure 2**).

Analysis of Influence From the Environment and Medication

Moreover, we tested whether breath gas sampling in the hospital for inpatients differed from breath gas sampling at home considering depression severity, age, and gender as covariates. Therefore, the six patients being in outpatient therapy were compared with the 19 patients in the hospital. No significant difference was found in the aforementioned significant different breath gas markers, except m/z 74. Levels of m/z 74 were significantly lower in patients sampling at home compared to those sampling in the hospital [$F(1/24) = 6.2$, $p = 0.02$]. No significant difference in concentration of these VOCs was detected between patients on antidepressants compared with those without antidepressants.

DISCUSSION

Endogenous VOCs provide a plethora of information regarding the metabolic processes. This is to our knowledge the first study using breath gas analysis to explore potential signatures for supporting diagnostics in MDD.

Some of the mass signatures found to be associated with MDD have a well-known origin. Mass signatures that were found to be significantly and stably reduced over the awakening period in patients compared with controls can be traced back butanoic or butyric acid (89 m/z) (18). Butyric acid plays an important role in oxidative generation of ATP, supplies anabolic pathways (gluconeogenesis and lipogenesis) and contributes to the regulation of cell metabolism by triggering signaling pathways (19). It is produced in the colon through microbial fermentation of dietary fiber that is primarily absorbed by colonocytes and metabolized in the liver for the generation of ATP during energy metabolism. Some butyric acid is absorbed in the distal colon, which is not connected to the portal vein, thereby allowing for the systemic distribution of butyric acid to multiple organ systems through the circulatory system (19). Reduction of butyric acid is in line with new findings from a large microbiome study that shows that patients with MDD have reduced amounts of butyric acid producing bacteria in the gut that in turn are associated with reduced quality of life

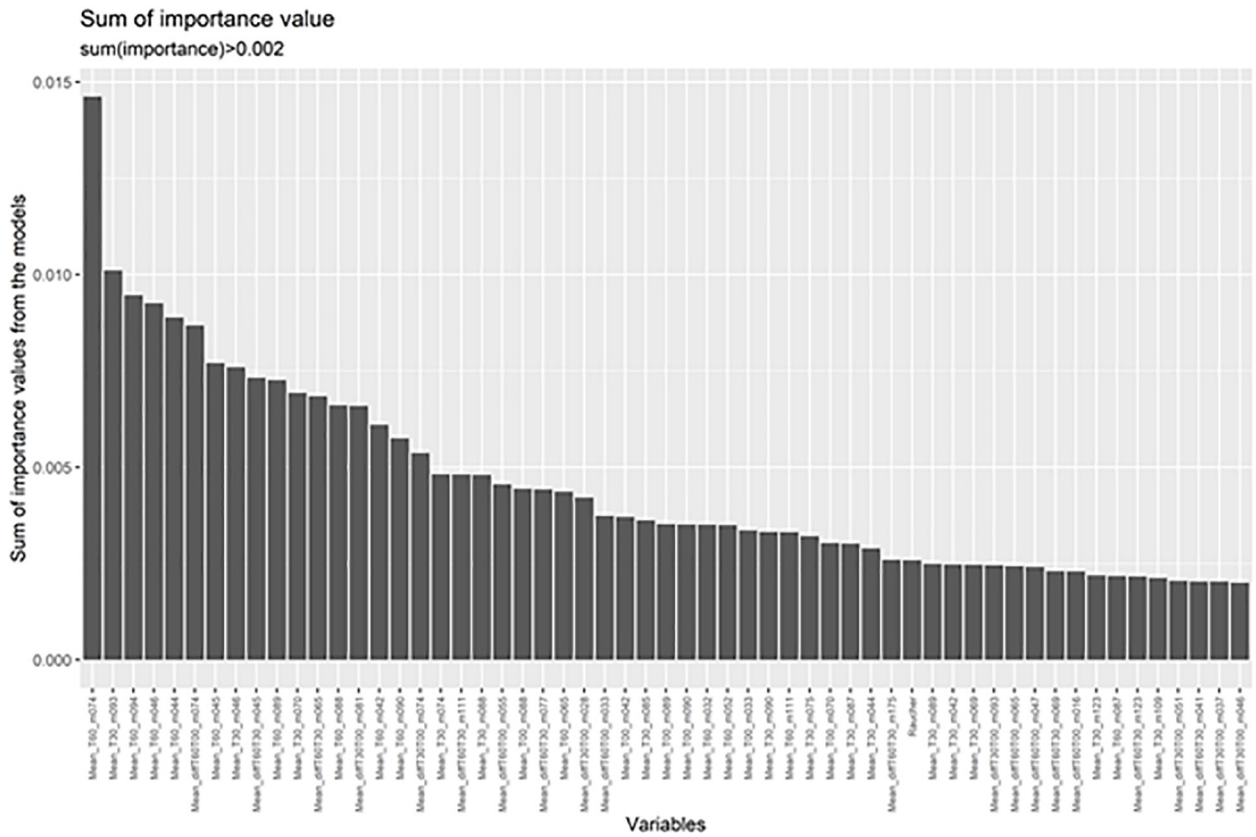

FIGURE 2 | Random forest analyses indicate the masses most important for differentiating between patients and controls. These are shown in order of importance.

(20). Moreover, in one study, using 16S rRNA gene-based next generation sequencing a total of 40 bacterial taxa were found to be altered in saliva of patients with MDD compared with healthy controls (21). Thus, oral microbiome and not only gut or lung microbiome might need to be considered when locating origins of altered VOCs.

It always is the question if an association like the one found in the present study is causal or not. Patients with MDD reduce their physical activity and thus the changes found here might be associated with the physical activity. In a study on prolonged exercise in not depressed subjects short-chain fatty acids (SCFAs) represented by acetic acid, butanoic acid, and propionic acid increased (22). In an animal experiment, it could be shown that rats that voluntarily exercise have an increased level of butyrate in their intestines (23). Butyrate is an ester of butyric acid. This would argue that reduced physical activity might be a contributing factor to butyric acid in breath. Thus, further studies are necessary to study the effect on exercise butyric acid in patients with MDD.

One other marker with relevance to MDD was isoprene (69 m/z) (24), which is derived from the cholesterol synthetic pathway (25). Cholesterol blood levels are significantly increased in patients with MDD compared with the healthy controls and are positively associated with depression severity (26). Isoprene was found to be reduced in breath gas in patients with MDD in particular at awakening compared with healthy controls in our study. During the awakening period the levels of the marker in controls approaches that of patients with MDD. Since isoprene is stored in muscles and gets released during muscle contraction (27), our finding might suggest that reduced activity in patients with MDD is associated with reduced isoprene levels despite increase of cholesterol levels. However, isoprene was found to decrease during prolonged exercise in humans (22). In acute exercise, this might be different due to pulmonary ventilation, where increases of isoprene have been detected. Moreover, m/z 74, m/z 93, and m/z 94 were not found to be associated with exercise so far, we are aware of in other studies.

It could also be proven for isoprene that it can be measured in increased concentration in the air breathed during physical activity. Here, it could be proven that the measured concentration also depends on the lung blood flow. Endogenous production is not increased during increased activity (28).

M/z 93 was significantly increased in MDD compared with the controls and significantly increased during the awakening response in patients more than in the healthy controls. This mass belongs to toluene (29), which is predominantly used as an industrial feedstock. Its exposure was previously found to be associated with cognitive dysfunctioning in the neuropsychological tests (30).

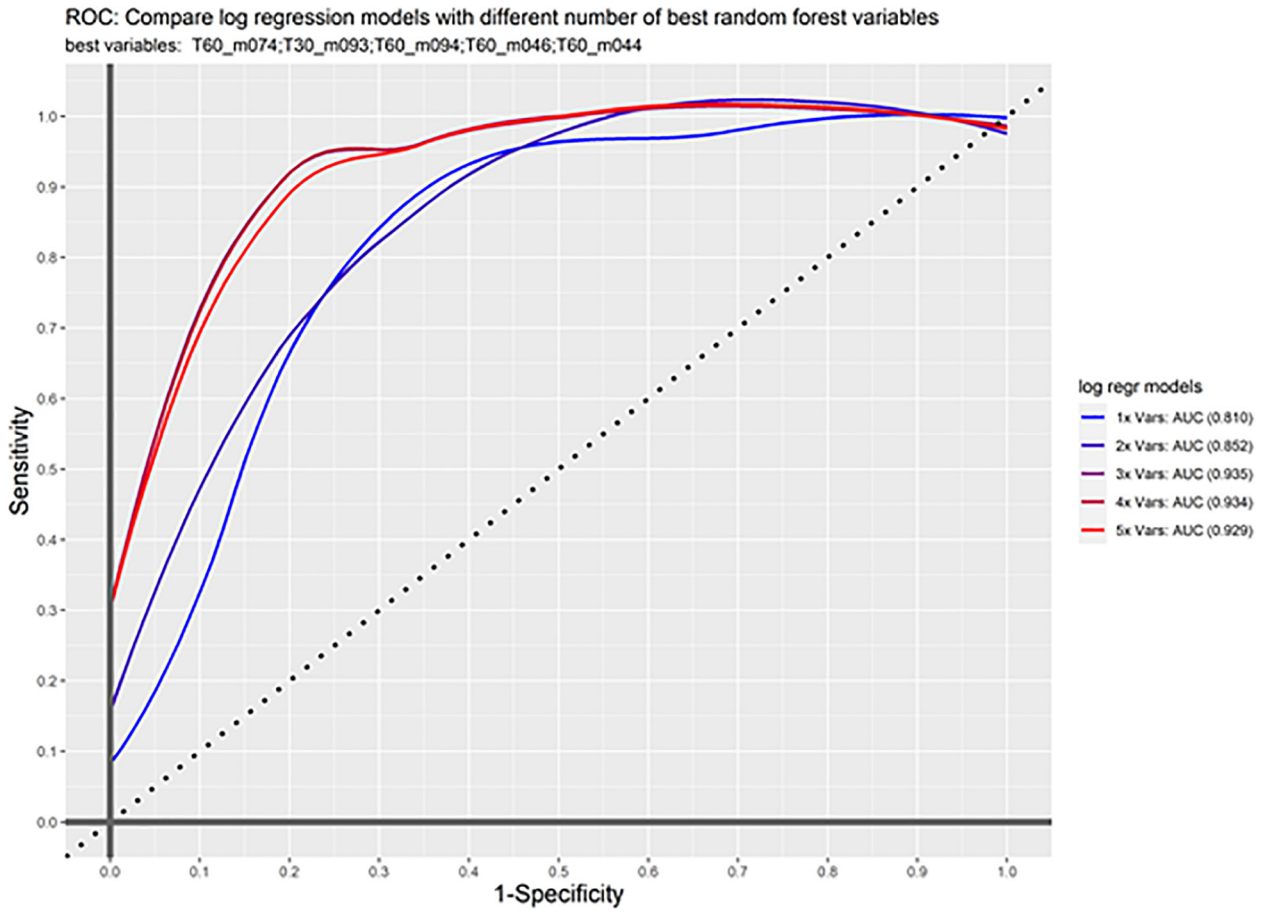

FIGURE 3 | ROC curve. Shown is sensitivity and 1-specificity for the combination of markers in the validation sample. First m/z 74 was calculated alone (1x Vars), then subsequently the other important markers are added showing an increase up to the first three markers.

Currently, diagnostics are still based on clinical interviews, psychiatric history and assessment of psychopathology. Breath gas analysis has the advantage against blood analyses or functional MRI that it is a non-invasive, easy to apply measurement. Measurement in patients with MDD was well-tolerated and is feasible also over several time points during the day. Thus, it allows multiple measurements over time, e.g., during the awakening period like in our study. In our experience, subjects were comfortable with the procedure even when they were severely depressed and were not stressed by it. Breath gas analysis did show a very good accuracy in predicting patients with MDD vs. healthy subjects in the test as well as the validation sample. An AUC of 0.93 for a three-factor solution seems to be promising for the next step in studying these signatures in the larger clinical studies including also other diagnoses.

The three most important markers from the random forest analysis were markers 74, 93, and 94. While m/z 93 is toluene (29), the origin of m/z 94 is unclear. For marker 74, lower levels were found in patients compared with the healthy controls. Interestingly, patients sampling at home showed the lowest levels suggesting that this marker might differ even more, when investigated only in the usual home environment. One possibility for the significantly higher levels in hospitalized patients could be that patients in the hospital receive more intense therapy, a professionally chosen diet plan and nursing support to motivate patients with depression to take their meals despite low appetite. Using TOF-PTR-MS analysis with a 100-fold better detection in addition to PTR–MS, we tentatively relate this mass to protonated methylguanidine (74 m/z), which is a guanidine compound and can be synthesized from creatine and creatinine (31). It might reflect creatine metabolism, but it also was found to be highly dependent on the diet, e.g., from boiled beef and fish (32). Therefore, the difference between in and outpatients might be due to better nutrition in the hospital. Interestingly, creatine deficiency was associated with MDD and in turn its supplementation showed positive therapeutic effects (33).

In this first study, the sample size was small thus limiting the generalizability of the findings. In a follow-up study, the sample size needs to be extended toward more outpatients treated in the community and patients in remission as well as longitudinal assessments during the disease course. This will allow to explore whether the markers are trait or state

dependent. While in the present study, antidepressant medication seems not to have a major effect, it should then be tested whether this might be the case for all the antidepressant classes. The type of diet can have an impact on metabolites excreted, and thus, these effects can be seen in exhaled breath. In this first attempt at a study, the exact components of the diet were not explicitly asked about. Thus, nutrition needs to be taken into consideration. So far, we are not aware of any of the masses we found to be associated with nutrition, but given the limited number of existing studies, and the small sample in our pilot study, it seems to be important to control for nutrition. Thus, breath gas analysis was carried out in patients and controls at awakening and the hour afterward on an empty stomach. In our sample, patients were more often smokers than non-smokers. Although VOCs known to be associated with smoking were excluded from analyses, in a larger sample the effect of smoking needs to be investigated.

In summary, the present study shows that breath gas analysis might be an interesting method to investigate the metabolic profile in patients with major depressive disorder (MDD).

DATA AVAILABILITY STATEMENT

The raw data supporting the conclusions of this article will be made available by the authors, without undue reservation.

ETHICS STATEMENT

The studies involving human participants were reviewed and approved by Ethics Committee of medical faculty of Otto von Guericke University Magdeburg. The patients/participants provided their written informed consent to participate in this study.

AUTHOR CONTRIBUTIONS

ML: acquisition, analysis and interpretation of the data, and drafting the manuscript. HD: analysis and interpretation of the data and revising the manuscript. LG and DG: interpretation of the data and revising the manuscript. GM-L: acquisition, interpretation of the data, and revising the manuscript. CH: design of the work, interpretation of the data, and revising the manuscript. TF: design of the work, acquisition, analysis and interpretation of the data, and drafting the manuscript. All authors agreed to be accountable for all aspects of the work ensuring that questions related to the accuracy or integrity of any part of the work are appropriately investigated, resolved, and gave approval for the final version.

FUNDING

TF received funding from the European Union Horizon 2020 Programme within the project Deep-Learning and HPC to boost biomedical applications for health (DeepHealth): Grant number: 825111.

SUPPLEMENTARY MATERIAL

The Supplementary Material for this article can be found online at: https://www.frontiersin.org/articles/10.3389/fpsyt.2022.819607/full#supplementary-material

REFERENCES

1. Smith K. Trillion-dollar brain drain. *Nature.* (2011) 478:15.doi: 10.1038/478015a
2. Kennedy SH, Giacobbe P. Treatment resistant depression–advances in somatic therapies. *Ann Clin Psychiatry.* (2007) 19:279–87. doi: 10.1080/10401230701675222
3. Zhang K, Zhu Y, Zhu Y, Wu S, Liu H, Zhang W, et al. Molecular, functional, and structural imaging of major depressive disorder. *Neurosci Bull.* (2016) 32:273–85.
4. Enache D, Pariante CM, Mondelli V. Markers of central inflammation in major depressive disorder: a systematic review and meta-analysis of studies examining cerebrospinal fluid, positron emission tomography and post-mortem brain tissue. *Brain Behav Immun.* (2019) 81:24–40. doi: 10.1016/j.bbi.2019.06.015
5. Binder EB, Nemeroff CB. The CRF system, stress, depression and anxiety-insights from human genetic studies. *Mol Psychiatry.* (2010) 15:574–88. doi: 10.1038/mp.2009.141
6. Kennis M, Gerritsen L, van Dalen M, Williams A, Cuijpers P, Bockting C. Prospective biomarkers of major depressive disorder: a systematic review and meta-analysis. *Mol Psychiatry.* (2020) 25:321–38.doi: 10.1038/s41380-019-0585-z
7. Kudielka BM, Hawkley LC, Adam EK, Cacioppo JT. Compliance with ambulatory saliva sampling in the Chicago health, aging, and social relations study and associations with social support. *Ann Behav Med.* (2007) 34:209–16. doi: 10.1007/BF02872675
8. Kraus C, Kadriu B, Lanzenberger R, Zarate CA Jr, Kasper S. Prognosis and improved outcomes in major depression: a review. *Transl Psychiatry.* (2019) 9:127.doi: 10.1038/s41398-019-0460-3
9. Novak BJ, Blake DR, Meinardi S, Rowland FS, Pontello A, Cooper DM, et al. Exhaled methyl nitrate as a noninvasive marker of hyperglycemia in type 1 diabetes. *Proc Natl Acad Sci USA.* (2007) 104:15613–8.doi: 10.1073/pnas.0706533104
10. Kistler M, Muntean A, Szymczak W, Rink N, Fuchs H, Gailus-Durner V, et al. Diet-induced and mono-genetic obesity alter volatile organic compound signature in mice. *J Breath Res.* (2016) 10:016009. doi: 10.1088/1752-7155/10/1/016009
11. Hashoul D, Haick H. Sensors for detecting pulmonary diseases from exhaled breath. *Eur Respir Rev.* (2019) 28:190011.doi: 10.1183/16000617.0011-2019
12. De Vincentis A, Vespasiani-Gentilucci U, Sabatini A, Antonelli-Incalzi R, Picardi A. Exhaled breath analysis in hepatology: state-of-the-art and perspectives. *World J Gastroenterol.* (2019) 25:4043–50. doi: 10.3748/wjg.v25.i30.4043
13. Ekselius L, Lindstrom E, von Knorring L, Bodlund O, Kullgren G. SCID II interviews and the SCID Screen questionnaire as diagnostic tools for personality disorders in DSM-III-R. *Acta Psychiatr Scand.* (1994) 90:120–3. doi: 10.1111/j.1600-0447.1994.tb01566.x
14. Hamilton M. A rating scale for depression. *J Neurol Neurosurg Psychiatry.* (1960) 23:56–62.doi: 10.1136/jnnp.23.1.56
15. Guy W. Clinical global impression. In: Guy W editor, *Assessment Manual for Psychopharmacology*. Rockville, MD: Department of Health, Education, and Welfare (1976). p. 217–22.

16. Beck AT, Ward CH, Mendelson M, Mock J, Erbaugh J. An inventory for measuring depression. *Arch Gen Psychiatry.* (1961) 4:561–71.
17. Buszewski B, Ulanowska A, Ligor T, Denderz N, Amann A. Analysis of exhaled breath from smokers, passive smokers and non-smokers by solid-phase microextraction gas chromatography/mass spectrometry. *Biomed Chromatogr.* (2009) 23:551–6. doi: 10.1002/bmc.1141
18. Adam ME, Fehervari M, Boshier PR, Chin ST, Lin GP, Romano A, et al. Mass-spectrometry analysis of mixed-breath, isolated-bronchial-breath, and gastric-endoluminal-air volatile fatty acids in esophagogastric cancer. *Anal Chem.* (2019) 91:3740–6. doi: 10.1021/acs.analchem.9b00148
19. Bourassa MW, Alim I, Bultman SJ, Ratan RR. Butyrate, neuroepigenetics and the gut microbiome: can a high fiber diet improve brain health? *Neurosci Lett.* (2016) 625:56–63. doi: 10.1016/j.neulet.2016.02.009
20. Valles-Colomer M, Falony G, Darzi Y, Tigchelaar EF, Wang J, Tito RY, et al. The neuroactive potential of the human gut microbiota in quality of life and depression. *Nat Microbiol.* (2019) 4:623–32.
21. Wingfield B, Lapsley C, McDowell A, Miliotis G, McLafferty M, O'Neill SM, et al. Variations in the oral microbiome are associated with depression in young adults. *Sci Rep.* (2021) 11:15009. doi: 10.1038/s41598-021-94498-6
22. Henderson B, Lopes Batista G, Bertinetto CG, Meurs J, Materic D, Bongers C, et al. Exhaled breath reflects prolonged exercise and statin use during a field campaign. *Metabolites.* (2021) 11:192. doi: 10.3390/metabo11040192
23. Matsumoto M, Inoue R, Tsukahara T, Ushida K, Chiji H, Matsubara N, et al. Voluntary running exercise alters microbiota composition and increases n-butyrate concentration in the rat cecum. *Biosci Biotechnol Biochem.* (2008) 72:572–6. doi: 10.1271/bbb.70474
24. Herbig J, Muller M, Schallhart S, Titzmann T, Graus M, Hansel A. On-line breath analysis with PTR-TOF. *J Breath Res.* (2009) 3:027004.doi: 10.1088/1752-7155/3/2/027004
25. Stone BG, Besse TJ, Duane WC, Evans CD, DeMaster EG. Effect of regulating cholesterol biosynthesis on breath isoprene excretion in men. *Lipids.* (1993) 28:705–8. doi: 10.1007/BF02535990
26. Wagner CJ, Musenbichler C, Bohm L, Farber K, Fischer AI, von Nippold F, et al. LDL cholesterol relates to depression, its severity, and the prospective course. *Prog Neuropsychopharmacol Biol Psychiatry.* (2019) 92:405–11. doi: 10.1016/j.pnpbp.2019.01.010
27. King J, Koc H, Unterkofler K, Mochalski P, Kupferthaler A, Teschl G, et al. Physiological modeling of isoprene dynamics in exhaled breath. *J Theor Biol.* (2010) 267:626–37.doi: 10.1016/j.jtbi.2010.09.028
28. King J, Kupferthaler A, Unterkofler K, Koc H, Teschl S, Teschl G, et al. Isoprene and acetone concentration profiles during exercise on an ergometer. *J Breath Res.* (2009) 3:027006. doi: 10.1088/1752-7155/3/2/027006
29. Sukul P, Schubert JK, Trefz P, Miekisch W. Natural menstrual rhythm and oral contraception diversely affect exhaled breath compositions. *Sci Rep.* (2018) 8:10838. doi: 10.1038/s41598-018-29221-z
30. Echeverria D, Fine L, Langolf G, Schork A, Sampaio C. Acute neurobehavioural effects of toluene. *Br J Ind Med.* (1989) 46:483–95.doi: 10.1136/oem.46.7.483
31. Tachikawa M, Hosoya K. Transport characteristics of guanidino compounds at the blood-brain barrier and blood-cerebrospinal fluid barrier: relevance to neural disorders. *Fluids Barriers CNS.* (2011) 8:13. doi: 10.1186/2045-8118-8-13
32. Gonella M, Barsotti G, Lupetti S, Giovannetti S. Factors affecting the metabolic production of methylguanidine. *Clin Sci Mol Med.* (1975) 48:341–7.doi: 10.1042/cs0480341
33. Kious BM, Kondo DG, Renshaw PF. Creatine for the treatment of depression. *Biomolecules.* (2019) 9:406.doi: 10.3390/biom9090406

Conflict of Interest: The authors obtained a patent for breath gas analysis in major depressive disorder. Thus, there is no embargo for the publication any more. TF received fees for presentation from Janssen-Cilag, Servier, Neuraxpharm, Recordati, and Otsuka.

The remaining authors declare that the research was conducted in the absence of any commercial or financial relationships that could be construed as a potential conflict of interest.

Publisher's Note: All claims expressed in this article are solely those of the authors and do not necessarily represent those of their affiliated organizations, or those of the publisher, the editors and the reviewers. Any product that may be evaluated in this article, or claim that may be made by its manufacturer, is not guaranteed or endorsed by the publisher.

frontiers | Frontiers in Psychiatry

ORIGINAL RESEARCH
published: 22 July 2022
doi: 10.3389/fpsyt.2022.904139

Altered Brain Function in Treatment-Resistant and Non-treatment-resistant Depression Patients: A Resting-State Functional Magnetic Resonance Imaging Study

Jifei Sun[1†], Yue Ma[1†], Limei Chen[1], Zhi Wang[1], Chunlei Guo[1], Yi Luo[1], Deqiang Gao[1], Xiaojiao Li[1], Ke Xu[1], Yang Hong[1], Xiaobing Hou[2], Jing Tian[2], Xue Yu[2], Hongxing Wang[3], Jiliang Fang[1] and Xue Xiao[2*]*

[1] Department of Radiology, Guang'anmen Hospital, China Academy of Chinese Medical Sciences, Beijing, China, [2] Department of Psychiatric, Beijing First Hospital of Integrated Chinese and Western Medicine, Beijing, China, [3] Department of Neurology, Xuanwu Hospital, Capital Medical University, Beijing, China

OPEN ACCESS

Edited by:
Masahiro Takamura, Shimane University, Japan

Reviewed by:
Thomas Frodl, University Hospital RWTH Aachen, Germany
Yifeng Rang, South China Agricultural University, China

***Correspondence:**
Jiliang Fang
Fangmgh@163.com
Xue Xiao
xiaoxuepsy@sina.com

[†]These authors have contributed equally to this work and share first authorship

Specialty section:
This article was submitted to Neuroimaging and Stimulation, a section of the journal Frontiers in Psychiatry

Received: *25 March 2022*
Accepted: *23 June 2022*
Published: *22 July 2022*

Citation:
Sun J, Ma Y, Chen L, Wang Z, Guo C, Luo Y, Gao D, Li X, Xu K, Hong Y, Hou X, Tian J, Yu X, Wang H, Fang J and Xiao X (2022) Altered Brain Function in Treatment-Resistant and Non-treatment-resistant Depression Patients: A Resting-State Functional Magnetic Resonance Imaging Study. Front. Psychiatry 13:904139. doi: 10.3389/fpsyt.2022.904139

Objective: In this study, we used amplitude of low-frequency fluctuation (ALFF) and regional homogeneity (ReHo) to observe differences in local brain functional activity and its characteristics in patients with treatment-resistant depression (TRD) and non-treatment-resistant depression (nTRD), and to explore the correlation between areas of abnormal brain functional activity and clinical symptoms.

Method: Thirty-seven patients with TRD, 36 patients with nTRD, and 35 healthy controls (HCs) were included in resting-state fMRI scans. ALFF and ReHo were used for image analysis and further correlation between abnormal brain regions and clinical symptoms were analyzed.

Results: ANOVA revealed that the significantly different brain regions of ALFF and ReHo among the three groups were mainly concentrated in the frontal and temporal lobes. Compared with the nTRD group, the TRD group had decreased ALFF in the left/right inferior frontal triangular gyrus, left middle temporal gyrus, left cuneus and bilateral posterior lobes of the cerebellum, and increased ALFF in the left middle frontal gyrus and right superior temporal gyrus, and the TRD group had decreased ReHo in the left/right inferior frontal triangular gyrus, left middle temporal gyrus, and increased ReHo in the right superior frontal gyrus. Compared with the HC group, the TRD group had decreased ALFF/ReHo in both the right inferior frontal triangular gyrus and the left middle temporal gyrus. Pearson correlation analysis showed that both ALFF and ReHo values in these abnormal brain regions were positively correlated with HAMD-17 scores ($P < 0.05$).

Conclusion: Although the clinical symptoms were similar in the TRD and nTRD groups, abnormal neurological functional activity were present in some of the same brain regions. Compared with the nTRD group, ALFF and ReHo showed a wider range of brain area alterations and more complex neuropathological mechanisms in the TRD group, especially in the inferior frontal triangular gyrus of the frontal lobe and the middle temporal gyrus of the temporal lobe.

Keywords: treatment-resistant depression, non-treatment-resistant depression, fMRI, amplitude of low-frequency fluctuation, regional homogeneity

INTRODUCTION

Major depressive disorder (MDD) is a common clinical disorder of the psychiatric system, characterized by significant and persistent depressed mood, reduced interest, reduced cognitive function and somatic disturbances (1). MDD has a high global prevalence, affecting over 300 million people worldwide, and is expected to be the leading global disease burden by the end of 2030 (2). Despite the availability of psychological, physical and pharmacological therapies, 30–40% of people with MDD still fail to respond to these treatments (3). According to the most common previous definition of treatment-resistant depression(TRD), the patient does not improve after at least two or more treatments of adequate dose and duration (4). Therefore, the study of TRD has become a challenging research domain, where substantial effort has been invested worldwide (5).

TRD is a complex disorder whose pathogenesis is not fully understood, and it reflects the coexistence of multiple depressive subtypes, psychiatric comorbidity, and coexisting medical illnesse (6). Compared with the non-treatment-resistant depression (nTRD), patients with TRD are more difficult to treat and consume more treatment costs (4, 7). Overall medical costs for TRD patients are almost twice or more than twice as high as those for nTRD patients (8, 9). In terms of clinical symptoms, compared with nTRD patients, TRD patients had more severe depressive symptoms, cognitive impairment, anxiety and distress, longer onset period, and lower work productivity (7, 10–12). Therefore, it is necessary to explore the biomarkers of TRD, which in turn will facilitate the understanding of the differences in the pathogenesis of TRD and nTRD.

Currently, although brain tissue or cerebrospinal fluid is an ideal resource for studying MDD biomarkers, it is more difficult to obtain in the clinic (13). Although peripheral blood proteins are easy to obtain but there are many types of studies and no uniform standards have been established (14). In recent years, resting-state functional magnetic resonance imaging (rs-fMRI) has been gradually applied in the field of psychiatric disorders, such as MDD (15, 16), schizophrenia (17) and autism (18), because of its simplicity and ease of acquisition. It has also been further applied to the study of subtypes of depression (19–21). The application of rs-fMRI technology facilitates a deeper understanding of the neuropathology of depression and the development of effective antidepressant drugs (22).

Regional homogeneity (ReHo) and amplitude of low-frequency fluctuations (ALFF) are commonly used in rs-fMRI to study functional brain activity. ReHo is used to assess the level of coordination of neural activity in local brain regions by calculating ReHo values to indirectly reflect the spontaneous activity of local neurons in time synchronization (23). ALFF reflects the intensity of spontaneous activity in a region of the brain over a short period of time by calculating the average amplitude of low-frequency oscillations in that region (24). However, the diseases currently studied using a combined ALFF and ReHo approach mainly include Parkinson's disease (26), generalized anxiety disorder (25), bipolar disorder (27), and migraine without aura (28), while differential studies of TRD and nTRD are lacking. So far, there have been some studies on the difference between TRD and nTRD, but most of them use ALFF or ReHo as a single indicator. Previous studies have shown differences in the default mode network (DMN), visual recognition circuits, right auditory, right sensory/somatomotor hand and cerebellar ALFF in the TRD group compared to the nTRD group (29, 30). In addition, other studies have shown differences in ReHo in the left inferior frontal gyrus, right middle temporal gyrus, left precuneus, middle cingulate gyrus and left fusiform gyrus in the TRD group compared to the nTRD group (31, 32). The above rs-fMRI study found that ALFF and ReHo may be highly sensitive to changes in TRD. Previous studies have consistently shown that changes in different indices may represent different sensitivities and that changes in multiple indices in the same brain region during the same period can help improve the sensitivity of the diagnosis (33). In addition, from the results of previous studies, it also can be seen that the main difference between TRD and nTRD is in the frontal and temporal lobes and other brain regions. It has also been shown that patients with TRD have gray matter volume changes in frontal and temporal lobe regions (34). The frontal and temporal lobes are not only important brain regions in the pathogenesis of MDD, but also closely related to the DMN and cognitive control network (CCN) (35–38).

Therefore, we used ALFF and ReHo to differentiate the differences in functional brain activity among the TRD group, nTRD group and healthy control (HC) group based on previous studies, and further analyzed the correlation between the differential brain areas and clinical characteristics. We hypothesized that there are differences in neural circuits in the brain of TRD and nTRD patients, especially closely related to the frontal lobe, temporal lobe. This study will provide a neuroimaging basis for the differences in neuropathological mechanisms between TRD and nTRD, which will also contribute more to the understanding of the pathogenesis of TRD.

MATERIALS AND METHODS

Participants

Seventy-three patients with MDD were from Guang'anmen Hospital, China Academy of Chinese Medical Sciences, Beijing First Hospital of Integrated Chinese and Western Medicine, and Xuanwu Hospital, Capital Medical University. All patients met the MDD criteria of the Diagnostic and Statistical Manual of Mental Disorders, Fifth Edition (DSM-5). We used the 17-item Hamilton Rating Scale for Depression scale (HAMD-17) to assess the severity of depression in all MDD patients and divided these patients into those with TRD (TRD, $n = 37$) and those with nTRD (nTRD, $n = 36$). The inclusion criteria for all patients were: (1) age 18–55 years; (2) HAMD-17 score >17; (3) right-handedness; (4) The TRD group was eligible to receive two or more adequate doses and courses of antidepressant therapy that were not effective and had been stable for more than 6 weeks on antidepressant medication prior to enrollment, with non-responsiveness defined as a decrease in HAMD-17 score of <50%. The nTRD group was in symptomatic remission on one antidepressant, with responsiveness defined as a decrease of more than 50% in HAMD-17 scores, relapse prior to enrollment.

Thirty-five gender- and age-matched HCs (21 females and 14 males): (1) age 18–55 years; (2) HAMD-17 score < 7; (3) right-handedness; (4) no history of any mental illness in first-degree relatives.

The exclusion criteria for patients and HCs were as follows: (1) history of drug abuse; (2) any contraindications to MRI, such as presence of a heart pacemaker, metal fixed false teeth, or severe claustrophobia; (3) pregnant or lactating status; (4) bipolar disorder, suicidal thoughts, and any other mental illness; (5) tumors, history of head trauma with loss of consciousness, and any cardiovascular, kidney or other major medical condition; (6) previous participation in electrical stimulation therapy.

All patients were required to sign an informed consent form before enrollment. This study was approved by the ethics committee of Guang'anmen Hospital, China Academy of Chinese Medical Sciences.

Scan Acquisition

All patients in this study underwent MRI using a Magnetom Skyra 3.0-T scanner (Siemens, Erlangen, Germany). Before the scanning procedure, the patients were instructed to remain awake and avoid active thinking. During the scanning process, the patients were required to wear earplugs and noise-canceling headphones, to use a hood to immobilize the head, and to lie flat on the examination bed. The scanning procedure involved a localizer scan, high-resolution three-dimensional T1-weighted imaging, and BOLD-fMRI.

The scanning parameters were as follows: for three-dimensional T1-weighted imaging, time repetition/time echo = 2500/2.98 ms, flip angle = 7°, matrix = 64 × 64, field of view = 256 mm × 256 mm, slice thickness = 1 mm, slice number = 48, slices = 192, scanning time = 6 min 3 s; for BOLD-fMRI, time repetition/time echo = 2000/30 ms, flip angle = 90°, matrix = 64 × 64, field of view = 240 mm × 240 mm, slice number = 43, slice thickness/spacing = 3.0/1.0 mm, number of obtained volumes = 200, and scanning time = 6 min 40 s.

Image Processing

fMRI Data Preprocessing

The acquired rs-fMRI data were pre-processed using MATLAB-based DPARSF 5.1 software (DPARSF 5.1, http://www.rfmri.org/DPARSF). (1) conversion of DICOM raw data to NIFTI format; (2) removal of the first 10 time points in order to put the data in a stable state; (3) slice-timing; (4) realignment of head-motion (removal of patients with head movements > 2 mm in any direction and motor rotation >2°); (5) regression of covariates, including brain white matter signal, cerebrospinal fluid signal and head movement parameters; (6) spatial normalization: functional images of all subjects were converted to Montreal Neurological Institute (MNI) standard space using DARTEL; (7) linear detrending and filtering (0.01 to 0.08 Hz).

ALFF Analysis

The data were spatially normalized and smoothed, and then a fast fourier transform (FFT) was performed to switch the time series to the frequency domain to obtain the power spectrum. The square root of the power spectrum at each frequency is calculated to obtain the average square root of the ALFF measurement for each voxel in the range of 0.01 to 0.08 Hz. Finally, time bandpass filtering (0.01 to 0.08 Hz) is then performed. To reduce inter-individual variability, ALFF was transformed to zALFF by Fisher's z transformation prior to statistical analysis.

ReHo Analysis

The similarity of the time series of each voxel to its neighboring voxels (26 neighboring voxels) was assessed using the Kendall's coefficient concordance(KCC), i.e., ReHo values. The whole-brain ReHo images of the subjects were obtained by calculating the KCC values of the whole-brain voxels. To improve the signal-to-noise ratio, the ReHo images were spatially smoothed using a 6 mm×6 mm×6 mm full-width half-height Gaussian kernel.

Statistical Analyses

Clinical Data Analysis

Clinical data were analyzed with SPSS 23.0 statistical software (IBM Corporation, Somers, New York). One-way analysis of variance (ANOVA) was used to compare ages and education levels among the three groups, and the chi-square test was used to compare gender. A two-sample *t*-test was used to compare the duration of disease and HAMD-17 scores between the two groups, with $P < 0.05$ (two-tailed) as the threshold for statistical significance.

fMRI Data Analysis

Image data were analyzed using the DPARSF toolbox, and a voxel-based one-way ANOVA was performed to compare whole-brain ALFF/ReHo map of the three groups. Gender, age, education level and framewise displacement (FD) metric (derived from Jenkinson's formula) of the three groups of subjects were used as covariates, and brain areas with ALFF/ReHo differences between the three groups were corrected for Gaussian random fields (GRF), and corrected cluster levels were set as $P<0.05$ (two-tailed) and threshold voxel levels $P < 0.005$ were defined as statistically different. We performed *post-hoc t*-test analysis using DPARSF 5.1 software for two-by-two comparisons between groups, and Bonferroni correction was applied to the results, setting a threshold of $P < 0.016$ (0.05/3) for statistical significance.

In order to verify the relationship between ALFF/ReHo values and clinical symptoms, we extracted the mean ALFF/ReHo values of the three different brain regions and did Pearson correlation analysis with the clinical scale scores of each group, and the statistical threshold of $P < 0.05$ (two-tailed) was statistically significant.

RESULTS

Characteristics of Research Samples

Two patients with TRD and one patient with nTRD were excluded because of excessive head movement. Therebefore, a total of 35 patients with TRD, 35 patients with nTRD, and 35 HCs were eligible for the study criteria. There were no statistical differences among the three groups in terms of gender, age and years of education. There was no statistical difference between

TABLE 1 | Demographic and clinical characteristics of the study participants.

Variable	TRD group (*n*, 35)	nTRD group (*n*, 35)	HC group(*n*, 35)	*t(F)*/χ2	*P*-value
Gender (M/F)	13/22	15/20	14/21	0.238	0.888[a]
Age (years)	36.65 ± 9.63	37.14 ± 9.85	37.48 ± 10.82	0.059	0.943[b]
Education (years)	14.20 ± 3.07	14.48 ± 2.70	14.37 ± 3.56	0.074	0.929[b]
Duration of illness (months)	48.45 ± 18.75	23.57 ± 13.99	NA	6.292	<0.001[c*]
HAMD-17 score	23.28 ± 3.73	22.57 ± 3.55	NA	0.820	0.415[c]

TRD, treatment resistant depression; nTRD, non-treatment-resistant depression; HC, healthy control; HAMD-17, 17-item Hamilton Rating Scale for Depression; NA; not applicable.
[a]The P-values of gender distribution among the three groups were obtained by chi-square test.
[b]The P-values were obtained by one-way analysis of variance tests.
[c]The P-value obtained by two-sample t-test.
**Significant difference.*

TABLE 2 | ALFF differences in TRD group; nTRD group; and HC group.

Clusters	Brain regions	MNI Peak			Cluster size	*F*/*T*–value (peak)
		X	Y	Z		
Differences among three groups						
1	Left inferior frontal triangular gyrus	−42	24	27	19	12.195
2	Right inferior frontal triangular gyrus	39	30	18	44	19.130
3	Left middle temporal gyrus	−39	−57	21	67	28.318
4	Right superior temporal gyrus	45	−42	21	60	17.731
5	Left precental gyrus	−33	9	33	34	23.937
6	Left cuneus	−6	−78	30	29	10.982
7	Left superior occipital gyrus	−21	−81	36	21	10.729
8	Bilateral posterior lobes of the cerebellum	−15	−75	−24	102	15.192
TRD group vs. nTRD group						
1	Left inferior frontal triangular gyrus	−45	27	27	18	−2.914
2	Right inferior frontal triangular gyrus	36	33	18	35	−2.837
3	Left middle frontal gyrus	−36	12	36	31	5.129
4	Left middle temporal gyrus	−42	−54	9	14	−2.932
5	Right superior temporal gyrus	45	−42	21	23	5.108
6	Left cuneus	−15	−81	24	24	−2.813
7	Bilateral posterior lobes of the cerebellum	15	−72	−24	87	−2.813
TRD group vs. HC group						
1	Right inferior frontal triangular gyrus	45	30	21	18	−2.850
2	Left middle frontal gyrus	−33	9	33	25	5.529
3	Left middle temporal gyrus	−48	−57	9	40	−2.831
nTRD group vs. HC group						
1	Left angular gyrus	−39	−60	27	27	−2.808
2	Right superior temporal gyrus	45	−36	21	13	3.839

MNI Peak; Coordinates of primary peak locations in the Montreal Neurological Institute space.

the TRD and nTRD groups in terms of HAMD-17 scores and a statistical difference in terms of illness duration (**Table 1**).

Differences in ALFF/ ReHo Among the TRD Group, nTRD Group, and HC Group

A one-way ANOVA revealed significant differences in ALFF and ReHo among the three groups in the left/right inferior frontal triangular gyrus, left middle temporal gyrus and right superior temporal gyrus. Meanwhile, there were significant differences among the three groups in ALFF in the left precentral gyrus, left cuneus, left superior occipital gyrus, and bilateral posterior lobes of the cerebellum, and significant differences in ReHo in the right superior frontal gyrus (**Tables 2**, **3** and **Figures 1**, **2**).

Compared with the nTRD group, the TRD group had increased ALFF in the left middle frontal gyrus, right superior temporal gyrus, and decreased ALFF in the left/right inferior frontal triangular gyrus, left middle temporal gyrus, left cuneus, and bilateral posterior lobes of the cerebellum. On the other hand, the TRD group had increased ReHo in the right superior frontal gyrus and decreased ReHo in the left/right inferior frontal

TABLE 3 | ReHo differences in TRD group; nTRD group; and HC group.

Clusters	Brain regions	MNI Peak			Cluster size	*F*/*T*–value (peak)
		X	Y	Z		
Differences among three groups						
1	Left inferior frontal triangular gyrus	−36	21	24	32	15.834
2	Right inferior frontal triangular gyrus	39	30	18	53	16.467
3	Right superior frontal gyrus	18	9	51	40	13.174
4	Left middle temporal gyrus	−36	−57	21	60	27.620
5	Right superior temporal gyrus	36	−27	21	42	13.949
TRD group vs. nTRD group						
1	Left inferior frontal triangular gyrus	−39	24	21	30	−2.944
2	Right inferior frontal triangular gyrus	42	30	18	29	−2.878
3	Right superior frontal gyrus	18	9	54	22	4.317
4	Left middle temporal gyrus	−45	−57	6	20	−2.833
TRD group vs. HC group						
1	Right inferior frontal triangular gyrus	42	33	15	27	−2.818
2	Left middle temporal gyrus	−45	−54	3	35	−2.834
nTRD group vs. HC group						
1	Left angular gyrus	−36	−63	21	27	−2.847
2	Right insula	36	−27	21	20	3.038

MNI Peak; Coordinates of primary peak locations in the Montreal Neurological Institute space.

triangular gyrus, and left middle temporal gyrus (**Tables 2**, **3** and **Figure 3**).

Compared with the HC group, the TRD group had increased ALFF in the left middle frontal gyrus and decreased ALFF in the right inferior frontal triangular gyrus and left middle temporal gyrus. On the other hand, the TRD group had decreased ReHo in the right inferior frontal triangular gyrus and left middle temporal gyrus (**Tables 2**, **3** and **Figure 4**).

Compared with the HC group, the nTRD group had increased ALFF in the right superior temporal gyrus and decreased ALFF in the left angular gyrus. On the other hand, the nTRD group had increased ReHo in the right insula and decreased ReHo in the left angular gyrus (**Tables 2**, **3** and **Figure 5**).

Significant Correlation Between Functional Image and Clinical Feature

To test the correlation between areas of abnormal brain activity and the severity of clinical depressive symptoms, we further performed Pearson correlation analysis. We found that the ALFF values of the left inferior frontal triangular gyrus, left middle temporal gyrus, and bilateral posterior lobes of the cerebellum in the TRD group were positively correlated with the HAMD-17 score ($r = 0.432$, $P = 0.009$; $r = 0.483$, $P = 0.003$; $r = 0.360$, $P = 0.033$). Meanwhile, the ReHo values of the left middle temporal gyrus in the TRD group were positively correlated with the HAMD-17 scores ($r = 0.335$, $P = 0.048$). On the other hand, the ALFF values of the left/right inferior frontal triangular gyrus in the nTRD group were positively correlated with the HAMD-17 score ($r = 0.342$, $P = 0.043$; $r = 0.395$, $P = 0.018$). In addition, the ReHo values of the right inferior frontal triangular gyrus in the nTRD group were positively correlated with the HAMD-17 score ($r = 0.407$, $P = 0.015$) (**Table 4** and **Figure 6**).

DISCUSSION

To our knowledge, this is the first study of the relationship between changes in local functional brain activity in TRD and nTRD using ALFF and ReHo. The results of this study showed no significant differences in clinical depressive symptoms between the TRD and nTRD groups, but abnormal neurofunctional activity in some of the same brain regions. Compared with the nTRD group, the brain regions of ALFF and ReHo in the TRD group were more extensively altered, and the neuropathological mechanisms was more complex. This study provides a reference value for the differences in functional brain activity between TRD and nTRD.

In this study, we found TRD group had decreased ALFF/ReHo in the left/right inferior frontal triangular gyrus compared to the nTRD group. The inferior frontal triangular gyrus is located in the pre-frontal lobe, near the orbito frontal cortex (OFC) and the middle frontal gyrus, and is a key brain region for emotional and cognitive control circuits, and is associated with certain types of behavioral inhibition (39–41). The inferior frontal triangular gyrus is not only an important part of the CCN, but is also closely related to MDD (38, 39). In addition, the inferior frontal triangle gyrus is known for its involvement in speech function and language processing (42). Patients with MDD are characterized by a wide range of abnormalities in language comprehension (43). A study suggests that glutamatergic neurotransmission may play a regulatory role in language acquisition, comprehension, and production (44). Abnormal glutamate signaling plays an

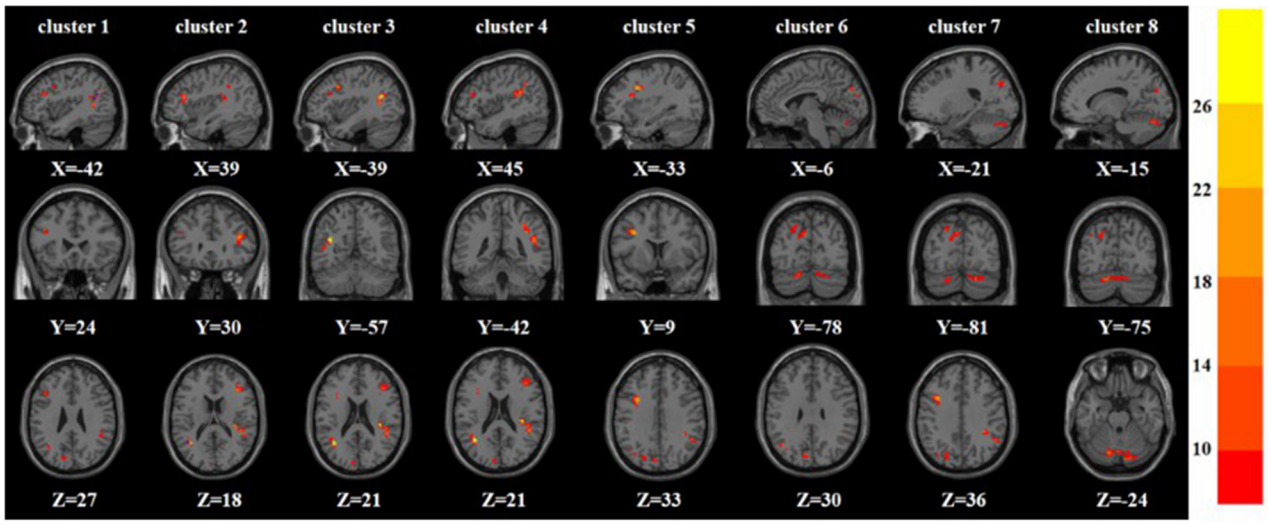

FIGURE 1 | Based on one-way ANOVA for three groups of ALFF abnormal brain regions. The color bars indicate the *F*-value.

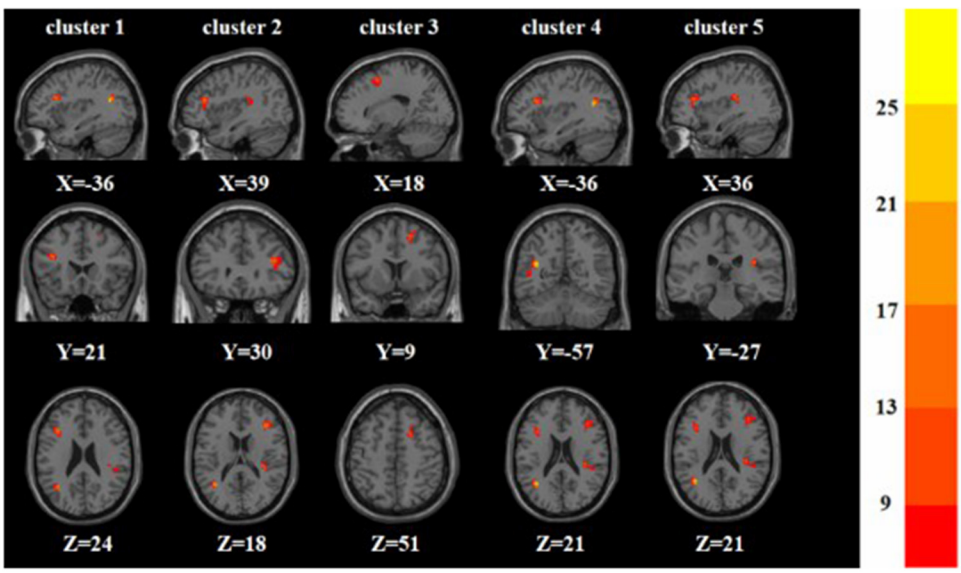

FIGURE 2 | Based on one-way ANOVA for three groups of ReHo abnormal brain regions. The color bars indicate the *F*-value.

important role in the etiology of MDD (45, 46). More research is needed to understand how MDD-related genes affect the inferior frontal triangular gyrus. Previous studies have also found ALFF differences in the TRD group, treatment response depression (TSD) group and HC group in the inferior frontal gyrus (32). Another study found that TRD had decreased ReHo in the left inferior frontal gyrus than in the nTRD group, which is consistent with the results of this study (31). A study also found that significantly dereduced glucose metabolism in the right inferior frontal gyrus of patients with MDD was associated with the severity of pleasure deficits in depression (47). Therefore, the results of this study showed that ALFF and ReHo were decreased in the TRD group compared to the nTRD group, suggesting a more severely impaired inferior frontal triangular gyrus in the TRD group. Correlation analysis showed that ALFF/ReHo values in the left/right inferior frontal triangular gyrus of the nTRD group were positively correlated with HAMD-17 scores, suggesting that the occurrence of depressive symptoms in the nTRD group was more closely related to dysfunction in the inferior frontal triangular gyrus, and that the inferior frontal triangular gyrus was an important differential brain area between the TRD and nTRD groups.

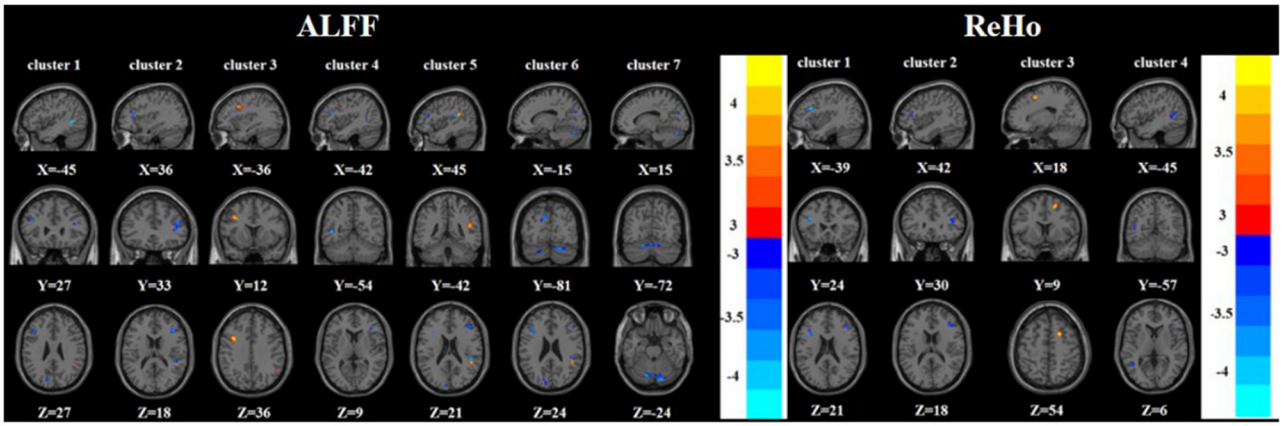

FIGURE 3 | Brain regions with abnormal ALFF (left) and ReHo (right) between TRD group and nTRD group based on *post hoc T*-tests. The color bars indicate the *T*-value.

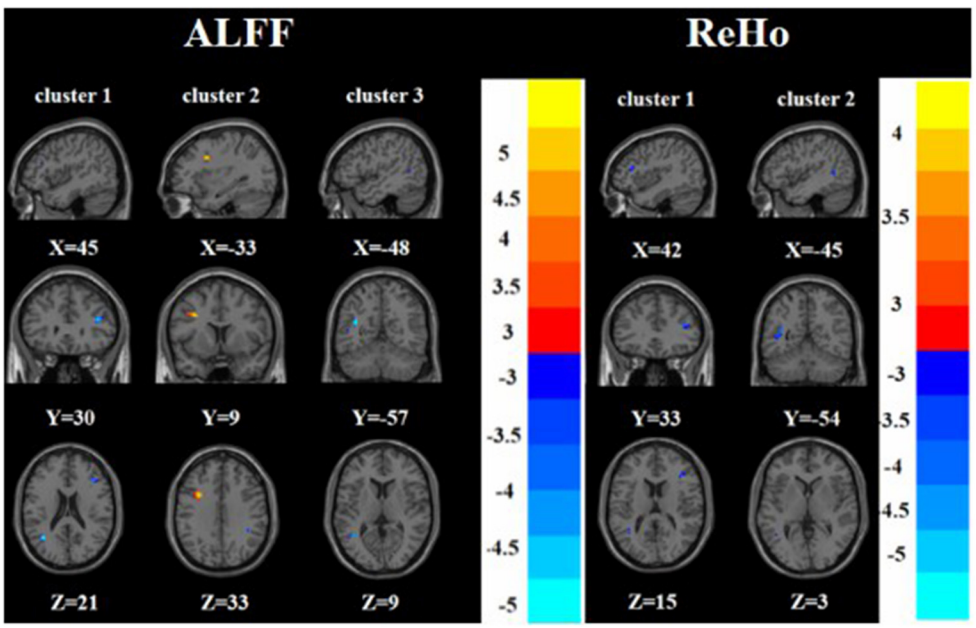

FIGURE 4 | Brain regions with abnormal ALFF (left) and ReHo (right) between TRD group and HC group based on *post hoc T*-tests. The color bars indicate the *T*-value.

We found that the TRD group had increased ALFF in the left middle frontal gyrus and ReHo in the right superior frontal gyrus compared to the nTRD group. The left middle frontal gyrus and the right superior frontal gyrus are key brain regions of the dorsolateral prefrontal cortex (DLPFC) and an important component of the CCN (48, 49). Several studies have shown that treatment with repetitive transcranial magnetic stimulation and transcranial direct current stimulation in the CCN, especially DLPFC, can directly improve core symptoms such as mood and cognition in MDD patients (50). Previous studies also found that the TRD group had significantly increased ALFF in the left DLPFC compared to the nTRD group, which is consistent with the results of the present study (30). Therefore, the results of this study suggest that both ALFF and ReHo are sensitive to the left middle frontal gyrus in TRD patients, suggesting that impaired function of the DLPFC is one of the causes of the complex pathological mechanisms in TRD patients.

We also found that ALFF/ReHo in the left middle temporal gyrus was decreased in the TRD group compared to the nTRD group. The middle temporal gyrus is involved in tasks related to lexical cognition and semantic understanding in humans and is important for understanding visual and auditory information (51, 52). The possibility of functional disruption of the middle temporal gyrus in MDD and schizophrenia exists (53, 54). The

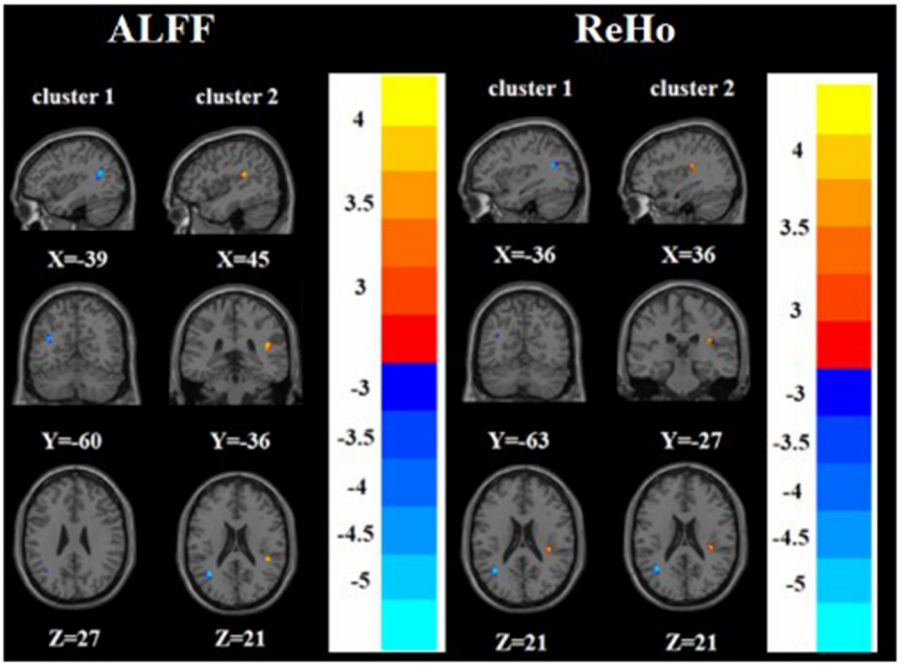

FIGURE 5 | Brain regions with abnormal ALFF (left) and ReHo (right) between nTRD group and HC group based on *post hoc T*-tests. The color bars indicate the *T*-value.

TABLE 4 | Correlation of abnormal brain areas with clinical symptoms.

Variables	Group	Brain regions	HAMD−17 score	
			Coefficient	*P*–value
ALFF	TRD	Left inferior frontal triangular gyrus	0.432	0.009[d#]
		Left middle temporal gyrus	0.483	0.003[d#]
		Bilateral posterior lobes of the cerebellum	0.360	0.033[d#]
	nTRD	Left inferior frontal triangular gyrus	0.342	0.043[d#]
		Right inferior frontal triangular gyrus	0.395	0.018[d#]
ReHo	TRD	Left middle temporal gyrus	0.335	0.048[d#]
	nTRD	Right inferior frontal triangular gyrus	0.407	0.015[d#]

[d] *P–value for pearson correlation(not corrected).*
[#] *Statistical significance.*

middle temporal gyrus is also closely related to the DMN and is the basis of the DMN in the functional role of language (51). Previous studies have also found differences in ReHo in the right middle temporal gyrus between the TRD and nTRD groups (31). A clinical study also showed that electroconvulsive therapy improved TRD and was associated with the ability to enhance high connectivity between the anterior subgenual anterior cingulate and the middle temporal gyrus (55). Therefore, both ALFF and ReHo in the left middle temporal gyrus were decreased in the TRD group in this study, suggesting that compensatory hypofunction of the left middle temporal gyrus may be an important mechanism in the pathogenesis of TRD patients. In addition, correlation analysis showed that ALFF and ReHo values of the left middle temporal gyrus in the TRD group were positively correlated with HAMD-17 scores, while this was not found in the nTRD group, suggesting that the left middle temporal gyrus may be a neuroimaging marker of TRD.

The right superior temporal gyrus also plays an important role in social-emotional processing as part of the DMN (56, 57). Patients with TRD are vulnerable to suicide risk during adolescence, and reduced volume of the right superior temporal gyrus can be a marker for suicide attempts during adolescence (57). Previous studies have found ReHo was decreased in the right superior temporal gyrus in TRD group than in the HC group (31). The results of this study showed that ALFF in the right superior temporal gyrus was increased in the TRD group compared to the nTRD group, indicating an important

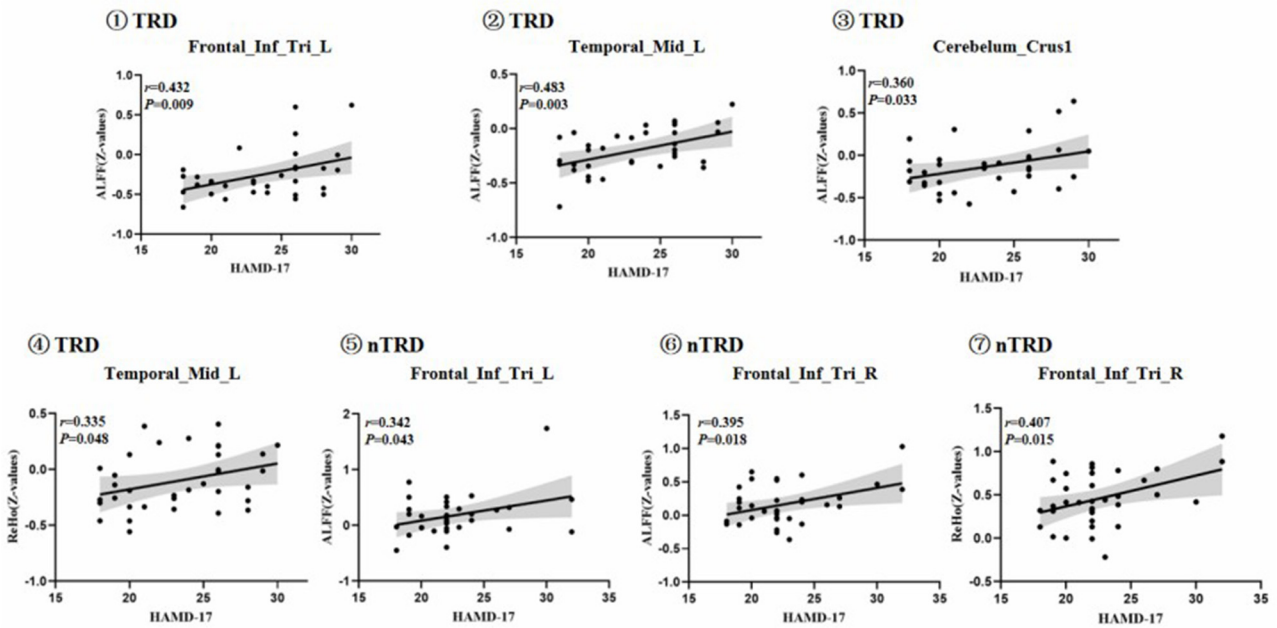

FIGURE 6 | Positive correlation between the ALFF and ReHo of the abnormal brain regions: ①Frontal_Inf_Tri_L, Left inferior frontal triangular gyrus; ALFF value of TRD group; ②Temporal_Mid_L, left middle temporal gyrus; ALFF value of TRD group; ③Cerebelum_Crus1, bilateral posterior lobes of the cerebellum(Crus I); ALFF value of TRD group; ④ Temporal_Mid_L, left middle temporal gyrus; ReHo value of TRD group; ⑤Frontal_Inf_Tri_L, Left inferior frontal triangular gyrus; ALFF value of nTRD group; ⑥Frontal_Inf_Tri_R, Right inferior frontal triangular gyrus; ALFF value of nTRD group; ⑦Frontal_Inf_Tri_R, Right inferior frontal triangular gyrus; ReHo value of nTRD group.

differential brain area between TRD and nTRD in the right superior temporal gyrus.

In this study, ALFF in the left cuneus was decreased in the TRD group compared to the nTRD group. The cuneus is part of the occipital lobe and is involved in visual perception functions (e.g., facial emotion) and plays an important role in social interaction (58, 59). Functional changes in the cuneus lobe are also closely related to MDD (60, 61). A study of an fMRI reward processing task found that adolescents with unremitting depression showed greater activation in the frontal middle gyrus and less activation in the cuneus compared to adolescents with remitting depression (62). Previous studies found that the ReHo in the left precuneus was decreased in the TRD group compared to the nTRD group (31). Another study also found decreased FC between the medial pre-frontal cortex and the cuneus in the TRD group compared to the nTRD group (63). Therefore, the results of this study suggest that abnormal function of the left cuneus is one of the reasons for the complex neuropathological mechanism of TRD.

Compared with the nTRD group, the ALFF of bilateral posterior lobes of the cerebellum in the TRD group was decreased compared to the nTRD group. In addition to the motor domain, the cerebellum is also involved in the cognitive and emotional aspects of the human body (64). Atrophy of the cerebellum often leads to cognitive and emotional symptoms, sometimes referred to as "cerebellar cognitive-emotional syndrome" (65). Cerebellar damage predisposes to language processing, aspects of executive function, and emotional dysregulation (66). Animal model studies have shown that electrical stimulation experiments also link cerebellar neural activity to depression and impulsive behavior (67). Previous studies have shown that ReHo was decreased in the bilateral cerebellum in the TRD group compared to the TSD group. Therefore, the results of the present study suggest that the posterior lobes of the cerebellum is further involved in emotion regulation in patients with TRD. In addition, correlation analysis showed a positive correlation between ALFF values and HAMD-17 scores in the bilateral posterior lobes of the cerebellum. Therefore, bilateral posterior lobes of the cerebellum may be a neuroimaging marker in patients with TRD.

Meanwhile, we also found that the TRD group had decreased ALFF/ReHo in the right inferior frontal triangular gyrus and left middle temporal gyrus compared to the HC group. Previous studies found that the TRD group had decreased ALFF in the right inferior frontal gyrus and left middle temporal gyrus compared to the HC group, which is consistent with the present study (68). However, it has also been found that the ReHo in the TRD group was decreased in the left lateral inferior frontal gyrus than in the HC group, and increased in the right middle temporal gyru scompared to the HC group, which is different from the present study (31). This variation in results may be related to differences in patient medication use, sample size and scanning and analysis methods. However, all of the above studies suggest that the inferior frontal gyrus and middle temporal gyrus are important differential brain regions between the TRD and

HC groups. Interestingly, the inferior frontal triangular gyrus and middle temporal gyrus were also important differences between the TRD and nTRD groups, while no differences were found between the nTRD and HC groups in these two brain regions, therefore, further attention and research on these two brain regions are needed in the future.

Some limitations should be considered. First, although the patients in this study were included strictly according to the inclusion criteria, there were still some factors that potentially influenced the results of this study, such as the time of onset, the use of antidepressants and the duration of the disease. Second, this study focused on only one scale, the HAMD-17, and more scales need to be used in the future to focus in more detail on the correlation between cognitive, anxiety, insomnia, and somatic subtypes of symptoms with TRD and nTRD in patients with MDD, thus improving the scientific value of this study. Third, we did not clarify the gender differences between the different groups of the sample in this study, so this is an important direction for future research. Finally, Setting a GRF correction threshold voxel level of $P < 0.001$ is more statistically valid (69, 70), but we did not find significant cluster. Setting a threshold of $P < 0.005$ in this study may be slightly statistically weak, and in future studies, we will further expand the sample size and use more stringent statistical validity to enhance the scientific value of this study.

CONCLUSION

In conclusion, we used ALFF and ReHo based on rs-fMRI technique to preliminarily analyze the differences in local neurological functional activity between TRD and nTRD brains. We found that although the clinical symptoms were similar in the TRD and nTRD groups, there was abnormal neurofunctional activity in some of the same brain regions, and ALFF and ReHo were more extensively altered in the TRD group with more complex neuropathological mechanisms, especially in the inferior frontal triangular gyrus of the frontal lobe and the middle temporal gyrus of the temporal lobe.

DATA AVAILABILITY STATEMENT

The raw data supporting the conclusions of this article will be made available by the authors, without undue reservation.

ETHICS STATEMENT

The studies involving human participants were reviewed and approved by the Ethics Committee of Guang'anmen Hospital, Chinese Academy of Traditional Chinese Medicine (NO. 2017-021-SQ). The patients/participants provided their written informed consent to participate in this study.

AUTHOR CONTRIBUTIONS

JF conceived and designed this experiment. JS drafted the manuscript and participated in data collection and analysis. YM drew diagrams and made statistical analysis of data. LC, ZW, CG, YL, DG, XL, and KX involved in data analysis and data collection. YH performed fMRI on the subjects. XH, JT, XY, HW, and XX involved in case collection and symptom assessment of patients. All authors contributed to the article and approved the submitted version.

FUNDING

This research was supported by the China Academy of Chinese Medical Sciences Innovation Fund (CI2021A03301), National Natural Science Foundation of China (82174282 and 81774433), National Key Research and Development Program of China (2018YFC1705802), and Clinical Efficacy and Brain Mechanism of Transcutaneous Auricular Vagus Nerve Stimulation for patients With Mild to Moderate Depression (QYSF-2020-02).

ACKNOWLEDGMENTS

We thank all the subjects who participated in the experiment for their support.

REFERENCES

1. Hasin DS, Sarvet AL, Meyers JL, Saha TD, Ruan WJ, Stohl M, et al. Epidemiology of adult DSM-5 major depressive disorder and its specifiers in the United States. *JAMA Psychiatry.* (2018) 75:336–46. doi: 10.1001/jamapsychiatry.2017.4602
2. Ahmed HU, Hossain MD, Aftab A, Soron TR, Alam MT, Chowdhury MWA, et al. Suicide and depression in the world health organization South-East Asia Region: a systematic review. *WHO South East Asia J Public Health.* (2017) 6:60–6. doi: 10.4103/2224-3151.206167
3. Ionescu DF, Rosenbaum JF, Alpert JE. Pharmacological approaches to the challenge of treatment-resistant depression. *Dialogues Clin Neurosci.* (2015) 17:111–26. doi: 10.31887/DCNS.2015.17.2/dionescu
4. Gaynes BN, Lux L, Gartlehner G, Asher G, Forman-Hoffman V, Green J, et al. Defining treatment-resistant depression. *Depress Anxiety.* (2020) 37:134–45. doi: 10.1002/da.22968
5. Pandarakalam JP. Challenges of treatment-resistant depression. *Psychiatr Danub.* (2018) 30:273–84. doi: 10.24869/psyd.2018.273
6. Berlim MT, Fleck MP, Turecki G. Current trends in the assessment and somatic treatment of resistant/refractory major depression: an overview. *Ann Med.* (2008) 40:149–59. doi: 10.1080/07853890701769728
7. Jaffe DH, Rive B, Denee TR. The humanistic and economic burden of treatment-resistant depression in Europe: a cross-sectional study. BMC Psychiatry. (2019) 19:247. doi: 10.1186/s12888-019-2222-4
8. Ivanova JI, Birnbaum HG, Kidolezi Y, Subramanian G, Khan SA, Stensland MD. Direct and indirect costs of employees with treatment-resistant and non-treatment-resistant major depressive disorder. *Curr Med Res Opin.* (2010) 26:2475–84. doi: 10.1185/03007995.2010.517716
9. Crown WH, Finkelstein S, Berndt ER, Ling D, Poret AW, Rush AJ, et al. The impact of treatment-resistant depression on health care utilization and costs. *J Clin Psychiatry.* (2002) 63:963–71. doi: 10.4088/JCP.v63n1102
10. DiBernardo A, Lin X, Zhang Q, Xiang J, Lu L, Jamieson C, et al. Humanistic outcomes in treatment resistant depression: a secondary analysis of the STAR∗D study. *BMC Psychiatry.* (2018) 18:352. doi: 10.1186/s12888-018-1920-7

11. Li QS, Tian C, McIntyre MH, Sun Y; 23andMe Research Team, Hinds DA, Narayan VA. Phenotypic analysis of 23andMe survey data: treatment-resistant depression from participants' perspective. *Psychiatry Res.* (2019) 278:173–9. doi: 10.1016/j.psychres.2019.06.011
12. Qiao J, Geng D, Qian L, Zhu X, Zhao H. Correlation of clinical features with hs-CRP in TRD patients. *Exp Ther Med.* (2019) 17:344–8. doi: 10.3892/etm.2018.6914
13. Enache D, Pariante CM, Mondelli V. Markers of central inflammation in major depressive disorder: a systematic review and meta-analysis of studies examining cerebrospinal fluid, positron emission tomography and post-mortem brain tissue. *Brain Behav Immun.* (2019) 81:24–40. doi: 10.1016/j.bbi.2019.06.015
14. Liu JJ, Wei YB, Strawbridge R, Bao Y, Chang S, Shi L, et al. Peripheral cytokine levels and response to antidepressant treatment in depression: a systematic review and meta-analysis. *Mol Psychiatry.* (2020) 25:339–50. doi: 10.1038/s41380-019-0474-5
15. Gong J, Wang J, Qiu S, et al. Common and distinct patterns of intrinsic brain activity alterations in major depression and bipolar disorder: voxel-based meta-analysis. *Transl Psychiatry.* (2020) 10:353. doi: 10.1038/s41398-020-01036-5
16. Cui P, Kong K, Yao Y, Huang Z, Shi S, **Liu P**, et al. Brain functional alterations in MDD patients with somatic symptoms: a resting-state fMRI study. *J Affect Disord.* (2021) 295:788–96. doi: 10.1016/j.jad.2021.08.143
17. Mwansisya TE, Hu A, Li Y, Chen X, Wu G, Huang X, et al. Task and resting-state fMRI studies in first-episode schizophrenia: A systematic review. *Schizophr Res.* (2017) 189:9–18. doi: 10.1016/j.schres.2017.02.026
18. Dapretto M, Davies MS, Pfeifer JH, Scott AA, Sigman M, Bookheimer SY, et al. Understanding emotions in others: mirror neuron dysfunction in children with autism spectrum disorders. *Nat Neurosci.* (2006) 9:28–30. doi: 10.1038/nn1611
19. Drysdale AT, Grosenick L, Downar J, Dunlop K, Mansouri F, Meng Y, et al. Resting-state connectivity biomarkers define neurophysiological subtypes of depression. *Nat Med.* (2017) 23:264. doi: 10.1038/nm.4246
20. Borserio BJ, Sharpley CF, Bitsika V, Sarmukadam K, Fourie PJ, Agnew LL. Default mode network activity in depression subtypes. *Rev Neurosci.* (2021) 32:597–613. doi: 10.1515/revneuro-2020-0132
21. Guo CC, Hyett MP, Nguyen VT, Parker GB, Breakspear MJ. Distinct neurobiological signatures of brain connectivity in depression subtypes during natural viewing of emotionally salient films. *Psychol Med.* (2016) 46:1535–45. doi: 10.1017/S0033291716000179
22. Fagiolini A, Kupfer DJ. Is treatment-resistant depression a unique subtype of depression? *Biol Psychiatry.* (2003) 53:640–8. doi: 10.1016/S0006-3223(02)01670-0
23. Zang Y, Jiang T, Lu Y, He Y, Tian L. Regional homogeneity approach to fMRI data analysis. *Neuroimage.* (2004) 22:394–400. doi: 10.1016/j.neuroimage.2003.12.030
24. Zang YF, He Y, Zhu CZ, Cao QJ, Sui MQ, Liang M, et al. Altered baseline brain activity in children with ADHD revealed by resting-state functional MRI. *Brain Dev.* (2007) 29:83–91. doi: 10.1016/j.braindev.2006.07.002
25. Shen Z, Zhu J, Ren L, Qian M, Shao Y, Yuan Y, et al. Aberrant amplitude low-frequency fluctuation (ALFF) and regional homogeneity (ReHo) in generalized anxiety disorder (GAD) and their roles in predicting treatment remission. *Ann Transl Med.* (2020) 8:1319. doi: 10.21037/atm-20-6448
26. Yue Y, Jiang Y, Shen T, Pu J, Lai HY, Zhang B. ALFF and ReHo mapping reveals different functional patterns in early- and late-onset parkinson's disease. *Front Neurosci.* (2020) 14:141. doi: 10.3389/fnins.2020.00141
27. Chrobak AA, Bohaterewicz B, Sobczak AM, Marszał-Wiśniewska M, Tereszko A, Krupa A, et al. Time-Frequency characterization of resting brain in bipolar disorder during Euthymia-a preliminary study. *Brain Sci.* (2021) 11:599. doi: 10.3390/brainsci11050599
28. Wei HL, Tian T, Zhou GP, et al. Disrupted dynamic functional connectivity of the visual network in episodic patients with migraine without aura. *Neural Plast.* (2022) 2022:9941832. doi: 10.1155/2022/9941832
29. Guo WB, Sun XL, Liu L, Xu Q, Wu RR, Liu ZN, et al. Disrupted regional homogeneity in treatment-resistant depression: a resting-state fMRI study. *Prog Neuropsychopharmacol Biol Psychiatry.* (2011) 35:1297–302. doi: 10.1016/j.pnpbp.2011.02.006
30. Zhang A, Li G, Yang C, Liu P, Wang Y, Kang L, et al. Alterations of amplitude of low-frequency fluctuation in treatment-resistant versus non-treatment-resistant depression patients. *Neuropsychiatr Dis Treat.* (2019) 15:2119–28. doi: 10.2147/NDT.S199456
31. Wu QZ, Li DM, Kuang WH, Zhang TJ, Lui S, Huang XQ, et al. Abnormal regional spontaneous neural activity in treatment-refractory depression revealed by resting-state fMRI. *Hum Brain Mapp.* (2011) 32:1290–9. doi: 10.1002/hbm.21108
32. Guo WB, Liu F, Xue ZM, Xu XJ, Wu RR, Ma CQ, et al. Alterations of the amplitude of low-frequency fluctuations in treatment-resistant and treatment-response depression: a resting-state fMRI study. *Prog Neuropsychopharmacol Biol Psychiatry.* (2012) 37:153–60. doi: 10.1016/j.pnpbp.2012.01.011
33. Suo N, He B, Cui S, Yang Y, Wang M, Yuan Q, et al. Convergent functional changes of default mode network in mild cognitive impairment using activation likelihood estimation. *Front Aging Neurosci.* (2021) 13:708687. doi: 10.3389/fnagi.2021.708687
34. Li CT, Lin CP, Chou KH, Chen IY, Hsieh JC, Wu CL, et al. Structural and cognitive deficits in remitting and non-remitting recurrent depression: a voxel-based morphometric study. *Neuroimage.* (2010) 50:347–56. doi: 10.1016/j.neuroimage.2009.11.021
35. Raichle ME, MacLeod AM, Snyder AZ, Powers WJ, Gusnard DA, Shulman GL, et al. default mode of brain function. *Proc Natl Acad Sci U S A.* (2001) 98:676–82. doi: 10.1073/pnas.98.2.676
36. Raichle ME, Snyder AZ. A default mode of brain function: a brief history of an evolving idea. *Neuroimage.* (2007) 37:1083–99. doi: 10.1016/j.neuroimage.2007.02.041
37. Depping MS, Wolf ND, Vasic N, Sosic-Vasic Z, Schmitgen MM, Sambataro F, et al. Aberrant resting-state cerebellar blood flow in major depression. *J Affect Disord.* (2018) 226:227–31. doi: 10.1016/j.jad.2017.09.028
38. Pan F, Xu Y, Zhou W, Chen J, Wei N, Lu S, et al. Disrupted intrinsic functional connectivity of the cognitive control network underlies disease severity and executive dysfunction in first-episode, treatment-naive adolescent depression. *J Affect Disord.* (2020) 264:455–63. doi: 10.1016/j.jad.2019.11.076
39. Du J, Rolls ET, Cheng W, et al. Functional connectivity of the orbitofrontal cortex, anterior cingulate cortex, and inferior frontal gyrus in humans. *Cortex.* (2020) 123:185–99. doi: 10.1016/j.cortex.2019.10.012
40. Briggs RG, Lin YH, Dadario NB, Kim SJ, Young IM, Bai MY, et al. Anatomy and white matter connections of the middle frontal Gyrus. *World Neurosurg.* (2021) 150:e520–9. doi: 10.1016/j.wneu.2021.03.045
41. Badre D, Nee DE. Frontal cortex and the hierarchical control of behavior. *Trends Cogn Sci.* (2018) 22:170–88. doi: 10.1016/j.tics.2017.11.005
42. Greenlee JD, Oya H, Kawasaki H, Volkov IO, Severson MA 3rd, Howard MA 3rd et al. Functional connections within the human inferior frontal gyrus. *J Comp Neurol.* (2007) 503:550–9. doi: 10.1002/cne.21405
43. Zhuo C, Zhou C, Lin X, Tian H, Wang L, Chen C, et al. Common and distinct global functional connectivity density alterations in drug-naïve patients with first-episode major depressive disorder with and without auditory verbal hallucination. *Prog Neuropsychopharmacol Biol Psychiatry.* (2020) 96:109738. doi: 10.1016/j.pnpbp.2019.109738
44. Li W, Kutas M, Gray JA, Hagerman RH, Olichney JM. The role of glutamate in language and language disorders - evidence from ERP and pharmacologic studies. *Neurosci Biobehav Rev.* (2020) 119:217–41. doi: 10.1016/j.neubiorev.2020.09.023
45. Bernard R, Kerman IA, Thompson RC, Jones EG, Bunney WE, Barchas JD, et al. Altered expression of glutamate signaling, growth factor, and glia genes in the locus coeruleus of patients with major depression. *Mol Psychiatry.* (2011) 16:634–46. doi: 10.1038/mp.2010.44
46. Pham TH, Gardier AM. Fast-acting antidepressant activity of ketamine: highlights on brain serotonin, glutamate, and GABA neurotransmission in preclinical studies. *Pharmacol Ther.* (2019) 199:58–90. doi: 10.1016/j.pharmthera.2019.02.017
47. Su H, Zuo C, Zhang H, Jiao F, Zhang B, Tang W, et al. Regional cerebral metabolism alterations affect resting-state functional connectivity in major depressive disorder. *Quant Imaging Med Surg.* (2018) 8:910–24. doi: 10.21037/qims.2018.10.05
48. Zhang B, Qi S, Liu S, Liu X, Wei X, Ming D. Altered spontaneous neural activity in the precuneus, middle and superior frontal gyri, and hippocampus

in college students with subclinical depression. *BMC Psychiatry*. (2021) 21:280. doi: 10.1186/s12888-021-03292-1
49. Li W, Li Y, Yang W, Zhang Q, Wei D, Li W, et al. Brain structures and functional connectivity associated with individual differences in Internet tendency in healthy young adults. *Neuropsychologia*. (2015) 70:134–44. doi: 10.1016/j.neuropsychologia.2015.02.019
50. Amidfar M, Ko YH, Kim YK. Neuromodulation and cognitive control of emotion. *Adv Exp Med Biol.* (2019) 1192:545–64. doi: 10.1007/978-981-32-9721-0_27
51. Briggs RG, Tanglay O, Dadario NB, Young IM, Fonseka RD, Hormovas J, et al. The unique fiber anatomy of middle temporal gyrus default mode connectivity. *Oper Neurosurg (Hagerstown).* (2021) 21:E8–E14. doi: 10.1093/ons/opab109
52. Xu J, Wang J, Fan L, Li H, Zhang W, Hu Q, et al. Tractography-based parcellation of the human middle temporal gyrus. *Sci Rep*. (2015) 5:18883. doi: 10.1038/srep18883
53. Jiang J, Chen X, Qiu Y, Wang B, Yu Y, Zhu ZZ, et al. Hyperconnectivity between the posterior cingulate and middle frontal and temporal gyrus in depression: Based on functional connectivity meta-analyses. *Brain Imaging Behav*. (2022) 23:61. doi: 10.1007/s11682-022-00628-7
54. Joo SW, Chon MW, Rathi Y, Shenton ME, Kubicki M, Lee J. Abnormal asymmetry of white matter tracts between ventral posterior cingulate cortex and middle temporal gyrus in recent-onset schizophrenia. *Schizophr Res.* (2018) 192:159–66. doi: 10.1016/j.schres.2017.05.008
55. Subramanian S, Lopez R, Zorumski CF, Cristancho P. Electroconvulsive therapy in treatment resistant depression. *J Neurol Sci.* (2022) 434:120095. doi: 10.1016/j.jns.2021.120095
56. Buckner RL, Andrews-Hanna JR, Schacter DL. The brain's default network: anatomy, function, and relevance to disease. *Ann N Y Acad Sci.* (2008) 1124:1–38. doi: 10.1196/annals.1440.011
57. McLellan Q, Wilkes TC, Swansburg R, Jaworska N, Langevin LM, MacMaster FP. History of suicide attempt and right superior temporal gyrus volume in youth with treatment-resistant major depressive disorder. *J Affect Disord.* (2018) 239:291–4. doi: 10.1016/j.jad.2018.07.030
58. Fusar-Poli P, Placentino A, Carletti F, et al. Functional atlas of emotional faces processing: a voxel-based meta-analysis of 105 functional magnetic resonance imaging studies. *J Psychiatry Neurosci.* (2009) 34:418–32. doi: 10.1111/j.1365-2850.2009.01434.x
59. Parker JG, Zalusky EJ, Kirbas C. Functional MRI mapping of visual function and selective attention for performance assessment and presurgical planning using conjunctive visual search. *Brain Behav*. (2014) 4:227–37. doi: 10.1002/brb3.213
60. Groves SJ, Pitcher TL, Melzer TR, et al. Brain activation during processing of genuine facial emotion in depression: Preliminary findings. *J Affect Disord.* (2018) 225:91–6. doi: 10.1016/j.jad.2017.07.049
61. Farah R, Greenwood P, Dudley J, Hutton J, Ammerman RT, Phelan K„ et al. Maternal depression is associated with altered functional connectivity between neural circuits related to visual, auditory, and cognitive processing during stories listening in preschoolers. *Behav Brain Funct*. (2020) 16:5. doi: 10.1186/s12993-020-00167-5
62. Fischer AS, Ellwood-Lowe ME, Colich NL, Cichocki A, Ho TC, Gotlib IH. Reward-circuit biomarkers of risk and resilience in adolescent depression. *J Affect Disord.* (2019) 246:902–9. doi: 10.1016/j.jad.2018.12.104
63. de Kwaasteniet BP, Rive MM, Ruhé HG, Schene AH, Veltman DJ, Fellinger L, et al. Decreased resting-state connectivity between neurocognitive networks in treatment resistant depression. *Front Psychiatry*. (2015) 6:28. doi: 10.3389/fpsyt.2015.00028
64. Depping MS, Schmitgen MM, Kubera KM, Wolf RC. Cerebellar contributions to major depression. *Front Psychiatry*. (2018) 9:634. doi: 10.3389/fpsyt.2018.00634
65. Schmahmann JD, Weilburg JB, Sherman JC. The neuropsychiatry of the cerebellum - insights from the clinic. *Cerebellum.* (2007) 6:254–67. doi: 10.1080/14734220701490995
66. Hoche F, Guell X, Vangel MG, Sherman JC, Schmahmann JD. The cerebellar cognitive affective/Schmahmann syndrome scale. *Brain.* (2018) 141:248–70. doi: 10.1093/brain/awx317
67. Huguet G, Kadar E, Temel Y, Lim LW. Electrical stimulation normalizes c-Fos expression in the deep cerebellar nuclei of depressive-like rats: implication of antidepressant activity. *Cerebellum.* (2017) 16:398–410. doi: 10.1007/s12311-016-0812-y
68. Guo WB, Liu F, Chen JD, Gao K, Xue ZM, Xu XJ, et al. Abnormal neural activity of brain regions in treatment-resistant and treatment-sensitive major depressive disorder: a resting-state fMRI study. *J Psychiatr Res.* (2012) 46:1366–73. doi: 10.1016/j.jpsychires.2012.07.003
69. Roiser JP, Linden DE, Gorno-Tempinin ML, Moran RJ, Dickerson BC, Grafton ST. Minimum statistical standards for submissions to neuroimage: clinical. *Neuroimage Clin*. (2016) 12:1045–47. doi: 10.1016/j.nicl.2016.08.002
70. Eklund A, Nichols TE, Knutsson H. Cluster failure: Why fMRI inferences for spatial extent have inflated false-positive rates. *Proc Natl Acad Sci U S A*. (2016) 113:7900–5. doi: 10.1073/pnas.1602413113

Conflict of Interest: The authors declare that the research was conducted in the absence of any commercial or financial relationships that could be construed as a potential conflict of interest.

Publisher's Note: All claims expressed in this article are solely those of the authors and do not necessarily represent those of their affiliated organizations, or those of the publisher, the editors and the reviewers. Any product that may be evaluated in this article, or claim that may be made by its manufacturer, is not guaranteed or endorsed by the publisher.

frontiers | Frontiers in Psychiatry

TYPE Original Research
PUBLISHED 09 August 2022
DOI 10.3389/fpsyt.2022.950328

OPEN ACCESS

EDITED BY
Takashi Nakano,
Fujita Health University, Japan

REVIEWED BY
Fengqin Wang,
Hubei Normal University, China
Carolina Torres,
Serviço de Neurologia, Hospital de Clínicas de Porto Alegre, Brazil
Andrew Fukuda,
Brown University, United States

*CORRESPONDENCE
Yvonne Höller
yvonne@unak.is

SPECIALTY SECTION
This article was submitted to Computational Psychiatry, a section of the journal Frontiers in Psychiatry

RECEIVED 22 May 2022
ACCEPTED 19 July 2022
PUBLISHED 09 August 2022

CITATION
Höller Y, Jónsdóttir ST, Hannesdóttir AH and Ólafsson RP (2022) EEG-responses to mood induction interact with seasonality and age. *Front. Psychiatry* 13:950328. doi: 10.3389/fpsyt.2022.950328

EEG-responses to mood induction interact with seasonality and age

Yvonne Höller[1]*, Sara Teresa Jónsdóttir[1,2], Anna Hjálmveig Hannesdóttir[1] and Ragnar Pétur Ólafsson[2]

[1]Faculty of Psychology, University of Akureyri, Akureyri, Iceland, [2]Faculty of Psychology, University of Iceland, Reykjavík, Iceland

The EEG is suggested as a potential diagnostic and prognostic biomarker for seasonal affective disorder (SAD). As a pre-clinical form of SAD, seasonality is operationalized as seasonal variation in mood, appetite, weight, sleep, energy, and socializing. Importantly, both EEG biomarkers and seasonality interact with age. Inducing sad mood to assess cognitive vulnerability was suggested to improve the predictive value of summer assessments for winter depression. However, no EEG studies have been conducted on induced sad mood in relation to seasonality, and no studies so far have controlled for age. We recorded EEG and calculated bandpower in 114 participants during rest and during induced sad mood in summer. Participants were grouped by age and based on a seasonality score as obtained with the seasonal pattern assessment questionnaire (SPAQ). Participants with high seasonality scores showed significantly larger changes in EEG power from rest to sad mood induction, specifically in the alpha frequency range ($p = 0.027$), compared to participants with low seasonality scores. Furthermore, seasonality interacted significantly with age ($p < 0.001$), with lower activity in individuals with high seasonality scores that were older than 50 years but the opposite pattern in individuals up to 50 years. Effects of sad mood induction on brain activity are related to seasonality and can therefore be consider as potential predicting biomarkers for SAD. Future studies should control for age as a confounding factor, and more studies are needed to elaborate on the characteristics of EEG biomarkers in participants above 50 years.

KEYWORDS

mood induction, seasonality, seasonal affective disorder, winter depression, EEG

1. Introduction

Rosenthal et al. (1) were the first to describe seasonal affective disorder (SAD) as a mood disorder that is characterized by recurrent depressions that occur annually at the same time of the year. Depressive symptoms in SAD are known to occur in both summer and winter, but winter depression with remission in spring is its most common representation (2).

Prevalence of SAD is estimated to be as high as 9.7% worldwide although it has been found to vary substantially based on location (3). The condition is more common

among adolescents or young adults compared to elderly individuals (4, 5). The main distinctive feature of SAD as compared to major depressive disorder is that it occurs repeatedly at the same time of the year. Early screening in summer or fall could be used to plan timely prevention before first symptoms occur. It is partly possible to predict SAD based on subjective reports about the annual seasonal changes in mood, appetite, energy, sleep, and social interaction. Given that subjectively experienced seasonal changes are an important indicator for SAD, screening instruments for SAD were developed in order to measure these changes in the form of a score for an individual's *seasonality* (1). The most commonly used tool for assessing seasonality is the Seasonal Pattern Assessment Questionnaire (SPAQ) developed by (1) for the diagnosis of SAD. Presently, the SPAQ is administered as a screening tool rather than a formal diagnosis (6) as SAD requires a clinical diagnosis based on standardized criteria, such as those found in the DSM-5 (7). The SPAQ allows to calculate a global seasonality score (GSS) which is higher when individuals indicate large fluctuations of sleep, social activity, mood, weight, appetite, and energy. The SPAQ is the most widely used questionnaire to assess seasonality; For example, a systematic review yielded that 46 out of 55 samples were examined with the SPAQ (8).

Seasonal and non-seasonal depression are supposed to share the same cognitive vulnerabilities (9–11). The level of automatic thoughts and dysfunctional assumptions in individuals with SAD are comparable to the elevated scores of patients with non-seasonal depression (9). Furthermore, patients with SAD and those with non-seasonal depression might exhibit a similar style in negative attributions (10).

People being vulnerable to the onset of depression are distinguished from non-vulnerable people only if being confronted with certain stressors (12, 13). Another study confirmed the role of cognitive vulnerabilities in combination with sad mood induction, and that dysfunctional attitudes were more severe after mood induction (11). However, no prior studies included mood induction when examining individuals with SAD.

Electroencephalographic (EEG) studies have provided promising results in identifying possible indicators of psychological states and psychiatric disorders, such as depression and the cognitive processes associated with the condition (14–16). Individuals suffering from major depression disorder were reported to show lower absolute power in the electroencephalogram (EEG) in the frontal lobe compared to healthy controls, in all frequency bands but mainly in the alpha range (17). Alpha activity has been associated with emotional experience (18), self-reflection (19), and has shown a negative relationship with cognitive function and attention (20).

Asymmetrical alpha band activity between the frontal hemispheres has been found to be a likely indicator of depression, with depressed individuals having relatively higher alpha power in the left hemisphere compared to healthy controls (21–23). The frontal lobe was also reported to respond to sad mood induction (24–26) or to predict responses to mood induction (27), but it was argued that the dispositional state, examined under resting conditions may be less conclusive than the measurement under specific emotional contexts, which allows capturing emotional responses (25).

Lowered alpha activity in the prefrontal cortex is especially thought to predict higher tendency to ruminate (28). The relevance of the frontal cortex as well as the alpha frequency range for mood disorders points to the role of cognitive control over negative thoughts. High alpha power is acknowledged to reflect active inhibition (29). Therefore, the relative enhancement of alpha power in the left hemisphere can be interpreted as reduced cortical activity. It was theorized that hypoactivation of the left frontal area leads to ruminative tendencies and consequently to negative emotional interpretation (30). The frontal cortex is also relevant for cognitive flexibility (31), which has been reported to be impaired in individuals with depression (32). It was suggested that individuals with major depressive disorders exhibit ruminative and negative automatic thoughts because being cognitively inflexible in a negative emotional context (33). Depressed individuals exhibit a tendency to pay greater attention to adverse stimuli, and this tendency was linked to an abnormal activation in the lower left frontal cortex (17, 34). Abnormalities in the activation or structure of the emotion circuit have been suggested to underlie depressive disorders, including the prefrontal cortex, anterior cingulate cortex, hippocampus, and amygdala (35).

In addition to alpha abnormalities, abnormal synchronization of theta and beta oscillations was suggested to reflect unstable states of cognitive processing, specifically of working memory in individuals with depression (36). Lower power in the alpha and theta range has been reported during mind wandering (37). Moreover, increases in the delta band are generally related to pathology such as mental slowing in dementia (38), as well as psychopathology (39).

Frontal EEG asymmetry has also been studied during induced mood states (40). The induction of sad mood is related to asymmetry as compared to the induction of euphoria (41), and the level of asymmetry is related to the level of negative affect (27). A review summarized that it is likely that the hypoactivation of the left frontal lobe in response to negative stimuli reflects a predisposition to mood disorders (40). However, several findings contradict this point of view (25, 42).

Frontal alpha asymmetry seems to be subject to seasonal variation (43). Asymmetry of spectral EEG-power in frontal and parieto-temporal networks was documented also in individuals with SAD (44–47). Patients with SAD showed lower delta, theta, and alpha activity than controls (46, 47). In contrast, in remitted patients, an increase in theta power has been noted globally compared to controls (46). A similar pattern with lower EEG

power can be found in patients with depression (17). This suggests that the brain activity changes in SAD and non-seasonal depression reflecting a similar mechanism of a cognitive instability. However, the rather small samples of previous studies warrant rigorous replication of these findings. Studies in healthy controls showed that there is seasonal variation of beta and alpha power, with especially high amplitudes in summer (48, 49).

When discussing EEG studies on SAD one should critically note that SAD is more common at young age (4, 5, 50), while EEG bandpower changes with age in so far as the dominant rhythm—usually alpha—shifts to a lower frequency range (51). This shift consists typically of higher power in lower frequency ranges (delta-theta) and lower power in higher frequency ranges (alpha-beta). Since depressive states coincide with lower power in the alpha range, as well, it is necessary to consider a potential interaction between age and seasonality when examining abnormalities in brain activity related to seasonality. Frontal power asymmetry is stronger in young healthy controls as compared to individuals with major depression, but the difference diminishes and even reverses with age (52). Whether or not differences in brain activity between individuals who are vulnerable to experience SAD vs. those who don't also depend on age has not been investigated, yet. Furthermore, no EEG research has been conducted on induced sad mood in individuals who score high on seasonality indices in order to identify potential neurophysiological biomarkers for SAD. Especially studies comparing brain activity of individuals with high seasonality during remission to controls with low seasonality are rather rare. The differences found between people with and without SAD in winter-time might be due to physiological changes induced by the winter's darkness that are evident only in those individuals with high seasonality. However, it would be more useful to detect differences between people with and without high seasonality in a season with more daylight. In other words, detecting neurophysiological differences between patients with and without SAD already in summer could indicate whether predispositions exist or not. Those cognitive processes that induce sad mood might potentially distinguish between individuals with high or low seasonality even during remission and support the understanding of cognitive vulnerabilities in SAD.

The novel contribution of the present study was, thus, (1) that we examined a sample with a broad age range as compared to young participants, only, (2) we examined them during late summer/early fall instead of winter, and (3) we used a procedure to induct sad mood. With this setup we aimed to answer the following questions:

- **How is a potential interaction of age and seasonality reflected in EEG band power?** Remission states of SAD come along with higher theta power. Seasonality is more common among younger individuals, and EEG band power exhibits increase of power in slower compared to faster rhythms with age. We expect a similar effect of high seasonality and higher age on EEG band power, with higher power in lower frequency ranges (delta-theta) and reduced power in higher frequency ranges (alpha-beta).
- **How does EEG band power change during induced sad mood in people with high-seasonality?** We expect participants with high seasonality to show a larger change during the induction of sad mood in the form of a stronger broadband decrease in EEG absolute power, but especially in frontal alpha.

2. Methods

This data was also analyzed in a previously published study by the same authors (53), where more details on the study parts that were not analyzed in the present report can be retrieved.

2.1. Ethics

This study was approved by The National Bioethics Committee which confirmed our application on May 28th 2019 (study number 19-090-V1). All who worked on this study signed a non-disclosure contract. We obtained written informed consent for participation from all participants.

2.2. Recruitment

Recruitment was done between June and September 2019 *via* publication of a webform on the University website and by posting the link to that webform on social media. The biggest outreach was obtained by sending out invitation emails to psychology students of the University of Akureyri. Psychology students could use the participation certificate obtained after completing the study as a compensation for physical attendance at a hands-on session in a seminar. Overall, 23 psychology students participated in the study. Inclusion criteria were a minimum age of 18 along with a sound mind and enough judgement to give informed consent. Proficiency in Icelandic was a requirement for participation in the study as all materials used were in Icelandic. Thus, we excluded all participants that did not speak Icelandic fluently. The study at hand was part of a more extensive project, where participants were required to complete online-follow up surveys. For completing all phases of the study, participants were offered a 4000 ISK gift certificate.

2.3. Questionnaires

For the purpose of assessing mood and behavioral change according to the seasons participants completed the SPAQ (1).

The version used in this study was validated in Iceland against a diagnostic clinical interview with a resulting sensitivity of 94%, a specificity of 73% and a combined positive predictive value of 45% for SAD and subsyndromal SAD (54). The questionnaire has proven to be an effective screening tool for SAD, is internal consistent (α = 0.74–0.81), reliable (with a test-retest reliability of 0.76 at an interval of 2 months), and widely used in SAD research compared to similar measures to which it was compared, such as the inventory for seasonal variation (55). However, a high seasonality score does not equal a diagnosis of SAD according to the DSM-5 criteria (56). To obtain participants' global seasonality scores (GSS), we calculated the sum of the global seasonality questions in the SPAQ. As a non-clinical estimate for SAD, we grouped participants into low- and high seasonality by means of the Kasper criteria (57), according to which SAD is defined as a GSS above 10. A larger score indicates that the individuals report to be more likely to experience seasonal variation in mood, energy, weight, appetite, sleep, and social activity. We did not further distinguish between SAD and subsyndromal SAD, as the ability of the SPAQ to differentiate between these two subsamples was found to be rather poor (54).

In addition, participants completed the Depression Anxiety Stress Scale (DASS, 88), Patient Health Questionnaire (PHQ, 87), and Bergen Insomnia Scale (BIS, 58). The BIS can be used to measure insomnia according to the formal and clinical diagnostic criteria (DSM- IV-TR) and consists of six items. The first three items assess to sleep onset, sleep maintenance, and early morning awakening. The last three items ask about not feeling adequately rested, experiencing daytime impairment, and dissatisfaction with sleep. The scale can be scored with a total composite score ranging from 0 to 42. The original scale was validated by (58) and the Icelandic version had been translated and validated previously (50).

Participants were also asked about their age, gender, education, handedness, and first language.

Mood was measured on a visual analog scale as relation between the indicated position to the total length of the bar, measured in millimeters. The total length was 150 mm with arrows indicating increase strength of mood from the middle of the scale with the left arrow indicating sad mood and the right arrow indicating happy mood. This tool was used previously in similar sad mood induction task studies (59, 60). Cognitive flexibility was measured as reaction time difference between congruent and incongruent conditions in the Stroop task. For this purpose we subtracted the mean of reaction time in congruent trials from the mean of reaction time in incongruent trials, and we grouped participants by a median-split.

2.4. Procedure

Measurements were performed at the EEG-laboratory of the University of Akureyri between end of July and beginning of October 2019. Experimenters were present in the laboratory throughout the whole procedure. After completion of informed consent, participants answered all questionnaires mentioned in Section 2.3 and the EEG-cap was mounted.

The first two conditions recorded were at rest for 3 min with eyes open and 3 min with eyes closed, with the screen of the stimulus computer turned off and dimmed light. Subsequently participants performed an emotional pictures memory task, which was not used for the present study.

The next condition was a Stroop task where participants were asked to indicate the font color of words displayed on the stimulus computer by pressing a correspondingly colored key on a keyboard where the color of the font corresponded to the word. There were 105 congruent trials and 210 incongruent trials presented in a randomized order, with an inter-trial interval of 1 s + a jitter of 0-10 screen flip intervals during which a central fixation cross was presented.

In the final condition participants first received a printed three part form containing the questions about current mood in the form of the visual analog scale and measurement of induced rumination that was not used for the purpose of the present study. Time spent on answering the written questions on mood and rumination did not count toward the indicated time-periods. All instructions were given verbally through headphones or on the screen of the stimulus computer. Firstly, participants rated their current mood on the visual analog scale and state rumination *via* a short state rumination inventory questionnaire. Next, participants listened to an 8 min musical piece, thought to evoke temporary sadness or dysphoria. Participants were asked to freely experience any emotions they might feel. We used a musical excerpt from Prokofiev's "Russia Under the Mongolian Yoke", remastered at half speed. This has been used and found to be effective in inducing a transient dysphoric mood in previous research on cognitive vulnerability to depression (60–62).

Immediately after the music had finished, participants rated their current mood again on the visual analog scale. Then, they were then instructed to wait for 5 min for a challenging cognitive task. From this 5 min free thinking period we extracted the first 3 min for EEG analysis. However, no cognitive task followed but the waiting period served as a free contemplation time in anticipation of a task. This instruction for the free thinking period is a new procedure and was chosen in order to try to keep participants focused on themselves and the upcoming experiment and to counter that their mind starts to wander about other issues such as their surrounding. Finally, participants rated their current mood for a third time on the visual analog scale and completed the rumination state evaluation *via* the short state rumination questionnaire for a second time. After this, participants were informed that no difficult task would follow and that the study was completed.

To sum up, for the present study, we used the EEG data recorded during 3 min rest with eyes open condition and during

the first 3 min of the free-thinking period after listening to the sad music, which was intended to induce sad mood. Due to the emotional pictures memory task and Stroop task that were conduced in between these two conditions, the free-thinking period followed about half an hour after the resting condition. We did not control for drowsiness/wakefulness but participants were asked to keep their eyes open during both of these periods, to keep the overall background condition comparable and to prevent participants from falling asleep.

2.5. EEG recording and analysis

EEG data was gathered using BrainVision BrainAmp Recorder and Amplifier (Brain Products GmbH, Gilching, Germany) and digitized at a sampling rate of 256 Hz. Recording was conducted using 32 electrodes (Fp1, Fp2, F3, F4, C3, C4, P3, P4, O1, O2, F7, F8, T7, T8, P7, P8, Fz, Cz, Pz, FC1, FC2, CP1, CP2, FC5, FC6, CP5, CP6, FT9, FT10, TP9, TP10) referenced to FCz and grounded at AFz. One additional electrode served as lower vertical electrooculogram. Electrode positioning was in accordance with the standardized international 10-20 system by using an EasyCap. Electrodes were filled with electrolyte containing a mild abrasive (OneStep Abrasive Plus) in order to achieve low impedance of $<10k\Omega$ in all channels.

We analyzed EEG-data from 3 min rest with eyes open condition and the first 3 min of the free-thinking period after listening to the sad music. EEG-data was pre-processed using BrainVision Analyzer (Brain Products GmbH, Gilching, Germany). Data was filtered from 0.5 to 30 Hz with zero-phase shift Butterworth filters. Then, re-referencing was performed by averaging the activity of all electrodes and subtracting this mean from all other channels. Next, an independent component analysis (ICA, infomax restricted) was performed in order to automatically remove eye-blink artifacts. The vertical lower oculogram was used as a vertical activity channel. The whole recording epochs per condition were fed into the algorithm, i.e., at least 3 min per condition as the shortest condition was 3 min of rest with eyes open or closed. The ICA (63) is an algorithm that separates the EEG signals into the same number of temporally maximally independent component time courses. The ocular component represents eye movements and blinks and, thus, has a characteristic pattern in time and topography, which is used for the automatic selection of the component. To this end, the ocular correction ICA first performed a blink marker placement by searching the oculogram channel for blinks and marking them according to the mean slope algorithm (64). For identification of components related to the vertical electrooculogram only the time intervals that are identified by this algorithm as blinks are used. Then, the share of each ICA component in the variance of the selected ocular channel activation was calculated, which was then excluded from back-projection. As a last pre-processing step, a raw data inspection was done by applying the standard thresholds as implemented in Brain Vision Analyzer, in order to automatically identify and exclude movement and muscle artifacts: check gradient: the maximal allowed voltage step is 50 microvolt/ms; check difference: the maximal allowed difference of values in intervals of 200 ms: 200 microvolt; lowest activity allowed in 100 ms intervals is 0.5 microvolts; bad events were marked ±20 0 m around the identified artifacts. The two 3 min recordings were divided into 2 s segments. For each segment, we calculated the Fast Fourier Transform (FFT). The FFT of all segments that were not marked as containing artifacts were averaged for each participant, separately for the two conditions rest and sad mood induction. From the average FFT we extracted average band power in the delta (1–4 Hz), theta (5–7 Hz), alpha (8–13 Hz), and beta (14–30 Hz) range for statistical analysis. EEG channels were grouped for lobes and hemisphere for the purpose of conducting an analysis of variance with factors lobe and hemisphere, but used individually for *post-hoc* illustrations of results. When more than one electrode was recorded for one such region, averaging was performed. These regions were frontal-left (Fp1, F3, F7), frontal right (Fp2, F4, F8), central left (C3), central right (C4), parietal left (P3, P7), parietal right (P4, P8), temporal left (T7), temporal right (T8), occipital left (O1), and occipital right (O2).

2.6. Statistical analysis

For comparing psychometric characteristics between the group with low and high seasonality we used non-parametric tests because all data was ordinal, and thus, no parametric tests are allowed. Therefore, we calculated 7 non-parametric Mann–Whitney *U*-tests. The results were interpreted at the Bonferroni-corrected level of significance, that is, $p < 0.007$.

We tested for behavioral effects of mood induction with non-parametric repeated measures ANOVA with a parametric bootstrap (65) for the change in mood. When testing for interactions between seasonality and condition we also controlled for age and cognitive flexibility (31–33). Cognitive flexibility was added as a grouping variable according to a median split of reaction time increase between the congruent and incongruent color naming condition in a Stroop task. Age was also used as a grouping variable with people being up to 50 years vs. those who were older. Because there were only 18 participants older than 50, the additional combination with low vs. high seasonality and cognitive flexibility left too few participants in the subcategories of older participants with higher seasonality and low vs. high cognitive flexibility. Therefore, two separate analyses of variance were conducted, one with seasonality as a grouping factor and one with age as a grouping factor. Therefore, results were interpreted at the Bonferroni-corrected level of significance, that is $p < 0.025$.

The EEG data was evaluated using a semi-parametric repeated measures ANOVA with a parametric bootstrap (65)

with between-subjects factor GSS (low vs. high seasonality), and within subjects factors hemisphere (left vs. right), lobe (frontal, central, temporal, parietal, and occipital), frequency (delta, theta, alpha, and beta), and condition (rest vs. sad mood induction). Additionally, we included factor age into the analysis, since EEG changes with age. We divided the sample into participants up to 50 years and participants older than 50 years, because prior EEG-research on SAD investigated only subjects up to age 50 (46) and because prior research indicates that 50 is a significant turning point in EEG signal properties (66).

We chose a semi-parametric repeated measures ANOVA that only requires metric data, but allows for non-normality and variance heterogeneity (65). This method is implemented in the function RM of the R-package MANOVA.RM (67). We used it with the parametric bootstrap with 1000 iterations. The parametric bootstrap showed the most favorable performance in unbalanced designs like in our case where low seasonality is much more frequent than high seasonality and, additionally, the older subgroup shows fewer cases of high seasonality than the younger subgroup (65). The method was shown to be robust and advantageous in unbalanced designs and for a large number of factors as well as EEG data previously because these data typically violate assumptions of classical methods (65).

For *post-hoc* analyses of significant interactions and effects we used *z*-values from Wilcoxon rank sum test or signed rank test for creating topographic plots of the data.

3. Results

3.1. Sample

A total of 119 participants were recruited for this study. For the statistical analysis, 3 participants were excluded due to missing data in the EEG recording. Furthermore, 2 participants (nr. 2 and nr. 76) did not complete the SPAQ and were therefore excluded. The final sample consisted of 114 participants, 10 tested in second half of July, 28 in August, 72 in September, and 3 in the first week of October. It should be noted that the weather in the Icelandic summer between end of July and beginning of October is comparable to the central-European fall between September and November.

Participants' age ranged from 18 to 66 years with the average age of 33.75 (*SD*=13.43) years. The sample consisted of 92 women and 22 men. The odds ratio for gender to suffer from SAD is 1.8 according to (68) justifying an overrepresentation of female participants. However, in our sample there were even more women to men, due to the recruitment among psychology students which are about 90% women, and also the increased availability of female voluntary participants. Eight participants were left handed, and three participants indicated to have no preference for left or right.

In the sample, 9.91% had completed primary education, only, 55.86% had higher education entrance qualification, 6.31% had learned a trade, 18.92% had completed undergraduate education at a University, and 9.01% had completed master or doctoral level education at a University. The native language was Icelandic in 95% of the sample, however, all participants were fluent in Icelandic.

We found that 57.66% reported taking any kind of medication regularly. However, this included also oral contraceptives, which explained major part of this large proportion. Furthermore, 25.44% consumed tobacco regularly. It should be noted that this consumption includes not only smoking, but also vapes, e-cigarettes, and chewing tobacco. While 20.72% reported never drinking alcohol at all, 36.94% reported drinking once a month or less, 36.94% reported drinking two to four times a month and only 5.4% reported drinking two to three times a week or more frequent drinking. Participants reported drinking on average 2.83 cups of coffee or caffeinated drinks per day (median = 2; SD = 2.54). The hours of sleep in the night before the experiment were on average 7.10 h (median = 7; SD = 1.70).

3.2. Psychometric and grouping data

Participants were divided into two groups based on an estimated likelihood of them experiencing mild to moderate seasonal affective disorder, measured by the GSS obtained from the SPAQ. According to (68) and (3), which used the same SPAQ questionnaire in Icelandic as we did in our study and where SAD was determined by means of the Kasper criteria (57) with a GSS score of 11 or higher. Therefore, in our study a score of $\leq$10 was categorized as a low seasonality score and a score of $>$10 as a high-seasonality score. Out of 114 participants that completed the SPAQ, 37 had a high GSS and 77 had a low GSS.

Descriptive statistics for the psychometric scales, separately for the two groups as well as results from Mann–Whitney *U*-tests comparing the two samples are shown in Table 1.

3.3. Behavioral responses to mood induction

The experiment involved a mood induction phase (listening to sad music) and a free thinking period. We measured mood before (t1) and after (t2) listening to sad music and after the free thinking period (t3). Mood ratings and cognitive flexibility measures in the form of reaction times for congruent and incongruent conditions in the Stroop task are given in Table 2. There were 17 participants who did show an absolute increase of mood according to the visual analog scale. However, given the inaccuracy of such a scale, we investigated how many actually meant that their mood did not change. Out of these

TABLE 1 Psychometric characteristics of the sample separately for the low and high-seasonality groups.

	GSS≤10		GSS>10		*U*-Test	
Scale	**Mean**	***SD***	**Mean**	***SD***	***z***	***p***
age	36.43	14.07	29.34	10.30	2.48	0.013
GSS	4.53	2.87	14.11	2.64	−8.64	**<0.001**
BIS	13.36	8.42	21.49	7.77	−4.68	**<0.001**
PHQ	4.97	3.67	10.80	4.46	−6.00	**<0.001**
DASS depression	2.97	3.68	5.72	4.05	−3.96	**<0.001**
DASS anxiety	2.18	2.60	6.49	4.65	−5.07	**<0.001**
DASS stress	5.40	4.15	9.59	4.20	−4.45	**<0.001**

GSS, global seasonality score; DASS, depression/anxiety/stress scale.
PHQ, patient health questionnaire; BIS, Bergen insomnia scale.
Bold *p*-values: significant at Bonferroni-corrected level $p < 0.007$.

TABLE 2 Mood induction reports and cognitive flexibility separately for the low and high-seasonality groups.

	GSS≤10		GSS>10	
Scale	**Mean**	***SD***	**Mean**	***SD***
Mood t1	113.43	25.65	92.93	24.90
Mood t2	80.23	38.44	68.69	36.43
Mood t3	98.24	32.85	74.08	32.65
RT congruent	778	170	749	187
RT incongruent	847	193	811	220

t1, t2, t3: time points during experiment.
RT: reaction time in milliseconds.

17 participants, 6 had a change smaller than 5 mm, 5 had a change between 5 and 10 mm, 2 had a change between 10 and 20 mm, and only 4 had a change larger than 20 mm. Thus, there were 4 with an atypical change in mood during mood induction. Among them, only 2 showed more positive mood also at t3.

According to the ANOVA, there was a significant effect of time, i.e., an) induction of sad mood from t1 to t2 and t3 [$F_{(1.90,Inf)} = 6.38$; $p = 0.006$] as well as a significant group effect, thus, lower mood in participants with higher seasonality [$F_{(1,364.85)} = 13.30$; $p < 0.001$]. Furthermore, an interaction indicated that there was a significantly stronger effect of mood induction in the group with higher seasonality [$F_{(1.9,Inf)} = 8.83$; $p = 0.001$], but there was no three-way interaction with cognitive flexibility. However, there was a significant interaction between cognitive flexibility and mood induction [$F_{(1.89,Inf)} = 4.85$; $p = 0.008$], such that participants with a smaller increase in reaction time in the Stroop task responded more intensely to mood induction. Younger participants showed lower mood [$F_{(1,115.87)} = 7.05$; $p = 0.022$]. The interaction between age and cognitive flexibility was not significant after Bonferroni-correction for multiple comparisons.

3.4. Brain responses to mood induction

In order to test the interaction of effects between seasonality (two groups by GSS, low and high) and age(<51 and older) on brain activity at rest and during mood induction (factor condition) we performed a semi-parametric ANOVA. Furthermore, the model included EEG-frequency band, hemisphere, and brain lobe as factors. The results of the semi-parametric ANOVA with $p < 0.1$ are shown in Table 3.

There was a significant effect of seasonality, such that high-seasonality participants had a higher overall average power in EEG oscillations (mean = 0.51; *SD* = 0.13) than low-seasonality participants (mean = 0.50; *SD* = 0.12). This difference was calculated across all frequency ranges and regions and is therefore rather small, as there were frequency ranges with opposing differences and the difference depended additionally on age (see Figure 1). The older group had a lower overall average EEG activity (mean = 0.44; *SD* = 0.17) than younger participants (mean = 0.50; *SD* = 0.12). There was a significant interaction between age, seasonality, and frequency (Figure 1). In the younger group, high-seasonality participants exhibited larger power (average between rest and mood induction) in the delta, theta and beta frequency band but lower power in the alpha range, especially in the left temporo-parietal region. In the older participant group, high-seasonality participants exhibited lower power in all frequency ranges, especially in the alpha range.

There was also a significant interaction between seasonality and frequency, such that in all frequency bands the activity was higher in high-seasonality participants except for the alpha band, where the activity was lower in that group (see Figure 1). The higher power in high-seasonality participants was most pronounced in the delta band, irrespective of condition, while higher power in low-seasonality

TABLE 3 ANOVA-type semi-parametric analysis of variance with parametric bootstrap on EEG measures for factors condition (within: rest vs. after mood induction), seasonality (between: GSS low vs. high), age (between: young vs. old), hemisphere (within: left vs. right), lobe (within: frontal, central, temporal, parietal, occipital), frequency (within: delta, theta, alpha, beta).

Factor	ATS	df1	df2	*p*-value
GSS	11.05	1	693.03	<0.001
Age	96.13	1	693.03	<0.001
GSS×age	30.02	1	693.03	<0.001
Lobe	87.42	3.24	693.03	<0.001
Age×lobe	4.14	3.24	693.03	.002
Frequency	1218.38	1.97	Inf	<0.001
GSS×frequency	10.51	1.97	Inf	<0.001
Age×frequency	29.79	1.97	Inf	<0.001
GSS×age×frequency	6.72	1.97	Inf	<0.001
Lobe×frequency	39.05	5.85	Inf	<0.001
Age×lobe×frequency	1.40	5.85	Inf	.018
Condition	185.17	1	Inf	<0.001
GSS×condition	3.23	1	Inf	.089
Age×condition	4.70	1	Inf	.039
Lobe×condition	46.34	2.53	Inf	<0.001
Frequency×condition	239.77	2.23	Inf	<0.001
GSS×frequency×condition	3.08	2.23	Inf	.027
Age×frequency×condition	4.73	2.23	Inf	<0.001
Lobe×frequency×condition	18.73	5.54	Inf	<0.001

Only effects with $p < 0.1$ are shown.
ATS, ANOVA-type statistic; df, degrees of freedom; GSS, grouping by global seasonality score; condition, rest vs. mood induction.

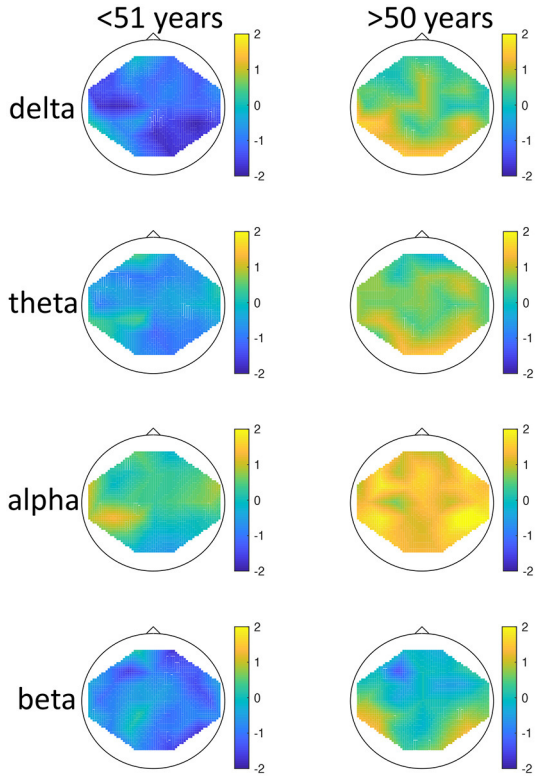

FIGURE 1
Topographical maps of activity distribution: colors represent difference between participants with low and high global seasonality score, indicated by approximated *z*-values from a Wilcoxon rank sum test, for frequency ranges from **top** to **bottom**: delta, theta, alpha, beta; and for age groups <51 years **(left)** and >50 years **(right)**. Negative *z*-values indicate lower activity in the low- compared to high-seasonality group, positive *z*-values indicate higher activity in the low- compared to high-seasonality group.

participants in the alpha band was most pronounced during mood induction.

The effect of mood induction was significant with a higher activity after induced mood than during rest, especially in the delta range and inferior frontal regions for low seasonality participants, while the largest difference was found in the alpha range for high-seasonality participants with lower activity after mood induction than during rest (see Figures 2, 3). In other words, the alpha band desynchronizes in response to mood induction, which is stronger in participants with high-seasonality. In the theta range the central region showed a desynchronization during induced sad mood while higher power was found in the frontal area.

4. Discussion

In this study, we examined brain activity in the delta, theta, alpha, and beta frequency bands in low and high-seasonality individuals during rest and mood induction. In addition, we controlled for age effects. Table 4 summarizes the main findings.

4.1. Brain activity, seasonality, and age

We found significant overall difference in brain activity according to seasonality, but also significant effects of age. The aging effect in the EEG was to be expected as with age, slowing of the EEG occurs, and a relative increase of delta compared to higher frequency ranges can be observed (69). Our results showed opposing directions of effects in the younger compared to the older sample. Our main interaction of age and seasonality warrants an attempt of an interpretation, i.e., younger, high-seasonality participants exhibited overall larger power, while in the older participant group, high-seasonality participants exhibited overall lower power, especially in the alpha range. Such a reversal effect that appears to be caused by age was previously documented also in patients with major depressive disorder (52) where young healthy controls showed higher frontal asymmetry in the delta, alpha, and beta frequency range,

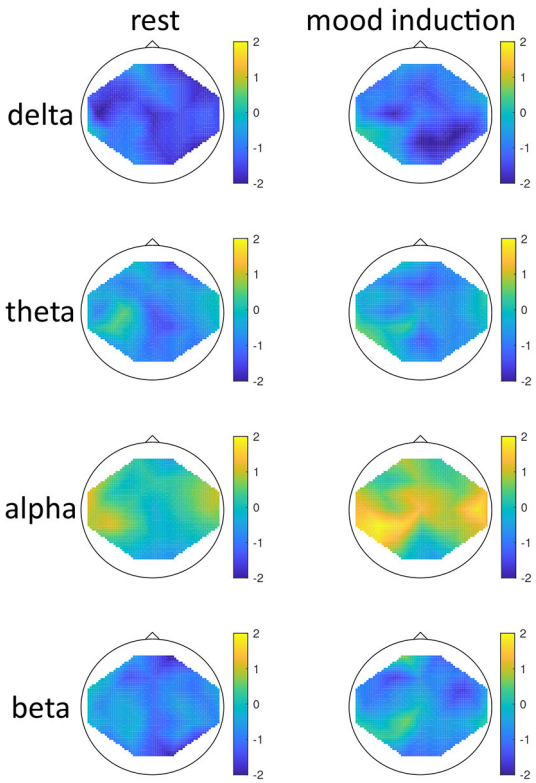

FIGURE 2
Topographical maps of activity distribution: colors represent difference between participants with low and high global seasonality score, indicated by approximated *z*-values from a Wilcoxon rank sum test, for frequency ranges from **top** to **bottom**: delta, theta, alpha, beta; and for conditions rest **(left)** and after mood induction, during the free-thinking period **(right)**. Negative *z*-values indicate lower activity in the low- compared to high-seasonality group, positive *z*-values indicate higher activity in the low- compared to high-seasonality group.

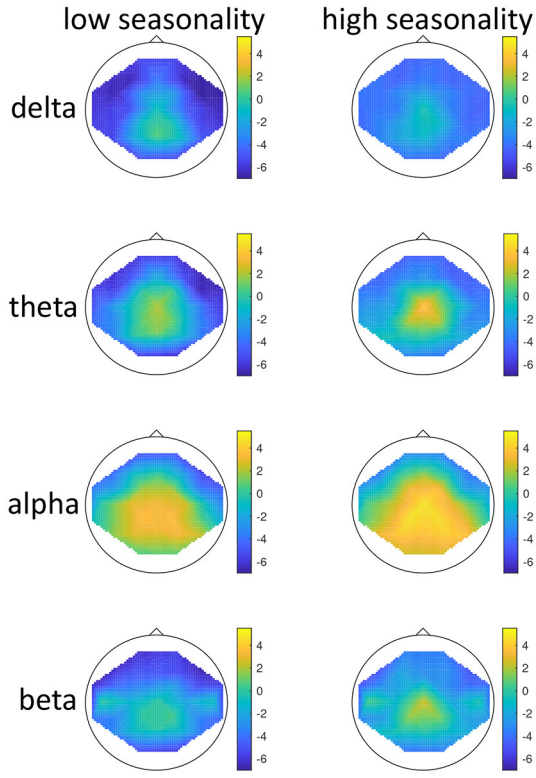

FIGURE 3
Topographical maps of activity distribution: Colors represent difference between rest and after mood induction, indicated by approximated *z*-values from a Wilcoxon signed rank test, for frequency ranges from **top** to **bottom**: delta, theta, alpha, beta; and for groups with low **(left)** and high **(right)** global seasonality score. Negative *z*-values indicate lower activity during rest compared to mood induction, positive *z*-values indicate higher activity during rest compared to mood induction.

while with age, major depressive disorder patients showed larger frontal asymmetry. While the higher activity in the theta band for young SAD patients in remission was reported previously (46), nothing is known so far about effects of seasonality in the EEG of older individuals. The increased activity in the younger sample could be seen as an overcompensatory effect during summer, as during depressed states, the amplitudes of brain activity get lowered. Another possible view on this finding is supported by previous reports on higher power in the alpha and beta band in a general population in the summer (48, 49). Our finding that even higher amplitudes are found in the subsample with high seasonality score could reflect the special situation of high-seasonality individuals overreacting to the bright light conditions in the summer. Indeed, this finding was not reported in an earlier study (49) where seasonality did not interact with seasonal changes in EEG power. However, our study was conducted in Iceland with abundant amounts of daylight in the summer, whereas (49) examined participants in southern Italy (Napels), where some hours of darkness are achieved during the night. This reactivity might reverse with age because the absolute power in the alpha range decreases naturally with age. Another potential explanation for the interaction with age are changes in sleep buildup that differs between younger and older participants, as the need for sleep decreases with age. The two groups differed also significantly by quality of sleep according to BSI, which might confound these findings. Sleep disturbances in summers with long photoperiods might be more common in people who show high degrees of seasonality and might be even more common in the elderly subgroup. This interpretation is also supported by prior research which demonstrated a more rapid buildup of subjective sleepiness and EEG theta-alpha activity in patients with SAD compared to a control group (70).

Therefore, we strongly recommend controlling for age in future studies. Previous research was conduced with participants aged 30–50 years (46) or 28–55 years (47). Our study also

10.3389/fpsyt.2022.950328

TABLE 4 Summary of the main findings of the study.

Frequency range	Seasonality	Seasonality × age	Mood induction
Delta	↑	↓	↑
Theta	↑	↓	↑↓
Alpha	↓	↓	↓
Beta	↑	↓	↑

↑, increased power; ↓, decreased power.

emphasizes that, although the condition is rather rare in the elderly, further research is needed on the specific effects seasonality might have in a senior population.

4.2. Brain activity and SAD vs. seasonality

In contrast to studies examining active SAD (46, 47), we found increased power in all frequency bands except for the alpha band in young high-seasonality participants. Thus, our results are in line with prior reports on SAD during remission, where young patients demonstrate higher band power in the delta, theta, and alpha band compared to controls (46). EEG studies on brain activity in major depressive disorder patients have also indicated a brain-wide decrease in theta activation as well as an increase in higher frequency beta activation (71).

It is noteworthy that although we included hemisphere as a factor, there was no significant effect or interaction related to it, which is unexpected. Prior research would have suggested that our data could show an interaction between seasonality, lobe, and hemisphere, as frontal EEG asymmetry has been a hallmark of depression (21–23). But our sample was examined during remission, which might explain the lack of such an effect.

4.3. Brain activity during mood induction

High-seasonality individuals showed a larger and more widespread difference in the alpha range between rest and sad mood induction compared to low-seasonality individuals. Studies on rumination in major depressive disorder have established that the frontal lobe is a critical area for cognitive processes linked to depressive symptoms (14). Specifically, the induction of sad mood is supposed to evoke frontal asymmetry (40, 41). However, contrary to expectations we did not find any interaction between hemisphere and condition in our study. The relatively mild dysphoria induced by the procedure chosen might explain the lack of a clear effect in our data.

An analysis of the change in brain activity from rest to induced sad mood revealed larger frontal activity in the delta and theta frequency range during sad mood induction compared to rest.

Frontal EEG activity is greater when emotion regulation is efficient, i.e., when the response to sad mood induction is smaller (25).

In addition to enhanced delta and theta activity, we also found enhanced frontal activity in the beta range during mood induction. Beta oscillations play a crucial role in both positive and negative emotional tasks, as well as cognitive tasks (72). Increased activation of theta is thought to underlie top-down cognitive control (73), evaluation of goal directed behavior (74), and cognitive workload (75).

4.4. Limitations

As a result of the limited time frame of assessments during summer and location of the study in a small town with limited access to large numbers of potential participants an equal distribution of seasonality, age, gender and other demographic variables did not prove possible. Furthermore, substantial percentage of the sample consisted of university students which usually are a more homogeneous group than the general population. Especially the gender distribution was heavily biased toward women, as more women volunteered for participation. The low number of participating men also hindered us from taking gender into account as a factor in our statistical model. Unequal group sizes were compensated by the choice of statistical tests that are valid under conditions with unequal sample sizes. Nevertheless, a limitation of generalization must be considered, such as the results might be more representative for women than men. So far, sex differences were examined with respect to SAD and seasonality only in terms of the higher prevalence of seasonal symptoms among women (50), while the knowledge about interactions between sex, seasonality and EEG activity is rather limited. According to our recently published longitudinal study, sex has not predictive value when used alone or in combination with the EEG for predicting winter-time depression based on summer-time measurements (53). However, sex is known to affect EEG band activity insofar as it is possible to derive the subject's sex from EEG biomarkers (76, 77). Future studies with well-balanced samples should investigate the potential role of sex in the moderation of EEG band power interactions with seasonality.

When interpreting the results of this study, it is also important to keep in mind that the measure of seasonality is based on a screening and not a formal clinical diagnosis. SAD is a type of seasonally recurrent major depression that requires diagnosis based on clinical criteria, such as those found in DSM-5 (6). In addition, the cut-off point of GSS scores used to distinguish high and low seasonality individuals does not necessarily serve as realistic categorization of SAD but rather an indication of a possible problem (6).

Furthermore, we did not apply clinical exclusion criteria, such as prior personal history of depression, prescribed medication that is active on the central nervous system, use of stimulants, presence of psychopathology, substance abuse, history of neurological diseases such as multiple sclerosis or epilepsy, previous brain surgery or head trauma. Therefore, the data of some participants might not be fully representative for a healthy population, but could be biased. The non-clinical nature of the study and, therefore, the lack of a diagnostic interview prevented us from ruling out additional diagnoses that may be not related to seasonality or depression. Therefore, we must also consider a bias by such conditions. There are other mental disorders that follow a seasonal pattern, such as schizophrenia (78), anxiety (79), bulimia nervosa (80), and posttraumatic stress disorder (81), which might interfere with the results.

Another limitation is the choice of the mood induction procedure, where we combined verbal instructions and a sad musical piece. Although previous studies have supported this procedure (60–62), the question remains whether interindividual differences in music taste might affect the result. On the other hand, there is evidence for interindividual differences in EEG-responses to self-selected music for different purposes (i.e., activating vs. relaxing music) (82) such that letting participants choose their favorite sad music might not have led to a more homogeneous result.

Finally, this study was conducted in a cross-sectional design, while longitudinal designs are needed to confirm the relation between EEG correlates of induced sad mood in one season, i.e., summer, and depressive symptoms in the season when SAD typically occurs, i.e., winter. Such data was published recently, showing that cognitive vulnerabilities are better suited to predict winter depression, but the combination of those markers with EEG features can be advantageous (53).

4.5. Future directions

Recent technological developments go beyond the simple documentation of regional and frequency differences and provide automatic means for classification of brain diseases (83), for example by the use of convolutional neural networks (CNN) as a means of artificial intelligence for the classification of patients with major depressive disorder (84), which allow to determine the most information bearing regions and frequency bands (85). These methods are most useful when higher-dimensional features are chosen, such as functional connectivity measures (86). The disadvantage of CNNs is the need for a large sample size as their learning ability and generalizability depends highly on the size of the ground truth. In seasonal affective disorder, a simple support vector machine classification can be used to predict winter-time depression based on summer-time psychological vulnerabilities and EEG-features (53). The present results might add to the selection of prior knowledge for future artificial intelligence models, i.e., by adding age to the feature vector.

5. Conclusions

With respect to the initially posed research questions, we can draw the following conclusions:

- *How is a potential interaction of age and seasonality reflected in EEG band power?* Younger participants with high seasonality showed increased EEG power in all bands but the alpha range, while the older group with high seasonality exhibited decreased EEG power in all frequency bands. This finding emphasizes that it is important to control for age in future studies on brain activity in seasonal affective disorder.
- *How does EEG band power change during induced sad mood in people with high-seasonality?* Participants with high seasonality showed a larger difference in the alpha band with higher activity during rest compared to activity during sad mood induction possibly reflecting a breakdown of inhibition, while low seasonality participants showed a stronger frontal activity during sad mood induction across frequency ranges, possibly reflecting effective inhibition of ruminative thoughts that lead to sad mood.

Future research can make use of our results and estimate whether EEG biomarkers during induced sad mood in combination with the seasonality score in summer could serve as a predictor for SAD in winter. It is furthermore of interest whether brain activity during sad mood induction among SAD patients changes with seasons.

Data availability statement

The datasets generated for this study can be found in Höller, Yvonne (2022), "Data for: EEG-responses to mood induction interact with seasonality", Mendeley Data, v1 http://dx.doi.org/10.17632/7bzjts53xv.1 and the raw EEG data in Höller, Yvonne (2022), "Data for: EEG responses to mood induction", Mendeley Data, v1, http://dx.doi.org/10.17632/vhwc42cmmy.1.

Ethics statement

The studies involving human participants were reviewed and approved by National Bioethics Committee Iceland. The

patients/participants provided their written informed consent to participate in this study.

Author contributions

YH and RPÓ: conceptualization and supervision. YH (for EEG) and RPÓ (for psychological tests): methodology. YH: software, resources, data curation, visualization, project administration, and funding acquisition. YH, STJ, and AHH: validation. YH and AH: formal analysis. STJ and AHH: investigation. YH and STJ: writing—original draft preparation. RPÓ, STJ, and AHH: writing—review and editing. All authors have read and agreed to the published version of the manuscript.

Funding

This study was supported by the Research Fund of University of Akureyri (RHA, R1916) and Icelandic Research Fund (Grant No. 228739-051).

Acknowledgments

We thank Elísa Huld Jensdóttir, Máni Snær Hafdísarson, Sigrún María Óskarsdóttir, and Silja Hlín Magnúsdóttir for recruitment and data collection.

Conflict of interest

The authors declare that the research was conducted in the absence of any commercial or financial relationships that could be construed as a potential conflict of interest.

Publisher's note

References

1. Rosenthal NE, Sack DA, Gillin JC, Lewy AJ, Goodwin FK, Davenport Y, et al. Seasonal affective disorder. A description of the syndrome and preliminary findings with light therapy. *Arch Gen Psychiatry*. (1984) 41:72–80. doi: 10.1001/archpsyc.1984.01790120076010

2. Magnússon A, Partonen T. The diagnosis, symptomatology, and epidemiology of seasonal affective disorder. *CNS Spectr*. (2005) 10:625–34. doi: 10.1017/S1092852900019593

3. Magnússon A. An overview of epidemiological studies on seasonal affective disorder. *Acta Psychiat Scand*. (2000) 101:176–84. doi: 10.1034/j.1600-0447.2000.101003176.x

4. Rastad C, Sjödén PO, Ulfberg J. High prevalence of self-reported winter depression in a Swedish county. *Psychiatry Clin Neurosci*. (2005) 59:666–75. doi: 10.1111/j.1440-1819.2005.01435.x

5. Lukmanji A, Williams JVA, Bulloch AGM, Bhattarai A, Patten SB. Seasonal variation in symptoms of depression: a Canadian population based study. *J Affect Disord*. (2019) 255:142–9. doi: 10.1016/j.jad.2019.05.040

6. Melrose S. Seasonal affective disorder: an overview of assessment and treatment approaches. *Depress Res Treat*. (2015) 2015:1–6. doi: 10.1155/2015/178564

7. American Psychiatric Association. *Diagnostic and Statistical Manual of Mental Disorders. DSM-5*. 5th ed. San Francisco: American Psychiatric Association (2013). doi: 10.1176/appi.books.9780890425596

8. Kasof J. Cultural variation in seasonal depression: cross-national differences in winter versus summer patterns of seasonal affective disorder. *J Affect Disord*. (2009) 115:79–86. doi: 10.1016/j.jad.2008.09.004

9. Hodges S, Marks M. Cognitive characteristics of seasonal affective disorder: a preliminary investigation. *J Affect Disord*. (1998) 50:59–64. doi: 10.1016/S0165-0327(98)00034-2

10. Levitan RD, Rector NA, Bagby RM. Negative attributional style in seasonal and nonseasonal depression. *Am J Psychiatry*. (1998) 155:428–30. doi: 10.1176/ajp.155.3.428

11. Enggasser JL, Young MA. Cognitive vulnerability to depression in seasonal affective disorder: predicting mood and cognitive symptoms in individuals with seasonal vegetative changes. *Cogn Ther Res*. (2007) 31:3–21. doi: 10.1007/s10608-006-9076-z

12. Monroe SM, Simons AD. Diathesis-stress theories in the context of life stress research: implications for the depressive disorders. *Psychol Bull*. (1991) 110:406–25. doi: 10.1037/0033-2909.110.3.406

13. Segal ZV, Ingram RE. Mood priming and construct activation in tests of cognitive vulnerability to unipolar depression. *Clin Psychol Rev*. (1994) 14:663–95. doi: 10.1016/0272-7358(94)90003-5

14. de Freitas SB, Marques AA, Bevilaqua MC, de Carvalho MR, Ribeiro P, Palmer S, et al. Electroencephalographic findings in patients with major depressive disorder during cognitive or emotional tasks: a systematic review. *Rev Bras Psiquiatr*. (2016) 38:338–46. doi: 10.1590/1516-4446-2015-1834

15. Höller Y, Bathke AC, Uhl A, Strobl N, Lang A, Bergmann J, et al. Combining SPECT and quantitative EEG analysis for the automated differential diagnosis of disorders with amnestic symptoms. *Front Aging Neurosci*. (2017) 9:290. doi: 10.3389/fnagi.2017.00290

16. Popa L, Dragos H, Pantelemon C, Verisezan Rosu O, Strilciuc S. The role of quantitative EEG in the diagnosis of neuropsychiatric disorders. *J Med Life*. (2020) 13:8–15. doi: 10.25122/jml-2019-0085

17. Ding X, Yue X, Zheng R, Bi C, Li D, Yao G. Classifying major depression patients and healthy controls using EEG, eye tracking and galvanic skin response data. *J Affect Disord*. (2019) 251:156–61. doi: 10.1016/j.jad.2019.03.058

18. Allen JJB, Urry HL, Hitt SK, Coan JA. The stability of resting frontal electroencephalographic asymmetry in depression. *Psychophysiology*. (2004) 41:269–80. doi: 10.1111/j.1469-8986.2003.00149.x

19. Aftanas LI, Golocheikine SA. Human anterior and frontal midline theta and lower alpha reflect emotionally positive state and internalized attention: high-resolution EEG investigation of meditation. *Neurosci Lett*. (2001) 310:57–60. doi: 10.1016/S0304-3940(01)02094-8

20. Gevins A, Smith ME. Neurophysiological measures of working memory and individual differences in cognitive ability and cognitive style. *Cereb Cortex*. (2000) 10:829–39. doi: 10.1093/cercor/10.9.829

21. Gollan JK, Hoxha D, Chihade D, Pflieger ME, Rosebrock L, Cacioppo J. Frontal alpha EEG asymmetry before and after behavioral activation treatment for depression. *Biol Psychol*. (2014) 99:198–208. doi: 10.1016/j.biopsycho.2014.03.003

22. Kaiser AK, Gnjezda MT, Knasmüller S, Aichhorn W. Electroencephalogram alpha asymmetry in patients with depressive disorders: current perspectives. *Neuropsychiatr Dis Treat*. (2018) 14:1493–504. doi: 10.2147/NDT.S137776

23. Park Y, Jung W, Kim S, Jeon H, Lee SH. Frontal alpha asymmetry correlates with suicidal behavior in major depressive disorder. *Clin Psychopharm Neurosci*. (2019) 17:377–87. doi: 10.9758/cpn.2019.17.3.377

24. Blackhart GC, Kline JP. Individual differences in anterior EEG asymmetry between high and low defensive individuals during a rumination/distraction task. *Pers Individ Diff*. (2005) 39:427–37. doi: 10.1016/j.paid.2005.01.027

25. Dennis TA, Solomon B. Frontal EEG and emotion regulation: electrocortical activity in response to emotional film clips is associated with reduced mood induction and attention interference effects. *Biol Psychol*. (2010) 85:456–64. doi: 10.1016/j.biopsycho.2010.09.008

26. Nixon E, Liddle PF, Nixon NL, Liotti M. On the interaction between sad mood and cognitive control: the effect of induced sadness on electrophysiological modulations underlying Stroop conflict processing. *Int J Psychophysiol*. (2013) 87:313–26. doi: 10.1016/j.ijpsycho.2012.11.014

27. Tomarken AJ, Davidson RJ, Henriques JB. Resting frontal brain asymmetry predicts affective responses to films. *J Pers Soc Psychol*. (1990) 59:791–801. doi: 10.1037/0022-3514.59.4.791

28. Putnam K, McSweeney L. Depressive symptoms and baseline prefrontal EEG alpha activity: a study utilizing ecological momentary assessment. *Biol Psychol*. (2008) 77:237–40. doi: 10.1016/j.biopsycho.2007.10.010

29. Klimesch W. EEG alpha and theta oscillations reflect cognitive and memory performance: a review and analysis. *Brain Res Rev*. (1999) 29:169–95. doi: 10.1016/S0165-0173(98)00056-3

30. Disner SG, Beevers CG, Haigh EA, Beck AT. Neural mechanisms of the cognitive model of depression. *Nat Rev Neurosci*. (2011) 12:467–77. doi: 10.1038/nrn3027

31. Kim C, Johnson NF, Cilles SE, Gold BT. Common and distinct mechanisms of cognitive flexibility in prefrontal cortex. *J Neurosci*. (2011) 31:4771–9. doi: 10.1523/JNEUROSCI.5923-10.2011

32. Murphy FC, Michael A, Sahakian BJ. Emotion modulates cognitive flexibility in patients with major depression. *Psychol Med*. (2012) 42:1373–82. doi: 10.1017/S0033291711002418

33. Deveney CM, Deldin PJ. A preliminary investigation of cognitive flexibility for emotional information in major depressive disorder and non-psychiatric controls. *Emotion*. (2006) 6:429–37. doi: 10.1037/1528-3542.6.3.429

34. Cisler JM, Koster EHW. Mechanisms of attentional biases towards threat in anxiety disorders: an integrative review. *Clin Psychol Rev*. (2010) 30:203–16. doi: 10.1016/j.cpr.2009.11.003

35. Davidson RJ, Pizzagalli D, Nitschke JB, Putnam K. Depression: perspectives from affective neuroscience. *Annu Rev Psychol*. (2002) 53:545–74. doi: 10.1146/annurev.psych.53.100901.135148

36. Li Y, Kang C, Wei Z, Qu X, Liu T, Zhou Y, et al. Beta oscillations in major depression -signalling a new cortical circuit for central executive function. *Sci Rep*. (2017) 7:18021. doi: 10.1038/s41598-017-18306-w

37. Atchley R, Klee D, Oken B. EEG frequency changes prior to making errors in an easy stroop task. *Front Hum Neurosci*. (2017) 11:521. doi: 10.3389/fnhum.2017.00521

38. Cassani R, Estarellas M, San-Martin R, Fraga FJ, Falk TH. Systematic review on resting-State EEG for Alzheimer's disease diagnosis and progression assessment. *Dis Mark*. (2018) 2018:5174815. doi: 10.1155/2018/5174815

39. Newson JJ, Thiagarajan TC. EEG frequency bands in psychiatric disorders: a review of resting state studies. *Front Hum Neurosci*. (2019) 12:521. doi: 10.3389/fnhum.2018.00521

40. Palmiero M, Piccardi L. Frontal EEG asymmetry of mood: a mini-review. *Front Behav Neurosci*. (2017) 11:224. doi: 10.3389/fnbeh.2017.00224

41. Tucker DM, Stenslie CE, Roth RS, Shearer SL. Right frontal lobe activation and right hemisphere performance. Decrement during a depressed mood. *Arch Gen Psychiatry*. (1981) 38:169–74. doi: 10.1001/archpsyc.1981.01780270055007

42. Gotlib IH, Ranganath C, Rosenfeld JP. Frontal EEG alpha asymmetry, depression, and cognitive functioning. *Cogn Emot*. (1998) 12:449–78. doi: 10.1080/026999398379673

43. Velo JR, Stewart JL, Hasler BP, Towers DN, Allen JJB. Should it matter when we record? Time of year and time of day as factors influencing frontal EEG asymmetry. *Biol Psychol*. (2012) 91:283–91. doi: 10.1016/j.biopsycho.2012.06.010

44. Allen JJ, Iacono WG, Depue RA, Arbisi P. Regional electroencephalographic asymmetries in bipolar seasonal affective disorder before and after exposure to bright light. *Biol Psychiatry*. (1993) 33:642–6. doi: 10.1016/0006-3223(93)90104-L

45. Volf NV, Senkova NI, Danilenko KV, Putilov AA. Hemispheric language lateralization in seasonal affective disorder and light treatment. *Psychiat Res*. (1993) 47:99–108. doi: 10.1016/0165-1781(93)90059-P

46. Passynkova N, Volf N. Seasonal affective disorder: spatial organization of EEG power and coherence in the depressive state and in light-induced and summer remission. *Psychiatry Res*. (2001) 108:169–85. doi: 10.1016/S0925-4927(01)00122-6

47. Volf NV, Passynkova NR. EEG mapping in seasonal affective disorder. *J Affect Disord*. (2002) 72:61–9. doi: 10.1016/S0165-0327(01)00425-6

48. Machleidt W, Gutjahr L. Ultradian periodicity, diurnal and circannual rhythms in the electroencephalogram. *Fortschr Neurol Psychiatr*. (1984) 52:135–45. doi: 10.1055/s-2007-1002011

49. Barbato G, Cirace F, Monteforte E, Costanzo A. Seasonal variation of spontaneous blink rate and beta EEG activity. *Psychiatry Res*. (2018) 270:126–33. doi: 10.1016/j.psychres.2018.08.051

50. Höller Y, Gudjónsdottir BE, Valgeirsdóttir SK, Heimisson GT. The effect of age and chronotype on seasonality, sleep problems, and mood. *Psychiatry Res*. (2021) 297:113722. doi: 10.1016/j.psychres.2021.113722

51. Al Zoubi O, Ki Wong C, Kuplicki RT, Yeh Hw, Mayeli A, Refai H, et al. Predicting age from brain EEG signals–a machine learning approach. *Front Aging Neurosci*. (2018) 10:184. doi: 10.3389/fnagi.2018.00184

52. Ciarleglio A, Petkova E, Harel O. Elucidating age and sex-dependent association between frontal EEG asymmetry and depression: an application of multiple imputation in functional regression. *J Am Stat Assoc*. (2022) 117:12–26. doi: 10.1080/01621459.2021.1942011

53. Höller Y, Urbschat MM, Kristófersson GK, Ólafsson RP. Predictability of seasonal mood fluctuations based on self-report questionnaires and EEG biomarkers in a non-clinical sample. *Front Psychiatry*. (2022) 13:870079. doi: 10.3389/fpsyt.2022.870079

54. Magnússon A. Validation of the seasonal pattern assessment questionnaire (SPAQ). *J Affect Disord*. (1996) 40:121–9. doi: 10.1016/0165-0327(96)00036-5

55. Young MA, Blodgett C, Reardon A. Measuring seasonality: psychometric properties of the seasonal pattern assessment questionnaire and the inventory for seasonal variation. *Psychiatry Res*. (2003) 117:75–83. doi: 10.1016/S0165-1781(02)00299-8

56. Raheja SK, King EA, Thompson C. The seasonal pattern assessment questionnaire for identifying seasonal affective disorders. *J Affect Disord*. (1996) 41:193–9. doi: 10.1016/S0165-0327(96)00087-0

57. Kasper S, Wehr TA, Bartko JJ, Gaist PA, Rosenthal NE. Epidemiological findings of seasonal changes in mood and behavior. A telephone survey of Montgomery County, Maryland. *Arch Gen Psychiatry*. (1989) 46:823–33. doi: 10.1001/archpsyc.1989.01810090065010

58. Pallesen S, Bjorvatn B, Nordhus B I H ans Sivertsen, Hjornevik M, Morin CM. A new scale for measuring insomnia: the Bergen Insomnia Scale. *Percept Motor Skills*. (2008) 107:691–706. doi: 10.2466/pms.107.3.691-706

59. Segal ZV, Kennedy S, Gemar M, Hood K, Pedersen R, Buis T. Cognitive reactivity to sad mood provocation and the prediction of depressive relapse. *Arch Gen Psychiatry*. (2006) 63:749–55. doi: 10.1001/archpsyc.63.7.749

60. Ólafsson RP, Gudmundsdóttir SJ, Björnsdóttir TD, Snorrason I. A test of the habit-goal framework of depressive rumination and its relevance to cognitive reactivity. *Behav Ther*. (2020) 51:474–87. doi: 10.1016/j.beth.2019.08.005

61. Jarrett RB, Minhajuddin A, Borman PD, Dunlap L, Segal ZV, Kidner CL, et al. Cognitive reactivity, dysfunctional attitudes, and depressive relapse and recurrence in cognitive therapy responders. *Behav Res Ther*. (2012) 50:280–6. doi: 10.1016/j.brat.2012.01.008

62. Lau MA, Segal ZV, Williams JMG. Teasdale's differential activation hypothesis: implications for mechanisms of depressive relapse and suicidal behaviour. *Behav Res Ther*. (2004) 42:1001–17. doi: 10.1016/j.brat.2004.03.003

63. Makeig S, Bell AJ, Jung TP, Sejnowski TJ. Independent component analysis of electroencephalographic data. In: *Proceedings of the 8th International Conference on Neural Information Processing Systems. NIPS'95*. Cambridge, MA: MIT Press (1995). p. 145–51.

64. Gratton G, Coles MG, Donchin E. A new method for offline removal of ocular artifact. *Electroencephalogr Clin Neurophysiol*. (1983) 55:468–84. doi: 10.1016/0013-4694(83)90135-9

65. Bathke AC, Friedrich S, Pauly M, Konietschke F, Staffen W, Strobl N, et al. Testing mean differences among groups: multivariate and repeated measures analysis with minimal assumptions. *Multivariate Behav Res*. (2018) 53:348–59. doi: 10.1080/00273171.2018.1446320

66. Zappasodi F, Marzetti L, Olejarczyk E, Tecchio F, Pizzella V. Age-related changes in electroencephalographic signal complexity. *PLoS ONE*. (2015) 10:e0141995. doi: 10.1371/journal.pone.0141995

67. Friedrich S, Konietschke F, Pauly M. *MANOVA.RM: A Package for Calculating Test Statistics and Their Resampling Versions for Heteroscedastic Semi-Parametric Multivariate Data or Repeated Measures Designs*. (2017). R-Package Version 0.1.1. Available online at: https://CRAN.R-project.org/package=MANOVA.RM

68. Magnússon A, Stefánsson JG. Prevalence of seasonal affective disorder in Iceland. *Arch Gen Psychiatry*. (1993) 50:941–946. doi: 10.1001/archpsyc.1993.01820240025002

69. Vlahou EL, Thurm F, Kolassa IT, Schlee W. Resting-state slow wave power, healthy aging and cognitive performance. *Sci Rep*. (2014) 4:5101. doi: 10.1038/srep05101

70. Cajochen C, Brunner DP, Kräuchi K, Graw P, Wirz-Justice A. EEG and subjective sleepiness during extended wakefulness in seasonal affective disorder: circadian and homeostatic influences. *Biol Psychiatry*. (2000) 47:610–7. doi: 10.1016/S0006-3223(99)00242-5

71. Das J, Yadav S. Resting state quantitative electroencephalogram power spectra in patients with depressive disorder as compared to normal controls: an observational study. *Indian J Psychol Med*. (2020) Jan-Feb;42:30-38. doi: 10.4103/IJPSYM.IJPSYM_568_17

72. Ray W, Cole HW. EEG alpha activity reflects emotional and cognitive processes. *Science*. (1985) 228:750–2. doi: 10.1126/science.3992243

73. Cross-Villasana F, Gröpel P, Ehrlenspiel F, Beckmann J. Central theta amplitude as a negative correlate of performance proficiency in a dynamic visuospatial task. *Biol Psychol*. (2018) 132:37–44. doi: 10.1016/j.biopsycho.2017.10.009

74. Moore R, Gale A, Morris P, Forrester D. Theta phase locking across the neocortex reflects cortico-hippocampal recursive communication during goal conflict resolution. *Int J Psychophysiol*. (2006) 60:260–73. doi: 10.1016/j.ijpsycho.2005.06.003

75. Borghini G, Astolfi L, Vecchiato G, Mattia D, Babiloni F. Measuring neurophysiological signals in aircraft pilots and car drivers for the assessment of mental workload, fatigue and drowsiness. *Neurosci Biobehav Rev*. (2014) 44:58–75. doi: 10.1016/j.neubiorev.2012.10.003

76. Höller Y, Bathke A, Uhl A. Age, sex, and pathology effects on stability of electroencephalographic biometric features based on measures of interaction. *Trans Inform Forensics Sec*. (2019) 14:459–71. doi: 10.1109/TIFS.2018.2854728

77. Bučková B, Brunovský M, Bareš, Hlinka J. Predicting sex from EEG: validity and generalizability of deep-learning-based interpretable classifier. *Front Neurosci*. (2020) 14:589303. doi: 10.3389/fnins.2020.589303

78. Hinterbuchinger B, König D, Gmeiner A, Listabarth S, Fellinger M, Thenius C, et al. Seasonality in schizophrenia-An analysis of a nationwide registry with 110,735 hospital admissions. *Eur Psychiatry*. (2020) 63:e55. doi: 10.1192/j.eurpsy.2020.47

79. Winthorst WH, Post WJ, Meesters Y, Penninx BW, Nolen WA. Seasonality in depressive and anxiety symptoms among primary care patients and in patients with depressive and anxiety disorders; results from the Netherlands Study of Depression and Anxiety. *BMC Psychiatry*. (2011) 11:198. doi: 10.1186/1471-244X-11-198

80. Lam RW, Goldner EM, Grewal A. Seasonality of symptoms in anorexia and bulimia nervosa. *Int J Eat Disord*. (1996) 19:35–44. doi: 10.1002/(SICI)1098-108X(199601)19:1<35::AID-EAT5>3.0.CO;2-X

81. Solt V, Chen CJ, Roy A. Seasonal pattern of posttraumatic stress disorder admissions. *Compr Psychiatry*. (1996) 37:40–2. doi: 10.1016/S0010-440X(96)90049-8

82. Höller Y, Thomschewski A, Schmid EV, Höller P, Crone JS, Trinka E. Individual brain-frequency responses to self-selected music. *Int J Psychophysiol*. (2012) 86:206–13. doi: 10.1016/j.ijpsycho.2012.09.005

83. Ke H, Chen D, Shi B, Zhang J, Liu X, Zhang X, et al. Improving brain e-health services via high-performance EEG classification with grouping Bayesian optimization. *IEEE Trans Serv Comput*. (2020) 13:696–708. doi: 10.1109/TSC.2019.2962673

84. Ke H, Chen D, Shah T, Liu X, Zhang X, Zhang L, et al. Cloud-aided online EEG classification system for brain healthcare: a case study of depression evaluation with a lightweight CNN. *Softw Pract Exp*. (2020) 50:596–610. doi: 10.1002/spe.2668

85. Ke H, Cai C, Wang F, Hu F, Tang J, Shi Y. Interpretation of frequency channel-based CNN on depression identification. *Front Comput Neurosci*. (2021) 15:773147. doi: 10.3389/fncom.2021.773147

86. Ke H, Wang F, Ma H, He Z. ADHD identification and its interpretation of functional connectivity using deep self-attention factorization. *Know Based Syst*. (2022) 250:109082. doi: 10.1016/j.knosys.2022.109082

87. Kroenke K, Spitzer RL, Williams JB. The PHQ-9: validity of a brief depression severity measure. *J Gen Intern Med*. (2001) 16:606–13. doi: 10.1046/j.1525-1497.2001.016009606.x

88. Lovibond PF, Lovibond SH. The structure of negative emotional states: comparison of the depression anxiety stress scales (DASS) with the beck depression and anxiety inventories. *Behav Res Ther*. (1995) 33:335–433. doi: 10.1016/0005-7967(94)00075-U

frontiers | Frontiers in Psychiatry

TYPE Original Research
PUBLISHED 05 October 2022
DOI 10.3389/fpsyt.2022.841999

OPEN ACCESS

EDITED BY
Masahiro Takamura,
Shimane University, Japan

REVIEWED BY
Fengqin Wang,
Hubei Normal University, China
Krisztina Monory,
Johannes Gutenberg University Mainz, Germany

*CORRESPONDENCE
Xiangdong Tang
2372564613@qq.com
Larry D. Sanford
SanforLD@evms.edu

SPECIALTY SECTION
This article was submitted to Computational Psychiatry, a section of the journal Frontiers in Psychiatry

RECEIVED 23 December 2021
ACCEPTED 20 September 2022
PUBLISHED 05 October 2022

CITATION
Zhu J, Zhang Y, Ren R, Sanford LD and Tang X (2022) Blood transcriptome analysis: Ferroptosis and potential inflammatory pathways in post-traumatic stress disorder. *Front. Psychiatry* 13:841999. doi: 10.3389/fpsyt.2022.841999

Blood transcriptome analysis: Ferroptosis and potential inflammatory pathways in post-traumatic stress disorder

Jie Zhu[1], Ye Zhang[1], Rong Ren[1], Larry D. Sanford[2]* and Xiangdong Tang[1]*

[1]Sleep Medicine Center, Department of Respiratory and Critical Care Medicine, Mental Health Center, West China Hospital, Sichuan University, Chengdu, China, [2]Sleep Research Laboratory, Center for Integrative Neuroscience and Inflammatory Diseases, Pathology and Anatomy, Eastern Virginia Medical School, Norfolk, VA, United States

Background: Transcriptome-wide analysis of peripheral blood in post-traumatic stress disorder (PTSD) indicates widespread changes in immune-related pathways and function. Ferroptosis, an iron-dependent regulated cell death, is closely related to oxidative stress. However, little is known as to whether ferroptosis plays a role in PTSD.

Methods: We conducted a comprehensive analysis of combined data from six independent peripheral blood transcriptional studies in the Gene Expression Omnibus (GEO) database, covering PTSD and control individuals. Differentially expressed genes (DEGs) were extracted by comparing PTSD patients with control individuals, from which 29 ferroptosis-related genes (FRGs) were cross-matched and obtained. The weighted gene co-expression network analysis (WGCNA), the Extreme Gradient Boosting (XGBoost) model with Bayesian Optimization, and the least absolute shrinkage and selection operator (LASSO) Cox regression were utilized to construct a PTSD prediction model. Single-sample Gene Set Enrichment Analysis (ssGSEA) and CIBERSORT revealed the disturbed immunologic state in PTSD high-risk patients.

Results: Three crucial FRGs (ACSL4, ACO1, and GSS) were identified and used to establish a predictive model of PTSD. The receiver operating characteristic (ROC) curve verifies its risk prediction ability. Remarkably, ssGSEA and CIBERSORT demonstrated changes in cellular immunity and antigen presentation depending on the FRGs model.

Conclusion: These findings collectively provide evidence that ferroptosis may change immune status in PTSD and be related to the occurrence of PTSD, which may help delineate mechanisms and discover treatment biomarkers for PTSD.

KEYWORDS

ferroptosis, post-traumatic stress disorder, transcriptome analysis, computational modeling, inflammatory pathways

Introduction

Post-traumatic stress disorder (PTSD) is a psychiatric syndrome involving the interaction of environments and genes. PTSD occurs after a traumatic experience and is followed by flashbacks, hallucinations, nightmares, constant alertness, and enhanced arousal (1). By definition, PTSD is associated with a traumatic event. However, data also suggest that the development of PTSD requires a genetic tendency that alters, to varying degrees, an individual's response to, or recovery from, traumatic exposure (2).

The development of high-throughput sequencing technology has enabled unbiased identification of genes, pathways, and proteins related to PTSD pathophysiology. Data from five PTSD peripheral blood studies indicated that transcriptional disruption affects multiple immune-related pathways and molecules (3). In a review of similar studies, Heinzlemann and Gill concluded that PTSD develops as a result of altered epigenetic regulation and inflammatory genes that are highly active (4).

Despite the widespread observation of immune fluctuations, it remains unclear how specific mechanisms are activated or how key processes are regulated. On the other hand, the nervous system is particularly vulnerable to oxidative stress due to its high metabolic demands and dense composition of oxidation-sensitive lipid cells (5, 6). PTSD patients showed elevated serum lipid peroxidation and depleted antioxidant enzymes (7). Down-regulated expression of the antioxidant protease, superoxide dismutase (SOD), also was observed in PTSD patients (8).

Oxidative stress is a cellular state that occurs when the pro-oxidant molecules, such as reactive oxygen species (ROS), exceed the elimination power of the antioxidants (9). Antioxidant depletion leads to cell degeneration and apoptosis, making oxidative stress a primary molecular aging mechanism widely involved in multiple diseases.

In the presence of excess iron, or more precisely, the divalent ferrous ion Fe^{2+}, can produce abundant ROS such as soluble hydroxyl radicals or lipid alkoxy radicals (10). Known as the Fenton reaction, this is the main source of ROS in the cell produced by Fe^{2+}. By generating ROS, mitochondrial respiration is reduced, lipids are peroxidized, enzymes are oxidized, and neuronal damage is possible (11). Moreover, ROS and mitochondrial function seem to be closely related to the innate immune system. Mitochondria-derived ROS can trigger some inflammasomes such as nucleotide-binding and oligomerization domain (NOD)-like receptors (NLRs), and Melanoma (AIM) 2-like receptors (ALRs) (12, 13).

Another process closely related to iron metabolism and ROS is ferroptosis. Ferroptosis is a form of iron-dependent cell death induced by oxidative stress, and that involves molecular pathways common to oxidative stress, such as lipid peroxidation and glutathione (GSH) depletion (14). The Fenton reaction is the critical step of ferroptosis. A high level of iron produces excessive ROS and leads to liposome peroxidation, which leads to cell death. Although first found in cancer cells, ferroptosis has been linked to several neurological illnesses, such as Alzheimer's, Parkinson's, and stroke (15–17). Stefanovic et al. found lower GSH transferase levels in PTSD (18), suggesting that ferroptosis may be involved in the pathophysiological process of PTSD. These studies suggest that ferroptosis may be a key influence in the pathological processes of PTSD.

The main aim of the current study is to synthesize available data from transcriptional studies of PTSD and to elucidate the association of ferroptosis-related genes (FRGs) with the pathophysiology of PTSD. Six independent studies from the Gene Expression Omnibus (GEO) database were included. Multiple algorithms were used in this study to establish a risk prediction model for PTSD, including the weighted gene co-expression network analysis (WGCNA), the Extreme Gradient Boosting (XGBoost) model with Bayesian Optimization, and the least absolute shrinkage and selection operator (LASSO) Cox regression (**Figure 1**). Furthermore, immune cell and function analyses were conducted to reveal the possible underlying mechanism of PTSD assessments.

Materials and methods

Data availability

The RNA sequencing (RNA-seq) data of PTSD patients were obtained from the GEO database (accession numbers: GSE97356, GSE81761, GSE63878, GSE64813, GSE67663, and GSE109409) (**Table 1**). GSE97356 contains 324 World Trade Center responders, of which 123 individuals are in the PTSD group, and 201 individuals are controls. GSE81761 includes military service members with PTSD (n = 39) and controls without PTSD (n = 27) at baseline. GSE63878 contains 96 samples from U.S. Marines deployed to conflict zones, half of whom returned with PTSD. GSE64813 involved 188 samples of service members, and half with PTSD. GSE67663 summarizes the gene expression profiles of 112 PTSD cases and 72 controls. GSE109409 contains 85 Canadian infantry soldiers, of whom 27 were positive for PTSD. All research projects used peripheral blood to obtain transcriptome-wide RNA-Seq data, and both are publicly available. Thus, the present study was exempt from requiring approval from local ethics committees. The GSE97356 and GSE81761 datasets were used as training sets, while the others were used as independent validation datasets. The ferroptosis-related genes

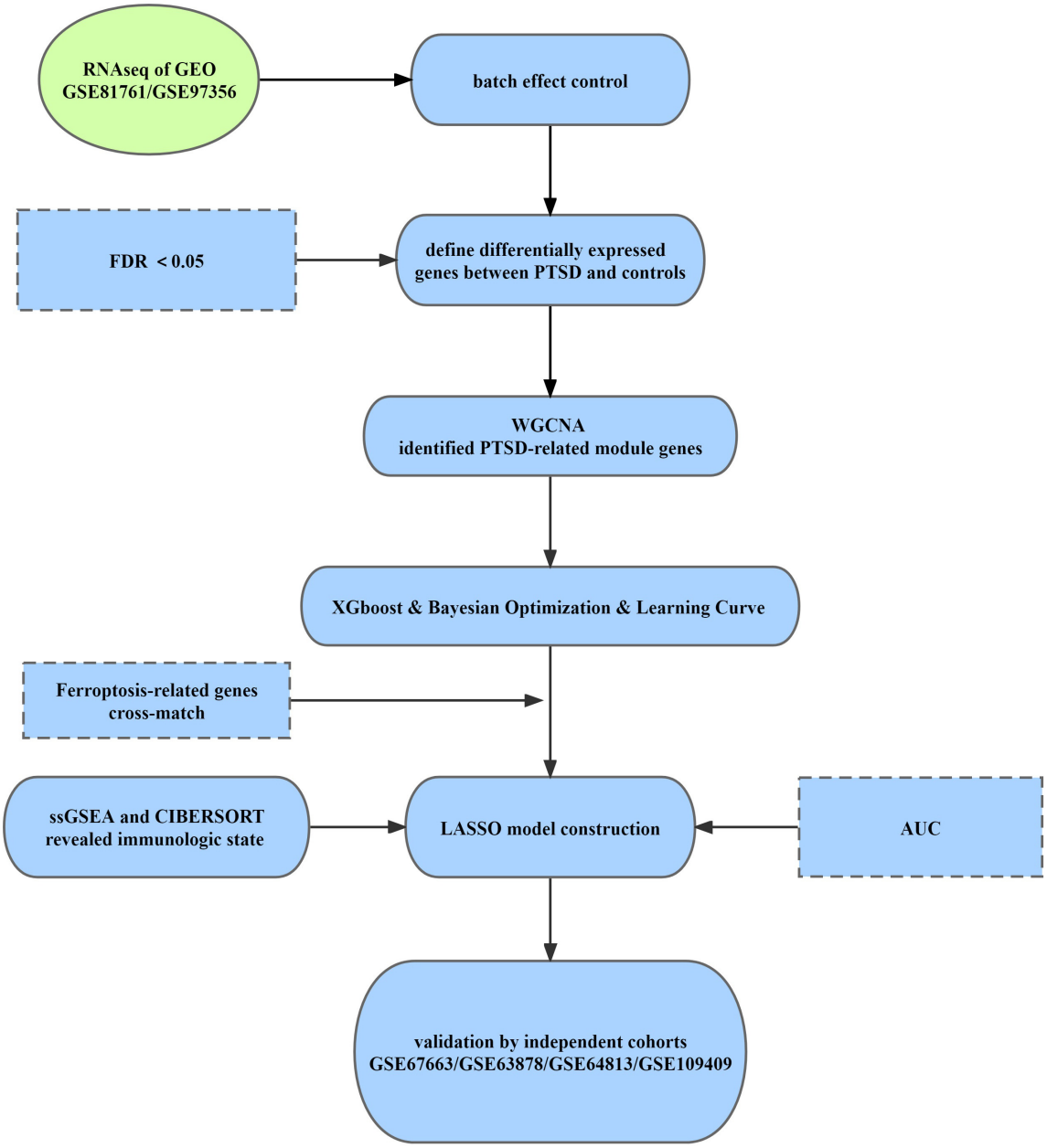

FIGURE 1
Workflow of the study.

(FRGs) list was derived from previously published research (19–23).

Combined transcriptional data-processing and batch effect control

All statistical analyses were conducted using the R program version 3.6.2 and GraphPad software (Prism 8). Each individual's gene expression profiles were summarized after the microarray probes were mapped with gene symbols according to the chips and platforms. If multiple microarray probes were mapped to one single gene, the expression level was expressed as the mean value. The analysis did not include missing data or samples with low coverage. The gene expression values were log2-transformed, namely log2 Fold Change (log2FC), before normalization. The batch correction was conducted using the R package ComBat and sva functions to reduce cohort effects and remove system

10.3389/fpsyt.2022.841999

TABLE 1 Baseline of included datasets.

GSE97356	PTSD group (*N* = 123)	Control group (*N* = 201)
Age (mean)	52.5	51.4
Race (*n*%)		
Caucasian	102 (82.9%)	181(90.0%)
Other	21(17.1%)	20(9.9%)
Sex (*n*%)	Not applicable	Not applicable
GSE81761	**PTSD group (*N* = 39)**	**Control group (*N* = 27)**
Age (mean)	31.1	35.9
Race (*n*%)		
White	25 (64.1%)	20 (74.1%)
Non-white	14 (35.9%)	7 (25.9%)
Sex (*n*%)		
Male	37 (94.9%)	26 (96.3%)
Female	2 (5.1%)	1 (3.7%)
GSE63878	**PTSD group (*N* = 48)**	**Control group (*N* = 48)**
Age (mean)	22.2	22.4
Race (*n*%)		
Caucasian	26 (54.2%)	26 (54.2%)
African American	4 (8.3%)	4 (8.3%)
Native American Mexican	13 (27.1%)	13 (27.1%)
Asian and Other	5 (10.4%)	5 (10.4%)
Sex (*n*%)		
Male	48 (100%)	48 (100%)
Female	0 (0%)	0 (0%)
GSE64813	**PTSD group (*N* = 94)**	**Control group (*N* = 94)**
Age (mean)	23.1	23.4
Race (*n*%)		
Caucasian	52 (55.3%)	52 (55.3%)
African American	8 (8.5%)	8 (8.5%)
Native American Mexican	26 (27.7%)	26 (27.7%)
Asian and Other	10 (10.6%)	10 (10.6%)
Sex (*n*%)		
Male	94 (100%)	94 (100%)
Female	0 (0%)	0 (0%)
GSE67663	**PTSD group (*N* = 112)**	**Control group (*N* = 72)**
Age (mean)	41.9	43.3
Race (*n*%)		
African American	102 (91.1%)	71 (98.6%)
Others	10 (8.9%)	1 (1.4%)
Sex (*n*%)		
Male	25 (22.3%)	21 (29.2%)
Female	87(77.7%)	51 (70.8%)
GSE109409	**PTSD group (*N* = 27)**	**Control group (*N* = 58)**
Age (mean)	28.7	30.3
Race (*n*%)	Not applicable	Not applicable
Sex (*n*%)	Not applicable	Not applicable

variability from technical, clinical, or demographic factors (3, 24). Subsequently, combined and normalized cohorts contained gene expression data from two GEO cohorts that included PTSD and control individuals. We performed a principal component analysis (PCA) to verify whether the batch effect was eliminated. Continuous variables were compared between groups using the equal-variance *T*-test. Unless otherwise noted, the significance threshold for the *P*-value was set to 0.05.

Weighted correlation network analysis

The Wilcoxon test for non-parametric distributions was performed to detect differential gene expressions (DGEs) between PTSD and controls samples by the limma package. The weighted gene co-expression network analysis (WGCNA) is a common method to transform gene expression data into a co-expression network and identify disease-related gene modules and key genes affecting phenotypic traits (25, 26). The R program's WGCNA package was utilized on DGEs data to identify highly connected modules, which summarized specific gene expression patterns related to PTSD. Under the proper soft threshold power, clustering analysis can successfully establish a standard scale-free network, and then overlapping WGCNA function was used to get a Topological Overlap Matrix (TOM). Similar modules were merged by the hierarchical clustering method with a height cut-off of 0.25. Module eigengenes (MEs) were principal components and summarized all gene expression patterns into a specific module. Subsequently, module-trait associations were estimated using spearman's correlation analysis (in our study, clinical trait refers to PTSD). The module with the highest spearman's correlation coefficient was extracted. Genes clustered in the module genes were then cross-matched with FRGs, thus identifying FRGs potentially crucial in PTSD development.

Hyperparameter optimization and feature importance ranking

In order to further refine the screening of key genes, we employed the Extreme Gradient Boosting (XGBoost)

algorithm. The XGBoost algorithm excels as a method for combining multiple learning algorithms into one superior predictive algorithm. It consists primarily of two parts: a decision tree algorithm and a gradient boosting algorithm (27). Boosting is accomplished by setting up weak evaluators individually and integrating multiple weak evaluators iteratively. Because hyperparameters can greatly impact the classification performance of the XGBoost model, the Bayesian parameter optimization based on Gaussian processes was applied as a way to adjust them (28). Four main hyperparameters were associated with the Bayesian optimization in this article: Eta (Learning rate), Max depth (Maximum depth of a tree), Min child weight (Minimum sum of instance weight needed in a child), and Subsample (Subsample ratio of the training instances). We used the area under the curve (AUC) as the objective function. Ranks of features were determined by the average gain of each feature across all trees. High-value features can be considered more significant for prediction than low-value features. An analysis of the model's performance was compared according to the learning curve. As a result, the classification model's generalization ability (overfitting or underfitting) could be effectively evaluated (29).

Functional annotation and protein-protein interaction networks

Gene Ontology (GO) enrichment and Kyoto Encyclopedia of Genes and Genomes (KEGG) pathway analyses were conducted to better understand the biologic function of DGEs and FRGs. GO analysis utilized the Biological Process term, which provides current scientific information about the functions of encoding and non-coding genes and allows exploring how individual genes contribute to an organism's biology at the molecular, cellular, and organism levels. KEGG database provides information for biological system functions such as cells, organisms, and ecosystems, mainly generated from large-scale datasets produced by genome sequencing and other high-throughput technologies. The intersection of DGEs and FRGs was assessed via the R VennDiagram package. The GO Biological Process and KEGG pathway analyses identified major biological terms via the R "clusterProfiler" package. The R "GOplot" package was employed to visualize the enrichment terms.

The Search Tool for the Retrieval of Interacting Genes database[1] provides protein interaction information from large-scale sequencing sources (30). Using this tool, the physical and functional associations among specific gene clusters (based on user requirements) can be computationally predicted. A protein–protein interaction (PPI) network among intersection genes of DGEs and FRGs was calculated by topology analysis using Maximal Clique Centrality (MCC).

Establishment of the risk prediction model

Genome-wide analysis of gene expression levels and high throughput technology produces a large amount of data that allows statistical analyses of complex diseases' genetic causes. Regularization via the least absolute shrinkage and selection operator (LASSO) is often used to reduce the selected set of explanatory variables in examining the associations between all biomarkers and a given phenotype (31). The LASSO model construction was accomplished using the R package "glmnet." After tenfold cross-validation with minimum standards to determine the penalty parameters (λ), the Lasso model was established. The Receiver Operating Characteristic (ROC) curve verified the prediction ability for the risk of illness.

Gene set enrichment derived from immune cell markers and CIBERSORT analysis

Single-sample Gene Set Enrichment Analysis (ssGSEA) classified gene sets with immune biological roles by identified immune markers (32, 33). The immune markers comprised 782 immune-related genes representing diverse immunologic cells and functions (34). The expression data were changed into ssGSEA scores to predict the abundance of each gene set type in individual samples. The gene expression profile of two combined PTSD studies was transformed into a gene set enrichment profile.

Cell-type identification by estimating relative subsets of RNA transcript, also named CIBERSORT, is a computational algorithm that distinguishes 22 immune cell types retrieved from RNA-sequencing gene expression profiles (35). Cell types including B cells naïve, B cells memory, Plasma cells, T cells CD8, T cells CD4 naïve, T cells CD4 memory resting, T cells CD4 memory activated, T cells follicular helper, T cells regulatory (Tregs), T cells gamma delta, NK cells resting, NK cells activated, Monocytes, Macrophages M0, Macrophages M1, Macrophages M2, Dendritic cells resting, Dendritic cells activated, Mast cells resting, Mast cells activated, Eosinophils, and Neutrophils were estimated in each sample. And in that way, the gene

1 http://string-db.org/

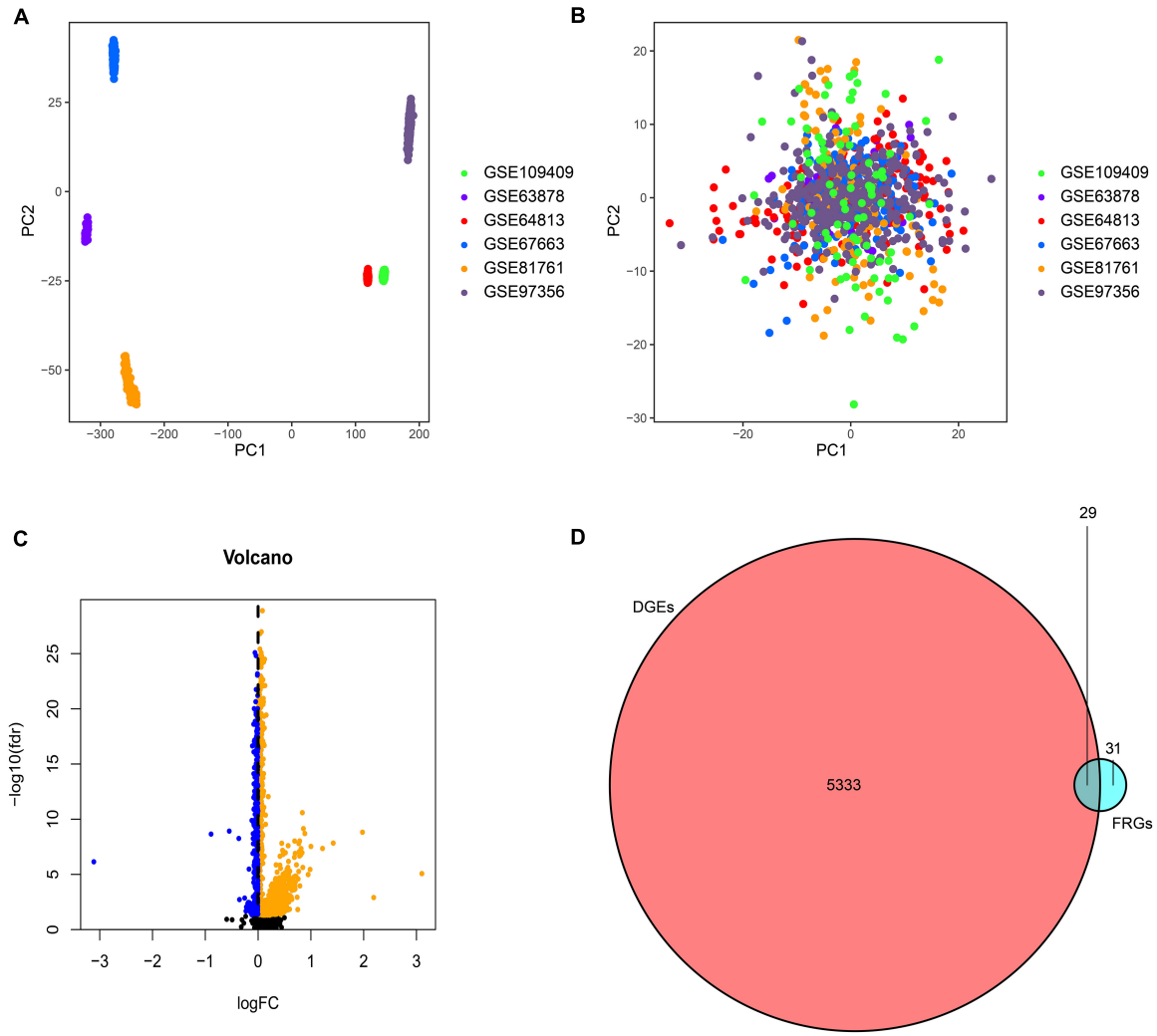

FIGURE 2
Principal component analysis (PCA) of the six GEO datasets. **(A)** Scatter plots present the samples based on two principal components (PC1 and PC2) without removing the batch effect. **(B)** Scatter plots to present the samples with the removal of batch effect. **(C)** Volcano plot of DGEs in the combined GEO cohort. The orange spots represented the up-regulated genes, and the blue spots represented the down-regulated genes between PTSD and controls. **(D)** Venn diagram of DGEs and FRGs showed the cross-match gene set contained 29 crucial FRGs.

expression profile was transformed into an immune cell profile.

Results

Differentially expressed genes and ferroptosis-related genes in the combined gene expression omnibus cohort

The samples based on the unnormalized expression values showed a distribution bias by batch (Figure 2A). After normalization, the PCA plot indicated that the batch effect was removed from the different platforms (Figure 2B), and 185 PTSD subjects and 248 controls were included in the training datasets. The batch correction had a significant impact on the log2FC value of the differential genes. The absolute value of average log2FC decreased from 89 to less than 1. Therefore, instead of utilizing log2FC, we used a stronger *P*-value criterion, namely the *P*-value after FDR (false discovery rate) correction. A total of 5362 DGEs were screened from 19,281 genes at baseline using an FDR value less than 0.05, of which 369 were up-regulated, and 4993 were down-regulated (Figure 2C). After matching with 60 FRGs reported in previous studies, we obtained 29 differential FRGs (Figure 2D): ACACA, ACO1, ACSF2, ACSL3, ACSL4,

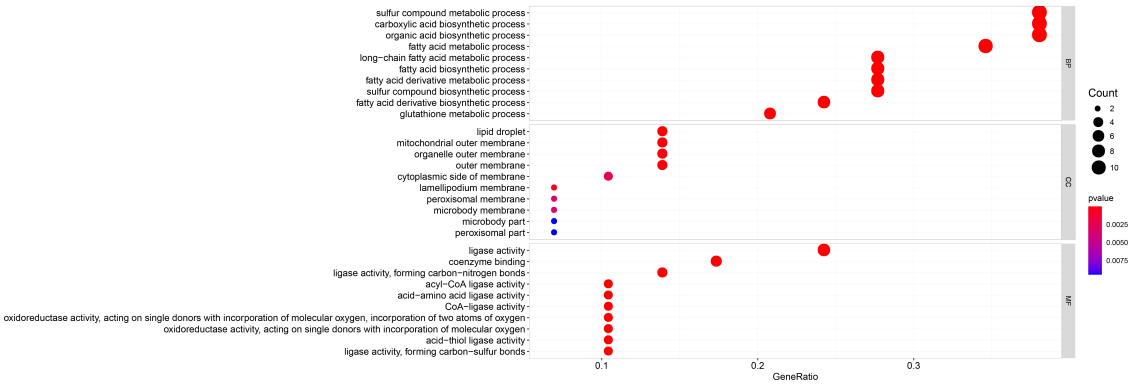

FIGURE 3
Gene Ontology enrichment of 29 differential FRGs. The count shows the number of genes enriched in the pathway. Gene ratio: the ratio of the FRGs number in this term to the total number of FRGs.

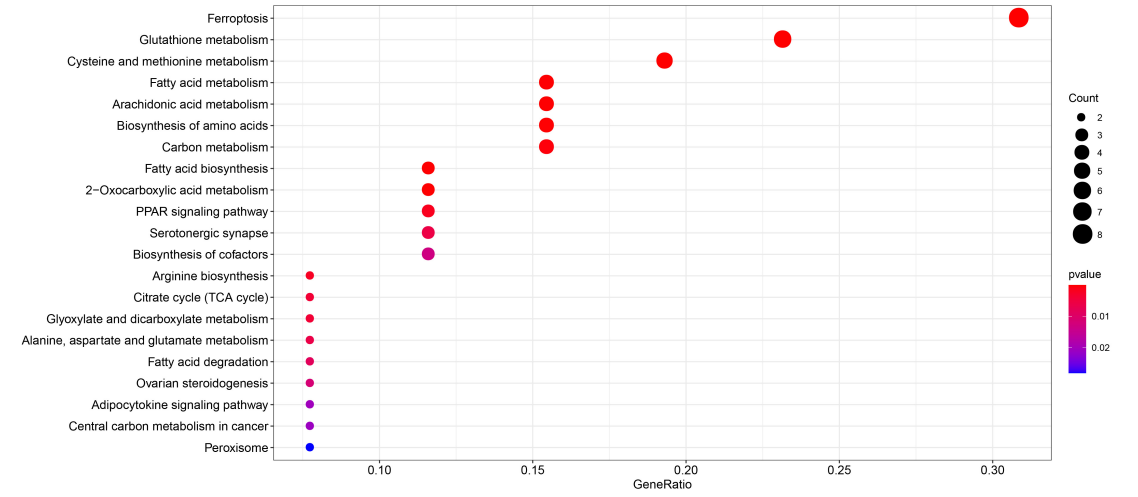

FIGURE 4
Kyoto encyclopedia of genes and genomes enrichment of 29 differential FRGs. The count shows the number of genes enriched in the pathway. Gene ratio: the ratio of the FRGs number in this term to the total number of FRGs.

AIFM2, AKR1C3, ALOX5, ALOX12, ALOX15, CBS, CD44, CHAC1, CISD1, CRYAB, CS, DPP4, EMC2, FADS2, FANCD2, FDFT1, FTH1, G6PD, GCLC, GCLM, GLS2, GOT1, GPX4, and GSS.

Functional annotation of the differential ferroptosis-related genes

Gene Ontology enrichment analysis related to biological processes (BP) found that the 29 differential FRGs were enriched in several metabolic pathways, including carboxylic acid biosynthesis, organic acid biosynthesis, long-chain fatty acid metabolism, and glutathione metabolism. Cellular components (CC) genes were concentrated in various organelle membranes, e.g., organelle outer membrane, mitochondrial outer membrane, and microbody membrane. Molecular function (MF) genes were mainly enriched in terms of the activity of multiple enzymes, including acyl-CoA ligase activity, acid-amino acid ligase activity, and acid-thiol ligase activity (Figure 3). Not surprisingly, in the KEGG pathway analyses, the 29 differential FRGs were notably associated with ferroptosis and some metabolic pathways similar to those revealed by GO enrichment, such as fatty acid biosynthesis, 2-Oxocarboxylic acid metabolism, and glutathione metabolism (Figure 4).

Construction and analysis of protein–protein interaction network

The PPI network was constructed with the 29 differential FRGs using the STRING database (Figure 5A).

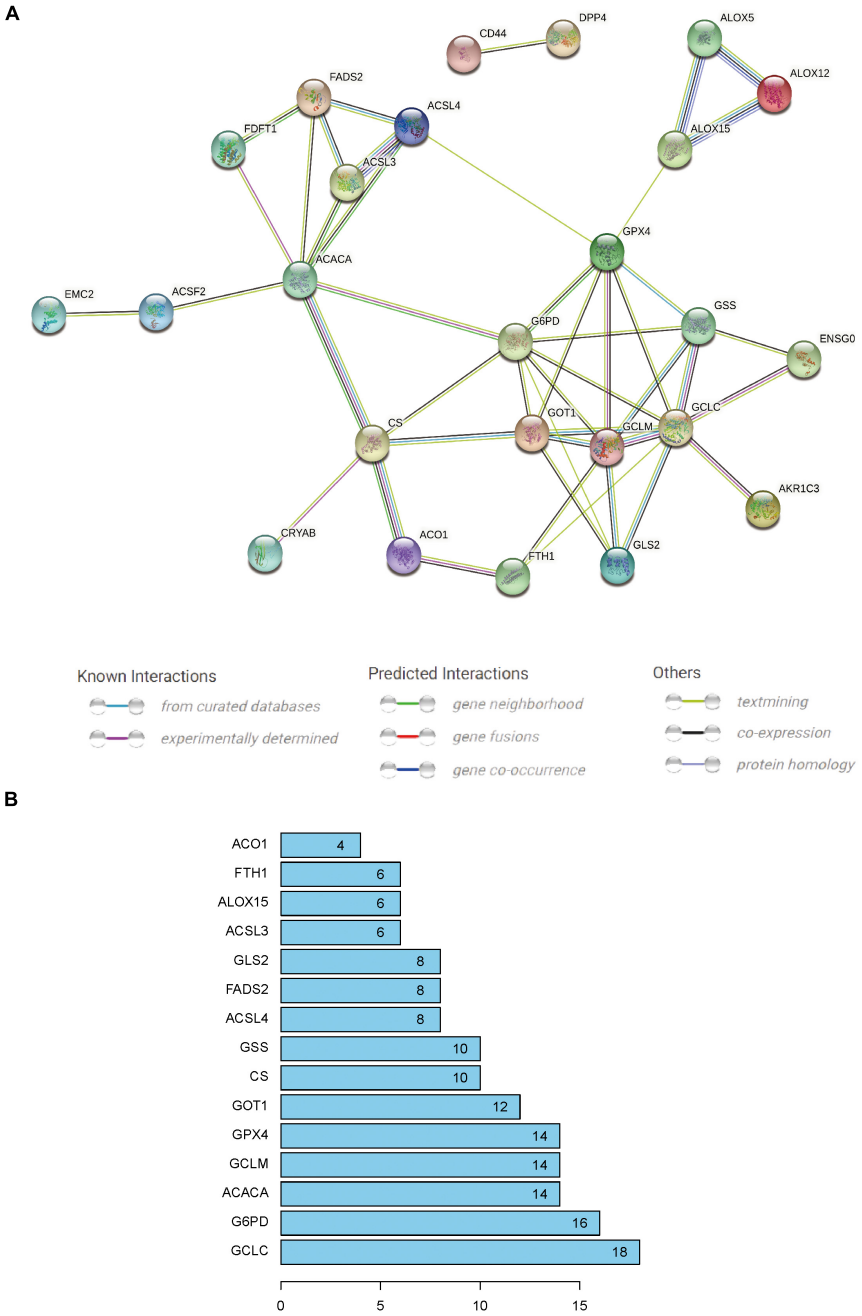

FIGURE 5
(A) Protein–protein interaction network generated by STRING database analysis indicating direct and indirect associations among 29 crucial FRGs. **(B)** Fifteen significant nodes of the PPI network were screened using an interaction score > 0.4; these were the most widely connected and are sorted by the number of connected nodes.

Subsequently, 15 significant network nodes (GCLC, G6PD, ACACA, GCLM, GPX4, GOT1, CS, GSS, ACSL4, FADS2, GLS2, ACSL3, ALOX15, FTH1, ACO1) were identified with a PPI combined score > 0.4, which indicated a medium to high confidence network (Figure 5B).

Co-expression network construction

We used WGCNA to assess highly connected modules by integrating DGEs of PTSD cases compared to all control individuals. The gene hierarchy clustering plots showed two clusters in PTSD patients and controls by the WGCNA

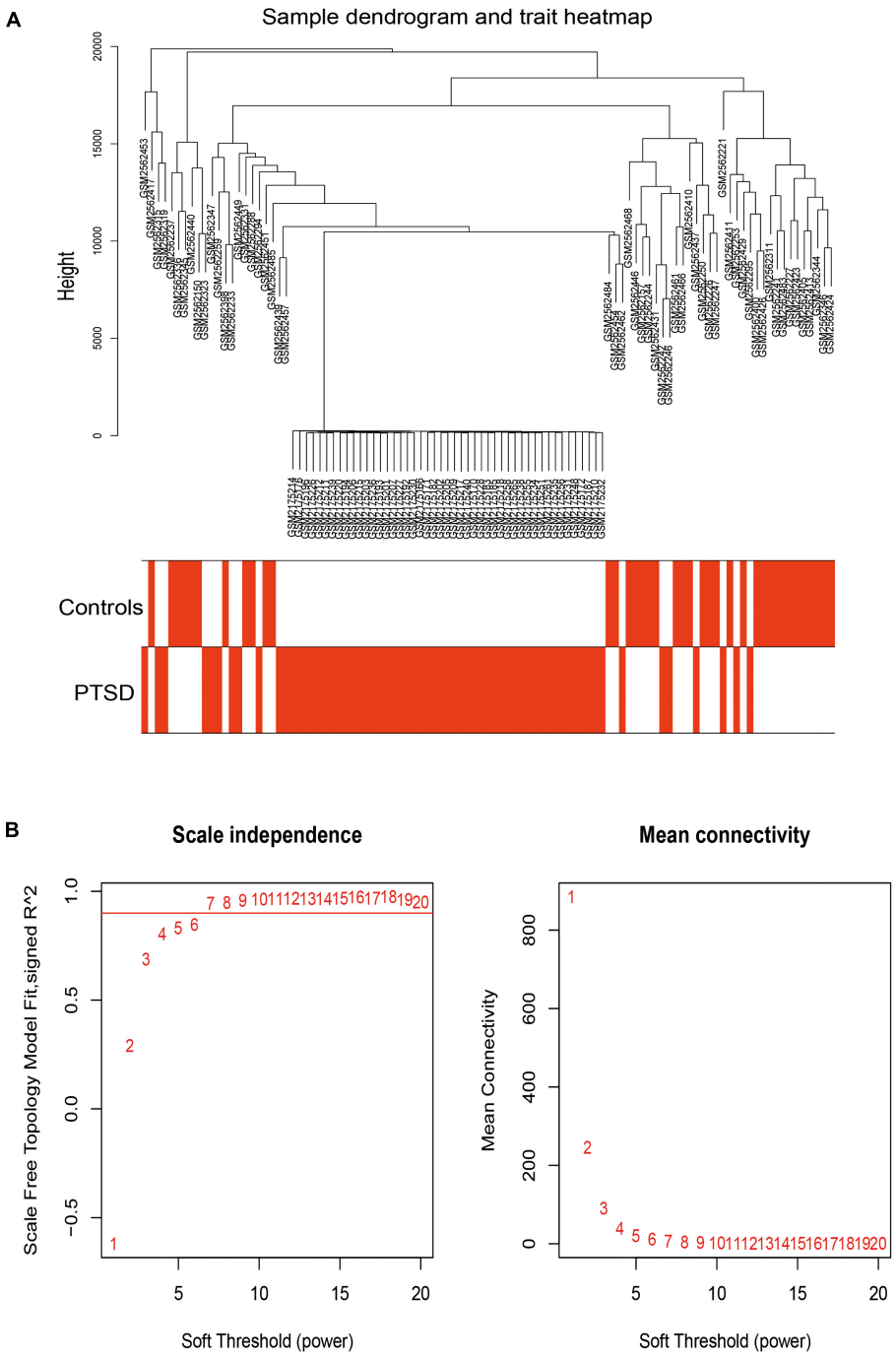

FIGURE 6
(A) The gene hierarchy clustering plots showed that all samples were divided into two clusters (in the red and white plot) with the WGCNA algorithm method. **(B)** A scale-free network distribution was with stable average connectivity when the soft threshold power β was set to 7.

algorithm method (Figure 6A). Outliers in height above 20,000 were removed. When the soft threshold power β was set to 7, the scale-free Topology fitting index R^2 was greater than 0.9 and the mean connectivity was stabilized, indicating a good network connection (Figure 6B). After removing highly similar modules (Figure 7A), 12 gene cluster modules (Figure 7B) were generated as MEcyan (96 genes), MEblack (258 genes), MEblue (1550 genes), MEpurple (173 genes), MEbrown (989 genes), MEsalmon (135 genes), MEgreenyellow (149 genes), MEred (274 genes), MEtan (149 genes), MEmagenta (434

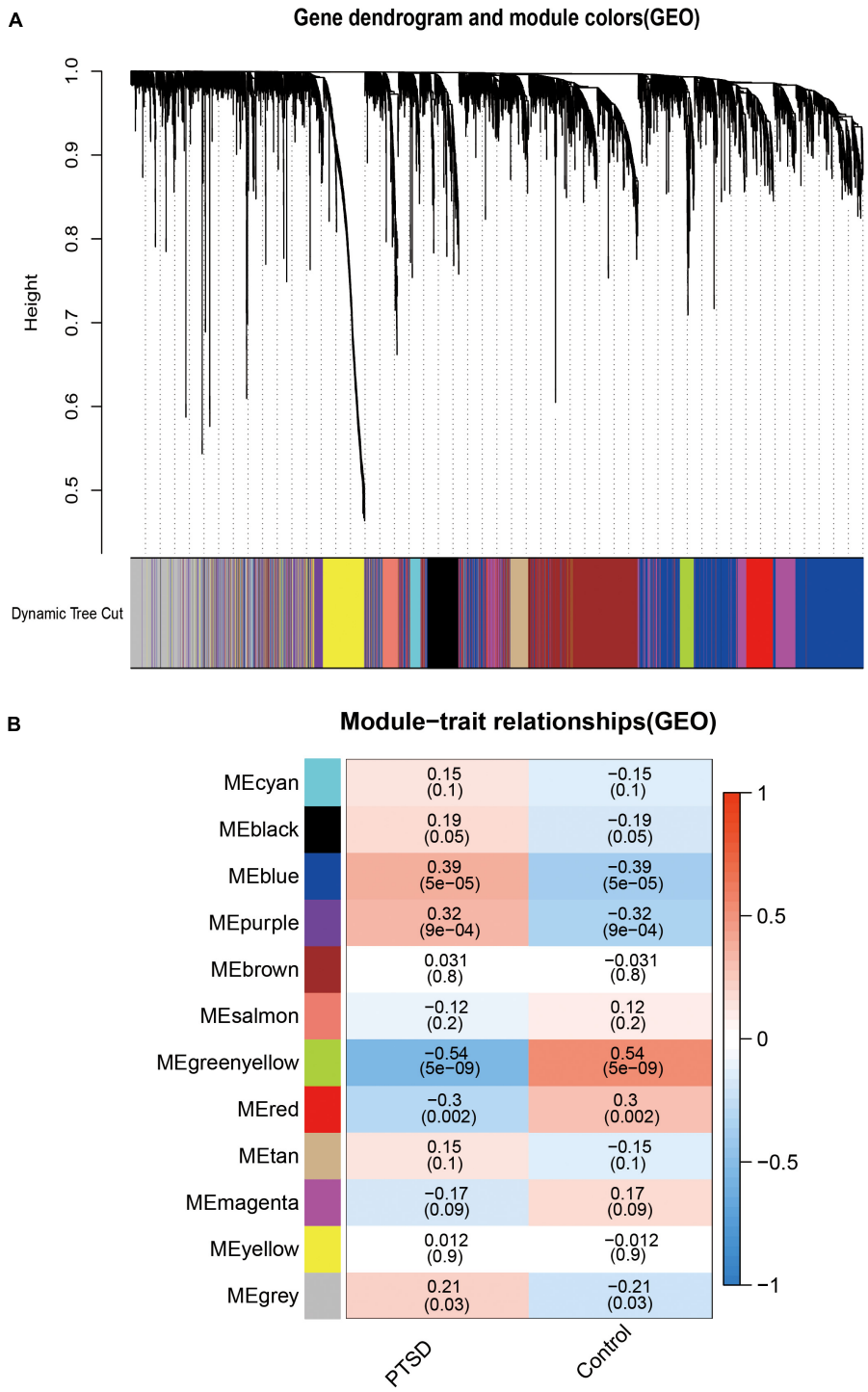

FIGURE 7
(A) Through the hierarchical clustering method, similar modules were clustered in 12 module eigengenes (MEs), which summarized all gene expression patterns into a specific module. **(B)** Spearman's correlation analysis between the MEs and PTSD indicated that the most relevant object module was MEgreenyellow (correlation coefficient = −0.54, *P* = 5e-09).

genes), MEyellow (385 genes), and MEgray (770 genes). The spearman's correlation analysis revealed each module's correlation coefficient with PTSD. We chose the module with the largest correlation coefficient, MEgreenyellow (correlation coefficient = -0.54, *P* = 5e-09), as the critical module for further analysis.

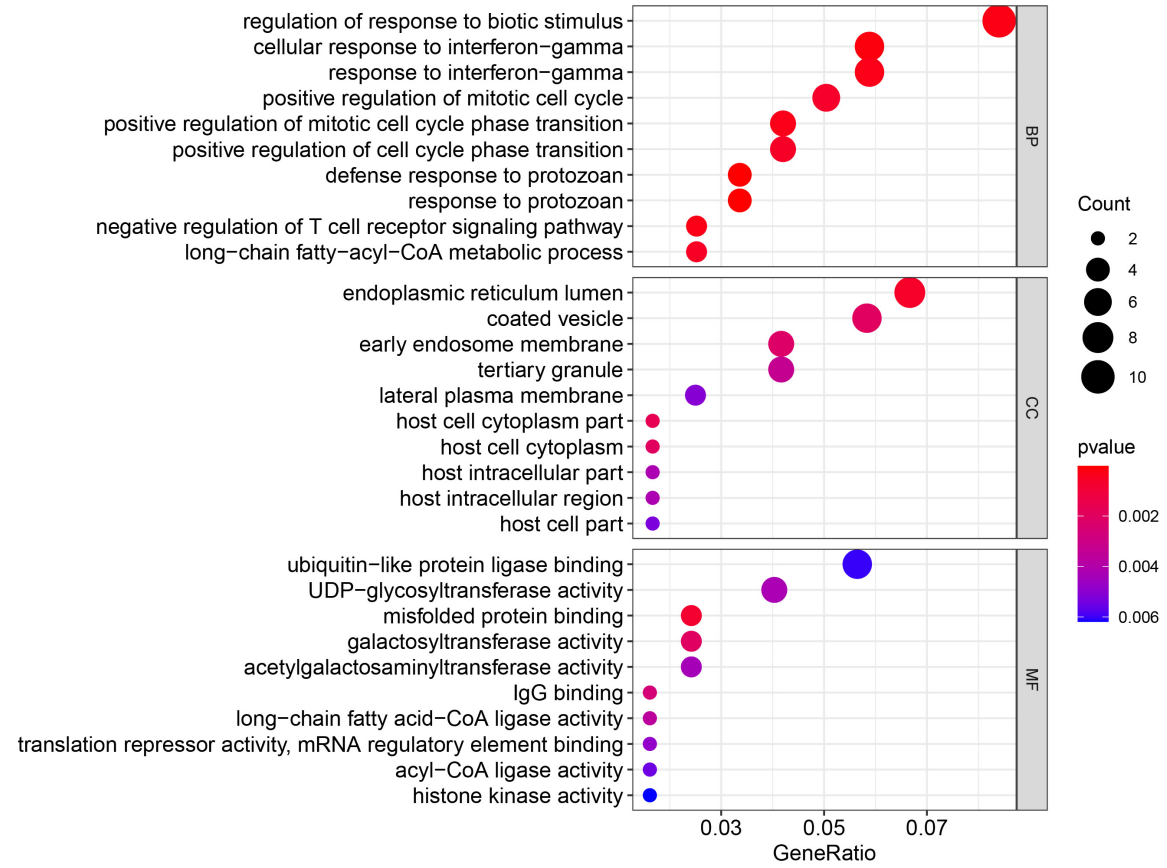

FIGURE 8
Gene Ontology enrichment of 149 MEgreenyellow genes. The count shows the number of genes enriched in the pathway. Gene ratio: the ratio of the gene number in this term to the total number of the MEgreenyellow module.

Functional annotation of the MEgreenyellow module genes

The GO enrichment and KEGG pathway analyses were performed again for the 149 MEgreenyellow genes (Figures 8, 9). For GO analysis, these genes aggregated in multiple immune-related responses, such as cellular response to interferon-gamma, negative regulation of T cell receptor signaling pathway, and IgG binding. It is worth noting that the 149 MEgreenyellow genes were also enriched in ferroptosis in the KEGG pathway and were involved in some similar metabolic pathways, including long-chain fatty acid-CoA ligase activity and fatty acid biosynthesis.

Key genes assessed by XGBoost

Table 2 shows parameter ranges and optimized values for the XGBoost model. Accordingly, we obtained the optimal feature subset and the hyperparameter combination that provided the highest AUC. In the learning curve, the optimal model satisfied both the accuracy of the training set and the validation set at the same time (Figure 10B). Based on the rank order of each feature in the XGBoost model, the top 20 key genes were retained (Figure 10A).

The least absolute shrinkage and selection operator model construction

After cross-matching 60 FRGs and 20 key genes, we identified three crucial FRGs related to PTSD development: ACSL4, ACO1, and GSS (Figure 10C). They were also significant nodes of our PPI network. *t*-Tests showed that all three genes were down-expressed in the training datasets and the validation datasets (Figures 11A–F) compared with control individuals. The LASSO model of PTSD was constructed using the three intersecting genes. As shown in Figure 10D, the optimal value of λ was set when a 3-FRG signature was generated as follows: estimation score = ACSL4 × 0.000296 + ACO1 × − 0.001032 + GSS × 0.001216. The PTSD group received a

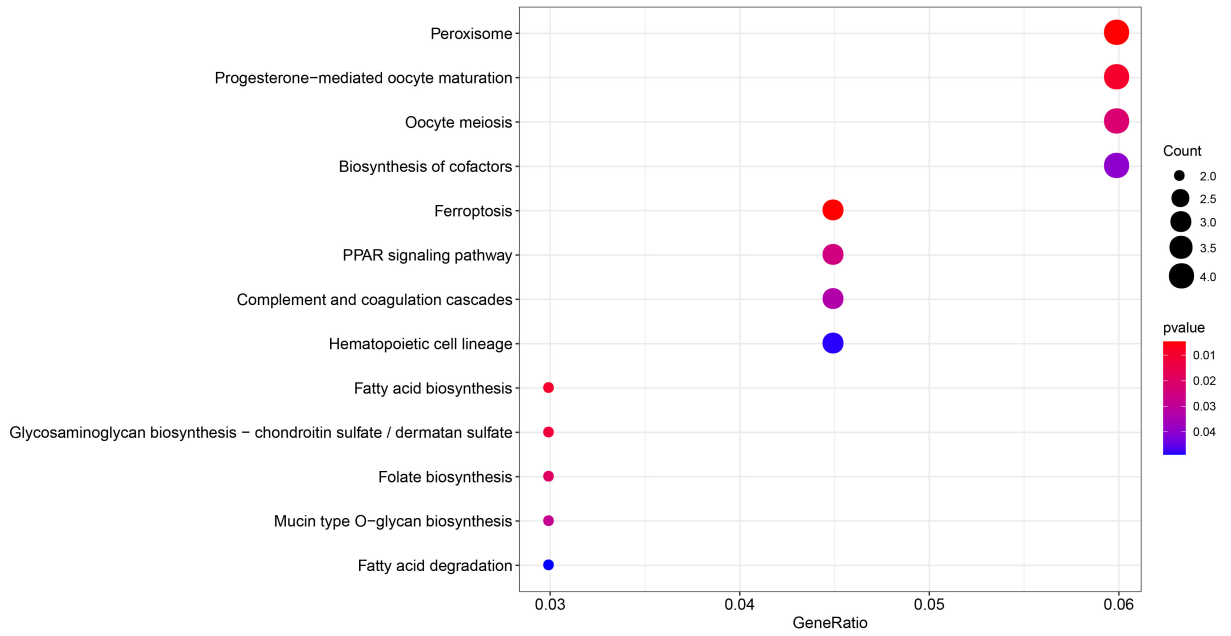

FIGURE 9
Kyoto encyclopedia of genes and genomes enrichment of 149 MEgreenyellow genes. The count shows the number of genes enriched in the pathway. Gene ratio: the ratio of the gene number in this term to the total number of the MEgreenyellow module.

TABLE 2 Main hyper-parameter range and optimized value.

Hyperparameter	Range	Optimized value
Eta	(0.01, 0.046)	0.03577263
Max depth	(6, 8)	8
Min child weight	(1, 9)	2
Subsample	(0.5, 0.8)	0.6688349

higher score than the control group ($P < 0.001$). ROC curves evaluated the estimation score's predictive performance for PTSD, and the AUC reached 0.769 in the training datasets and 0.922 in the validation datasets (Figures 11G,H).

Relationship between immune status and estimation risk of post-traumatic stress disorder

We quantified the ssGSEA enrichment scores of each sample and took the median value of the estimation score as the threshold to divide the high and low-risk groups. As shown in Figure 12A, elements related to antigen presentation process contents such as aDCs (activated dendritic cells), B cells, and DCs (dendritic cells) were significantly up-regulated in the high-risk group. Elements related to cellular immunity, such as neutrophils, T helper cells, NK cells, Tfh (follicular helper T cells), Th2 Cells, TIL (tumor-infiltrating lymphocytes), and Tregs (regulatory T cells), were up-regulated in the high-risk group. The antigen presentation process includes APC (antigen-presenting cell) co-inhibition, CCR (CC chemokine receptor), Check-point, Cytolytic activity, HLA (human leukocyte antigen), T cell co-inhibition, T cell co-stimulation, and Type II IFN Response were also up-regulated in the high-risk group (Figure 12B). The high-risk group showed elevated levels in cellular immunity and antigen presentation function, which may be associated with disturbances in ferroptosis.

The abundance of 22 immune cells in each sample was compared between the high- and low-risk groups. Pearson correlation coefficient was used to calculate the correlation between components. T cells follicular helper, NK cells activated, Macrophages M1, Dendritic cells resting, and Mast cells activated were excluded because they were present in zero amounts in each sample. Figure 13A displayed the correlation among the above 17 immune cell types. A total of four immune cell types were obviously correlated. Neutrophils negatively related to T cells CD4 memory resting ($r = -0.46$), Monocytes ($r = -0.56$), and NK cells resting ($r = -0.40$), suggesting that there may be an antagonistic relationship between neutrophils, T cells CD4 memory resting, Monocytes, and NK cells resting.

The differential expression of immune cells assessed by CIBERSORT was shown in Figure 13B. B cells naïve, B cells memory, T cells CD8, T cells CD4 naïve, T cells CD4 memory resting, T cells CD4 memory activated, NK cells resting, Monocytes, and Mast cells resting were up-regulated in the

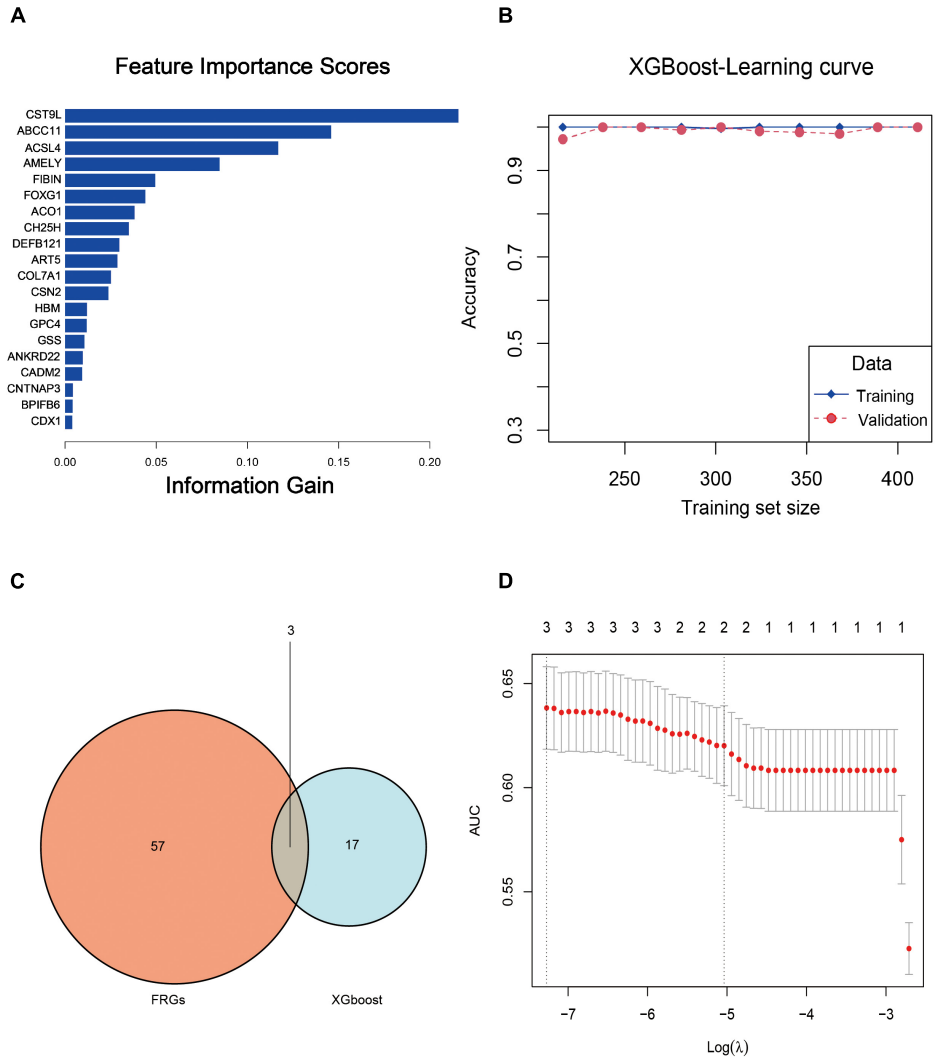

FIGURE 10
(A) Feature importance rankings for the top 20 genes identified by the XGBoost model. **(B)** Accuracy rates in the training and validating processes upon the learning curve. **(C)** Venn diagram of the top 20 genes and FRGs. After cross-matching 20 XGBoost genes and 60 FRGs, we identified three crucial FRGs related to PTSD development, which were ACSL4, ACO1, and GSS. **(D)** LASSO coefficient profile plot of the three crucial FRGs plotted against the log (lambda) sequence.

high-risk group, taking $P < 0.05$ as the threshold. These results also confirmed the ssGSEA enrichment result, indicating that ferroptosis is involved in the disorder of the immune state in PTSD patients. FRGs are potential indicators to evaluate the PTSD risk and underlying immune status.

Discussion

We conducted a comprehensive transcriptome-wide analysis covering PTSD cases and control individuals by combining six independent research datasets, intending to reveal the potential involvement of FRGs in the pathophysiology of PTSD. As the first step of the study, we applied batch normalization to reduce the batch effect, allowing us to improve statistical capabilities and explicitly validate different molecular pathways in PTSD. The enrichment analysis of GO and KEGG suggested a direct relationship with glutathione metabolism, which is a critical process in ferroptosis (36). GSH is an essential intracellular antioxidant against oxidative stress (19, 37) synthesized from glutamate, cysteine, and glycine (19). Glutamate accumulation in oxidative stress inhibits the import of cysteine, resulting in GSH depletion and lipid peroxide accumulation (38, 39).

Dixon et al. first described ferroptosis (40), which was subsequently defined as iron-dependent regulated necrosis accompanied by lipid peroxidation (19). The main biochemical mechanism of ferroptosis is the catalysis of polyunsaturated

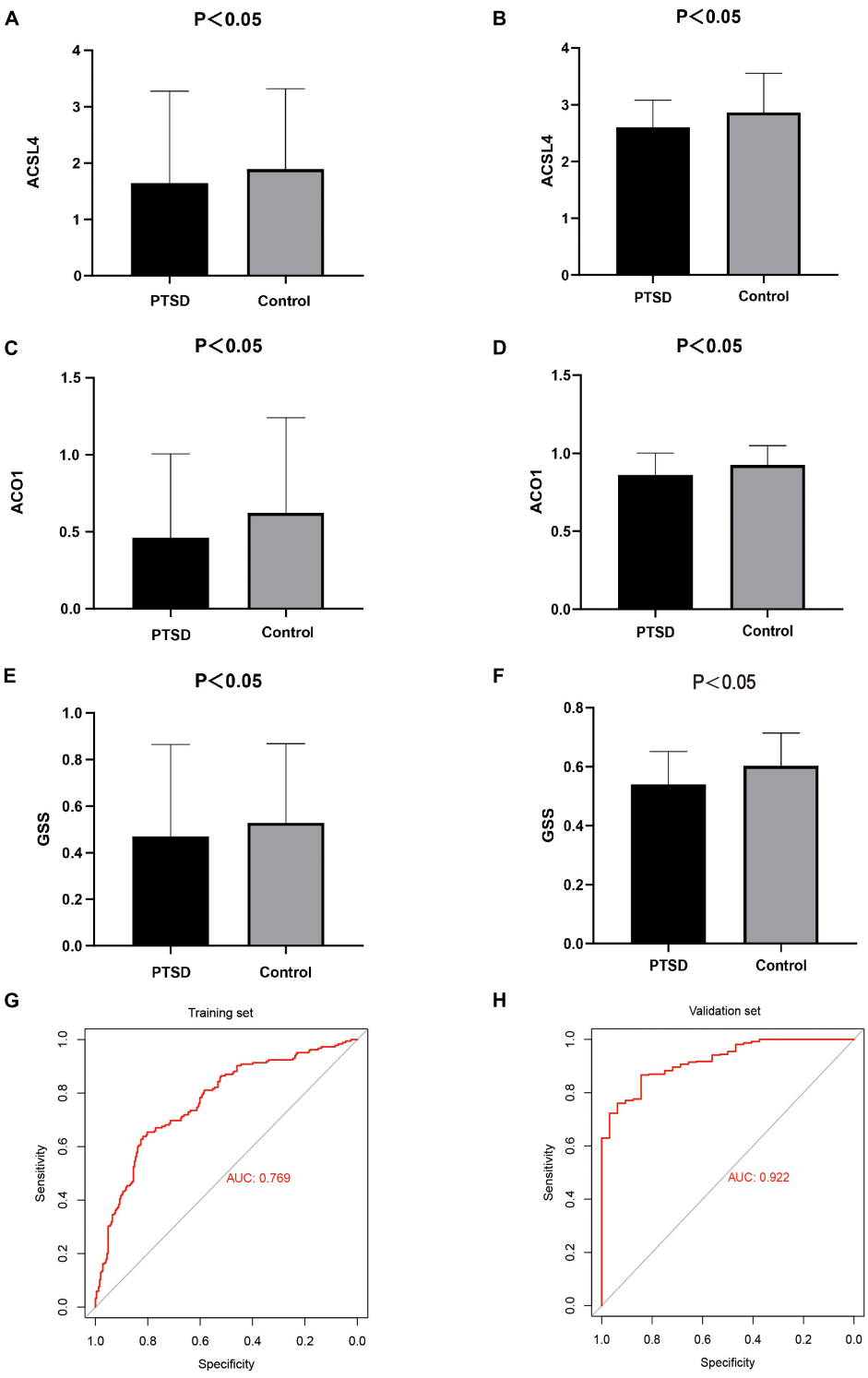

FIGURE 11
(A,B) *t*-Tests found that ACSL4 was down-expressed in the training datasets and the validation datasets. **(C,D)** ACO1 was down-expressed in the training datasets and the validation datasets. **(E,F)** GSS was down-expressed in the training datasets and the validation datasets. **(G,H)** The AUC of ROC curves reached 0.769 and 0.922 in the training datasets and the validation datasets, indicating the LASSO model has good diagnostic accuracy.

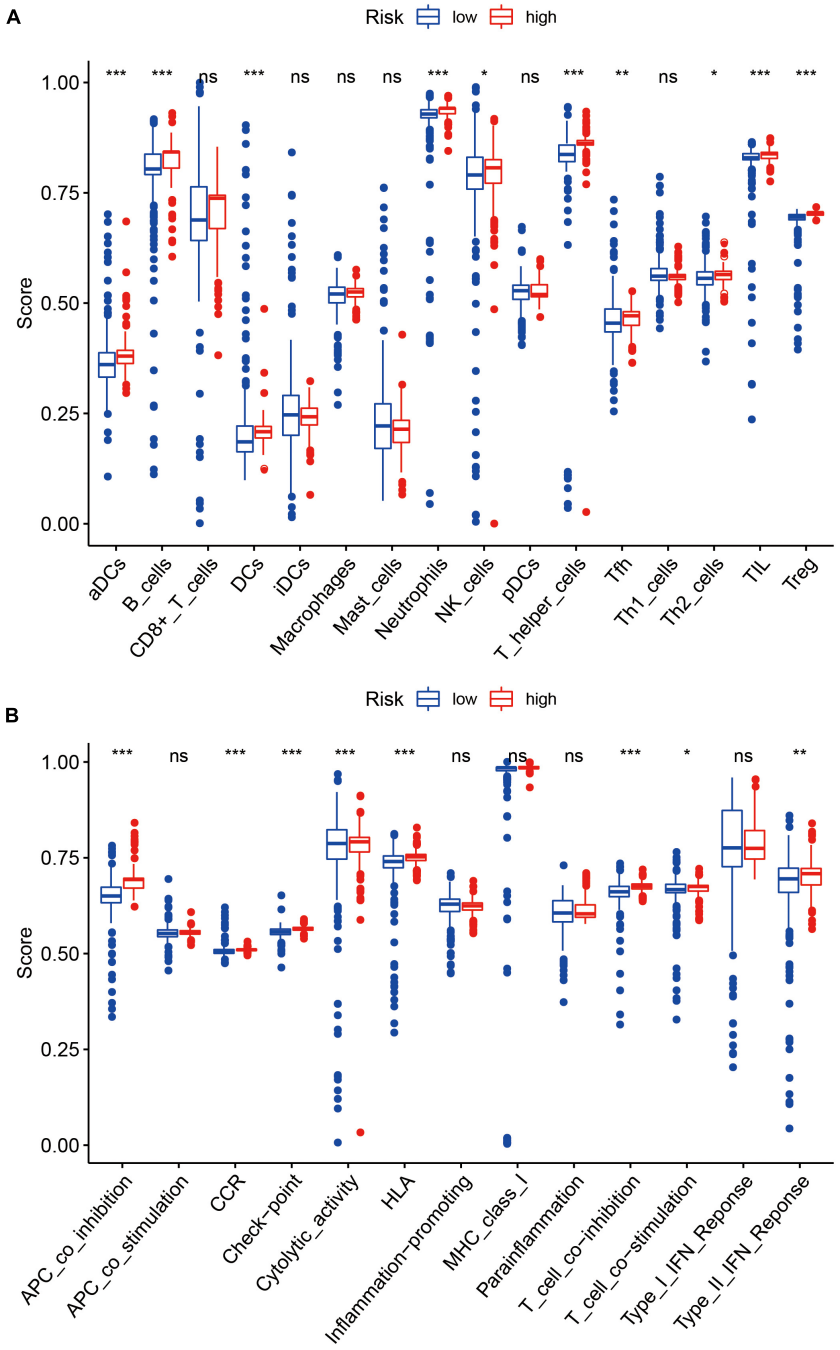

FIGURE 12
(A) Elements related to antigen presentation process contents such as aDCs, B cells, and DCs were significantly up-regulated in the high-risk group (all $P < 0.05$). Elements related to cellular immunity, such as neutrophils, NK cells, T helper cells, Tfh, Th2 Cells, TIL, and Tregs, were also up-regulated in the high-risk group. *$P < 0.05$; **$P < 0.01$; ***$P < 0.001$. **(B)** The contents of the antigen presentation process, including APC co-inhibition, CCR, Check-point, Cytolytic activity, HLA, T cell co-inhibition, T cell co-stimulation, and Type II IFN Response were significantly up-regulated in the high-risk group. *$P < 0.05$; **$P < 0.01$; ***$P < 0.001$.

fatty acids (PUFAs) that causes lipid peroxidation under the action of catalytic Fe (II) (41). Animal models of PTSD suggest increased iron in cognition-related brain regions, resulting in neuronal injury (42). Hence, high catalytic Fe (II) abundance indicates high levels of oxidative stress. PUFAs are frequently oxidized by lipoxygenases and reduced by the enzyme glutathione peroxidase 4 (GPX4) and its cofactor, GSH (20, 43). Intracellular GSH is synthesized from cysteine. Thus

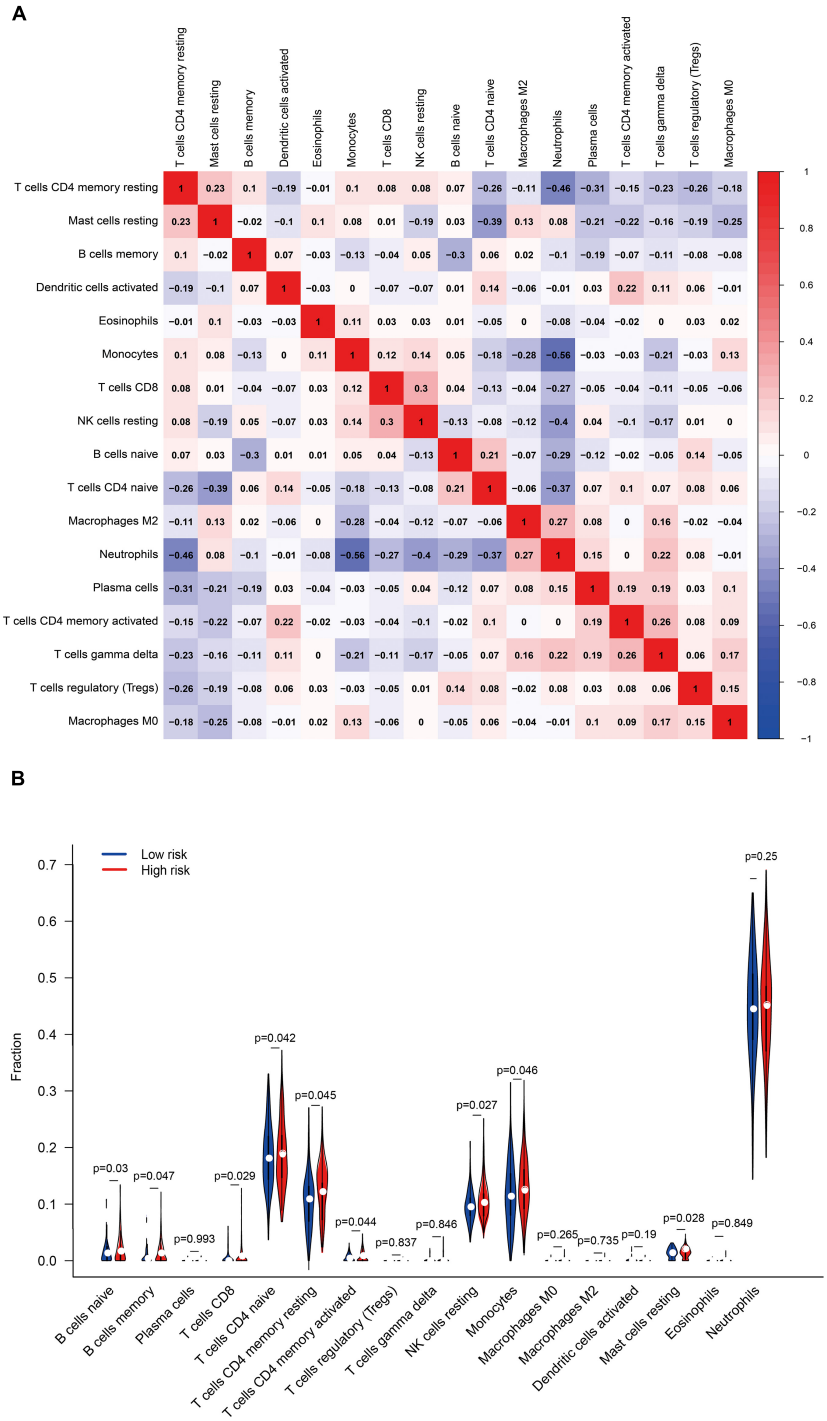

FIGURE 13
(A) Pearson correlation coefficient revealed the correlation between 17 immune cells. **(B)** The differential expression of immune cells in the high- and low-risk groups.

cysteine depletion leads to intracellular GSH exhaustion and triggers ferroptosis (40), indicating that maintaining certain cysteine levels is critical for protecting cells from ferroptosis. The requirement for cysteine for protection from ferroptosis is related to the activity of GPX4 (38, 44). Therefore, the inhibition of GPX4 and depletion of GSH results in elevated lipid peroxides and cell death induced by ferroptosis (19, 40, 43). Our study identified three crucial genes predictive

for the risk of developing PTSD, which are also important components of ferroptosis. ACSL4, ACO1, and GSS regulate lipid, iron, cysteine, and glutathione metabolic processes, which participate in the complex biological interplay of ferroptosis (45).

ACSL4 (Acyl-CoA ligase 4) encodes an isozyme of the long-chain fatty-acid-coenzyme A ligase family, thereby exerting significant effects in lipid biosynthesis (46). ACSL4 helps produce arachidonic acid (AA) or adrenic acid (AdA) containing phosphatidylethanolamine, which is involved in lipid peroxidation for ferroptosis (47, 48). ACSL4 activation contributes to ferroptosis-induced brain injury and neuroinflammation in ischemic stroke (49). ACO1 (Aconitase 1) encodes an essential enzyme that can regulate iron levels inside cells, and knockdown of ACO1 can suppress ferroptosis induced by amino acid/cysteine deprivation (20, 50). Intracellular iron and ACO1 expression were found to engage in a directional cross-talk relationship in adipose tissue, simultaneously affecting its adipogenic capacity and connecting iron metabolism and adipogenesis (51). GSS (Glutathione Synthetase) is the core gene that affects glutathione synthesis and metabolism (52). Mutations in GSS cause glutathione synthetase deficiency and result in various metabolic diseases (53–55).

The enrichment analysis of highly connected module genes in WGCNA revealed immune response pathways, including the cellular response to interferon-gamma, negative regulation of T cell receptor signaling pathway, and IgG binding. Meanwhile, the ssGSEA and CIBERSORT analysis based on the FRGs model revealed specific immune status differences between risk groups, particularly in cellular immunity and antigen presentation, which primarily were up-regulated in the high-risk group. Our result is consistent with recent research that reported direct or indirect relationships between the immune response and PTSD. For example, combined data analysis extracted from five transcriptome studies found perturbed gene expression in aggregated inflammatory pathways, including cytokine, innate immune, and type I interferon (3). Immune responses are up-regulated in PTSD at baseline and down-regulated after symptom improvement (1). The pro-inflammatory cytokines in peripheral blood cells were examined, revealing that increased CRP, IL-6, TNF-α, IL-1β, and IFN-γ were related to PTSD symptoms (56). Transcriptional sequencing of peripheral blood from PTSD patients also supported roles for innate immune and interferon signaling genes in developing the pathophysiology underlying PTSD (57).

Recent work indicates that ferroptosis-related cell death is a potent activator of the innate immune system (36). Ruptured ferroptosis cells may release pro-inflammatory factors, such as damage-associated molecular patterns (DAMPs) (36), an immunogenic process that can increase the secretion of numerous proinflammation cytokines (58, 59). Moreover, ROS and oxidized lipoproteins are also key components of DAMPs. DAMPs stimulate inflammation by binding to pattern recognition receptors (PPRs), such as Toll-like receptors (TLRs), NLR families and the ALR families (12, 60). Activating these receptors further increase inflammatory responses by recruiting immune cells. Some ferroptosis cells release signals, such as PGE2, which could impact the local immune environment (44). Immunotherapy-activated CD8 + T cells have been found to promote ferroptosis-specific lipid peroxidation, which increased the efficacy of antitumor therapy in tumor diseases (61). It is thus reasonable to assume that ferroptosis could be a potential regulatory pathway in the immune changes associated with PTSD, making it a potential marker that could aid in recognizing the development of PTSD and treatment target for the disorder.

Limitations

There are some limitations to our study. First, our model was established with a public database with a limited scale. Research across multiple centers will be required to verify our findings and assess their clinical utility. Second, a single hallmark to estimate the risk of PTSD development is insufficient because, as we know, the occurrence of PTSD is also related to a variety of environmental factors. The lack of time complexity is another limitation of our study. Due to the nature of the original data, cross-sectional studies were used to analyze the results. Further research is required to determine the validity of our conclusions in prospective studies. Our study suggests a potential role of ferroptosis in PTSD, even suggesting that it may serve as a therapeutic target for the treatment of PTSD. However, it should be emphasized that the link between ferroptosis and PTSD needs to be experimentally determined.

Conclusion

In summary, our study defined a novel model associated with PTSD. The present work also indicated the potential immunological effect of ferroptosis in PTSD occurrence. Further investigation is needed to understand the mechanisms linking ferroptosis and the development of PTSD.

Data availability statement

This data can be found here: Public datasets were available in the GEO database (https://www.ncbi.nlm.nih.gov/geo/). The corresponding accession numbers were given in the main text.

Author contributions

JZ generated the original concept and performed the statistical analysis. YZ and RR helped writing the first draft of the manuscript. LS revised the entire manuscript. LS and XT supervised the entire study. All authors had full access to all study data and analyses, participated in preparing this report, and approved of its final, submitted form.

Funding

This present work was supported by the Ministry of Science and Technology of the People's Republic of China (2021ZD0201900) and the National Natural Science Foundation of China (Grant No. 82120108002).

Conflict of interest

The authors declare that the research was conducted in the absence of any commercial or financial relationships that could be construed as a potential conflict of interest.

Publisher's note

References

1. Rusch HL, Robinson J, Yun S, Osier ND, Martin C, Brewin CR, et al. Gene expression differences in PTSD are uniquely related to the intrusion symptom cluster: a transcriptome-wide analysis in military service members. *Brain Behav Immun.* (2019) 80:904–8. doi: 10.1016/j.bbi.2019.04.039

2. Howie H, Rijal CM, Ressler KJ. A review of epigenetic contributions to post-traumatic stress disorder. *Dialogues Clin Neurosci.* (2019) 21:417–28. doi: 10.31887/DCNS.2019.21.4/kressler

3. Breen MS, Tylee DS, Maihofer AX, Neylan TC, Mehta D, Binder EB, et al. PTSD blood transcriptome mega-analysis: shared inflammatory pathways across biological sex and modes of trauma. *Neuropsychopharmacology.* (2018) 43:469–81. doi: 10.1038/npp.2017.220

4. Heinzelmann M, Gill J. Epigenetic mechanisms shape the biological response to trauma and risk for PTSD: a critical review. *Nurs Res Pract.* (2013) 2013:417010. doi: 10.1155/2013/417010

5. Schiavone S, Jaquet V, Trabace L, Krause KH. Severe life stress and oxidative stress in the brain: from animal models to human pathology. *Antioxid Redox Signal.* (2013) 18:1475–90. doi: 10.1089/ars.2012.4720

6. Uttara B, Singh AV, Zamboni P, Mahajan RT. Oxidative stress and neurodegenerative diseases: a review of upstream and downstream antioxidant therapeutic options. *Curr Neuropharmacol.* (2009) 7:65–74. doi: 10.2174/157015909787602823

7. Atli A, Bulut M, Bez Y, Kaplan I, Ozdemir PG, Uysal C, et al. Altered lipid peroxidation markers are related to post-traumatic stress disorder (PTSD) and not trauma itself in earthquake survivors. *Eur Arch Psychiatry Clin Neurosci.* (2016) 266:329–36. doi: 10.1007/s00406-015-0638-5

8. Zieker J, Zieker D, Jatzko A, Dietzsch J, Nieselt K, Schmitt A, et al. Differential gene expression in peripheral blood of patients suffering from post-traumatic stress disorder. *Mol Psychiatry.* (2007) 12:116–8. doi: 10.1038/sj.mp.4001905

9. Aquilano K, Baldelli S, Ciriolo MR. Glutathione: new roles in redox signaling for an old antioxidant. *Front Pharmacol.* (2014) 5:196. doi: 10.3389/fphar.2014.00196

10. Tang S, Gao P, Chen H, Zhou X, Ou Y, He Y. The role of iron, its metabolism and ferroptosis in traumatic brain injury. *Front Cell Neurosci.* (2020) 14:590789. doi: 10.3389/fncel.2020.590789

11. Fischer TD, Hylin MJ, Zhao J, Moore AN, Waxham MN, Dash PK. Altered mitochondrial dynamics and TBI pathophysiology. *Front Syst Neurosci.* (2016) 10:29. doi: 10.3389/fnsys.2016.00029

12. Chen Y, Zhou Z, Min W. Mitochondria, oxidative stress and innate immunity. *Front Physiol.* (2018) 9:1487. doi: 10.3389/fphys.2018.01487

13. Lamkanfi M, Kanneganti TD, Franchi L, Nunez G. Caspase-1 inflammasomes in infection and inflammation. *J Leukoc Biol.* (2007) 82:220–5. doi: 10.1189/jlb.1206756

14. Ren JX, Li C, Yan XL, Qu Y, Yang Y, Guo ZN. Crosstalk between oxidative stress and ferroptosis/oxytosis in ischemic stroke: possible targets and molecular mechanisms. *Oxid Med Cell Longev.* (2021) 2021:6643382. doi: 10.1155/2021/6643382

15. Weiland A, Wang Y, Wu W, Lan X, Han X, Li Q, et al. Ferroptosis and its role in diverse brain diseases. *Mol Neurobiol.* (2019) 56:4880–93. doi: 10.1007/s12035-018-1403-3

16. Yan HF, Tuo QZ, Yin QZ, Lei P. The pathological role of ferroptosis in ischemia/reperfusion-related injury. *Zool Res.* (2020) 41:220–30. doi: 10.24272/j.issn.2095-8137.2020.042

17. Yan N, Zhang J. Iron metabolism, ferroptosis, and the links with Alzheimer's disease. *Front Neurosci.* (2019) 13:1443. doi: 10.3389/fnins.2019.01443

18. Borovac Stefanovic L, Kalinic D, Mimica N, Beer Ljubic B, Aladrovic J, Mandelsamen Perica M, et al. Oxidative status and the severity of clinical symptoms in patients with post-traumatic stress disorder. *Ann Clin Biochem.* (2015) 52:95–104. doi: 10.1177/0004563214528882

19. Stockwell BR, Friedmann Angeli JP, Bayir H, Bush AI, Conrad M, Dixon SJ, et al. Ferroptosis: a regulated cell death nexus linking metabolism, redox biology, and disease. *Cell.* (2017) 171:273–85. doi: 10.1016/j.cell.2017.09.021

20. Hassannia B, Vandenabeele P, Vanden Berghe T. Targeting ferroptosis to iron out cancer. *Cancer Cell.* (2019) 35:830–49. doi: 10.1016/j.ccell.2019.04.002

21. Bersuker K, Hendricks JM, Li Z, Magtanong L, Ford B, Tang PH, et al. The CoQ oxidoreductase FSP1 acts parallel to GPX4 to inhibit ferroptosis. *Nature.* (2019) 575:688–92. doi: 10.1038/s41586-019-1705-2

22. Doll S, Freitas FP, Shah R, Aldrovandi M, da Silva MC, Ingold I, et al. FSP1 is a glutathione-independent ferroptosis suppressor. *Nature.* (2019) 575:693–8. doi: 10.1038/s41586-019-1707-0

23. Liang JY, Wang DS, Lin HC, Chen XX, Yang H, Zheng Y, et al. A novel ferroptosis-related gene signature for overall survival prediction in patients with hepatocellular carcinoma. *Int J Biol Sci.* (2020) 16:2430–41. doi: 10.7150/ijbs.45050

24. Leek JT. svaseq: removing batch effects and other unwanted noise from sequencing data. *Nucleic Acids Res.* (2014) 42:21. doi: 10.1093/nar/gku864

25. Langfelder P, Horvath S. WGCNA: an R package for weighted correlation network analysis. *BMC Bioinform.* (2008) 9:559. doi: 10.1186/1471-2105-9-559

26. Zhao W, Langfelder P, Fuller T, Dong J, Li A, Hovarth S. Weighted gene coexpression network analysis: state of the art. *J Biopharm Stat.* (2010) 20:281–300. doi: 10.1080/10543400903572753

27. Lv CX, An SY, Qiao BJ, Wu W. Time series analysis of hemorrhagic fever with renal syndrome in mainland China by using an XGBoost forecasting model. *BMC Infect Dis.* (2021) 21:839. doi: 10.1186/s12879-021-06503-y

28. Ke H, Chen D, Shi B, Zhang J, Liu X, Zhang X, et al. Improving brain E-health services via high-performance EEG classification with grouping bayesian optimization. *IEEE Trans Serv Comput.* (2020) 13:696–708. doi: 10.1109/TSC.2019.2962673

29. Ke H, Chen D, Shah T, Liu X, Zhang X, Zhang L, et al. Cloud-aided online EEG classification system for brain healthcare: a case study of depression evaluation with a lightweight CNN. *Softw Pract Exp.* (2020) 50:596–610. doi: 10.1002/spe.2668

30. Franceschini A, Szklarczyk D, Frankild S, Kuhn M, Simonovic M, Roth A, et al. STRING v9.1: protein-protein interaction networks, with increased coverage and integration. *Nucleic Acids Res.* (2013) 41:D808–15. doi: 10.1093/nar/gks1094

31. Wang H, Lengerich BJ, Aragam B, Xing EP. Precision lasso: accounting for correlations and linear dependencies in high-dimensional genomic data. *Bioinformatics.* (2019) 35:1181–7. doi: 10.1093/bioinformatics/bty750

32. Barbie DA, Tamayo P, Boehm JS, Kim SY, Moody SE, Dunn IF, et al. Systematic RNA interference reveals that oncogenic KRAS-driven cancers require TBK1. *Nature.* (2009) 462:108–12. doi: 10.1038/nature08460

33. Xiao B, Liu L, Li A, Xiang C, Wang P, Li H, et al. Identification and verification of immune-related gene prognostic signature based on ssGSEA for osteosarcoma. *Front Oncol.* (2020) 10:607622. doi: 10.3389/fonc.2020.607622

34. Angelova M, Charoentong P, Hackl H, Fischer ML, Snajder R, Krogsdam AM, et al. Characterization of the immunophenotypes and antigenomes of colorectal cancers reveals distinct tumor escape mechanisms and novel targets for immunotherapy. *Genome Biol.* (2015) 16:64. doi: 10.1186/s13059-015-0620-6

35. Newman AM, Liu CL, Green MR, Gentles AJ, Feng W, Xu Y, et al. Robust enumeration of cell subsets from tissue expression profiles. *Nat Methods.* (2015) 12:453–7. doi: 10.1038/nmeth.3337

36. Proneth B, Conrad M. Ferroptosis and necroinflammation, a yet poorly explored link. *Cell Death Differ.* (2019) 26:14–24. doi: 10.1038/s41418-018-0173-9

37. Schulz JB, Lindenau J, Seyfried J, Dichgans J. Glutathione, oxidative stress and neurodegeneration. *Eur J Biochem.* (2000) 267:4904–11. doi: 10.1046/j.1432-1327.2000.01595.x

38. Friedmann Angeli JP, Schneider M, Proneth B, Tyurina YY, Tyurin VA, Hammond VJ, et al. Inactivation of the ferroptosis regulator Gpx4 triggers acute renal failure in mice. *Nat Cell Biol.* (2014) 16:1180–91. doi: 10.1038/ncb3064

39. Ratan RR. The chemical biology of ferroptosis in the central nervous system. *Cell Chem Biol.* (2020) 27:479–98. doi: 10.1016/j.chembiol.2020.03.007

40. Dixon SJ, Lemberg KM, Lamprecht MR, Skouta R, Zaitsev EM, Gleason CE, et al. Ferroptosis: an iron-dependent form of nonapoptotic cell death. *Cell.* (2012) 149:1060–72. doi: 10.1016/j.cell.2012.03.042

41. Jiang X, Stockwell BR, Conrad M. Ferroptosis: mechanisms, biology and role in disease. *Nat Rev Mol Cell Biol.* (2021) 22:266–82. doi: 10.1038/s41580-020-00324-8

42. Zhao M, Yu Z, Zhang Y, Huang X, Hou J, Zhao Y, et al. Iron-induced neuronal damage in a rat model of post-traumatic stress disorder. *Neuroscience.* (2016) 330:90–9. doi: 10.1016/j.neuroscience.2016.05.025

43. Seiler A, Schneider M, Forster H, Roth S, Wirth EK, Culmsee C, et al. Glutathione peroxidase 4 senses and translates oxidative stress into 12/15-lipoxygenase dependent- and AIF-mediated cell death. *Cell Metab.* (2008) 8:237–48. doi: 10.1016/j.cmet.2008.07.005

44. Yang WS, SriRamaratnam R, Welsch ME, Shimada K, Skouta R, Viswanathan VS, et al. Regulation of ferroptotic cancer cell death by GPX4. *Cell.* (2014) 156:317–31. doi: 10.1016/j.cell.2013.12.010

45. Friedmann Angeli JP, Krysko DV, Conrad M. Ferroptosis at the crossroads of cancer-acquired drug resistance and immune evasion. *Nat Rev Cancer.* (2019) 19:405–14. doi: 10.1038/s41568-019-0149-1

46. Wang J, Wang Z, Yuan J, Wang J, Shen X. The positive feedback between ACSL4 expression and O-GlcNAcylation contributes to the growth and survival of hepatocellular carcinoma. *Aging (Albany NY).* (2020) 12:7786–800. doi: 10.18632/aging.103092

47. Doll S, Proneth B, Tyurina YY, Panzilius E, Kobayashi S, Ingold I, et al. ACSL4 dictates ferroptosis sensitivity by shaping cellular lipid composition. *Nat Chem Biol.* (2017) 13:91–8. doi: 10.1038/nchembio.2239

48. Wenzel SE, Tyurina YY, Zhao J, St Croix CM, Dar HH, Mao G, et al. PEBP1 wardens ferroptosis by enabling lipoxygenase generation of lipid death signals. *Cell.* (2017) 171:628–41.e26. doi: 10.1016/j.cell.2017.09.044

49. Cui Y, Zhang Y, Zhao X, Shao L, Liu G, Sun C, et al. ACSL4 exacerbates ischemic stroke by promoting ferroptosis-induced brain injury and neuroinflammation. *Brain Behav Immun.* (2021) 93:312–21. doi: 10.1016/j.bbi.2021.01.003

50. Gao M, Monian P, Quadri N, Ramasamy R, Jiang X. Glutaminolysis and transferrin regulate ferroptosis. *Mol Cell.* (2015) 59:298–308. doi: 10.1016/j.molcel.2015.06.011

51. Moreno M, Ortega F, Xifra G, Ricart W, Fernandez-Real JM, Moreno-Navarrete JM. Cytosolic aconitase activity sustains adipogenic capacity of adipose tissue connecting iron metabolism and adipogenesis. *FASEB J.* (2015) 29:1529–39. doi: 10.1096/fj.14-258996

52. Al-Jishi E, Meyer BF, Rashed MS, Al-Essa M, Al-Hamed MH, Sakati N, et al. Clinical, biochemical, and molecular characterization of patients with glutathione synthetase deficiency. *Clin Genet.* (1999) 55:444–9. doi: 10.1034/j.1399-0004.1999.550608.x

53. Shi ZZ, Habib GM, Rhead WJ, Gahl WA, He X, Sazer S, et al. Mutations in the glutathione synthetase gene cause 5-oxoprolinuria. *Nat Genet.* (1996) 14:361–5. doi: 10.1038/ng1196-361

54. Dahl N, Pigg M, Ristoff E, Gali R, Carlsson B, Mannervik B, et al. Missense mutations in the human glutathione synthetase gene result in severe metabolic acidosis, 5-oxoprolinuria, hemolytic anemia and neurological dysfunction. *Hum Mol Genet.* (1997) 6:1147–52. doi: 10.1093/hmg/6.7.1147

55. Njalsson R, Carlsson K, Winkler A, Larsson A, Norgren S. Diagnostics in patients with glutathione synthetase deficiency but without mutations in the exons of the GSS gene. *Hum Mutat.* (2003) 22:497. doi: 10.1002/humu.9199

56. Passos IC, Vasconcelos-Moreno MP, Costa LG, Kunz M, Brietzke E, Quevedo J, et al. Inflammatory markers in post-traumatic stress disorder: a systematic review, meta-analysis, and meta-regression. *Lancet Psychiatry.* (2015) 2:1002–12. doi: 10.1016/S2215-0366(15)00309-0

57. Breen MS, Maihofer AX, Glatt SJ, Tylee DS, Chandler SD, Tsuang MT, et al. Gene networks specific for innate immunity define post-traumatic stress disorder. *Mol Psychiatry.* (2015) 20:1538–45. doi: 10.1038/mp.2015.9

58. Linkermann A, Stockwell BR, Krautwald S, Anders HJ. Regulated cell death and inflammation: an auto-amplification loop causes organ failure. *Nat Rev Immunol.* (2014) 14:759–67. doi: 10.1038/nri3743

59. Mulay SR, Linkermann A, Anders HJ. Necroinflammation in kidney disease. *J Am Soc Nephrol.* (2016) 27:27–39. doi: 10.1681/ASN.2015040405

60. Sellge G, Kufer TA. PRR-signaling pathways: learning from microbial tactics. *Sem Immunol.* (2015) 27:75–84. doi: 10.1016/j.smim.2015.03.009

61. Wang W, Green M, Choi JE, Gijon M, Kennedy PD, Johnson JK, et al. CD8(+) T cells regulate tumour ferroptosis during cancer immunotherapy. *Nature.* (2019) 569:270–4. doi: 10.1038/s41586-019-1170-y

Frontiers in Psychiatry

Explores and communicates innovation in the field of psychiatry to improve patient outcomes

The third most-cited journal in its field, using translational approaches to improve therapeutic options for mental illness, communicate progress to clinicians and researchers, and consequently to improve patient treatment outcomes.

Discover the latest Research Topics

See more →

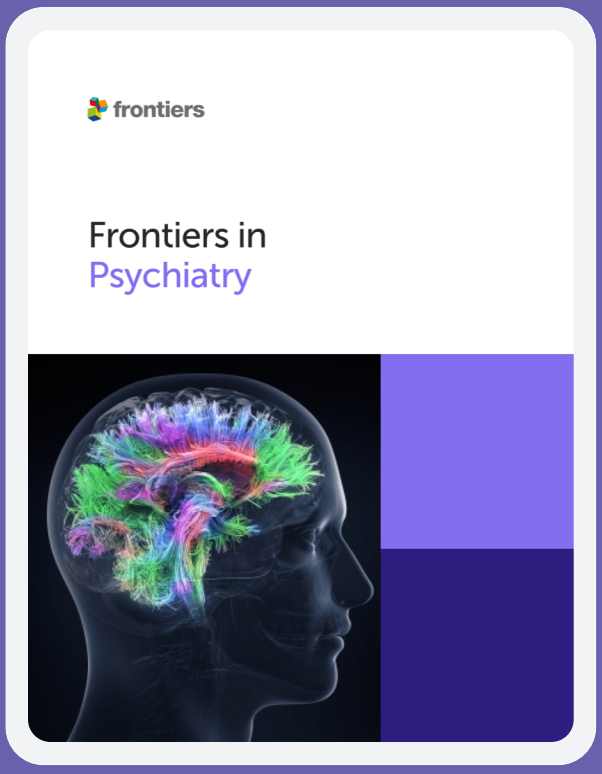

Frontiers

Avenue du Tribunal-Fédéral 34
1005 Lausanne, Switzerland
frontiersin.org

Contact us

+41 (0)21 510 17 00
frontiersin.org/about/contact